
Investigation of the modulation
of murine repeat element DNA
methylation by ionising radiation
in vivo

A thesis submitted in fulfilment for the degree of Doctor of Philosophy

Michelle Renee Newman, B.Sc, B.HSc (Hons)

Haematology and Genetic Pathology

School of Medicine, Faculty of Health Sciences

Flinders University

November 2012

TABLE OF CONTENTS

TABLE OF CONTENTS	I
FIGURES	VIII
TABLES	XII
SUMMARY	XIV
DECLARATION	XVIII
ACKNOWLEDGEMENTS	XIX
ABBREVIATIONS AND UNITS OF MEASUREMENT	XXII
<i>STANDARD INTERNATIONAL UNITS OF MEASURE</i>	XXIV
<i>INDICATORS OF MAGNITUDE</i>	XXIV
PUBLICATIONS AND PRESENTATIONS ARISING FROM THIS THESIS	XXV
PUBLICATIONS	XXV
PRESENTATIONS.....	XXV
1 INTRODUCTION	1
1.1 IONISING RADIATION	3
1.1.1 <i>Quantifying ionising radiation</i>	4
1.2 BIOLOGICAL EFFECTS OF RADIATION.....	6
1.2.1 <i>Mouse models in radiation research</i>	6
1.2.2 <i>High dose radiation exposure</i>	9
1.2.2.1 Tissue effects from high dose radiation exposure	9
1.2.2.2 Sub-cellular effects from high dose radiation exposure	10
1.2.2.3 Repair of DNA following high dose radiation exposure	13
1.2.3 <i>Low dose radiation exposure</i>	14
1.2.4 <i>Ageing and radiation exposure</i>	16
1.3 MAINTENANCE OF GENOMIC STABILITY	17
1.3.1 <i>Chromatin structure</i>	17
1.3.2 <i>DNA methylation</i>	21

1.3.2.1	Methods for the detection of DNA methylation.....	24
1.3.3	<i>Telomeres and genomic stability</i>	30
1.3.4	<i>Retrotransposons and genomic stability</i>	33
1.4	DNA METHYLATION AND RADIATION EXPOSURE.....	39
1.5	AIMS OF THIS THESIS.....	44
2	MATERIALS AND METHODS.....	45
2.1	MOUSE STRAINS.....	45
2.2	A11 CELL LINE.....	46
2.3	RADIATION DOSIMETRY AND X-IRRADIATION OF MICE.....	46
2.4	MOUSE TISSUES.....	48
2.4.1	<i>Mouse tissue isolation</i>	48
2.4.2	<i>Isolation of peripheral blood</i>	48
2.5	ANALYSIS OF DNA METHYLATION.....	49
2.5.1	<i>Extraction of genomic DNA</i>	49
2.5.2	<i>Bisulphite modification of genomic DNA</i>	50
2.5.3	<i>Primer design</i>	51
2.5.4	<i>PCR and high resolution melt analysis (HRM)</i>	51
2.5.5	<i>Calculation of the Net Temperature Shift</i>	52
2.5.6	<i>Gel electrophoresis of PCR products</i>	52
2.5.7	<i>Sequence analysis of PCR products</i>	53
2.5.7.1	Sanger sequencing.....	53
2.5.7.2	Pyrosequencing.....	53
2.5.8	<i>Liquid chromatography-Mass spectrometry (LC-MS)</i>	54
2.5.8.1	DNA hydrolysis.....	54
2.5.8.2	LC-MS Procedure.....	54
2.6	TELOMERE LENGTH ANALYSIS.....	55
2.7	L1 TRANSCRIPT ANALYSIS.....	56
2.7.1	<i>RNA extraction</i>	56
2.7.1.1	RNA quality control.....	57
2.7.1.2	DNaseI treatment.....	57
2.7.2	<i>Reverse transcription</i>	58

2.7.3	<i>Quantitative real-time PCR</i>	58
2.7.3.1	Primer design	59
2.7.3.2	Analysis of reference gene stability	59
2.8	WESTERN BLOT ANALYSIS	59
2.8.1	<i>Acid extraction of histone proteins</i>	59
2.8.2	<i>Determination of protein concentration</i>	60
2.8.3	<i>Gel Electrophoresis of protein lysates</i>	61
2.8.4	<i>Semi-dry transfer of proteins</i>	62
2.8.5	<i>Detection of proteins</i>	62
2.8.5.1	Antibody detection of proteins.....	62
2.8.5.2	Quantitation of protein bands	63
2.9	IMMUNOHISTOCHEMISTRY	63
2.9.1	<i>Preparation of tissue sections</i>	63
2.9.2	<i>Detection of spleen T-cells</i>	63
2.9.3	<i>Microscopy of spleen sections</i>	64
2.10	STATISTICAL ANALYSIS.....	65
3	DEVELOPMENT AND VALIDATION OF A MURINE LINE1 DNA METHYLATION HIGH RESOLUTION MELT ASSAY	66
3.1	RESULTS.....	69
3.1.1	<i>Design of a murine L1 repeat element high resolution melt assay</i>	69
3.1.1.1	Identification of murine LINE1 repeat element	69
3.1.1.2	Primer Design.....	69
3.1.1.3	Sequence analysis of LINE1 repeat elements	70
3.1.1.4	Development of PCR methylation controls.....	72
3.1.1.5	High resolution melt analysis of control DNA	73
3.1.2	<i>Detection of demethylation using the L1-HRM assay</i>	74
3.1.2.1	Detection of demethylation induced by 5-aza treatment	74
3.1.2.2	Biasing of PCR primers to enhance sensitivity	77
3.1.2.3	Statistical analysis of methylation differences between samples using the Net Temperature Shift.....	79
3.1.3	<i>Validation of L1-HRM assay</i>	80

3.1.3.1	Pyrosequencing	80
3.1.3.2	Liquid chromatography-mass spectrometry	82
3.1.3.3	Sensitivity, reproducibility and linearity of the L1-HRM assay	84
3.1.4	<i>Application of the HRM methylation assay to other murine repeat elements</i>	87
3.1.4.1	SINE1 and IAP_LTR repeat elements	87
3.2	DISCUSSION	89
3.2.1	<i>Detection of demethylation using the L1-HRM assay</i>	89
3.2.2	<i>Validation of HRM assay detection of methylation differences</i>	92
3.2.3	<i>Reproducibility, sensitivity and linearity of the L1-HRM assay</i>	94
3.2.4	<i>Conclusion</i>	96
4	ANALYSIS OF REPEAT ELEMENT DNA METHYLATION CHANGES IN MOUSE STRAINS WITH DIFFERING RADIATION SENSITIVITIES FOLLOWING EXPOSURE TO IONISING RADIATION	97
4.1	RESULTS	99
4.1.1	<i>L1 methylation levels in mouse spleen 6-7 days following 1 Gy X-irradiation</i>	99
4.1.1.1	Pyrosequencing analysis of spleen L1-HRM assay samples from male BALB/c and female CBA mice 6 days following 1 Gy X-irradiation	101
4.1.2	<i>LC-MS analysis of male BALB/c and female CBA mouse spleen total genomic DNA methylation levels 6 days following 1 Gy X-irradiation</i> ...	104
4.1.3	<i>B1 and IAP repeat element methylation levels of male and female BALB/c and CBA mouse spleen 6 days following 1 Gy X-irradiation</i>	105
4.1.4	<i>Analysis of temporal spleen methylation changes in C57Bl/6 mice following 1 Gy X-irradiation</i>	106
4.1.4.1	Pyrosequencing analysis of spleen L1 methylation changes in C57Bl/6 mice 1 and 14 days following 1 Gy X-irradiation	107
4.1.4.2	LC-MS analysis of spleen tissue genomic DNA from C57Bl/6 mice 1 and 14 days following 1 Gy X-irradiation	109
4.1.4.3	Spleen B1 and IAP element methylation levels in C57Bl/6 mice 14 days following 1 Gy X-irradiation	110

4.1.4.4	Pyrosequencing analysis of the methylation changes at all CpGs within the L1-HRM assay target sequence in the spleens of C57Bl/6 mice 14 days following 1 Gy X-irradiation	111
4.1.4.5	L1 promoter analysis.....	114
4.1.4.6	Analysis of histone H3 tri-methylation in the spleens of C57Bl/6 mice 14 days following 1 Gy X-irradiation	119
4.1.5	<i>Analysis of spleen temporal L1 methylation changes in BALB/c and CBA mice following 1 Gy X-irradiation</i>	<i>121</i>
4.1.6	<i>Tissue L1 methylation levels of untreated BALB/c, CBA and C57Bl/6 mice</i>	<i>123</i>
4.1.7	<i>Tissue responses 6 days following 1 Gy X-irradiation in male and female BALB/c and CBA mice</i>	<i>126</i>
4.1.8	<i>Immunohistochemical analysis of spleen tissue cell populations</i>	<i>127</i>
4.2	DISCUSSION	133
4.2.1	<i>Strain differences in response to irradiation</i>	<i>133</i>
4.2.2	<i>Sex differences in L1 methylation levels in response to X-irradiation.....</i>	<i>142</i>
4.2.3	<i>Analysis of the effect of changes in methylation to the L1 promoter.....</i>	<i>143</i>
4.3	CONCLUSION.....	147
5	LONGITUDINAL STUDY OF REPEAT ELEMENT METHYLATION IN PERIPHERAL BLOOD IN RESPONSE TO LOW DOSE RADIATION.....	148
5.1	RESULTS.....	150
5.1.1	<i>Longitudinal study of repeat element DNA methylation in mice up to 299 days following 10 mGy X-irradiation (Longitudinal Study #1)</i>	<i>150</i>
5.1.1.1	Outline of study	150
5.1.1.2	Analysis of mouse weight and repeat element methylation changes following 10 mGy X- irradiation.....	151
5.1.2	<i>Longitudinal study of repeat element DNA methylation in mice up to 420 days following 10 mGy X-irradiation (Longitudinal Study #2)</i>	<i>159</i>
5.1.2.1	Outline of longitudinal study #2	159
5.1.2.2	Weight changes of male and female mice over time	160

5.1.2.3	Analysis of the effect of irradiation and ageing on peripheral blood genomic DNA up to 420 days following irradiation with 10 mGy X-rays.....	162
5.1.2.4	Analysis of the effect of 10 mGy X-irradiation and ageing on spleen genomic DNA from mice at 420 days post-irradiation	169
5.2	DISCUSSION	172
5.2.1	<i>Analysis of variation in NTS between PCRs</i>	172
5.2.2	<i>The longitudinal effect of 10 mGy X-irradiation on telomere length and repeat element methylation in spleen and peripheral blood up to 420 days post-irradiation</i>	175
5.3	CONCLUSION.....	182
6	GENERAL DISCUSSION.....	184
	REFERENCES.....	191
	APPENDIX A: ANALYSIS OF THE EFFECT OF C57BL/6-PKZ1 TRANSGENIC STATUS ON NTS	233
	APPENDIX B: PCR PRIMERS.....	234
	HRM PRIMERS.....	234
	<i>KATO</i>	234
	<i>LINE1</i>	234
	<i>B1_MM.....</i>	235
	<i>IAP_LTR</i>	235
	SEQUENCING PRIMERS.....	235
	QRT-PCR PRIMERS.....	236
	<i>L1-ORF1.....</i>	236
	<i>L1-ORF2.....</i>	236
	<i>COCH (COAGULATION FACTOR C HOMOLOGUE)</i>	236
	<i>CPB1 (CARBOXYPEPTIDASE B1).....</i>	237
	<i>GAPDH (GLYCERALDEHYDE-3-PHOSPHATE DEHYDROGENASE)</i>	237
	<i>PNLIP (PANCREATIC TRIACYLGLYCEROL LIPASE)</i>	237
	<i>POLR2C (POLYMERASE (RNA) II (DNA DIRECTED) POLYPEPTIDE C)</i>	238
	<i>RN18S (RIBONUCLEOTIDE PROTEIN SUBUNIT 18).....</i>	238
	<i>SPI-C (TRANSCRIPTION FACTOR SPI-C)</i>	238
	TELOMERE ASSAY PRIMERS	239

<i>TELOMERE</i>	239
TELOMERE OLIGONUCLEOTIDE STANDARD	239
<i>36B4 (LARGE RIBOSOMAL PROTEIN, PO)</i>	239
<i>36B4</i> OLIGONUCLEOTIDE STANDARD	239
APPENDIX C: SOLUTIONS AND BUFFERS.....	240
AGAROSE GEL ELECTROPHORESIS	240
0.5 X TRIS-BORATE EDTA (TBE) BUFFER	240
2% AGAROSE GEL	240
6 X FICOLL LOADING BUFFER.....	240
WESTERN BLOT.....	240
HISTONE LYSIS BUFFER.....	240
TRIS-EDTA	241
1 X RUNNING BUFFER	241
4 X LOADING BUFFER.....	241
1 X TRANSFER BUFFER	241
10 X TRIS BUFFERED SOLUTION (TBS).....	242
1 X TBS-TWEEN (TBS-T)	242
IMMUNOHISTOCHEMISTRY.....	242
APES SOLUTION	242
2% FORMALDEHYDE.....	242
BLOCKING SOLUTION	242
APPENDIX D: L1 PROMOTER AND ORF SEQUENCES.....	243
APPENDIX E: TELOMERE LENGTH AND GENOME COPY NUMBER	
CALCULATIONS	246
CALCULATION OF TELOMERE LENGTH	246
TELOMERE OLIGONUCLEOTIDE STANDARDS	247
CALCULATION OF GENOME COPY NUMBER.....	247
<i>36B4</i> OLIGONUCLEOTIDE STANDARDS	248
TELOMERE LENGTHS OF MICE FROM LONGITUDINAL STUDY OF METHYLATION IN PB IN RESPONSE TO LOW DOSE RADIATION.....	249
APPENDIX F: CELLPROFILER™ PIPELINE	250
APPENDIX G: PUBLICATIONS ARISING FROM THIS THESIS	251

FIGURES

Figure 1-1: Sources of radiation exposure.....	2
Figure 1-2: Linear no-threshold model.....	2
Figure 1-3: Measurement of radiation exposure.....	4
Figure 1-4: Tissue/organ radiation weighting factors.....	6
Figure 1-5: Damage to DNA following high dose radiation exposure.....	12
Figure 1-6: Control of chromatin structure by epigenetic modifications.....	19
Figure 1-7: Methylation of cytosine.....	22
Figure 1-8: Facilitation of mutations via demethylation of cytosine.....	24
Figure 1-9: Techniques that utilise bisulphite modification to evaluate methylation levels.....	26
Figure 1-10: Structure of telomeres.....	32
Figure 1-11: Types of retrotransposons.....	34
Figure 1-12: L1 transcription and retrotransposition.....	36
Figure 1-13: IAP transcription and retrotransposition.....	37
Figure 3-1: Agarose gel analysis of L1 PCR products.....	70
Figure 3-2: The L1 sequence confirmed by DNA sequencing.....	72
Figure 3-3: High resolution melt analysis of control DNA.....	74
Figure 3-4: Melt curve analysis of unmodified genomic DNA.....	76
Figure 3-5: Detection of 5-aza induced partial demethylation of murine L1 elements in A11 cells using methylation-status unbiased L1 primers.....	76
Figure 3-6: Detection of 5-aza induced partial demethylation of murine L1 elements in A11 cells using unmethylated-biased L1 primers.....	78
Figure 3-7: Quantitation of methylation differences using the Net Temperature Shift.....	80
Figure 3-8: Schematic diagram of the L1 pyrosequencing target sequence.....	81
Figure 3-9: Pyrosequencing of 5-aza treated A11 cells L1-HRM PCR products.....	82
Figure 3-10: Analysis of total genomic 5mdC content in 5-aza treated A11 cells.....	83
Figure 3-11: Linearity of L1-HRM assay.....	85

Figure 3-12: Murine B1 and Intracisternal-A-Particle Long Terminal Repeat element sequences..... 88

Figure 3-13: Demethylation of B1 and IAP_LTR repeat elements after 5-aza treatment..... 88

Figure 4-1: Spleen tissue L1 methylation in BALB/c, CBA and C57Bl/6 mice 6-7 days following irradiation with 1 Gy X-rays..... 100

Figure 4-2: LC-MS and pyrosequencing analysis of spleen methylation levels in male BALB/c and female CBA mice 6 days following 1 Gy X-irradiation. 103

Figure 4-3: LC-MS analysis of total splenic genomic DNA methylation levels in male BALB/c and female CBA mice 6 days following 1 Gy X-irradiation. 104

Figure 4-4: B1 and IAP repeat element methylation in spleen tissues from BALB/c and CBA mice 6 days following 1 Gy X-irradiation..... 105

Figure 4-5: L1 methylation levels in C57Bl/6 spleen tissue up to 14 days following irradiation with 1 Gy X-rays..... 107

Figure 4-6: Pyrosequencing analysis of spleen methylation levels from C57Bl/6 mice 1 and 14 days following irradiation with 1 Gy X-rays..... 108

Figure 4-7: LC-MS analysis of spleen genomic 5mdC levels from C57Bl/6 mice 14 days following irradiation with 1 Gy X-rays..... 109

Figure 4-8: C57Bl/6 mouse spleen tissue B1 and IAP element methylation 14 days following irradiation with 1 Gy X-rays..... 110

Figure 4-9: L1 pyrosequencing dispensation sequence..... 112

Figure 4-10: Pyrosequencing analysis of all CpGs within the L1 CpG island of spleen samples from C57Bl/6 mice 14 days following irradiation with 1 Gy X-rays..... 113

Figure 4-11: Analysis of the L1 promoter sequence..... 116

Figure 4-12: L1 transcript levels in the spleen tissues of C57Bl/6 mice 14 days following irradiation with sham or 1 Gy X-rays..... 118

Figure 4-13: L1 transcript expression in 5-aza treated A11 cells..... 119

Figure 4-14: Analysis of histone H3 tri-methylation in spleen tissue of C57Bl/6 mice 14 days following 1 Gy X-irradiation..... 120

Figure 4-15: BALB/c and CBA L1 methylation levels 1, 6 and 14 days following irradiation with 1 Gy X-rays..... 122

Figure 4-16: L1 methylation in various tissues from the BALB/c, CBA and C57Bl/6 mouse strains..... 124

Figure 4-17: Analysis of male BALB/c tissue panel with methylation-status unbiased L1 primers. 125

Figure 4-18: Detection of splenic T-cells in male BALB/c and CBA mice using immunohistochemistry. 128

Figure 4-19: CellProfiler™ identification of splenic T-cells. 130

Figure 4-20: The roving mean of T-cell areas in BALB/c spleen..... 131

Figure 4-21: Mean splenic T-cell staining area frequency of male BALB/c and CBA mice. 132

Figure 4-22: Correlation of NTS and splenic T-cell area frequency. 132

Figure 5-1: Outline of longitudinal study..... 150

Figure 5-2: Mean weight over time of mice irradiated with sham and 10 mGy X-rays up to 299 days post-irradiation. 152

Figure 5-3: Outline of sample randomisation for HRM analysis..... 153

Figure 5-4: Mean PB L1 NTS of mice up to 85 days post-irradiation with 10 mGy X-rays. 154

Figure 5-5: PB L1 and B1 element NTS of mice up to 299 days post-irradiation with sham or 10 mGy X-rays. 155

Figure 5-6: Mean L1 and B1 element NTS of PB samples up to 299 days following irradiation with sham or 10 mGy X-rays. 157

Figure 5-7: Spleen NTS of L1 and B1 elements from mice 299 days post-irradiation with sham and 10 mGy X-rays..... 158

Figure 5-8: Outline of second longitudinal study. 159

Figure 5-9: Mean weight over time for male and female mice irradiated with sham and 10 mGy X-rays. 161

Figure 5-10: Telomere length of individual male and female mice pre- and post-irradiation with 10 mGy X-rays. 163

Figure 5-11: Mean telomere length of male and female mice pre- and post-irradiation with 10 mGy X-rays.	164
Figure 5-12: PB NTS for L1 and B1 elements for mice up to 420 days post-irradiation with sham or 10 mGy X-rays.	166
Figure 5-13: Mean PB NTS for L1 and B1 elements from mice up to 420 days post-irradiation with sham or 10 mGy X-rays.	168
Figure 5-14: Correlation of L1 and B1 element NTS for PB.....	169
Figure 5-15: Analysis of spleen telomere length at 420 days post-irradiation with sham or 10 mGy X-rays compared to young untreated mice.	170
Figure 5-16: Spleen L1 NTS of mice 420 days post-irradiation compared with untreated young mice and analysis of B1 element NTS of mice 420 days post-irradiation with sham and 10 mGy X-rays.....	171

TABLES

Table 1: LD _{50:30} of inbred mouse strains following single whole body X-irradiation.....	8
Table 2: Days survival following daily whole-body X-irradiation with 10 Gy of the C57Bl/6, BALB/c and CBA mouse strains in a study of twenty-seven mouse strains.	9
Table 3: Number of events of the different types of DNA damage that can occur in a cell following irradiation with 1 Gy X-rays.	13
Table 4: Summary of published <i>in vivo</i> murine DNA methylation and ionising radiation studies.	41
Table 5: Summary of published <i>in vivo</i> transgenerational murine DNA methylation and ionising radiation studies.	42
Table 6: Dosimetry parameters for irradiation experiments.....	48
Table 7: Frequency of sequence variants detected at 10 nucleotide positions in the L1-HRM target sequence.....	71
Table 8: Analysis of variability of L1-HRM assay.....	86
Table 9: Pearson correlation of L1, B1 and IAP repeat element NTS values for the 5-aza treated A11 cell line samples.	89
Table 10: L1 CpG methylation levels (%) for male BALB/c and female CBA mice 6 days following 1 Gy X-irradiation using pyrosequencing.....	102
Table 11: Correlation of L1 transcript levels with LC-MS and pyrosequencing mean methylation.	118
Table 12: Mean L1 NTS for tissues from BALB/c and CBA mice treated with 1 Gy X-rays.....	126
Table 13: Mean L1 NTS for peripheral blood samples from BALB/c and CBA mice treated with 1 Gy X-rays.....	127
Table 14: Age of mice at PB sampling in longitudinal study (#1) up to 299 days post-irradiation with 10 mGy X-rays.	151
Table 15: Analysis of changes in PB L1 and B1 element NTS up to 299 days following irradiation with 10 mGy X-rays.....	156

Table 16: Age of mice at PB sampling in longitudinal study (#2) up to 420 days post-irradiation with 10 mGy X-rays.	160
Table 17: Analysis of changes in mouse weight up to 420 days post-irradiation with 10 mGy X-rays.	161
Table 18: Analysis of changes in PB L1 and B1 repeat element NTS in male and female mice up to 420 days post-irradiation with 10 mGy X-rays.	167
Table 19: Mean difference in L1 NTS between bisulphite modification and PCR groups for PB samples up to 85 days post-irradiation amplified with the unmethylated-biased primers.	173
Table 20: Comparison of the mean L1 NTS for three PCR groups from longitudinal study #2 amplified with the methylation status-unbiased primers.	174
Table 21: Independent samples T-test analysis of pKZ1-C57Bl/6 transgenic status.	233
Table 22: Telomere oligonucleotide standard lengths.	247
Table 23: 36B4 oligonucleotide standard copy numbers.	248
Table 24: Mean length per telomere of PB samples from Chapter 5 (Section 5.1.2.3.1).	249
Table 25: Mean length per telomere of spleen samples from Chapter 5 (Section 5.1.2.4.1).	249

SUMMARY

Mouse models that are used to investigate the biological effects of ionising radiation exposure have shown that different inbred strains respond differently to radiation exposure. Based on end-points such as time to lethality, repair of DNA damage and the development of cancers, these strains are defined as radiation-sensitive or resistant. Ionising radiation has been reported to induce a loss of DNA methylation, a modification of cytosine residues (predominantly when in sequence with a guanine; termed a CpG) that plays an important role in maintaining genome stability by influencing the expression of genes through chromatin structure. The most heavily methylated regions of the genome are found at transposable repeat elements, where a loss of methylation may result in transposition and increased genomic instability. It is not known whether the radiation sensitivity that these animals exhibit is influenced by the modulation of DNA methylation by ionising radiation. This thesis describes the investigation of the modulation of DNA methylation of a class of repeat elements known as LINE1 (L1), in three strains of laboratory mice that differ in radiosensitivity: the C57Bl/6 (radiation-resistant), BALB/c and CBA (radiation-sensitive) mouse strains. A sensitive PCR-based assay was developed in order to investigate the changes in L1 methylation following radiation exposure. The L1 assay utilised high resolution melt technology (HRM), which is able to distinguish between single nucleotide differences in sequences of DNA following PCR amplification. The L1-HRM assay was demonstrated to be able to detect differences in heterogeneous CpG methylation as small as 3%; and was also able to detect changes in methylation between samples that could not be

detected by the gold standard method for total genomic 5mdC quantitation (liquid chromatography mass-spectrometry). Compared with other PCR-based methods for DNA methylation analysis, the L1-HRM assay was shown to be a sensitive, high through-put screening tool that did not require post-PCR manipulation in order to detect differences in methylation between samples.

Following high dose irradiation (1 Gy), the radiosensitive mouse strains (BALB/c and CBA) exhibited early increases in spleen L1 methylation, which had returned to sham methylation levels by 14 days following irradiation. Differences in responses between male and female mice were also observed, with the male CBA mice demonstrating an earlier response in comparison with the female CBA mice. The radiation-resistant C57Bl/6 mice demonstrated a late change in methylation, where a loss of methylation was observed by 14 days following irradiation. The modulation of L1 DNA methylation was shown to only affect some CpGs within the L1-HRM assay target region, which was consistent across the three strains. This is the first analysis of the modulation of murine L1 element CpGs following radiation exposure. Furthermore, the loss of methylation in the C57Bl/6 mice did not result in an increase in L1 element transcripts. Other murine repeat DNA elements (B1 and Intracisternal-A particle long terminal repeat elements) were found to display similar modulation to that of the L1 elements following irradiation. These results show that strains that differ in radiosensitivity exhibit temporal differences in repeat element methylation responses following exposure to ionising radiation, highlighting the importance of timing of analysis, particularly when analysing the effects of a modulator of DNA methylation that does not appear to affect every

CpG. This is the first direct comparison of the temporal DNA methylation response of three strains of mice that differ in radiosensitivity.

Low doses of ionising radiation have been shown to demonstrate a protective role for endpoints such as DNA damage and tumour progression, termed the radioadaptive response. The exact mechanism(s) involved in the radioadaptive response are still being identified, and it has been suggested that stabilisation of the genome via the modulation of DNA methylation may be involved. Both radiation exposure and ageing are associated with increased genomic instability, shorter telomeres and reduced DNA methylation. Studies described in this thesis investigated whether a low dose radiation (10 mGy) exposure would modulate repeat element DNA methylation to induce an adaptive response. Following irradiation, the modulation of L1 and B1 DNA methylation of ageing mice was monitored over time using peripheral blood (PB) sampling. A decline in PB L1 and B1 element methylation levels was not observed by 420 days (~18 months of age) post-irradiation; however spleen L1 methylation levels increased with age. No effect of irradiation was detected on PB and spleen L1 and B1 methylation levels or telomere length in the ageing mice. These results indicate that there may be an age-threshold at which repeat element methylation levels decline in ageing animals. Furthermore, these results suggest that a low dose ionising radiation exposure does not elicit a long term effect on DNA methylation levels, nor is an adaptive response induced. This is the first study of the long term effect of a low dose ionising radiation exposure on DNA methylation levels.

Very little is known about the effect of radiation exposure on repeat element DNA methylation at the doses used in this thesis. This is the first *in vivo* methylation study to use low doses of radiation that are in the adaptive response range. The results obtained using the L1-HRM assay exemplify the dynamic nature of DNA methylation over time, both in ageing animals and in response to ionising radiation exposure, highlighting the importance of timing of analysis, tissue type and age of an animal when interpreting DNA methylation responses to exogenous agents.

DECLARATION

I certify that this thesis does not incorporate without acknowledgment any material previously submitted for a degree or diploma in any university; and that to the best of my knowledge and belief it does not contain any material previously published or written by another person except where due reference is made in the text.

Michelle Renee Newman

ACKNOWLEDGEMENTS

First and foremost I would like to thank Professor Pam Sykes for giving me the opportunity to undertake a PhD in her laboratory. It is always a gamble to take on a new student, more so when that student was a research assistant for a number of years and has many habits to break! I would also like to thank Pam for providing me with the opportunities that I have had during my PhD to advance my scientific career and help me grow as a scientist. Furthermore, I would not have been able to undertake my PhD if it were not for the scholarship provided by the Flinders Medical Centre Foundation and BHP Billiton.

Special thanks to my co-supervisor Dr Rebecca Ormsby. Thank you for your support, both with useful discussions, suggestions, countless hours of proof-reading, and friendship throughout my time here.

Most of the work described in this thesis was performed using mice. These experiments involved numerous irradiation experiments for which I would like to thank Associate Professor Eva Bezak for donating her time to perform the irradiations, calculation of the dosimetry, as well as undertaking some proof-reading. I am extremely grateful to have had the opportunity to have her involved in my research.

For their help with the mice used during the course of this study I thank the Flinders University School of Medicine Animal Facility.

The work from this thesis could not have been performed if it were not for the hours of time donated by both past and present members of the Sykes' lab. A big thankyou in no particular order goes to Dr Rebecca Ormsby, Mark Lawrence, Dr Benjamin Blyth, Dr Alex Staudacher, Ami Cochrane, Anzhen Jian, Katrina Bexis, Katherine Tulloch and Cameron Dougherty. I would also like to thank Dr Tanya Day, whose archival tissue culture experiments were used in this thesis.

Thanks also, to Dr Damian Hussey and Dr George Mayne for their help in the initial optimisation of the HRM assay; Dr Daniel Jardine for performing the LC-MS, and Dr Peta Macardle for useful discussion regarding the immunohistochemistry.

I would also like to thank the Low Dose Radiation Research Program, Biological and Environmental Research, U.S. Department of Energy for funding; and to Flinders University, the Flinders Medical Centre Volunteers Service, the Australian Radiation Protection Society and the Australian Institute of Nuclear Science and Engineering for providing funding to attend national and international conferences.

Personally, I would like to thank Dr Tina Bianco-Miotto, who unintentionally became a mentor, and encouraged me to take the big step to undertake a PhD. Thanks also to Tania Pfeiffer, whose regular coffee visits, especially during writing-up, were a much needed and welcomed break! I would like to thank my family and friends for their support over the years. Many of you were probably questioning my sanity at

times. In particular I would like to thank my mum, Monique, Carly, Steph and Jane for their support. Also to Em, Jase and James for the much needed climbing time.

Finally, a big thank you, hugs and kisses to Layla, Drew, Curtis and Zoe. Without you, life would have been boring and far too serious. Your smiles and giggles made the hard times easy to bear. You are the best nieces' and nephew anyone could ask for and I love you all to bits.

ABBREVIATIONS AND UNITS OF MEASUREMENT

A	amp
APES	aminopropylethoxysilane
5-aza	5-aza-2'-deoxycytidine
bp	base pair
BSA	bovine serum albumin
cDNA	complementary DNA
DAPI	4, 6-diamidino-2-phenylindole
DNA	deoxyribonucleic acid
DSB	double strand breaks
dsDNA	double-stranded DNA
DMSO	dimethyl sulphoxide
DNMT	DNA methyltransferase
DTT	dithiothreitol
FITC	fluorescein isothiocyanate
<i>g</i>	relative centrifugal force
gDNA	genomic DNA
GI	genomic instability
HDR	high dose radiation
HPLC	high performance liquid-chromatography
HRM	high resolution melt
HVL	half value layer
IAP_LTR	intracisternal-A-particle long terminal repeat
kb	kilo base
LC-MS	liquid chromatography mass-spectrometry
LDR	low dose radiation
LET	linear energy transfer
LINE; L1	long interspersed nucleic elements

5mdC	5-methyl-deoxycytosine
MLT	mean length per telomere
NTS	net temperature shift
ORF	open reading frame
PB	peripheral blood
PBS	phosphate buffered saline
PVDF	polyvinylidene difluoride
ROS	reactive oxygen species
RNA	ribonucleic acid
qRT-PCR	quantitative real-time polymerase chain reaction
SINE	short interspersed nucleic elements
SSB	single strand breaks
ssDNA	single stranded DNA
T_m	melting temperature
V	volt
v/v	volume for volume
w/v	weight for volume

Standard international units of measure

°C	degree Celsius
g	gram
Gy	Gray
h	hour
d	day(s)
L	litre
M	Mole
min	minutes
s	seconds
Sv	Seivert

Indicators of magnitude

k	Kilo	(x 10 ³)
m	milli	(x 10 ⁻³)
μ	micro	(x 10 ⁻⁶)
n	nano	(x 10 ⁻⁹)

PUBLICATIONS AND PRESENTATIONS ARISING FROM THIS THESIS

Publications

Michelle R Newman, Benjamin J. Blyth, Damian J. Hussey, Daniel Jardine, Pamela J. Sykes and Rebecca J. Ormsby. (2012) Sensitive quantitative analysis of murine LINE1 DNA methylation using high resolution melt analysis. *Epigenetics*. 7(1): 92-101.

Presentations

M.R. Newman, B.J. Blyth, E. Bezak, P.J. Sykes and R.J. Ormsby. Analysis of LINE1 repeat element Methylation changes following high dose radiation exposure in C57Bl/6, BALB/c and CBA mice. 4th Australian Epigenetics Scientific Conference, 7-9th May, Adelaide, Australia 2012.

M.R. Newman, B.J. Blyth, E. Bezak, P.J. Sykes and R.J. Ormsby. Changes to global DNA methylation in three inbred mouse strains with differing radiation sensitivities. AINSE Radiation Conference, 15th – 17th February, Lucas Heights, 2012.

M.R. Newman, B.J. Blyth, E. Bezak, D. Hussey, P.J. Hussey, P.J. Sykes and R.J. Ormsby. The use of high resolution melt analysis to investigate radiation sensitivity and changes to global DNA methylation in various mouse strains. 6th Chromatin Structure and Function, 5th – 8th December, Aruba, 2011.

Sykes P.J., **Newman M.R.**, Ormsby R.J., Blyth B.J. and Bezak E. Global DNA Methylation Responses to Low Dose Radiation Exposure. 36th Annual Conference of the Australasian Radiation Protection Society, Melbourne, Australia. 16-19 October, 2011.

Sykes P.J., **Newman M.R.**, Blyth B.J. and Ormsby R.J. Global methylation responses to low dose exposure. 14th International Congress on Radiation Research, Warsaw, Poland, 28th August – 1st September, 2011.

Newman M.R., Ormsby R.J., Blyth B.J., Bezak E., and Sykes P.J. Global DNA methylation responses to low dose radiation exposure. The Engineering and Physical Sciences in Medicine and the Australian Biomedical Engineering Conference, Darwin, NT, 14th-18th August 2011.

Newman, M.R., Blyth, B.J., Bezak, E., Sykes, P.J., and Ormsby, R.J. Detecting changes in global DNA methylation levels *in vivo* following low dose ionizing radiation exposure. 56th Annual Radiation Research Society Meeting, Maui, Hawaii. 25th-29th September 2010.

Newman, M.R., Blyth, B.J., Bezak, E., Sykes, P.J., and Ormsby, R.J. Investigation of DNA methylation levels *in vivo* in response to low dose radiation exposure. ARPS SA student oral presentation competition, Adelaide, Australia. 22nd June 2010.

Newman, M.R., Blyth, B.J., Bezak, E., Sykes, P.J., and Ormsby, R.J. Investigating DNA methylation as a mechanism in the low dose radiation induced adaptive response. ASMR Scientific Meeting 2010, Adelaide, Australia. 9th June 2010.

Newman, M.R., Blyth, B.J., Sykes, P.J., and Ormsby, R.J. Quantitation of global DNA methylation levels in response to low dose radiation exposure using high resolution melt curve analysis. Epigenetics 2009 Australian Scientific Conference, Melbourne, Australia. 1st -3rd December 2009.

1 INTRODUCTION

Humans are continually exposed to natural background radiation. In Australia, the average total exposure to background radiation is 2 mSv per year and can include natural sources of radiation such as cosmic radiation, radioactive elements in the earth's crust producing radon gas, and naturally occurring radionuclides found in food and water. Exposure to radiation from medical procedures such as diagnostic X-rays, comprise approximately 35% of an average Australian citizen's total annual exposure (Figure 1-1).

The current model for radiation risk assessment, termed the linear no-threshold model (LNT), states that all doses of radiation including extremely low doses, are harmful. This model suggests a proportional relationship between dose and cancer risk (as reviewed by Tubiana et al., 2006; 2009). It is becoming increasingly apparent that the LNT model could lead to incorrect assumptions of safe radiation exposure. This model is based predominantly on epidemiological data obtained from Japanese atomic bomb survivors, and a linear extrapolation is used for doses below 100 mSv (Figure 1-2) and is extrapolated for doses below 100 mSv. Furthermore, the disparity between the biological effects of low and high dose radiation exposure indicate that little is still known regarding the mechanism(s) involved in the response(s) to radiation damage, and the doses that can potentially lead to radiation-induced cancer.

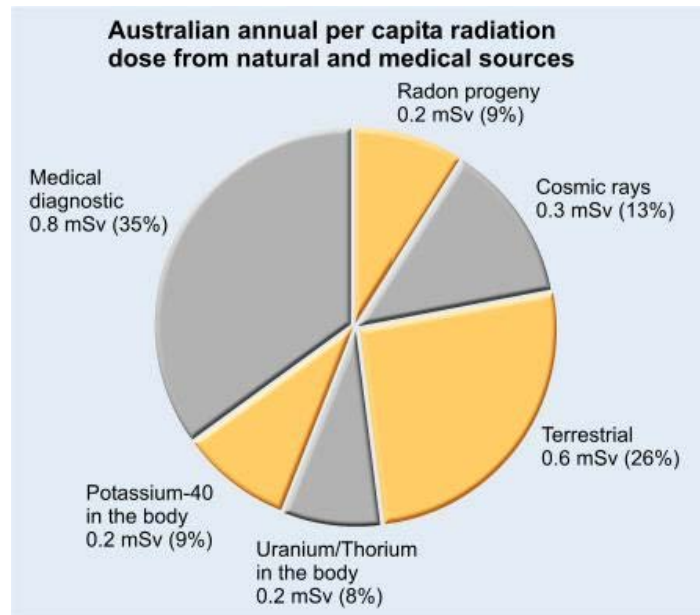


Figure 1-1: Sources of radiation exposure.

Natural and medical sources of radiation exposure (mSv) in Australia per capita.

Obtained from: <http://www.arpansa.gov.au/radiationprotection>. Accessed: 10th July, 2012.

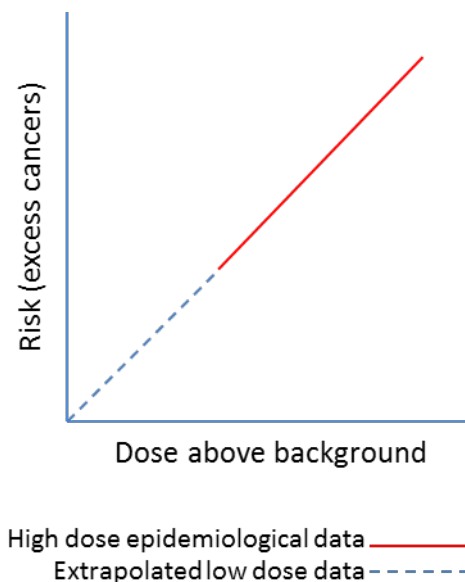


Figure 1-2: Linear no-threshold model.

The linear no threshold model is based on epidemiological data (solid red line), which is extrapolated for doses less than 100 mSv (broken blue line) and predicts that all doses of radiation above background exposure increase cancer risk proportionally.

1.1 Ionising Radiation

Radiation can be categorised as ionising or non-ionising. The classification of radiation type is based on the amount of energy available for transfer to biological material. Non-ionising radiation does not have enough energy to directly break chemical bonds. Examples of non-ionising radiation include microwaves and visible light. Ionising radiation can be categorised as radiation waves (X- and gamma (γ)-rays) or radiation particles such as α - and β -particles. X-rays are a man-made form of ionising radiation and are produced by energy transitions due to accelerating electrons. The α - and β -particles and γ -rays are naturally occurring forms of ionising radiation and are emitted from the decay of naturally occurring isotopes. Gamma-rays can also be produced from atmospheric interactions with cosmic rays. Ionising radiation is biologically hazardous due to its high energy which enables it to disrupt chemical bonds (as reviewed by the U.S. Environmental Protection Agency, 2007a; 2007b; Raabe, 2012). Radiation effects can be classified as “deterministic” or “stochastic”. The tissue effects of ionising radiation exposure are termed “deterministic effects”, that is, the direct effects of the ionising radiation exposure such as organ failure, which occurs when the number of cells undergoing apoptosis outweighs the ability of the cell to replace them (Edwards and Lloyd, 1998). “Stochastic effects” of ionising radiation exposure are defined as the damage that can occur at the DNA level resulting in genomic instability and cancer at a later time-point (sometimes years) following the irradiation (Edwards and Lloyd, 1998).

1.1.1 Quantifying ionising radiation

The different types of ionising radiation are classified based on their linear energy transfer (LET). X-rays are low LET, and can penetrate deep into tissues. However, they are sparsely ionising and deposit energy randomly. Alpha particles are considered to be high LET and have the ability to ionise atoms, and are therefore highly destructive to a cell. Radiation is measured based on activity and exposure. The activity is measured as a standard international unit (SI) called the Becquerel (Bq) which is a unit of radioactive decay equal to one disintegration per second. Exposure to ionising radiation is measured as absorbed dose, equivalent dose and effective dose (Figure 1-3).

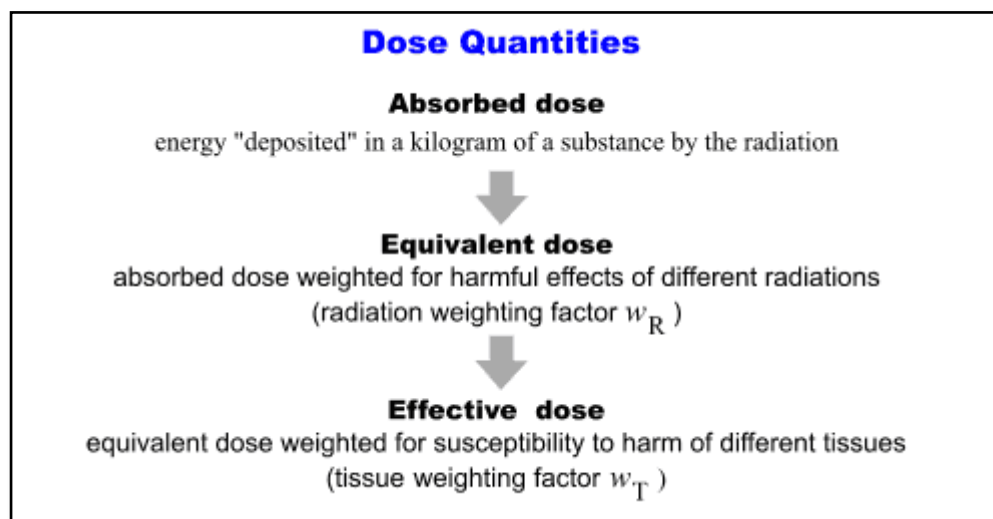


Figure 1-3: Measurement of radiation exposure.

Description of the measurement of radiation exposure of energy deposited in relation to the type of radiation i.e. α - particles or X-rays and the effect of the absorbed dose on tissues.

Adapted from: <http://www.arpansa.gov.au/radiationprotection/basics/units.cfm>. Accessed: 11th July, 2012.

Absorbed dose is measured in an SI unit of Gray (Gy). A Gray is the amount of absorbed energy deposited in one kilogram of mass. Not all types of radiation have the same biological effect for the same amount of absorbed dose, and therefore a measurement known as the equivalent dose, a Sievert (Sv) is used. The equivalent dose is determined by the absorbed dose multiplied by the weighting factor (W_R) of the radiation type. The weighting factor takes into account that some types of radiation produce more biological damage compared with others of the same absorbed dose. For example, X-rays have a W_R of 1, whilst α -particles have a W_R of 20; and hence 1 Gy X-rays equals 1 Sv, while 1 Gy α -particles equals 20 Sv. Finally, the effect on different tissues and organs that radiation will have is taken into account when quantifying radiation. This incorporates a tissue weighting factor (W_T ; Figure 1-4) to calculate the effective dose (E) to an organ (Sv), which is the equivalent dose of a radiation type multiplied by the tissue weighting factor. For example, tissue weighting factors will be used to determine the effective doses that different types of medical X-rays will have depending on the susceptibility to radiation-induced damage of the tissues and organs that are being imaged.

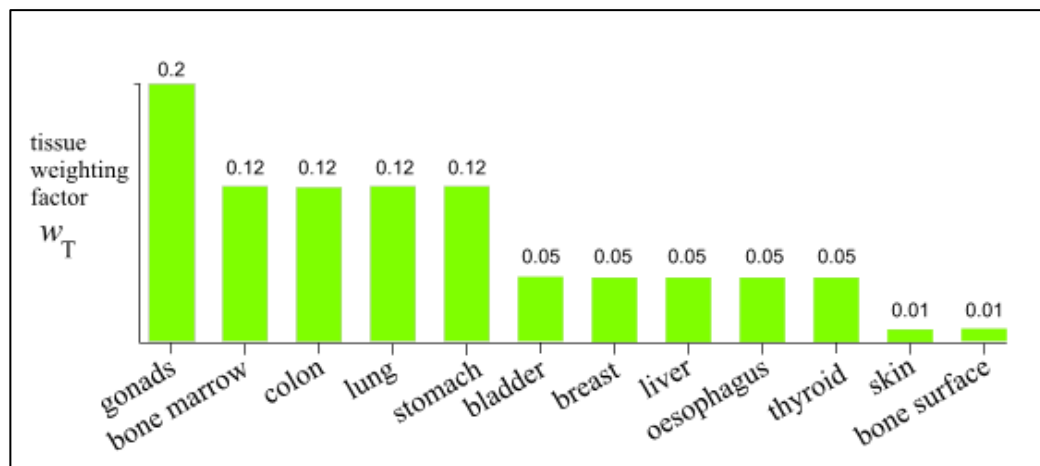


Figure 1-4: Tissue/organ radiation weighting factors.

The weighting factor for human tissues/organs for determining effective doses following radiation exposure.

Adapted from: <http://www.arpansa.gov.au/radiationprotection/basics/units.cfm>. Accessed: 12th July, 2012.

1.2 Biological Effects of Radiation

1.2.1 Mouse models in radiation research

The use of mice in research has become a powerful tool in the elucidation of the mechanisms that drive diseases such as cancer and diabetes, heart disease, as well as the effects of exogenous factors such as exposure to chemical carcinogens, diet and radiation. Mouse models provide insight into physiological and homeostatic responses that cannot be replicated *in vitro*. In radiation research, the mouse model is a particularly useful tool for understanding the effects of radiation on the whole organism, at the tissue, cellular and DNA level as well as specific systems such as the immune system. The most commonly used mouse strains in radiation research include the *scid* (severe compromised immunodeficiency), C57Bl/6, BALB/c and CBA

mouse strains. Grahn and Hamilton (1957), and Roderick (1963) investigated the effect of radiation exposure on inbred mouse strains, determining that some were more sensitive to radiation than others. Both studies demonstrated that the BALB/c followed by the CBA mouse strain were the most radiosensitive strains, while the C57Bl/6 strain exhibited less sensitivity to the radiation exposure. *Scid* mice are also extremely sensitive to radiation exposure due to a lack B and T-cells and deficiencies in DNA repair pathways. This strain is a good model organism for investigating the role of the immune system in response to ionising radiation (Fulop and Phillips, 1990; Biedermann *et al.*, 1991). BALB/c mice also exhibit deficiencies in DNA repair, and develop radiation-induced mammary cancers, leukaemia and other solid tumours (Storer *et al.*, 1988; Okayasu *et al.*, 2000). The CBA mouse strain is most commonly used in the study of leukaemogenesis, demonstrating low spontaneous leukemic frequency, but upon radiation exposure will develop acute myeloid leukaemia (AML) similar to human AML subsets (Rithidech *et al.*, 1999). While described as radiation resistant, C57Bl/6 mice can develop radiation-induced thymic lymphoma, which is most efficiently induced by repeated exposure to whole body irradiation with 1.8 Gy (Kaplan and Brown, 1952; Ina *et al.*, 2005), but on the whole can survive doses of radiation which would induce mortalities in the aforementioned strains (see Table 1 and Table 2). As a result, numerous studies have utilised these mice for the investigation of DNA repair pathways (Biedermann *et al.*, 1991; Okayasu *et al.*, 2000; Yu *et al.*, 2001), the induction of radiation-induced leukaemia (Plumb, 1998; Boulton, 2001; 2003; Giotopoulos *et al.*, 2006), haematopoietic recovery (Yugas and Storer, 1969; Hamasaki *et al.*, 2007) and differences in p53-mediated apoptosis in response to radiation exposure (Lindsay *et*

al., 2007). It should be noted that the three mouse strains discussed, C57Bl/6, BALB/c and CBA, all exhibit functional p53 responses, although the BALB/c strain has been reported to display reduced transcriptional activity in comparison to the C57Bl/6 mouse strain (Feng *et al.*, 2007; Lindsay *et al.*, 2007). Engineered mouse strains that contain mutations are also used, such as the Trp53 homozygous mice. These mice contain a mutated allele of the p53 gene and are used to understand the role that p53 plays in both radiation-induced carcinogenesis and the low-dose radioadaptive response (Mitchel *et al.*, 2003; 2004; 2008). Mouse studies are also a powerful tool for investigating the transgenerational effects of radiation exposure.

Table 1: LD_{50:30} of inbred mouse strains following single whole body X-irradiation.

Strain	Male		Female	
	LD _{50:30} ^a	SE	LD _{50:30} ^a	SE
BALB/cJ	<5.7		5.85	0.12
A/J	5.9	0.2	6.42	0.08
RF/J	6.28	0.2	7.13	0.15
SWR/J	6.29	0.1	6.14	0.06
C57BL/6J	6.5	0.15	6.7	0.06
CBA/J	6.56	0.09	6.89	0.08
C3HeB/J	6.76	0.11	6.89	0.07
SJL/J	7.13	0.11	7.74	0.13
C57BR/J	7.29	0.09	7.38	0.08
129/J	7.34	0.1	7.74	0.13

^adose of X-irradiation not specified

Adapted from the Biology of the Laboratory Mouse (Green, 1966)

Table 2: Days survival following daily whole-body X-irradiation with 10 Gy of the C57Bl/6, BALB/c and CBA mouse strains in a study of twenty-seven mouse strains.

Strain	<i>Male</i>		<i>Female</i>		Ranking in comparison to other strains ^b
	No. Days	SE	No. Days	SE	
C57Bl/6	24.58	1.18	23.03	0.42	14/27
BALB/c	17.00	0.45	16.76	0.48	26/27
CBA	16.44	0.56	16.55	0.55	27/27

^bAdapted from Roderick (1963)

1.2.2 High dose radiation exposure

1.2.2.1 Tissue effects from high dose radiation exposure

The effects of high dose radiation (HDR) exposure are most apparent in tissues such as bone marrow, thymus, spleen, gastrointestinal tract and lymphatic tissue – tissues that display high cellular turnover. HDR changes the tissue microenvironment, which can affect cell phenotype, tissue structure and signal transduction. This can result in persistent inflammation, which leads to greater cellular, and ultimately, tissue destruction (reviewed by Liu, 2010). High enough doses of radiation (>10 Sv) cause acute radiation sickness and symptoms such as gastrointestinal disorders can be evident within hours, while other symptoms can include bacterial infections, haemorrhaging, anaemia, loss of body fluids and electrolytes (as discussed by the U.S. Environmental Protection Agency, 2007b). Widespread cell death, or impaired activity within an organ or a tissue will result in the loss of organ function (as discussed by the Recommendations of the International Commission on Radiological Protection 2007).

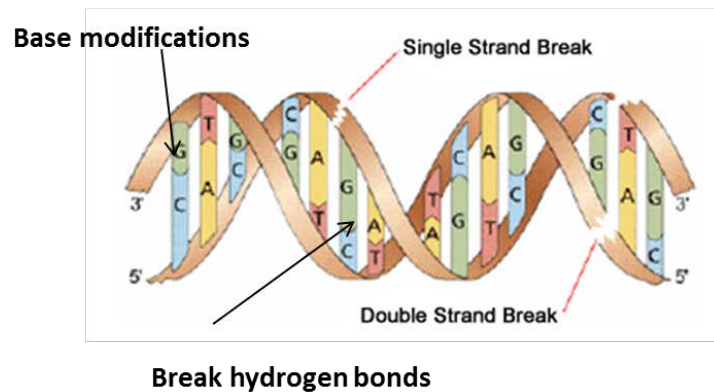
1.2.2.2 Sub-cellular effects from high dose radiation exposure

At the DNA level, there are three main outcomes of radiation exposure: 1) DNA lesions will result in the cell attempting to repair the damage induced. If the repair has been error free and the DNA is restored to its normal state, there will be no consequence to cell fate and therefore no risk of cancer; 2) the cell cannot repair the resulting DNA damage and programmed cell death (apoptosis) is induced. The damaged cell is removed and there is no risk of cancer. 3) The cell repairs the DNA damage, but with errors. The cell may detect the incorrectly repaired DNA and still activate apoptosis, or it may fail to detect the DNA damage thus allowing the cell to remain. DNA aberrations and mutations following the initial irradiation can lead to genomic instability, which is characterised by an increased rate of mutation. While mutations drive genetic diversity and therefore may not always result in a deleterious phenotype, genomic instability can lead to cancer.

Ionising radiation induced damage primarily affects DNA. This can be via direct or indirect ionisation of the DNA strands. Direct damage occurs from the electron track through the cell, causing proton loss of the sugar-phosphate backbone, resulting in single strand breaks (SSBs), and less frequently, double strand breaks (DSBs) of the DNA. Oxidation of the bases can lead to modified bases such as 8-hydroxyadenine and thymine dimers. Indirect damage to DNA following ionising radiation is the generation of reactive oxygen species (ROS) by the hydrolysis of water producing singlet oxygen atoms, hydroxyl radicals, superoxide radicals and hydrogen peroxide. The hydroxyl radicals (OH•) are considered to be the most damaging ROS, and can also be produced by the reduction of hydrogen peroxide. The hydroxyl radicals cause damage to the sugar-phosphate backbone, bases and results in SSB and DSBs

also (Figure 1-5). Most damage arising from ROS occurs from the indirect, hydroxyl radical damage (65% of the induced damage), compared to the damage induced by direct ionisation (35%) (Table 3)(Ward, 1988; Goodhead, 1989; Ward, 1990; Goodhead, 1994; Riley, 1994; Ward, 1995; Goodhead, 2009). Complex, clustered lesions in DNA (damages within one helical turn of each other) or DNA double strand breaks (DSB) are considered to be the most lethal type of DNA damage following ionising radiation exposure. Radiation-induced cell death can be due to errors in, or a lack of DNA repair at sites of damage. Persistent transgenerational changes to DNA can occur as a result of mutations arising from excessive damage or errors in repair (Charlton *et al.*, 1989; Goodhead, 1994; Barber *et al.*, 2002; 2006; Goodhead, 2009; Wright, 2010).

Direct damage



Break hydrogen bonds

Indirect damage

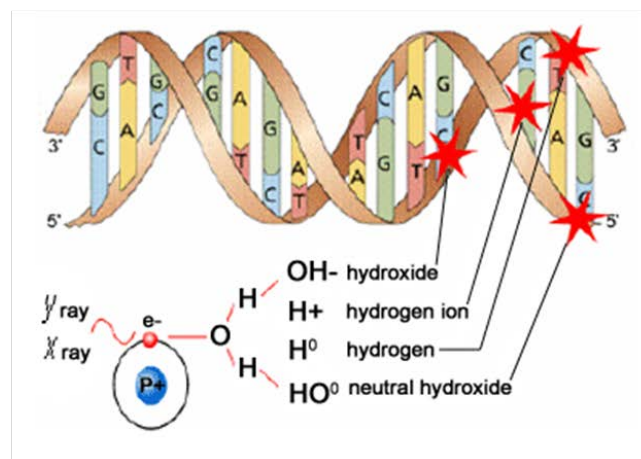


Figure 1-5: Damage to DNA following high dose radiation exposure.

DNA damage can occur following ionising radiation exposure either directly or indirectly. Direct damage occurs when the electron track occurs through the DNA causing proton loss to the sugar backbone, causing single strand and double strand breaks, inducing base damage or breaking the hydrogen bonds between bases. Indirect damage is the result of ionisation of water molecules, producing reactive oxygen species, of which the most damaging is the hydroxyl radical. These also cause damage to the sugar backbone, modify bases and break hydrogen bonds. Adapted from: <http://www.cna.ca/curriculum>. Accessed on the 19th September, 2012.

Table 3: Number of events of the different types of DNA damage that can occur in a cell following irradiation with 1 Gy X-rays.

	Damage	Number of events
Initial physical damage	ionisations in cell nucleus	100 000
	ionisation directly in DNA	2000
Biochemical damage	SSBs	1000
	8-hydroxyadenine	700
	thymine damage	250
	DSBs	40
	DNA-protein cross links	150

Adapted from Goodhead (1994)

1.2.2.3 Repair of DNA following high dose radiation exposure

DSBs damage both DNA strands and prevent the use of the complementary DNA strand as a template for repair, while for SSBs, the complementary strand can be used as a template for the new strand. Repair of DNA strand breaks is via base excision repair (BER), nucleotide excision repair (NER), mismatched repair (MMR), non-homologous end joining (NHEJ), or homologous recombination (HR). BER repairs non-helix distorting base modifications, abasic sites and SSB. It recognises and removes the inappropriate bases, while enzymes create an abasic site intermediate that is cleaved and the gap is filled in. NER can be involved in global repair or transcription-coupled repair, at places where RNA polymerase elongation has been blocked, removing thymidine dimers and bulky DNA adducts. MMR removes small mismatches, insertions and deletions that arise during replication or recombination. HR uses undamaged sister chromatid templates to repair DNA. DSBs caused by recombination are repaired by NHEJ machinery (reviewed by van Gent *et al.*, 2001; Kulkarni and Wilson, 2008). DSBs can also be caused by replication and

V(D)J gene recombination (the process by which immunoglobulin genes are rearranged to create immune diversity). Deficiencies in DNA repair mechanisms, such as in *scid* mice, have shown an inability to repair the damage induced by both V(D)J recombination and radiation (Biedermann *et al.*, 1991). Inefficient DNA repair as a result of ageing can result in the same accumulation of DSBs as induced by radiation exposure. Sedelnikova *et al* (2004) found that there was an accumulation of DSBs in ageing mice and also in cell cultures that had been allowed to reach senescence. The accumulation of DSBs in the cultured cells was equivalent to those induced in cells exposed to HDR. This indicates that regardless of the source of DNA damage, excessive damage still affects a cell's ability to repair the damage.

1.2.3 Low dose radiation exposure

According to the LNT model, all doses of radiation above background exposure no matter how small can increase cancer risk. However, there is increasing evidence indicating that low dose radiation (LDR) exposure does not elicit the same effect as high dose radiation exposure (HDR), and in some studies has been shown to be able to reduce the effect that HDR has on a cell/organism (as discussed by Dauer *et al.*, 2010). This has been termed the low dose radioadaptive response, and has been observed in a diverse range of organisms including bacteria, plants, yeast and animals (as discussed by Sakai *et al.*, 2006). A radioadaptive response is defined as "A post-irradiation cellular response which, typically, serves to increase the resistance of the cell to a subsequent radiation exposure" (Valentin, 2007).

The first radioadaptive response experiment reported showed that human lymphocytes cultured in ^3H thymidine had less chromosomal aberrations following exposure to X-radiation than cells exposed to the ^3H thymidine or X-rays alone (Olivieri *et al.*, 1984). Since then, many studies have demonstrated that a low dose of radiation can protect from the DNA damage induced by HDR exposure for a number of end-points including DNA DSB formation (Stoilov *et al.*, 2007) and micronuclei (Venkat *et al.*, 2001; Broome *et al.*, 2002; Mitchel, 2006). In animal studies, low doses have also been shown to reduce intra-chromosomal recombination in transgenic mice to below endogenous frequencies, as well as reduce the damage induced by a HDR exposure (Hooker *et al.*, 2004; Day *et al.*, 2006a; 2006b; Zeng *et al.*, 2006; Day *et al.*, 2007a), even if the high dose is delivered prior to the low dose (Day *et al.*, 2007b). In one study, it was demonstrated that the protection induced by the LDR still induced protection from a HDR exposure given 1 year after the LDR exposure, and was also able to reduce the accumulation of endogenous mutations over the life of an ageing animal (Zaichkina *et al.*, 2006). The radioadaptive response has also been demonstrated to be cross-adaptive, where one agent (such as LDR) can induce an adaptive response for a different agent. For example, conditioning doses of X-rays were demonstrated to be able to reduce mutations induced by treatment with an alkylating agent in mice (Yamauchi *et al.*, 2008).

While HDR exposure increases DNA damage and the frequency of mutations, which can ultimately lead to cancer, LDR has been reported to reduce cancer incidence. Single or multiple exposure to LDR (50 -100 mGy) has been demonstrated to reduce the incidence of thymic lymphoma, spontaneous and HDR-induced tumour

formation, as well as delay tumour formation in mice (Ishii *et al.*, 1996; Mitchel *et al.*, 2003; 2004; Ina *et al.*, 2005; 2007; 2008). LDR has also been shown to selectively inhibit damage to non-tumour cells when exposed to HDR in comparison to tumour cells (Jiang *et al.*, 2008); as well as induce the selective removal of pre-cancerous lesions (Portess *et al.*, 2007) and reduce neoplastic transformation frequency (Azzam *et al.*, 1994; 1996; Redpath *et al.*, 2001; Elmore *et al.*, 2008).

There is increasing evidence that the radioadaptive response may involve stimulation of the immune system, promoting increased efficiency to remove both damaged and cancerous cells. Exposure to LDR has been shown to increase the number of tumour tissue-infiltrating lymphocytes (Hashimoto *et al.*, 1999) and stimulate natural killer cell mediated cytotoxic activity (Cheda *et al.*, 2004). In addition to increased cytotoxic activity, there have also been reports of increased proliferation and repopulation of bone marrow/haematopoietic cells following LDR exposure (Matsubara *et al.*, 2000; Wang and Cai, 2000; Li *et al.*, 2004; Ina *et al.*, 2005).

1.2.4 Ageing and radiation exposure

Ageing is associated with an increased accumulation of DNA damage and an increased risk of cancer (as reviewed in Gorbunova *et al.*, 2007; Calvanese *et al.*, 2009). Age has been shown to influence radiation sensitivity (Lindop and Rotblat, 1962; Vesselinovitch *et al.*, 1971; Sasaki, 1991; Kato *et al.*, 2011), while reduced effectiveness of the adaptive response in *ex vivo* cells from elderly individuals has been observed (Gadhia, 1998). *In vitro* experiments in rodent cells have

demonstrated that glial cells from aged rats did not show an adaptive response compared with the cells from young rats (Miura *et al.*, 2002). In contrast, *in vivo* animal studies have shown that age at irradiation does not influence the radioadaptive response (Zaichkina *et al.*, 2006). The disparity between these experiments may be due to the endpoints analysed, tissues investigated, animal models used, dose and dose-rate, and highlights that further investigation on the relationship between the radioadaptive response and ageing is needed.

1.3 Maintenance of genomic stability

Both ageing and the effect of HDR exposure are characterised by reduced genomic stability. Genome stability (correct gene expression, protein functions and correct repair of DNA) is maintained by numerous mechanisms including histone modifications, telomere caps and DNA methylation. These modifications of DNA are stably inherited and work synergistically to influence the structure of chromatin, thereby controlling gene expression.

1.3.1 Chromatin structure

DNA methylation (discussed in Section 1.3.2) along with histone modification marks have been shown to be involved in the regulation of chromatin structure and promoter availability to transcriptional machinery, and ultimately gene expression.

Chromatin consists of DNA/protein structures called nucleosomes. The nucleosome consists of an octamer of four histones – H3, H4, H2A and H2B. Wrapped around

this octamer is ~147 bp of DNA. The histone proteins have N-terminal tails which can undergo post-translational modifications (marks) that include acetylation, methylation, phosphorylation, ubiquitination, sumoylation, ADP-ribosylation, deimination and proline isomerization. These histone marks influence the compaction and structure of the chromatin. For example, acetylation of histone H3 is associated with transcription and DNA repair, as it promotes an “open” chromatin structure, while lysine methylation is associated with repression of gene expression as it promotes a “closed” chromatin structure (Figure 1-6). CpG methylation also influences chromatin structure by inducing overwrapping of the DNA around the histone octamer (reviewed by Lee and Lee, 2011), and acting as a recruiting point for methyl binding proteins which form a platform. This platform recruits histone deacetylases (HDAC) that remove acetyl groups from the N-terminal tails, which in turn recruits histone lysine methyltransferases. It has been reported that these histone modifications then recruit proteins which bind the *de novo* DNA methyltransferases, which become anchored to the nucleosome, enhancing the repression (Sharma *et al.*, 2011). Therefore, heterochromatin regions are associated with reduced acetylation, increased histone H3 lysine 9 residue methylation and CpG methylation, while euchromatic regions are associated with increased acetylation, and reduced lysine and CpG methylation, and exhibit active transcription.

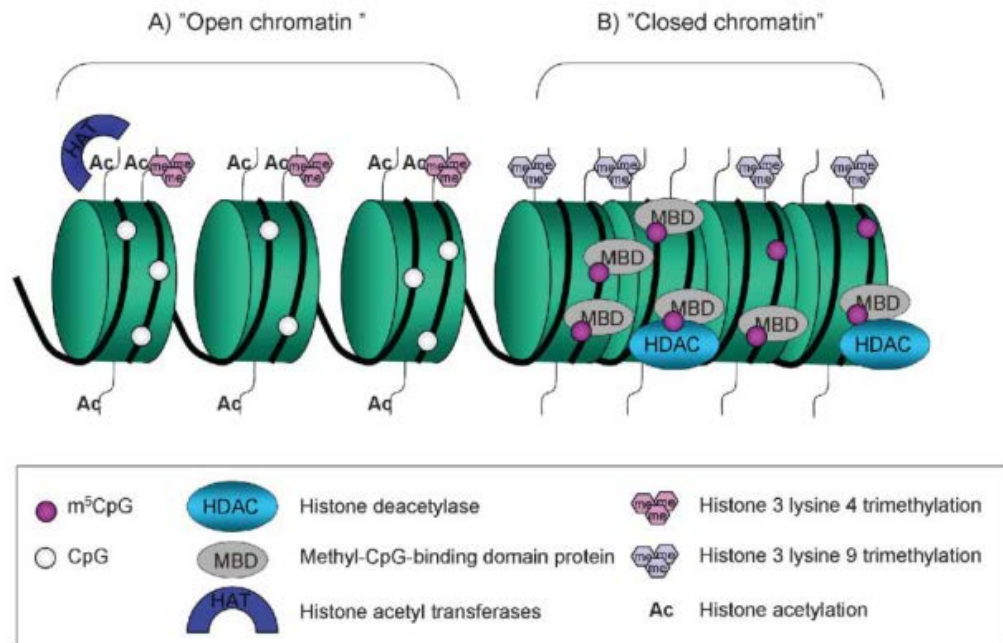


Figure 1-6: Control of chromatin structure by epigenetic modifications.

(A) Transcriptionally active chromatin is characterised by unmethylated cytosines (CpG) and acetylated histone tails. (B) Methylated cytosine residues (m⁵CpG) bind methyl binding domain proteins (MBD) that attract histone deacetylases (HDAC), which then remove acetyl (Ac) groups from the histone tails. The DNA becomes coiled into a "closed" chromatin structure carrying the silencing mark histone H3 lysine 9 tri-methylation. Adapted from Gronbaek et al (2007).

It has been shown that chromatin structure influences and is influenced by DNA repair mechanisms. It has been suggested that DNA damage in heterochromatin elicits faster repair responses compared to euchromatin due to the topology of the heterochromatin and the requirement to suppress any reactivation of transposable elements (Jakob *et al.*, 2011). However, other studies have shown that due to the tightly compacted nature of heterochromatin, it is repaired later than euchromatin (Cowell *et al.*, 2007; Goodarzi *et al.*, 2008; Chiolo *et al.*, 2011). Regardless, it is evident that following DSB formation, the DNA repair protein ATM phosphorylates the histone H2A variant, H2AX (termed γ H2AX). This then provides a docking

platform for other repair proteins, and also involves “eviction” of the nucleosome from the damaged DNA region, unwinding the DNA (Xu and Price, 2011). In order to unwind the DNA, CpG demethylation occurs. At the time γ H2AX is recruited to the site of the DSB, the DNA methyltransferase DNMT1 is also recruited, interacting with ATM (Mortusewicz *et al.*, 2005; Ha *et al.*, 2011), and other repair proteins such as GADD45 α (Barreto *et al.*, 2007; Lee *et al.*, 2011). The DNA methylating activity of DNMT1 is inhibited during this process, and leads to active demethylation of CpGs (Barreto *et al.*, 2007; Lee *et al.*, 2011). Thymine DNA glycosylase (TDG) is also implicated in DNA demethylation associated with base-excision repair, which results in destabilisation of the chromatin. The *de novo* methyltransferases are recruited during this process and are involved in the regulation of TDG and the subsequent re-methylation of the DNA (Li *et al.*, 2007). Following DNA repair, besides the restoration of CpG methylation, chromatin re-assembly and restoration of the nucleosome requires acetylation of histone H3 (Chen *et al.*, 2008).

Aberrant chromatin structure is associated with cancer, and is generally in the form of compacted chromatin, exhibiting increased lysine and CpG methylation and reduced acetylation (Nguyen *et al.*, 2002; Tryndyak *et al.*, 2006; Kondo *et al.*, 2007). These aberrations result in the incorrect gene expression patterns observed at proto-oncogenes and tumour suppressor genes. However, heterochromatic regions begin to exhibit properties of active euchromatin in the form of increased acetylation and reduced lysine and CpG methylation, which can result in transposition of repeat elements and microsatellite expansion (Fraga *et al.*, 2005; Howard *et al.*, 2007; Daskalos *et al.*, 2009; Estecio *et al.*, 2010; Muotri *et al.*, 2010; Ryu *et al.*, 2011).

1.3.2 DNA methylation

DNA methylation is a chemical modification to the fifth position of the cytosine pyrimidine ring. 5-methylcytosine (5mC) is generated when a methyl group from the universal methyl donor S-adenosylmethionine (SAM) is added via the DNA methyltransferase enzymes (DNMTs), which catalyse the transfer (Figure 1-7). A methylated cytosine in the context of DNA will be hitherto known as 5-methyldeoxycytidine (5mdC). Methylation of cytosine occurs during DNA replication, whereby the methylation pattern on the parental DNA strand is copied onto the newly synthesised strand by the maintenance methyltransferase DNMT1. *De novo* methylation, the process whereby a methyl group is added to a cytosine residue when there is no parental template, is performed by the methyltransferases DNMT3a and DNMT3b. These DNMTs play a large role in establishing methylation patterns during development (Costello and Plass, 2001; Curradi *et al.*, 2002; Liang *et al.*, 2002; Gronbaek *et al.*, 2007; DeAngelis *et al.*, 2008). In mammalian genomes, approximately 2-10% of cytosines are methylated. DNA methylation mainly occurs at a cytosine residue that is next to a guanine in sequence, separated by a phosphate that links the nucleotides. This is termed a CpG dinucleotide. Approximately 70-80% of the CpGs within the genome are methylated, however the majority of CpGs located within gene promoters are unmethylated. CpG-rich regions, known as CpG islands are most heavily methylated within heterochromatin, regions that contain repeated DNA elements. Heavy DNA methylation is also found to be involved in imprinting and X-inactivation, and patterns of methylation are tissue and development specific (Lorenz *et al.*, 1955; Puntschart and Vogt, 1998). During embryogenesis, the genome undergoes a wave of controlled demethylation,

following which *de novo* methylation occurs to establish methylation patterns that will be maintained.

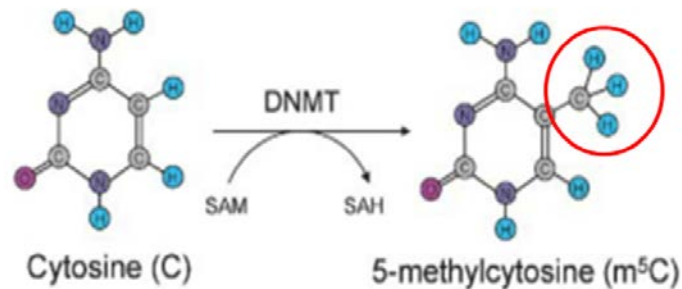


Figure 1-7: Methylation of cytosine.

Cytosine residues in DNA are converted to 5-methylcytosine by DNA methyltransferases (DNMTs). The universal methyl donor S-adenosylmethionine (SAM), which is converted to S-adenosylhomocysteine (SAH), donates the methyl group (ringed in red). Adapted from Gronbaek et al (2007).

DNA methylation levels can be altered by ageing (Wilson *et al.*, 1987; Christensen *et al.*, 2009) or exogenous factors such as diet (e.g. folate, which is a methyl donor), exposure to chemicals found in pollution (Yauk *et al.*, 2008), cigarette-smoke (Damiani *et al.*, 2008; Christensen *et al.*, 2009) and asbestos (Christensen *et al.*, 2009). In response to these modulators, a loss of DNA methylation is commonly observed and can result in increased mutation rates (Yauk *et al.*, 2008), increased frequency of cellular transformation and micronuclei formation (small nuclei formed as a result of damage to chromosomes) (Damiani *et al.*, 2008).

Research has demonstrated that there is a link between DNA damage and altered CpG methylation. Valinluck *et al* (2007) reported that inflammation-induced DNA-damaging products such as 5-chlorocytosine, mimic 5mdC and induce inappropriate

DNMT1 methylation within a CpG sequence. DNA methylation damage can also occur due to the conversion of 5mdC to thymine glycol by endogenous ROS, or an exogenous ROS-inducing agent such as ionising radiation. Oxidation of 5mdC can result in mismatches within the DNA sequence and can contribute to the increased number of transition mutations observed at methylated cytosine residues (Figure 1-8). Deamination of 5mdC can be followed by T:G base-excision repair by glycosylases, which can lead to an inherited loss of methylation at that CpG site (Slupphaug *et al.*, 2003; Popp *et al.*, 2010). An association between DNA DSBs and reduced or aberrant DNA methylation has been demonstrated, where a loss of methylation can result in excess DSB formation following exposure to DNA damaging agents (Beetstra *et al.*, 2005; Palii *et al.*, 2008). Furthermore, DNMT1 has been found to co-localise with γ -H2AX at sites of DSBs (Mortusewicz *et al.*, 2005; Palii *et al.*, 2008; Ha *et al.*, 2011), and aberrant DNMT1 protein levels have also been linked with aberrant *de novo* methylation of tumour suppressor genes, and reduced DNA repair (Trasler *et al.*, 2003; Ray *et al.*, 2006; Kondo *et al.*, 2007; Damiani *et al.*, 2008).

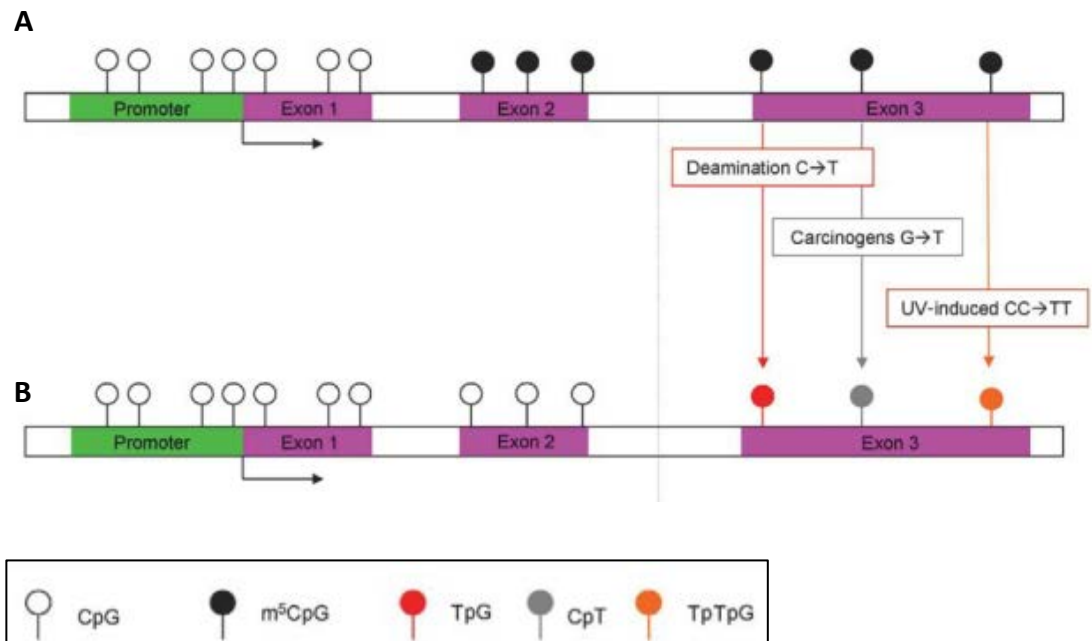


Figure 1-8: Facilitation of mutations via demethylation of cytosine.

(A) Methylated cytosine within the coding regions of genes may facilitate mutations by spontaneous hydrolytic deamination to thymine ($5mC \rightarrow T$), by exposure to carcinogens (resulting in $CpG \rightarrow CpT$ mutations), or UV-induced thymine adducts (resulting in $CCpG \rightarrow TTpG$). (B) Abberant methylation of promoters following repair. Adapted from Gronbaek et al (2007).

1.3.2.1 Methods for the detection of DNA methylation

There are a number of methods that are utilised to analyse CpG methylation. The choice of technique used is influenced by the experiment being performed, e.g. determination of the methylation levels at single gene loci vs. total genomic 5mdC.

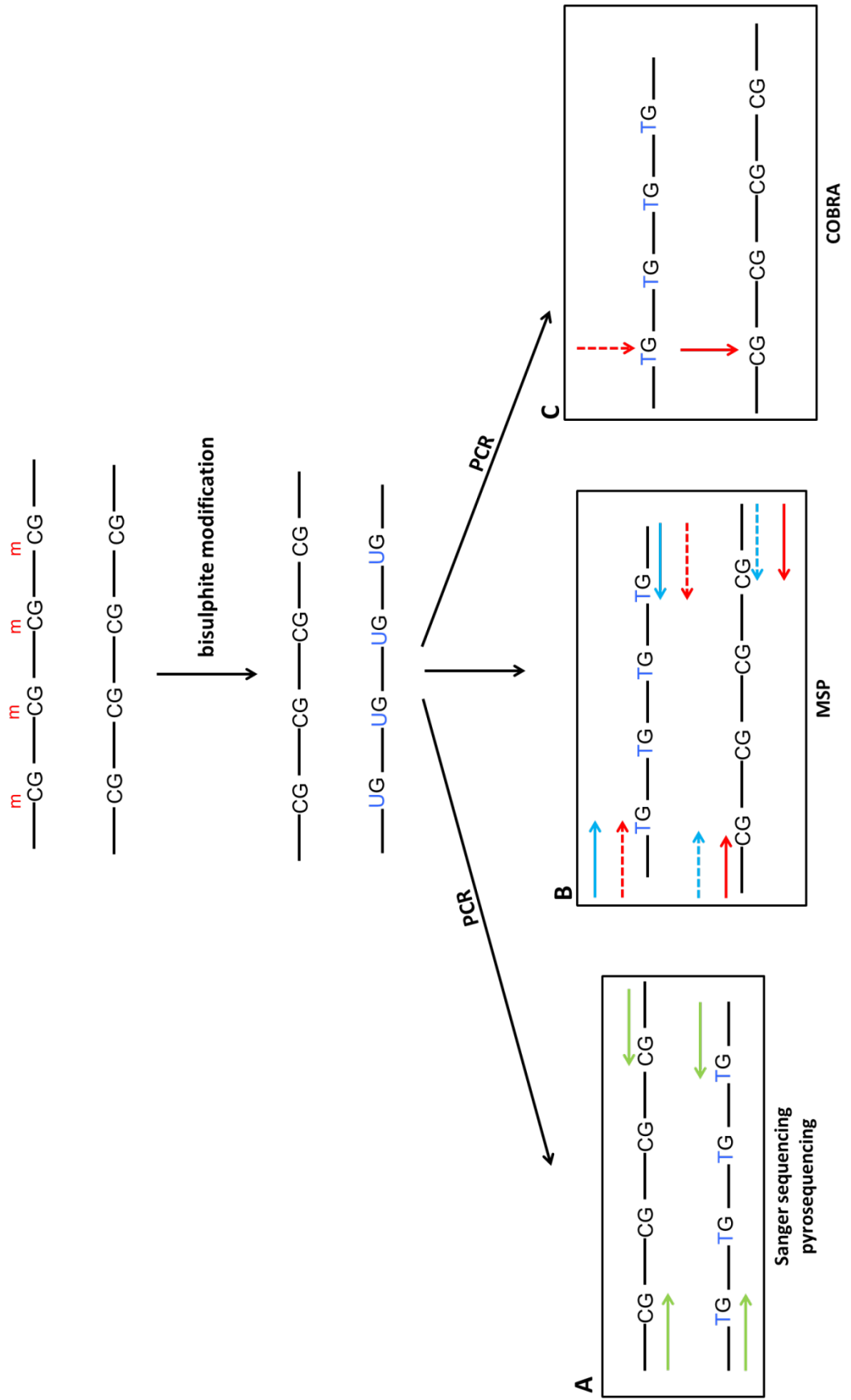
1.3.2.1.1 Single gene loci

Sodium bisulphite is most often used in the investigation of the methylation status of CpGs located within the promoters of gene loci. Sodium bisulphite treatment allows the distinction between cytosine residues that have a methyl group and

cytosine residues that are unmethylated. Following treatment of DNA with sodium bisulphite, unmethylated cytosines are converted to a uracil whereas a methyl group will protect the cytosine from conversion (Frommer *et al.*, 1992; Chen and Shaw, 1993). This process creates distinct sequences of DNA based on methylation status. PCR is then predominantly used to assess the methylation status of the target region (CpGs of interest) (Figure 1-9). The PCR products can be analysed using Sanger sequencing or pyrosequencing, methylation-specific PCR (MSP) or combined bisulphite restriction analysis (COBRA). Pyrosequencing detects pyrophosphate release upon nucleotide incorporation, allowing the level of fluorescence to be quantified at an individual CpG site. For MSP, separate primers specific for methylated versus unmethylated DNA are used. The methylation status of the CpG is then determined based on successful amplification with one of the primer sets. COBRA utilises methylation-sensitive restriction enzymes to determine methylation status. Restriction enzymes such as *HpaII* are chosen based on their sensitivity to methylated CpGs within the recognition sequence of the enzyme. An enzyme that would normally be unable to digest unmodified DNA due to the presence of a methyl group is able to cut DNA following bisulphite modification and PCR. DNA that was unmethylated prior to bisulphite modification will have a thymine in the recognition sequence following bisulphite modification and PCR, and will not be digested. Therefore, the methylation status of a CpG within the PCR product can be described as being methylated if the PCR product is digested, and unmethylated if undigested.

Figure 1-9: Techniques that utilise bisulphite modification to evaluate methylation levels.

When genomic DNA (gDNA) is treated with sodium bisulphite, cytosine residues that do not contain a methyl group will be converted to a uracil, while methylated cytosines will remain as a cytosine. The methylation status of a single gene locus can be determined following PCR (during which uracil residues are replaced by a thymine residue) by (A) Sanger sequencing or pyrosequencing of the PCR products (green arrows indicate sequencing primers); or (B) designing PCR primers that are specific for methylated CpGs (red arrow) or unmethylated CpGs (blue arrows). If the unmethylated-specific primers successfully amplify, the target region is unmethylated, and vice versa. This is known as Methylation-Specific PCR (MSP). (C) Following PCR, methylation sensitive enzymes can be used to digest the PCR products. Enzymes that would normally be unable to digest DNA if a methylated cytosine is within the recognition sequence will be able to digest DNA following bisulphite modification (red arrow), while unmethylated cytosine residues are converted to a uracil and the the enzyme no longer recognises the site (broken red arrow)(COBRA – combined bisulphite restriction analysis).



Although commonly used in methylation studies as these techniques are rapid and inexpensive, there are limitations. Pyrosequencing is limited to approximately 30 nucleotides, and is inhibited by the presence of non-CpG single nucleotide polymorphisms (SNPs). MSP is limited to only one CpG, while COBRA depends on efficient enzyme activity. Furthermore, in a target region that contains more than one CpG, heterogeneous methylation needs to be considered. Sanger sequencing can provide detailed information about the methylation status of individual CpGs when PCR products are cloned and single amplicons are sequenced, however this is laborious and low throughput. A post-PCR technique known as high resolution melt analysis (HRM) is also utilised to determine the methylation status of a target region that contains more than one CpG. Following quantitative real-time PCR, PCR products are subjected to increasing temperatures until the DNA strands become single stranded (ssDNA). Upon becoming single stranded, a fluorophore which was bound to the double stranded PCR products (dsDNA), is released. The temperature range at which fluorescence is detected is recorded. DNA that is GC rich requires greater temperature to break bonds and create ssDNA compared with DNA that is AT rich. Therefore, following bisulphite modification, DNA that is methylated will have a greater GC composition than unmethylated DNA, where all unmethylated cytosines were converted to a uracil. Thus, heterogeneously methylated DNA can be distinguished from fully methylated and unmethylated DNA, based on melting properties.

1.3.2.1.2 Genome-wide methylation

A reduction in total genomic 5mdC levels is a hallmark of cancer, along with the hypermethylation of certain loci. Hence, genome-wide methods for analysing DNA methylation are commonly performed in methylation studies. High purity liquid chromatography (HPLC) was first utilised to assess total genomic DNA methylation levels. Since then the more sensitive liquid chromatography-mass spectrometry (LC-MS) has been used. While highly sensitive, these techniques are not able to give the location of the CpGs that have been modulated, and are not ideal for analysing a large number of samples. This has led to next generation sequencing platforms being used to investigate genome-wide DNA methylation changes, to determine where these changes are occurring. While high-throughput, these platforms can be expensive and not available to all laboratories, and require complicated bioinformatics to process the data.

The methylation-sensitive enzyme *HpaII* and its isoschizomer *MspI* are also used in genome-wide methylation studies. The proportion of DNA that is digested by *HpaII* relative to *MspI* is used to determine the methylation levels of samples. An adaptation of this technique is the cytosine extension assay (Pogribny *et al.*, 1999). Following digestion of the DNA, radiolabelled cytosine is incorporated at the overhang created by the enzyme, which can then be quantified to determine the methylation level. This technique relies on efficient restriction digestion of the DNA, is low-throughput, and requires >1 µg of template DNA, which may not be available. Genome-wide changes to DNA methylation can also be investigated using the same techniques that are used for assessing single gene loci methylation. MSP, COBRA,

Sanger sequencing and pyrosequencing are used to determine the methylation status of repeat elements such as LINE1 (see Section 1.3.4), as a surrogate marker of changes to CpG methylation that are occurring across the genome, based on the fact that these elements are heavily methylated.

A recent report found that depending on the method used, different methylation data can be obtained for the same samples, particularly if the study is longitudinal and involves repeat sampling (Wu *et al.*, 2012). Therefore, careful consideration needs to be taken to determine the most appropriate method for determining methylation status, taking into account sample size, the amount of DNA available for analysis, as well as the expected changes in methylation i.e. complete demethylation/methylation vs. small changes at some CpGs; equipment and processing time.

1.3.3 Telomeres and genomic stability

The guanine-rich repeated sequences of DNA at the end of chromosomes are called telomeres, and consist of (TTAGGG) n repeated sequences. Telomeres serve to prevent degradation of the chromosome ends and to prevent fusion of chromosomes. The G-rich DNA strand (termed the G-strand) loops and is stabilised by telomere binding proteins TRF-1 and TRF-2 to form a physical structure at the end of the chromosome, called a “cap” (Figure 1-10). During replication, the enzyme telomerase replaces the telomere repeat sequence. Despite this dedicated enzyme, telomere lengths have been shown to become shorter with each round of cell division. Telomerase preferentially lengthens the shortest telomeres, leading to the

observation of varying telomere lengths within individuals and between individuals. In animal studies, telomere lengths have also been shown to vary depending on the age and sex of the animal and the tissue investigated (Cherif *et al.*, 2003). DNA methylation has also been linked with stable telomere length, where a loss of DNMT1 has been shown to reduce the methylation of the sequences immediately up-stream of the telomere hexamer repeat sequence (known as the sub-telomeric region), and results in shorter telomeres (Ng *et al.*, 2009). However, it has also been reported that a loss of DNMT1 can result in increased telomere length (Gonzalo *et al.*, 2006). Both these studies indicate that the altered DNA methylation of the sub-telomeric region results in altered maintenance of telomeres. Furthermore, it has been demonstrated that altered telomere length can result in increased radiation sensitivity (Goytisolo *et al.*, 2000; Wong *et al.*, 2000; Masutomi *et al.*, 2005). It has been hypothesised that the increased radiosensitivity that is observed in ageing animals may be partly due to reduced telomere length (Drissi *et al.*, 2011). Supporting the connection between altered telomere lengths and radiosensitivity is the observation that the radio-sensitive BALB/c mice have “uncapped” telomeres (Williams *et al.*, 2009).

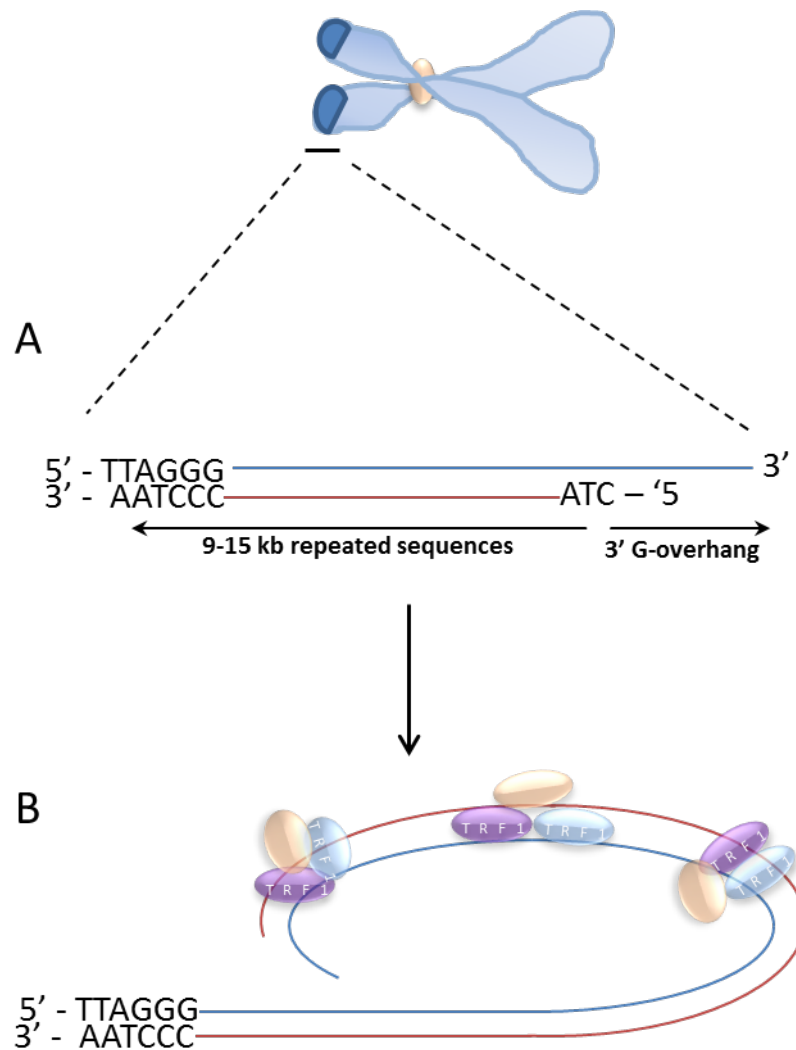


Figure 1-10: Structure of telomeres.

The repeated sequences of DNA at the end of chromosomes are known as telomeres. Telomeres consist of 9-15 kb TTAGGG repeats, with a G-rich leading strand (blue) and a C-rich lagging strand (red). (A) The G-strand (blue) extends in the 3' direction, forming the G-overhang. (B) The G-strand loops and binds to telomere binding proteins TRF-1 and TRF-2 which recruit other proteins to stabilise the telomere. Adapted from O'Sullivan and Karlseder (2010). Shown is the structure of a human telomere.

1.3.4 Retrotransposons and genomic stability

Retrotransposons are essentially parasitic sequences of DNA that through evolution have inserted into the eukaryotic genome. This evolutionary retrotransposition (the ability to change its position within the genome) has created sequence diversity through the creation of new mutations. Transposable elements include Long Interspersed Nucleotide Elements (LINE; L1), Short Interspersed Nucleotide Elements (SINE, Alu, B1) and Long Terminal Repeat elements (LTR) (such as the Intracisternal-A-Particle) (Figure 1-11) (Ostertag, 2001; McCarthy and McDonald, 2004; Farkash and Prak, 2006; Fedorov, 2009). Transposable elements can be described as autonomous or non-autonomous. Autonomous retrotransposons contain machinery necessary for mobility and are able to insert into other regions of the genome. Autonomous retrotransposons include LINE1 and LTR (IAP). Non-autonomous elements include SINE elements (Alu in humans, B1 in mice), and require LINE1 machinery to move across the genome.

The majority of the retrotransposons in the genome contain mutations and truncations that have rendered them incapable of transposition, however it has become evident that there are actively transposing elements within the human and murine genomes. Faulkner *et al* (2009) investigated L1 transcripts in the murine genome and found that 6-30% of mouse RNA transcripts initiate within repeat elements. Of the non-transposon transcripts from the murine genome, 18% had transcription start sites that occurred within repeat elements, and only ~5% of those transcription start sites were retrotransposons. Furthermore, it was evident that the transcription of the L1 elements varied between cell and tissue types, and

that the expression of different L1 families was also associated with cell and tissue type.

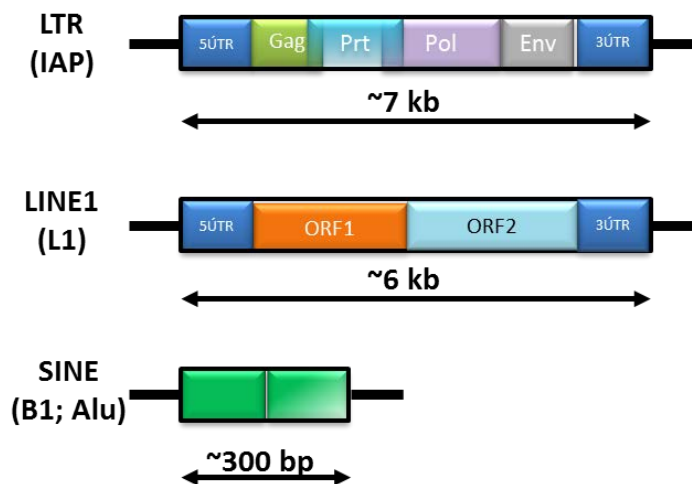


Figure 1-11: Types of retrotransposons.

The types of retrotransposons found in the genome: Long terminal repeat (LTR) elements such as the murine Intracisternal-A-Particle (IAP). These elements consist of long terminal repeat elements in the 5' and 3' UTR, and sequences encoding proteins involved in their autonomous transcription and retrotransposition. The autonomous Long Interspersed Nucleotide Elements (LINE1, L1) consist of a 5' and 3' UTR and open reading frames (ORF) encoding RNA binding proteins and an endonuclease. The non-autonomous Short Interspersed Nucleotide Elements (SINE1), B1 elements in the murine genome and Alu elements in the human genome, require the L1 proteins for transposition, and consist of two monomeric repeats. Adapted from Ostertag (2001).

L1 elements consist of a 5' and 3' UTR, two open reading frames, ORF1 and ORF2, and are ~6 kb in length. Transcripts of L1 elements have been found to consist of either ORF1 and 2 or just ORF2. A full-length L1 element is transcribed from its internal promoter to produce mRNA (Figure 1-12a). The RNA moves to the cytoplasm where ORF1 and ORF2 proteins (ORF1p and ORF2p) are translated. ORF1p is an RNA binding protein and is involved in the movement of the mRNA back into the nucleus, while ORF2p is an endonuclease. Following translation, a ribonucleoprotein complex forms between the RNA, an ORF2 and one or more

ORF1 proteins (Figure 1-12b). This complex is an intermediate to retrotransposition. The L1 ORF2p nicks DNA in a target site, creating a 3'OH (hydroxyl) overhang. The mRNA binds to the nicked DNA and reverse transcription takes place from the 3'OH overhang (Figure 1-12c-d). The newly synthesised cDNA is integrated into the DNA, following which the second strand is synthesised, creating a new L1 copy (Figure 1-12e-f). This process is known as target-primed reverse transcription and utilises the "host" cell's own transcriptional machinery. The SINE elements (human Alu and murine B1) are shorter repeat elements of approximately 300 bp. Despite being shorter than L1 elements, and lacking the proteins to actively transcribe and transpose, Alu/B1 elements are prevalent throughout the mammalian genome and show recent evolutionary insertions (reviewed in Batzer and Deininger, 2002; Akagi *et al.*, 2008). Alu/B1 element mobilisation appears to occur using the L1 ORF1 and 2 proteins for retrotransposition, as the sequence in the target site is flanked by target site sequence duplications that have close similarity to L1 target site duplications. Furthermore, the 5'UTR region of the Alu/B1 have been found to contain the ORF2p sequence motif (de Andrade *et al.*, 2011). The IAP Long Terminal Repeat element (IAP_LTR) is described as an endogenous retrovirus. It contains overlapping open-reading frames (ORFs) for a group-specific antigen (Gag), protease (Prt), polymerase (Pol), and terminal LTRs. The Pol genes encode a reverse transcriptase, ribonuclease H, and integrase to generate proviral complementary DNA (cDNA) from viral genomic RNA to insert into the target site. Following transcription, mRNA is moved to the cytoplasm where the particle proteins are translated (Figure 1-13a-b). Reverse transcription of the mRNA occurs in the cytoplasm following which the proviral cDNA is shuttled into the nucleus (Figure

1-13c). The IAP DNA is then incorporated into the target site via integrase, creating a new IAP copy (Figure 1-13d-e) (Mietz *et al.*, 1987; Kuff and Lueders, 1988; Gaubatz *et al.*, 1991; Dewannieux *et al.*, 2004).

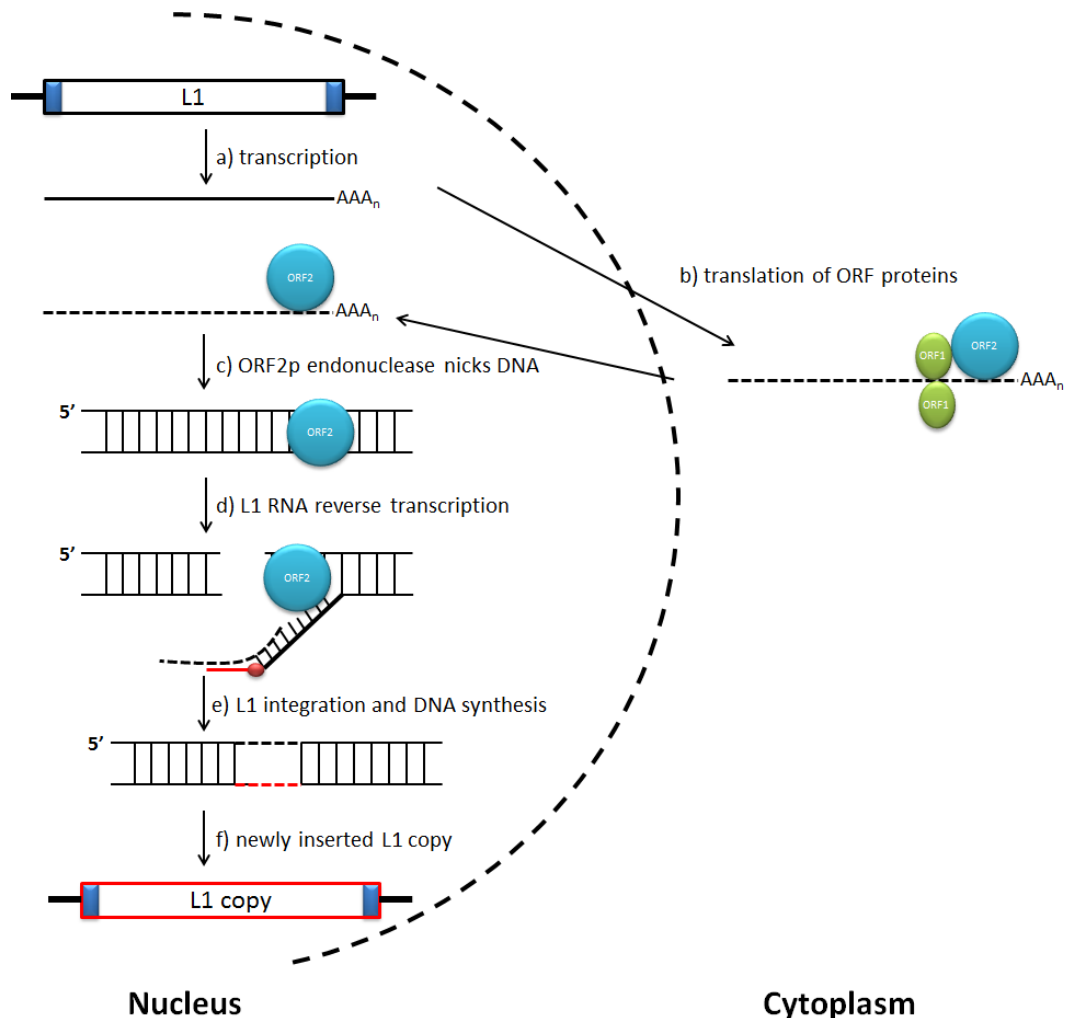


Figure 1-12: L1 transcription and retrotransposition.

(A) A full length L1 mRNA (solid line with poly-A tail) is transcribed from its promoter and moves to the cytoplasm. The L1 open reading frame (ORF) 1 and 2 proteins are translated (B), following which a ribonucleoprotein complex is formed between the mRNA (dotted line with poly-A tail), one ORF2p (blue circle) and one or more ORF1p (green circle). (C) The complex moves into the nucleus where the ORF2p, which is an endonuclease, nicks one DNA strand in a target site creating a 3'OH overhang (red circle). (D) The L1 mRNA binds to the nicked DNA strand following which reverse transcription takes place using the 3'OH as a priming site to produce L1 cDNA (solid red line). (E) The ORF2p endonuclease then nicks the other DNA strand and the L1 is integrated into the target site. (F) DNA synthesis occurs to produce a newly inserted L1 copy. Adapted from Ostertag (2001).

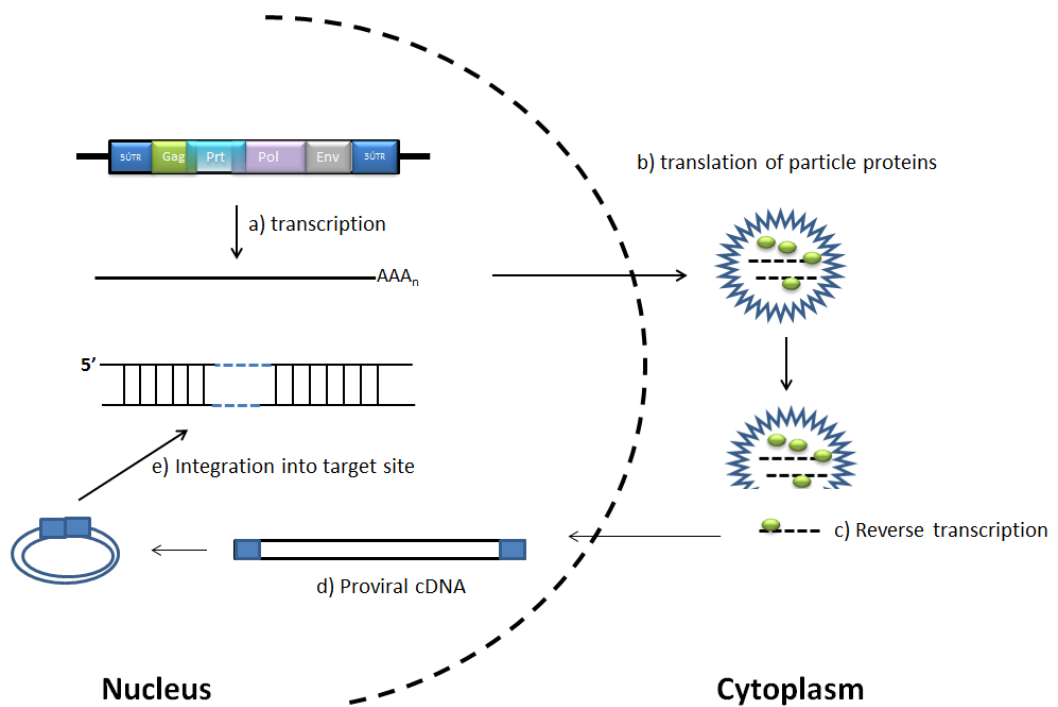


Figure 1-13: IAP transcription and retrotransposition.

(A) IAP mRNA (solid line with poly-A tail) is transcribed from its promoter and moves to the cytoplasm. (B) Translation of the particle proteins occurs, following which the IAP mRNA is reverse transcribed to proviral cDNA (dotted line) and (C) shuttled to the nucleus. (D) Proviral DNA is synthesised (box and circle) and (E) integrated into the target site via integrase (dotted blue line). Adapted from Koito and Iketa (2012).

Retrotransposons are located predominantly in heterochromatin and are associated with high CpG methylation and repressive histone marks, including histone H3 (lysine) K9, K27 and K20 tri-methylation (Martens *et al.*, 2005). However, recent studies have demonstrated that the repeat elements can be found upstream of coding genes and have been found to influence, and in some cases, control the expression of the genes. A well-known example is the A^{VY} allele. The *Agouti* gene encodes fur coat colour phenotype in mice. Normal *Agouti* expression results in a brown (pseudoagouti) phenotype. However, it has been found that there is an IAP element inserted upstream of the *Agouti* gene. Active transcription from the IAP 5'UTR promoter produces an alternate transcript which results in the A^{VY}

phenotype. Due to mosaic expression of A^{vy} , mice vary from agouti/yellow to pseudoagouti, but can also be mottled in appearance (Morgan *et al.*, 1999). Silencing of the IAP transcript upstream of *Agouti* has been demonstrated to be due to CpG methylation of the 5'UTR, and supplementation with a dietary methyl donor can produce offspring that shift from agouti to pseudoagouti compared with dams (Wolff *et al.*, 1998; Cooney *et al.*, 2002; Cropley *et al.*, 2010).

It is well documented that DNA damaging agents can induce a reduction in methylation of CpGs located within the promoters of the repeat elements and can result in increased transcript levels. Chemotherapeutic agents such as Etoposide, which induce double strand breaks and inhibit repair, and 5-aza-2'-deoxycytidine, an analogue of cytosine that cannot be methylated (Rudin and Thompson, 2001; Hagan *et al.*, 2003) both induce hypomethylation. Other examples of DNA damaging agents are chemicals used to manufacture plastics such as Bisphenol A (Dolinoy *et al.*, 2007), and particulate air pollution (Baccarelli *et al.*, 2009). Hypomethylation of the repeat element promoters has also been shown to occur following irradiation (Giotopoulos *et al.*, 2006; Filkowski *et al.*, 2010), and in some reports this has resulted in an increase in L1 and IAP transcripts (Faure *et al.*, 1997; Farkash *et al.*, 2006). However, in several reports, following irradiation, an increase in L1 methylation has also been observed (Kaup *et al.*, 2006; Kongruttanachok *et al.*, 2010; Aypar *et al.*, 2011; Goetz *et al.*, 2011). Hypomethylation of these elements also occurs with ageing (Barbot *et al.*, 2002; Bollati *et al.*, 2009; Jintaridith and

Mutirangura, 2010), cancer (Howard *et al.*, 2007; Ogino *et al.*, 2008a; 2008b; Irahara *et al.*, 2010), and in developmental defects (Wang *et al.*, 2010).

1.4 DNA methylation and radiation exposure

There is only one published report examining the effect of ionising radiation on promoter CpG methylation at individual loci, where investigators assessed the methylation levels of the tumour suppressor gene p16^{INKa} and the DNA repair gene O⁶-methylguanine-DNA methyltransferase (MGMT)(Kovalchuk *et al.*, 2004a). Nearly all studies investigating the effect of ionising radiation on DNA methylation levels have focussed on global DNA methylation levels. Kalinich *et al* (1989) were the first to demonstrate a dose dependent decrease in total (global) 5mdC content in cell lines following irradiation with 0.5 - 10 Gy. Subsequent *in vitro* studies have demonstrated variable methylation responses following HDR exposure including hyper- and hypomethylation, as well as no alteration in methylation levels (Kaup *et al.*, 2006; Kongruttanachok *et al.*, 2010; Aypar *et al.*, 2011; Goetz *et al.*, 2011; Armstrong *et al.*, 2012). *In vivo* studies have also shown variable responses of murine 5mdC levels following irradiation. Tawa *et al* (1998) demonstrated that radiation doses ranging from 4-10 Gy induced a loss of methylation in murine liver. Other mouse studies have demonstrated that there are tissue and sex differences in genomic DNA methylation levels following irradiation, as well as the timing of analysis. A summary of the published *in vivo* DNA methylation studies using ionising radiation is presented in Table 4. Of particular note are the differences in radiation dose, dose-rate, timing post-irradiation and the tissues investigated between the

studies. For example, a study conducted by Kovalchuk *et al* (2004a) demonstrated the importance of timing when 2 h following irradiation with 0.5 Gy at a low dose-rate (2 mGy/s) did not induce any changes in the liver or muscle tissues of irradiated mice, however a chronic irradiation at the same dose-rate resulting in an accumulated exposure of 0.5 Gy, induced a loss of methylation in muscle tissue.

The experiments presented in Table 4 have been performed in C57Bl/6 mice, which are considered to be radioresistant. One study has been conducted to determine if there is disparity in the modulation of DNA methylation between radioresistant (C57Bl/6) and radiosensitive (CBA) mice (Giotopoulos *et al.*, 2006). This study observed that at 4 days following irradiation with 3 Gy, there was a persistent loss of methylation in the bone marrow of the CBA mice, which was also observed in mice at 42 days post-irradiation. No effect was observed in the bone marrow of the C57Bl/6 mice, and spleen tissues from both strains did not demonstrate a loss of methylation at any time-point investigated. This evidence suggests that the mechanisms that contribute to the radiation-sensitivity of the CBA mice, as determined by time to lethality, tumour formation and overall genomic instability may involve the modulation of DNA methylation and are tissue-dependent.

Table 4: Summary of published *in vivo* murine DNA methylation and ionising radiation studies.

Mouse Strain	Sex	Dose	Dose Rate	Time Post-Irradiation	Tissue	Change to Methylation Levels	Author	
C57Bl/6	unknown	4, 7, 10 Gy	0.27 Gy/min	24, 48, 72 hours	spleen	n/c	Tawa <i>et al</i> , 1998	
					liver	↓		
					brain	n/c		
	male and female	acute 0.5 Gy	2 mGy/s	2 hours		liver	n/c	Kovalchuk <i>et al</i> , 2004
						muscle	n/c	
	chronic 0.5 Gy	50 mGy/day (2 mGy/s)	daily for 10 days; 2 hours following last irradiation		liver	n/c		
					muscle	↓ (males)		
	male and female	0.5, 1, 2.5, 5 Gy	5 Gy/min	6 hours	spleen	↓	Pogribny <i>et al</i> , 2004	
					liver	↓ (males)		
		4 weeks	spleen	n/c				
			liver	n/c				
		5 Gy	0.5 Gy/min	6 hours	spleen	↓		
					liver	↓ (females)		
	4 weeks	spleen	n/c					
		liver	n/c					
	male and female	acute 0.5 Gy	2 mGy/s	3 hours	liver	n/c	Raiche <i>et al</i> , 2004	
					spleen	↑ (males)		
		chronic 0.5 Gy	50 mGy/day (2 mGy/s)	daily for 10 days; 2 hours following last irradiation	liver	↓ (females)		
spleen					↓ (females) ↑ (males)			
male and female	5 Gy	5 Gy/min	6 hours	thymus	↓	Koturbash <i>et al</i> , 2005		
				muscle	↓			
	4 weeks	thymus	↓					
		muscle	n/c					
	5 Gy	0.5 Gy/min	6 hours	thymus	↓			
				muscle	n/c			
	4 weeks	thymus	↓ (males)					
		muscle	n/c					
male and female	acute 0.5 Gy	2 mGy/s	3 hours	thymus	↓	Pogribny <i>et al</i> , 2005		
	chronic 0.5 Gy	50 mGy/day (2 mGy/s)	daily for 10 days; 2 hours following last irradiation	thymus	↓			
CBA	unknown	3 Gy	0.5 Gy/min	4-42 days	BM	n/c	Giotopolous <i>et al</i> , 2006	
					spleen	n/c		
					BM	↓		
					spleen	n/c		
C57Bl/6	male	2.5 Gy	3 Gy/min	4 days	testes	↓	Fillowski <i>et al</i> , 2010	

n/c – no change

↑ - increase in methylation levels; ↓ - decrease in methylation levels

DNA methylation plays an important role in establishing gene expression patterns during development. Hence, the disruption of germline DNA methylation patterns may affect the genome stability of offspring. The effect of radiation on global DNA methylation levels in the germline has also been investigated (Table 5). Koturbash *et al* (2006) reported that offspring of C57Bl/6 mice irradiated with a whole body

dose of 2.5 Gy and mated one week following exposure, had reduced methylation levels in the thymus, but not in spleen or liver tissues. This has also been observed for the methylation of repetitive elements, where a decrease was detected in the thymus of offspring following paternal irradiation with 2.5 Gy (Filkowski *et al.*, 2010).

Table 5: Summary of published *in vivo* transgenerational murine DNA methylation and ionising radiation studies.

<i>Mouse Strain</i>	<i>Sex of irradiated parent</i>	<i>Dose</i>	<i>Dose-Rate</i>	<i>Age of progeny</i>	<i>Tissue</i>	<i>Change to Methylation Levels</i>	<i>Author</i>
C57Bl/6	male and female	2.5 Gy	unknown	15 days	spleen	n/c	Koturbash <i>et al.</i> , 2006
					liver	n/c	
					thymus	↓	
	male	2.5 Gy	3 Gy/min	6 months	thymus	↓	Filkowski <i>et al.</i> , 2010

↑ - increase in methylation levels; ↓ - decrease in methylation levels
n/c – no change

In some of the experiments found in Table 4, the loss of methylation can be attributed to a failure of maintenance methylation. Following chronic irradiation with 50 mGy/ day for ten days, it was shown that there were reduced levels of the maintenance methyltransferase, DNMT1. This loss of DNMT1 was also associated with an increase in the accumulation of γ -H2AX foci, indicating an association between a reduction in methylation and DNA DSBs (Pogribny *et al.*, 2005). Furthermore, there were reduced levels of the *de novo* methyltransferases DNMT3a/b, methyl-binding proteins implicated in chromatin compaction, as well as reduced tri-methylation of histone H4-Lys20. Tri-methylation of histone H4 is associated with transcriptionally active heterochromatic regions of DNA that are

generally CpG rich, heavily methylated and contain repetitive elements. Declining heterochromatin DNA methylation and histone H4-Lys20 methylation levels have been associated with both cancer and ageing (Fraga *et al.*, 2005).

Taken together, the few *in vivo* DNA methylation and radiation exposure studies that have been conducted indicate that very little is known about DNA methylation responses following irradiation, in particular the temporal and tissue-specific effects of the radiation-induced modulation and how this contributes to radiation-induced genomic instability and carcinogenesis.

1.5 Aims of this thesis

The modulation of DNA methylation, both genomic 5mC levels and repeat element methylation, has been shown to be affected by exogenous and endogenous factors which can result in increased genomic instability. The studies described in this thesis aimed to investigate repeat element methylation modulation *in vivo* following X-irradiation. The first aim of this thesis was to develop a sensitive, high throughput screening assay that was able to detect changes in methylation of L1 repeat elements. This assay was then used to investigate the temporal modulation of L1 repeat element DNA methylation in three strains of laboratory mice that differ in their radiosensitivity. It was hypothesised that the more radiosensitive mouse strains would elicit greater and more persistent modulation of repeat element DNA methylation. The assay was also used to monitor changes in peripheral blood L1 DNA methylation levels longitudinally in ageing mice that had been exposed to low dose X-radiation, with the hypothesis that the adaptive response would reduce, or prevent the decline in DNA methylation in ageing animals. Overall, the studies in this thesis sought to further understand the role that the modulation of DNA methylation plays in radiation-induced genomic instability by investigating the methylation levels of repeated sequences of DNA, whose demethylation has been implicated in increased genomic instability.

2 MATERIALS AND METHODS

2.1 Mouse strains

All experiments described in this thesis involving the use of animals were approved by the Flinders University Animal Welfare Committee and the South Australian Pathology/Child Health Network Animal Ethics Committee. The use and transport of transgenic animals was approved by the Office of the Gene Technology Regulator (OGTR) Australia and all animals were housed at the Flinders University School of Medicine Animal Facility and transported according to the OGTR transport guidelines. Animals were maintained in micro-isolators, on a 12 hour light/ dark cycle and were quality controlled for viruses, parasites and bacteria. Mice were fed on a joint stock ration (Gordons Speciality Stockfeeds and Ridley Agriproducts) and water provided *ad libitum*.

The C57Bl/6 mice used in this thesis are a transgenic mouse strain (pKZ1-C57Bl/6) containing an *E. coli* β -galactosidase-encoding *lacZ* gene in inverse orientation with respect to a chicken β -actin enhancer-promoter (EP) complex, and flanked by V κ 21c and J κ 5 mouse immunoglobulin recombination signal sequences (Matsuoka *et al.*, 1991). This strain is used in the laboratory for the study of chromosomal inversions and is, for all intents and purposes, C57Bl/6. The transgenic status of these animals did not influence the results obtained in this thesis (Table 21, Appendix A). Any references to C57Bl/6 mice used in this study refer to pKZ1-C57Bl/6 mice.

Three month old male and female BALB/c and CBA mice were obtained from the Australian Resource Centre (Perth, Australia) and the University of Adelaide (Adelaide, Australia).

2.2 A11 cell line

Archival frozen cell pellets of 5-aza-2'-deoxycytidine (5-aza) treated A11 cells were used in this thesis. A11 cells are a murine hybridoma cell line that was originally derived by fusion of pKZ1-C57Bl/6 transgenic spleen cells with P3653 murine myeloma cells (Hooker *et al.*, 2002). Cell culture and 5-aza treatments of the A11 cells was performed by Tanya Day (Tanya Day, 2006, PhD Thesis).

2.3 Radiation dosimetry and X-irradiation of mice

Radiation dosimetry and irradiations were performed by Chief Physicist A/Prof E. Bezak (Department of Medical Physics, Royal Adelaide Hospital, Adelaide, South Australia).

Different radiation doses were delivered by varying source-to-surface distance, lead or copper attenuators, and irradiation times (Table 6). Dose output calibration of ionising radiation appliances (Superficial X-ray unit) was performed according to the Institute of Physics and Engineering in Medicine and Biology (IPEMB) protocol (Aukett *et al.*, 1996; Aukett *et al.*, 2005). Calibration of the Varian 600 CD Accelerator was performed according to the International Multinational Atomic Energy Agency Technical Report Series 398 protocol on standards calibrated in water (International Atomic Energy Agency, 2000). The actual dose-rate after

applying distance and filter modifications was verified with a calibrated survey meter (Victoreen).

Mice were transported to the Royal Adelaide Hospital Radiotherapy Facility (Adelaide, South Australia) and restrained in a Perspex box (0.5 cm thick Perspex) with multiple ventilation holes. The mice in the Perspex box were placed upright against a block of solid water 8 cm thick to provide full backscatter and were irradiated with whole-body X-beam. C57Bl/6 mice that were irradiated and analysed 7 hours, 1 day or 7 days later were irradiated with a 100 kVp (8 mm Al half value layer (HVL)) Philips RT100 SXR superficial X-ray unit. The RT100 SXR X-ray unit was subsequently decommissioned. BALB/c and CBA mice were irradiated using a 6 MeV X-ray beam from a Varian 600 CD Linear Accelerator. A solid water build-up layer of 1 cm thickness was positioned on the top of the holder in order to achieve depth of electronic equilibrium at the mouse surface. Two parallel opposed beams with gantry rotated at 0° and 180°, radiation field size covering the whole Perspex holder and a 100 cm source-to-surface distance were used for irradiation. C57Bl/6 mice that were irradiated and euthanised 14 days later were irradiated with a 140 kVp (8mm Al HVL) Gulmay D3150 superficial X-ray unit. Mice used for the low-dose longitudinal study were irradiated with 10 mGy using the Gulmay D3150 superficial X-ray unit.

The Perspex box containing the mice was turned over after half the radiation dose had been delivered and the remaining half of the radiation dose was then delivered to ensure uniformity of the dose. Mice were returned to the Flinders University Animal Facility after irradiation and placed in quarantine prior to analysis.

Table 6: Dosimetry parameters for irradiation experiments.

X-ray Machine	Philips RT100 SXR and Gulmay D3150		Varian 600 CD Linear Accelerator
Dose (mGy)	10	1000	1000
Half Value Layer	8 mm Al [#]	8 mm Al [#]	1 cm water
Attenuator	2 mm Cu*	n/a	n/a
Distance (cm)	172	93.3	100
Dose Rate (mGy/ min)	13.9	179	1000
Irradiation Time (min/ side)	0.36	2.79	0.5
Total Irradiation Time (min)	0.72	5.58	1

[#]Aluminium

*Copper

n/a – not applicable

2.4 Mouse tissues

2.4.1 Mouse tissue isolation

Mouse tissues (kidney, liver, prostate and spleen) were surgically dissected following CO₂ asphyxiation and embedded in cryoprotectant (OCT compound, Tissue-Tek), frozen on dry ice and stored at -80°C until subsequent DNA extraction or tissue sectioning.

2.4.2 Isolation of peripheral blood

Peripheral blood (PB) sampling was performed via tail vein puncture. Prior to sampling, cages were placed in front of a heat lamp for several minutes. Mice were

then placed in a holding restraint. The tails were swabbed with ethanol and a small incision was made to the lateral tail vein using a GoldenRod lancet (MEDpoint Inc). No more than 100 μL of PB was collected in EDTA-collection tubes (Becton-Dickinson). Pressure was applied to the wound until bleeding ceased prior to returning animals to their cages. In some experiments, mice were euthanised immediately after CO_2 asphyxiation and tissues were collected as described in 2.4.1.

2.5 Analysis of DNA methylation

2.5.1 Extraction of genomic DNA

Genomic DNA (gDNA) was extracted from animal tissues or cultured cells using the DNeasy or QIAmp mini kits (Qiagen) following the manufacturer's instructions (both kits contain the same reagents). Briefly, 3 x 25 μm frozen tissue sections were cut using a cryostat (Reichert-Jung Cryocut 1800) and placed in a microcentrifuge tube containing 20 μL of proteinase K and 200 μL of Buffer ATL. Samples were placed at 56°C for 2.5 - 3 h. Tissues were homogenised by vortexing and passed through a 21 gauge needle. Two hundred microlitres of Buffer AL was added to each sample and vortexed prior to incubation at 70 °C for 10 min. One hundred microlitres of ethanol was added to each sample, vortexed and applied to the DNeasy mini spin columns. Supernatant was passed through the columns by centrifugation at 6000 x *g* for 1 min. Columns were placed into new collection tubes and samples underwent a series of washes with Buffers AW1 and AW2. DNA was eluted into microcentrifuge tubes with 100 μL of Buffer EB by centrifugation at 6000 x *g* for 1 min. Another 100 μL of Buffer EB was added to the columns and incubated at room temperature for 5

min. Samples were then centrifuged at 6000 x *g* for 1 min following which the entire eluate was re-applied to the columns, and incubated at room temperature for 5 minutes before a final centrifugation.

For pelleted cells and frozen blood samples, 200 μL of Buffer AL and 20 μL of proteinase K was applied to the samples, vortexed and placed at 56°C for 10 min. The samples were then extracted as for the frozen tissues. For PB samples, DNA was eluted with a single 100 μL volume.

A Nanodrop 8000 spectrophotometer (Thermo Scientific) was used to determine concentration and purity of gDNA samples. DNA concentration was calculated using the equation: concentration ($\mu\text{g}/\mu\text{L}$) = Absorbance at 260nm (A_{260}) \times dilution factor \times 50. A 50 μL aliquot of gDNA (20 μL for PB gDNA) was diluted to a working stock of 10 ng/ μL (5 ng/ μL for PB gDNA) that was stored at 4°C. The remaining DNA sample was stored at -20°C.

2.5.2 Bisulphite modification of genomic DNA

Genomic DNA was bisulphite modified using the Zymo EZ DNA Meth-Gold bisulphite modification kit (Zymo). Briefly, 130 μL of conversion reagent was added to 200 ng of gDNA or 40 ng of PB gDNA. Samples were denatured at 98°C for 10 min and underwent conversion at 64 °C for 2.5 h. Bisulphite converted DNA was chilled at 4°C for 30 min. The converted DNA was bound to a spin column and underwent wash and desulphonation steps prior to elution. DNA was eluted by centrifugation at 12 000 x *g* with 20 μL of Elution Buffer. Modified DNA was stored at -20°C.

2.5.3 Primer design

Primers (Geneworks) for *LINE1* (Long Interspersed Nucleic Elements – 1), *B1_Mm* (Mm family of SINE, Short Interspersed Nucleic Elements) and *IAP_LTR* (Intracisternal-A-Particle Long Terminal Repeat element) specific for bisulphite modified DNA were designed using MethPrimer (Li and Dahiya, 2002) (see Chapter 3 and Appendix B). Pyrosequencing primers and assays were designed using the PSQ Assay Design program (Qiagen). Each primer that was designed specifically for bisulphite modified DNA failed to amplify unmodified genomic DNA template.

2.5.4 PCR and high resolution melt analysis (HRM)

PCR cycling and HRM were performed on a Rotor-Gene Q (Qiagen). A 20 μ L reaction mix consisted of 20 ng equivalent of bisulphite modified gDNA (10 ng for PB gDNA); and a final concentration of: 1 x EpiTect HRM PCR Master Mix (Qiagen), 0.75 μ M forward primer and 0.75 μ M reverse primer (Geneworks), and water (Qiagen). Cycling conditions for *LINE1* PCRs were as follows: 95°C for 5 min followed by 35 cycles of 95°C for 20 s, 60°C for 30 s, and 72°C for 20 s. Melt curve analysis was from 73°C to 84°C rising by 0.1°C/2 s. Cycling conditions for *B1_Mm* and *IAP_LTR* PCRs were: 95°C for 5 min followed by 35 cycles of 95°C for 10 s, 52°C for 15 s, and 72°C for 10 s, for 35 cycles. Melt curve analysis was from 65°C - 80°C rising by 0.1°C/2 s. Unless stated, all samples underwent two separate PCRs in each experiment and these were averaged for analyses.

2.5.5 Calculation of the Net Temperature Shift

Differences in DNA methylation as detected by HRM were calculated using the average difference between the normalised melt curves of a test sample and the methylated control, termed the Net Temperature Shift (NTS). Calculation of the NTS is as follows: within the Rotor-Gene Q program, two normalisation regions (at temperatures before and after melt peak temperature) were nominated for HRM analysis. For LINE1, normalisation region 1 was between 74°C-75°C, whilst normalisation region 2 was between 82°C-84°C. For B1_Mm the regions were: 66°C-68°C and 79°C-80°C; for IAP_LTR: 70°C-72°C and 78°C-79°C. The subtraction of the methylated control normalised curve from each test normalised curve was performed automatically within the Rotor-Gene Q program and the summed difference of the fluorescence value at each temperature point within the entire melt range was divided by 100 to obtain the average distance between the curves, or the NTS (development and analysis of the NTS is discussed in Chapter 3).

2.5.6 Gel electrophoresis of PCR products

PCR products were analysed on a 2% (w/v) agarose gel in 0.5× TBE (Appendix C) containing 2 µg/µl ethidium bromide. Five µL of PCR product were mixed with 1 µL of Ficoll loading buffer (Appendix C) prior to electrophoresis. PCR product sizes were measured against a 100–700 bp ladder (Haematology and Genetic Pathology, Flinders University and Medical Centre). Gels were subject to electrophoresis in 0.5 × TBE running buffer at 120 V for 40 min. DNA bands were visualised under UV light

(250-360 nm) and imaged using the GeneGenius Gel Imaging system and Gene Snap Image Acquisition software (Syngene).

2.5.7 Sequence analysis of PCR products

2.5.7.1 Sanger sequencing

HRM PCR products were purified using the QIAquick PCR purification kit (Qiagen) and quantified on a Nanodrop 8000 (Thermo Scientific). Sequencing primers are outlined in Appendix B. Sequencing reactions were performed by the SouthPath and Flinders Sequencing Facility (Flinders University and Medical Centre, Adelaide, Australia).

2.5.7.2 Pyrosequencing

Pyrosequencing reactions were performed by EpigenDx (Massachusetts, USA) on a Qiagen-Pyrosequencing PSQ-MD. HRM-PCR replicates for each sample were combined and aliquoted into 96-well plates in duplicate (as pyrosequencing replicates) in a volume of 10 μ L. The target regions for analysis and pyrosequencing primers (see Appendix B) were determined using the PSQ Assay (Qiagen) (see section 3.1.3.1).

2.5.8 Liquid chromatography-Mass spectrometry (LC-MS)

2.5.8.1 DNA hydrolysis

Genomic DNA was hydrolysed as outlined in Song *et al* (2005). Briefly, 200 - 250 ng of DNA in a volume of 20 μ L was denatured at 100°C for 3 minutes and placed on ice. To the DNA, 2 μ L of 0.1 M ammonium acetate (Sigma), pH 5.3, containing 2 units of Nuclease P1 from *Penicillium citrinum* (Sigma) was added and samples were incubated at 45°C for 2 h. Following this, 2.2 μ L of 1 M ammonium bicarbonate (Sigma-Aldrich) containing 0.002 units of Phosphodiesterase I from *Crotalus adamanteus* venom (Sigma) was added and samples were incubated at 37°C for 2 h. Finally, 1 unit of calf intestinal phosphatase (Finnzymes) was added and the reaction was incubated at 37°C for 1 h. Hydrolysed samples were stored at -20°C. Each sample underwent two separate hydrolysis reactions and the average of the samples was used in analyses.

2.5.8.2 LC-MS Procedure

LC-MS was performed by Flinders Analytical (Flinders University, Adelaide, Australia). Briefly, liquid chromatography (LC) separation was performed on a Waters 2695 HPLC (Milford), at a flow rate of 0.25 mL/min with a column temperature of 22°C. The LC column was a Waters (Milford) Atlantis T3, 2.1 mm x 150 mm, 5 μ m particle. Two buffers were used: mobile phase A - 0.1% aqueous formic acid; and mobile phase B - 0.1% formic acid in acetonitrile. The LC program was 100% solvent A for 3 min, a linear gradient to 85% solvent A at 15 min, then back to 100% solvent A at 15.5 min where it was held for 6.5 min for re-

equilibration. A 20 μL volume of hydrolysed sample was diluted with 100 μL of type 1 water (Millipore Synergy System) and transferred to a 250 μL volume insert inside a 2 mL LC-MS vial and 10 μL of this solution was injected into the liquid chromatographer. Mass spectrometry was performed on a Waters Quattro micro, triple quadrupole mass spectrometer (Milford) fitted with an electrospray source. Positive ion electrospray and multiple reaction monitoring conditions were determined manually using ribo- and deoxy-ribonucleoside standards at a concentration of 10 $\mu\text{g}/\text{mL}$ in water (dC, 5mdC, C, U, 5mC, T, dA, A, dG and G; Sigma-Aldrich). Quantitation for 5mdC was monitored with a precursor ion of 242, fragment ion of 126 with a dwell time of 0.1 s. Cone voltage was 12 V and collision voltage was 8 V. For dG; the precursor ion was 267.8, the fragment ion was 152, dwell time was 0.1 s, cone voltage was 12 V and collision voltage was 12 V. Each sample was injected in duplicate. Percent methylation was calculated based on the ratio of 5mdC to dG [5mdC/dG].

2.6 Telomere length analysis

Telomere length was assessed using a qPCR method adapted from O'Callaghan and Fenech (2011). Twenty nanograms of genomic DNA was amplified in duplicate on either a Rotor-Gene Q (Qiagen) or ViiA™7 (Life Technologies) with murine telomere repeat sequence and 36B4 primers (for genome copy number determination) in a master mix containing final concentrations of: 1 x Platinum Taq PCR buffer (Invitrogen), 10 mM dNTPs (Fisher Biotech), 50 mM MgCl_2 (Invitrogen), 0.16 units x SybrGreen I (Life Technologies), 0.1 μM of forward and reverse primer (see

Appendix B) and 1 x Platinum *Taq* (Invitrogen) in a total reaction volume of 24 μ L. Cycling conditions were as follows: 94°C for 2 min followed by 35 cycles of 94°C for 15 s, 60°C for 30 s, 72°C for 15 s. Melt curve analysis was from 65°C to 95°C with 0.05°C/ s following 1 cycle at 95°C for 15 s. A standard curve of known telomere length and known *36B4* copy number/ diploid genome was included in each PCR (see Appendix E).

2.7 L1 transcript analysis

2.7.1 RNA extraction

RNA was extracted from animal tissues using the RNeasy mini kit (Qiagen) following the manufacturer's instructions. Briefly, 3 x 25 μ m frozen tissue sections were cut using a cryostat (Reichert-Jung Cryocut 1800) and placed in a chilled microcentrifuge tube. A11 cell pellets or tissue samples were homogenised with a 21 gauge needle in 350 μ L of Buffer RLT containing β -mercaptoethanol. Following the addition of 70% ethanol, samples were bound to a spin column and underwent a series of washes at 12,000 x *g* prior to an on-column DNaseI treatment (20 μ L of DNaseI and 140 μ L Buffer RDD; Qiagen). Bound RNA was washed with Buffers RW1 and RPE prior to elution with 40 μ L RNase-free water (Qiagen) after incubation at RT for 1 min. RNA was stored at -20°C. RNA purity and concentration was assessed using a Nanodrop 8000 spectrophotometer (Thermo Scientific). RNA concentration was calculated using the equation: concentration (μ g/ μ L) = Absorbance at 260nm (A_{260}) \times dilution factor \times 40.

2.7.1.1 RNA quality control

Residual gDNA in a RNA sample can give false positive results in quantitative real-time PCR (qPCR), therefore to assess whether there was any remaining gDNA in the RNA samples, an aliquot of RNA was used as a template for qPCR (see section 2.7.3 for qPCR protocol). The RNA samples were diluted to 10 ng/ μ L with water (Qiagen), and a volume of 2 μ L was used in the PCR.

2.7.1.2 DNaseI treatment

RNA samples that demonstrated amplification in a qPCR indicating the presence of residual gDNA underwent a second DNaseI treatment to remove gDNA. Following the addition of 60 μ L of water, 2.5 μ L of DNaseI and 10 μ L Buffer RDD (Qiagen) were added to the samples and incubated at RT for 10 min. To remove buffer and digested DNA, RNA was purified via isopropanol precipitation. Briefly, 1 μ L of 2 mg/mL glycogen (Sigma) was aliquoted to each sample following which 100 μ L of 75% isopropanol was added to the RNA. Samples were mixed by inversion and incubated at -20°C for 90 min. RNA was pelleted by centrifugation at 12,000 x *g* for 20 min at 4°C. Supernatant was removed and pellets were washed with 1 mL 75% ethanol by centrifugation at 12,000 x *g* for 20 min at 4°C. Ethanol was removed and pellets were air-dried briefly before the addition of 15 μ L of RNase-free water (Qiagen). RNA concentration and purity were assessed using a Nanodrop 8000.

2.7.2 Reverse transcription

RNA (200 – 300 ng) was reverse transcribed using the iScript cDNA synthesis kit (Bio-Rad), with the addition of 4 μL of 5x iScript reaction mix, 1 μL iScript reverse transcriptase and water made up to 20 μL . The reaction was incubated at RT for 5 min, 42°C for 30 min and finally, 85°C for 5 min. The cDNA samples were diluted 1/5 with water (Qiagen) and stored at 4°C.

2.7.3 Quantitative real-time PCR

Quantitative real-time PCR (qPCR) was performed in duplicate using a master mix containing final concentrations of: 1 x Platinum Taq PCR buffer (Invitrogen), 10 mM dNTPs (Fisher Biotech), 50 mM MgCl_2 (Invitrogen), 0.16 units SybrGreen I nuclei acid stain (Life Technologies), 0.1 μM of forward and reverse primer (see Appendix B) and 1 x Platinum Taq (Invitrogen). Target cDNA (2 μL) was amplified in a reaction volume of 22 μL on an Applied Biosystems ViiA™7 (Life Technologies) using the following cycling conditions: one cycle at 94°C for 2 min, 35 cycles at 94°C for 15 s, 58°C for 15 s, 72°C for 19 seconds. Melt curve analysis was from 60°C to 95°C with 0.05°C/ s following 1 cycle at 95°C for 15 s. A spleen gDNA sample was screened in three separate qPCRs to determine the average quantitative threshold cycle (Cq) value for inclusion in each PCR as a control for reaction efficiency.

2.7.3.1 Primer design

L1-ORF1 and L1-ORF2 primer sequences were obtained from Muotri *et al* (2010). Candidate reference genes were determined using Genevestigator® (Hruz *et al.*, 2008). Primer sequences were obtained from either PrimerBank (<http://pga.mgh.harvard.edu/primerbank/index.html>) or RTPrimerDB (<http://medgen.ugent.be/rtprimerdb/index.php>). For primer sequences and amplicon sizes see Appendix B.

2.7.3.2 Analysis of reference gene stability

Candidate reference genes (*Coch*, *Cpb-1*, *Gapdh*, *Pnlip*, *Pol2rc*, *Rn18s*, and *Spi-c*) (see Appendix B) for qPCR normalisation were assessed using geNorm (qBase^{PLUS}, Biogazelle) (Vandesompele *et al.*, 2002; Hellemans *et al.*, 2007). Fold expression of L1-open reading frame (ORF) genes was calculated using the ViiATM7 Comparative Ct ($\Delta\Delta Ct$) function or relative quantification based on RNA input (ΔCt).

2.8 Western blot analysis

2.8.1 Acid extraction of histone proteins

Histones were isolated from tissue sections as follows. Three fresh frozen tissue sections (25 μm) were cut using a cryostat (Reichert-Jung Cryocut 1800) and placed in a pre-chilled microcentrifuge tube containing 1 mL of chilled 1 x PBS. Samples were centrifuged at 12,000 x *g* for 1 min at RT to pellet tissues in order to remove cryoprotectant media. Once the supernatant was removed, all subsequent steps

were performed on ice and all solutions and buffers used were chilled to prevent protein degradation. Tissues were homogenised in 1 mL histone lysis buffer (Appendix C) with a 21 gauge needle. Lysates were centrifuged at 4°C at 1500 x *g* for 5 min. Supernatant was removed and nuclei were washed in 3 x 1 mL with histone lysis buffer at 4°C for 5 min at 1500 x *g*. Nuclei were then washed with 1 mL of Tris-EDTA (Appendix C) and centrifuged for 5 min at 1500 x *g* at 4°C. Pellets were resuspended in 100 µL of water. To the pellets, an aliquot of 0.4 N of concentrated HCl was added followed immediately by vortexing. Samples were incubated on ice for 1 h. Samples were then centrifuged at 14,000 x *g* for 10 min at 4°C. The supernatant was pipetted into a new tube and 1 mL of acetone was added. Samples were mixed by inversion and placed at – 20 °C overnight. Samples were centrifuged for 10 min at 4°C at 14,000 x *g*. The supernatant was discarded, the pellets were air dried briefly and resuspended in 100 µL of water, and stored at -20°C.

2.8.2 Determination of protein concentration

Lysates containing histones were quantitated using the Pierce BCA (bicinchoninic acid) protein assay kit as per the manufacturer's instructions. Briefly, BSA protein standards were prepared from a stock concentration of 2000 µg/mL and serially diluted using sterile 1 x PBS. The concentration range of the standards was: 2000, 1500, 1000, 750, 500, 250, 125 and 25 µg/mL. Twenty-five micro-litres of either sample or standard were pipetted into the well of a clear flat bottomed 96-well plate (Nunc). Two hundred micro-litres of working reagent consisting of 50 parts BCA Reagent A to 1 part BCA Reagent B were added to each well. Plates were gently

vortexed and incubated at 37°C for 30 min. Absorbance was measured at 562 nm on a microplate reader (VERSA_{max} microplate reader, Molecular Devices). Concentration of protein samples was determined using a standard curve of absorbance versus concentration of BSA standards.

2.8.3 Gel Electrophoresis of protein lysates

Proteins were separated via gel electrophoresis using a Bio-Rad Criterion™ electrophoresis system and Criterion™TGX™ Stain-Free pre-cast gels as per the manufacturer's instructions. Pre-cast gels were Tris-Glycine Laemmli-like gels with a trihalo compound that enables visualisation of protein bands on both gels and PVDF blots.

Briefly, Criterion™TGX™ Stain-Free pre-cast gels were placed into the gel tank and a Tris/SDS/Glycine running buffer added (Appendix C; Flinders Proteomics Facility). Ten micrograms of acid extracted histone lysate was loaded onto the gels with 4 x SDS loading buffer containing dithiothreitol (DTT) (Appendix C; Flinders Proteomics Facility). Samples were run at 300 V for 20 minutes.

Prior to semi-dry transfer, proteins were visualised on the gels using the Bio-Rad Gel-Doc Imaging System. The trihalo fluorescent compound within the gels was activated using UV light.

2.8.4 Semi-dry transfer of proteins

Proteins were transferred to low-fluorescence PVDF using the Bio-Rad Trans-Blot® Turbo™ Transfer System. Briefly, Criterion™TGX™ Stain-Free pre-cast gels were removed from the casing and equilibrated in 1 x Transfer Buffer for 10 min (Appendix C; Flinders Proteomics Facility). Two pieces of extra-thick blotting paper (Bio-Rad) (2.4 mm) were briefly equilibrated in 1 x Transfer Buffer. PVDF membrane was first activated by wetting with methanol and then equilibrated in 1 x Transfer Buffer. A transfer sandwich was assembled in a Trans-Blot® cassette as follows: 1 x blotting paper, PVDF, gel, 1 x blotting paper. Air bubbles were removed from the sandwich to ensure even transfer using a roller. Proteins were transferred at 25 V/1 A for 30 min.

Following transfer, membranes were imaged to determine efficiency of protein transfer. Protein bands were visualised as for gels as described in Section 2.8.3.

2.8.5 Detection of proteins

2.8.5.1 Antibody detection of proteins

PVDF membrane was rinsed briefly in RO water. Blots were then blocked at RT for 90 min in 1 x TBS-T (Appendix C) containing 5% skim milk powder, with gentle agitation. Blots were incubated at 4°C for two days in 1 x TBS-T/1% skim milk powder containing 1/2500 polyclonal rabbit anti-H3me3K9 (tri-methylation of the lysine 9 residue on histone H3) antibody (Abcam) with gentle agitation. Blots were then rinsed at RT in 1 x TBS-T three times for 10 min. Blots were incubated at RT for 90 min in 1/3000 dilution of HRP-conjugated goat anti-rabbit antibody (Abcam).

Unbound antibody was removed from the blots by 4 x 5 min rinses in 1 x TBS-T at RT. Blots were then incubated in 2 mL of enhanced chemiluminescence (ECL) reagent (Pierce) for 5 minutes and imaged using the Fuji LAS-4000 imager using auto-settings for ECL.

2.8.5.2 Quantitation of protein bands

Histone protein bands were quantitated as outlined in Aldridge *et al* (2008). Briefly, antibody-stained histone bands were normalised to account for variations in loading of samples using the mean intensity of all total histone H3 protein bands on an individual gel. Quantification of tri-methylation of lysine 9 residue on histone H3 was expressed as a ratio of histone H3 antibody band/mean of total histone H3.

2.9 Immunohistochemistry

2.9.1 Preparation of tissue sections

Frozen mouse spleen tissues were cut at -20°C using a Cryocut 1800 cryostat (Leica, USA) at a thickness of 5 µm per section. Sections were transferred to aminopropylethoxysilane (APES; Sigma)-coated glass slides (Appendix C).

2.9.2 Detection of spleen T-cells

Following mounting onto APES-coated slides, sections were fixed in 2% formaldehyde at RT for 10 min. Slides underwent three washes for 5 minutes each

with Phosphate Buffered Saline (PBS) (Sigma) at RT while shaking. Tissues were incubated at RT for 1 h in blocking solution (Appendix C) in a humidified chamber. One hundred microliters of primary antibody (hamster anti-mouse CD3e; Becton-Dickinson Pharmingen) diluted 1/100 in 1% goat serum (Sigma) was placed onto each spleen section and incubated overnight at 4°C. One slide was incubated overnight in 1% goat serum, without primary antibody to serve as a control for the secondary antibody. Primary antibody was washed from slides six times in PBS for 2 min each wash. Sections were then incubated at 37°C for 1 h in a humidified chamber with 100 µL of secondary antibody per slide (FITC-goat anti-hamster; Abcam) that had been diluted 1/200 in 1% goat serum. Unbound secondary antibody was removed from tissue sections by 6 x 2 min washes in PBS. Slides were dried briefly at RT and coverslipped using Vectashield mounting medium containing 4, 6-diamidino-2-phenylindole (DAPI; Vector Laboratories) and stored at -20°C until analysis.

2.9.3 Microscopy of spleen sections

Ten fields per spleen section (two sections per mouse) were examined using an Olympus AX70 epifluorescent microscope. Images of fields were captured using an ORCA high resolution digital camera (Hamamatsu Photonics, Japan). DAPI-labelled cells were visualised using a Chroma 31000 filter (peak excitation 340-380 nm, peak emission 435-485 nm; dichroic mirror 400 nm) and FITC-labelled cells were visualised using a Chroma 31001 NB filter (peak excitation 470-490 nm, peak emission 515-545 nm; dichroic mirror 505 nm).

Total T-cell areas per field were identified using a CellProfiler™ software pipeline (Carpenter *et al.*, 2006) (see Appendix F for pipeline). Mean T-cell area frequency per mouse was calculated as the average total T-cell area/total DAPI-labelled cells of the two spleen sections per mouse.

2.10 Statistical analysis

Data were analysed using the statistical program IBM SPSS Statistics (version 17, IBM Corp.). The effect of multiple treatment groups and the analysis of methylation differences between mouse tissues were first tested by ANOVA, with Bonferroni *post-hoc* analysis used to compare means between groups where equal variance was assumed. When sample numbers were unequal, Games-Howell *post-hoc* analysis was used. Linear bivariate correlations were analysed using Pearson correlation. The effect of treatment at a single measurement compared with sham-irradiated mice was analysed using the Independent samples T-test. Analyses of methylation changes over time for a single mouse in the longitudinal study were analysed using a general linear model multivariate analysis of variance (MANOVA)(Edwards, 2000) and repeated measures analysis. In all cases $P < 0.05$ was considered significant. All means are displayed with error bars representing ± 1 standard error of the mean.

3 DEVELOPMENT AND VALIDATION OF A MURINE LINE1 DNA METHYLATION HIGH RESOLUTION MELT ASSAY

Increasingly, mouse models are being used to study the acute and transgenerational effects of exogenous modulators of global DNA methylation such as diet (Finnell *et al.*, 2002; Sauer *et al.*, 2010; Vanhees *et al.*, 2011), chemical carcinogens (Koturbash *et al.*, 2011), ionising radiation (Tawa *et al.*, 1998; Pogribny *et al.*, 2004; Raiche *et al.*, 2004; Pogribny *et al.*, 2005; Giotopoulos *et al.*, 2006), as well as the study of DNA methylation in ageing animals (Singhal *et al.*, 1987; Barbot *et al.*, 2002). Accordingly, there is an increasing need for sensitive, robust, inexpensive and high throughput methods for the detection of changes to murine global DNA methylation levels. While High Performance Liquid Chromatography (HPLC) and Liquid Chromatography-Mass Spectrometry (LC-MS) are considered two of the gold standards for assessing total methylated cytosine content due to their high sensitivity, accuracy and reproducibility, they are low-throughput due to the requirements of sample preparation, lengthy analysis procedures, and cost per sample. More recently, whole genome sequencing and array technologies such as the *Illumina*, SOLiD (Invitrogen), and 454 platforms (Applied Biosystems) have been used to investigate global CpG methylation. While these platforms are able to determine the methylation status of thousands of genes at the single CpG site-level offering the highest level of resolution, they are not amenable for screening large numbers of experimental samples and the technology is not available to all

laboratories. Another common sequencing-by-synthesis technique used in methylation analysis is pyrosequencing, which offers information regarding the proportion of methylated cytosines in a target sequence. While this also is a powerful tool, it is limited by the size of the target region and cannot be used to analyse highly polymorphic sequences.

Approximately 2-10% (Gama-Sosa *et al.*, 1983) of the cytosine residues in the mammalian genome are methylated (5-methyl-deoxycytosine; 5mdC), predominantly when in sequence with a guanine (termed a CpG dinucleotide) and largely within transcriptionally silent regions of the genome. CpG-rich regions within transcriptionally active gene promoters are generally unmethylated although it has been reported that only key CpGs within the promoter region need be (un)methylated to exert control on gene expression (Cropley *et al.*, 2010). In cancer, DNA methylation changes can occur at individual genes, or across the genome (global methylation), resulting in transcriptionally silent regions becoming demethylated, leading to transcriptional activation, or transcriptionally active regions rendered silent by aberrant increases in DNA methylation.

The most heavily methylated regions of the genome are DNA sequences belonging to repetitive DNA elements, which comprise approximately 45% of the mammalian genome (Lander *et al.*, 2001), of which 20% consist of Long Interspersed Elements-1 (LINE1, L1)(Lander *et al.*, 2001; Ostertag, 2001; Fedorov, 2009). Short Interspersed Elements (SINE) and Long Terminal Repeat elements (LTR) are also distributed throughout the genome and are found to be highly methylated. These repeat elements can contain full length coding regions that upon demethylation may result

in transposition across the genome, which can cause disruption to gene expression and in some cases, disease (Scott *et al.*, 1987; Furano *et al.*, 1988). There are also reports that loss of repeat element methylation can be an early event in carcinogenesis or tumour progression. For example, loss of methylation at intracisternal-A particle (IAP) repeat elements in mice results in active transcription and transposition leading to insertion of the IAP element into the genomic locus of *Notch-1*. This retrotransposition induces expression of an oncogenic transcript of *Notch-1* in thymic tumours (Howard *et al.*, 2007). In several cases, it has been reported that a loss of methylation at repeat elements has resulted in increased chromosomal instability as well as the enhanced development of colorectal cancer, non-small cell lung cancer and bladder tumours (Gaudet *et al.*, 2003; Estecio *et al.*, 2007; Ogino *et al.*, 2008a; Ogino *et al.*, 2008b; Yamamoto *et al.*, 2008; Igarashi *et al.*, 2010; Saito *et al.*, 2010; Wolff *et al.*, 2010).

High resolution melt (HRM) PCR is now being used in methylation studies and is capable of detecting single nucleotide differences based on differences in melting temperatures (Ririe *et al.*, 1997). The widespread nature and high CpG density of L1 elements has resulted in the utilisation of L1 elements to investigate changes in DNA methylation at multiple locations within the genome (Yang *et al.*, 2004; Bollati *et al.*, 2009; Stanzer *et al.*, 2010).

The focus of this thesis is to study changes in murine L1 element DNA methylation levels following exposure to ionising radiation – a modulator of DNA methylation. Thus the first aim of this thesis was to develop an assay that could detect changes to L1 methylation across the genome that was high throughput and also had the

capacity to detect small changes in DNA methylation between animals. This chapter describes the development of a HRM assay that is capable of detecting small changes in murine L1 methylation.

3.1 Results

3.1.1 Design of a murine L1 repeat element high resolution melt assay

3.1.1.1 Identification of murine *LINE1* repeat element

The forward primer to a murine L1 element (Accession number: D84931.1) from Kato *et al* (2007) (see Appendix B) was used as a query sequence for a BLAT search (<http://genome.ucsc.edu/>) to identify a murine L1 element sequence that could be used to design PCR primers. The Kato primer sequence was found to align with a murine L1 repeat element Md family subunit T sequence. A target CpG island (a region of DNA sequence that contains more than 50% clustered CpGs) containing 13 CpGs upstream of the Kato primer binding site (located within open reading frame 2 (ORF2) of the consensus sequence) was identified using MethPrimer (Li and Dahiya, 2002).

3.1.1.2 Primer Design

The primers designed for this assay were created to be unbiased to the methylation status of the repeat elements. It was hypothesised that by creating the assay in this manner, all elements across the genome would be amplified regardless of their methylation status. The target L1 region contained 13 CpGs and was predicted to

produce a 192 bp PCR product (Appendix B). Bisulphite modified and unmodified murine genomic DNA were amplified with specific primers using annealing temperatures based on the predicted T_m of the primers and the protocol outlined by the EpiTect HRM PCR kit (Qiagen; see Chapter 2).

Figure 3-1 shows that the conditions used for PCR produced a single product that could only be amplified from bisulphite-modified genomic DNA.

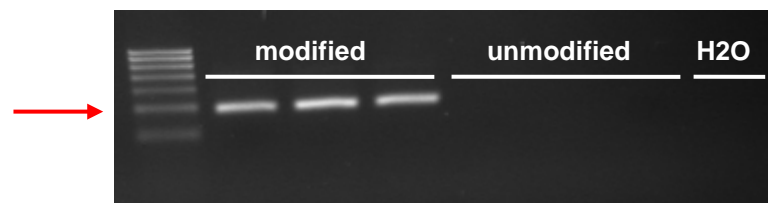


Figure 3-1: Agarose gel analysis of L1 PCR products.

L1-PCR products were run on a 2% agarose gel. Bisulphite modified and unmodified murine spleen genomic DNA was amplified using conditions outlined in Chapter 2 and subjected to agarose gel separation to determine specificity of the PCR. The red arrow indicates the 200 bp molecular weight marker band. The predicted size of the L1-PCR product from bisulphite modified genomic DNA is 192 bp.

3.1.1.3 Sequence analysis of LINE1 repeat elements

The L1-PCR products were separated by gel electrophoresis. The PCR bands were excised, purified and DNA sequenced using Sanger sequencing. The sequencing results confirmed that the primers were amplifying a murine L1 sequence. Sequence analysis of L1-PCR products identified six non-CpG nucleotide positions with more than one defined peak on the sequence chromatogram, indicating potential sequence variation. Using the unmodified-specific L1 primer sequences, the mouse genome was searched by *in silico* PCR (<http://genome.ucsc.edu/>) to

identify the predicted pool of L1 template sequences. Alignment of twenty randomly selected *in silico* PCR results (from >100 sequences) revealed ten nucleotide positions with sequence variation and that the frequency of the minority variants occurred in 5% to 40% of the analysed templates (Table 7) (Figure 3-2). Sequence variants 2, 5, and 7 occurred at the guanine base in CpG dinucleotides and as a result, 10 - 15% of the L1 elements did not contain a CpG at these sites. All six sequence variants identified from the sequencing of PCR products were observed in the twenty *in silico* predicted L1 template sequences.

Table 7: Frequency of sequence variants detected at 10 nucleotide positions in the L1-HRM target sequence.

Sequence Variant	Type	Frequency in alignment of <u>20</u> random <i>in silico</i> PCR results	Detected in L1-PCR product DNA sequencing
1	G>T	10% (T) (2/20)	No
2	G>A	10% (A) (2/20)	Yes
3	T>C	5% (C) (1/20)	No
	T>G	5% (G) (1/20)	Yes
4	G>A	5% (A) (1/20)	No
5	G>A	15% (A) (3/20)	Yes
6	C>T	5% (A) (1/20)	No
7	G>A	10% (A) (2/20)	Yes
8	G>A	30% (A) (6/20)	Yes
9	G>A	40% (G) (8/20)	Yes
10	C>A	5% (A) (1/20)	No

Unmodified genomic DNA specific L1 primers (F_unmod_mLINE1 and R_unmod_mLINE1) were used in an in silico PCR analysis (UCSC Genome). Twenty randomly selected in silico PCR results were aligned and the frequencies of sequence variants detected in the alignment in comparison to the L1-HRM PCR target sequence are shown.

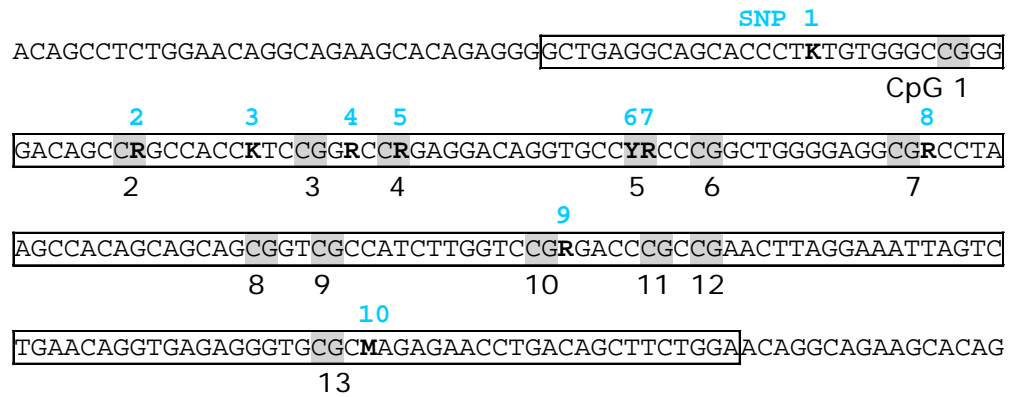


Figure 3-2: The L1 sequence confirmed by DNA sequencing.

The location of sequence variants in the target L1 region (boxed region) in unmodified genomic DNA identified from both sequence analysis of L1-PCR products (amplified with *F_unmod_mLINE1* and *R_unmod_mLINE1*) and in silico PCR analysis are shown in bold, numbered 1-10 in blue and characterised as an R (A/G), K (T/G) or M (A/C). CpGs are shaded and numbered in black 1-13.

3.1.1.4 Development of PCR methylation controls

Universal Methylated Mouse DNA (Zymo Research) was used as a methylated genomic DNA control. A LINE1 unmethylated control DNA was made as follows. L1 sequences from unmodified Universal Methylated DNA were amplified using *F_unmod_mLINE1* and *R_unmod_mLINE1* (see Appendix B). The resulting PCR products were purified (see Section 2.5.7) and bisulphite modified. During PCR amplification, any CpG that contained a methylated cytosine would be unmethylated in the final PCR product as methyl groups are not restored during PCR amplification. Thus the final PCR product would resemble unmethylated DNA and on bisulphite modification every cytosine within a CpG would be converted to a UpG.

3.1.1.5 High resolution melt analysis of control DNA

The methylated, unmethylated, and a 50% mixture of the methylated and unmethylated control samples were analysed by HRM following PCR with primers unbiased for methylation status in order to verify that sequence differences due to cytosine composition could be detected by HRM. As expected, the melt curve analysis showed that the methylated control had a higher melt temperature range compared with the unmethylated control DNA (Figure 3-3A). The 50% mixture had a melt temperature range that was between the two control DNA samples. The graph of the negative first derivative of the melting curve ($-dF/dT$) showed that the methylated and unmethylated control samples had only one major melt peak each, with the methylated control melting at a higher temperature compared to the unmethylated control (Figure 3-3B). The 50% mixture of the two control DNA samples showed melt peaks for both control DNA samples. Smaller peaks were observed which are considered to represent low melting heteroduplexes, some non-specific amplification products and residual primer dimer. As the unmethylated control sample template in the PCR was a purified PCR product, rather than a genomic DNA template, the melt peak was smoother, representing the absence of low-level non-specific amplification, which was verified by gel electrophoresis (data not shown).

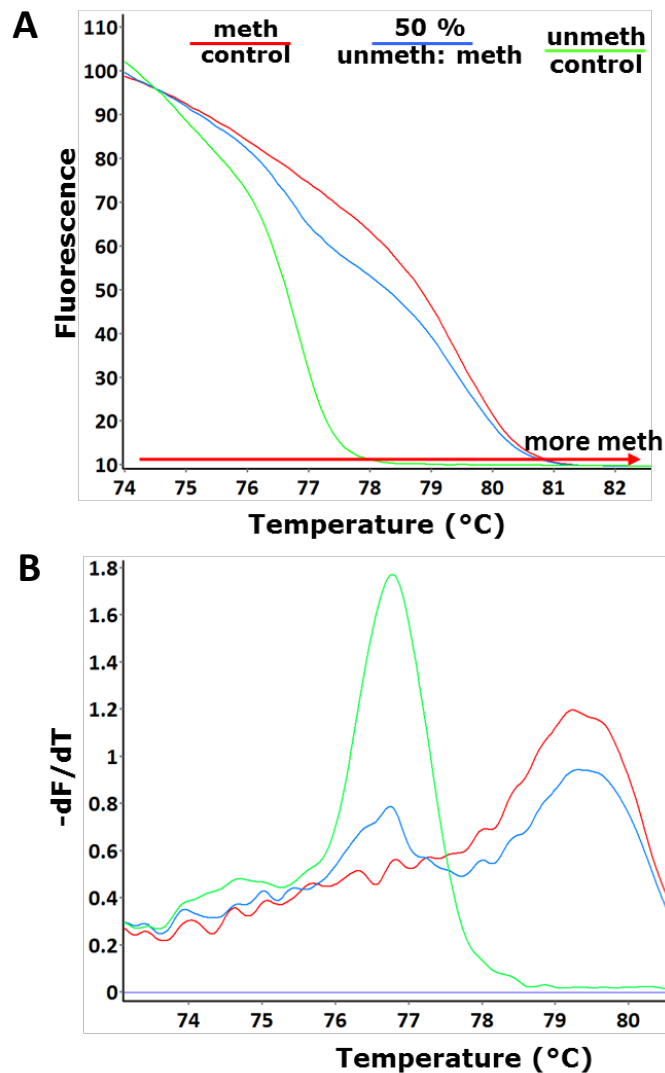


Figure 3-3: High resolution melt analysis of control DNA.

Melt curve analysis following amplification with the methylation-status unbiased L1 primers (*F_unbiased_mLINE1* and *R_unbiased_mLINE1*). (A) The HRM normalised melt curve and (B) the negative first derivative melt curve ($-dF/dT$), was performed on methylated (red) and unmethylated (green) control DNA as well as a 50% (methylated: unmethylated control) methylated sample (blue).

3.1.2 Detection of demethylation using the L1-HRM assay

3.1.2.1 Detection of demethylation induced by 5-aza treatment

Heterogeneous patterns of methylation at any individual CpG dinucleotide have been observed following modulation of methylation with exogenous agents or

during carcinogenesis (Eads *et al.*, 2000; Weeks and Morison, 2006; Suzuki *et al.*, 2007; Candiloro *et al.*, 2008; Zhang *et al.*, 2008; Fandy *et al.*, 2009; Gebhard *et al.*, 2010; Rand and Molloy, 2010; Stanzer *et al.*, 2010). In order to investigate if heterogeneous methylation patterns across numerous L1 elements distributed throughout the genome could be detected with this assay, genomic DNA isolated from A11 mouse hybridoma cells that had been treated with two different low doses (0.125 μM or 0.5 μM) of the chemical demethylating agent 5-aza-2'-deoxycytidine (5-aza) was utilised. HRM is used to detect single nucleotide polymorphisms (SNPs). Therefore, it was important to determine if there were differences in sequence due to non-CpG SNPs that could affect the melt curves of the samples. Analysis of the melt curves for L1 elements amplified from bisulphite unmodified genomic DNA revealed no difference in melt curves between the 5-aza and vehicle control (DMSO) treated samples (Figure 3-4). This result indicated that the identified non-CpG sequence variants were not influencing the melt curves, and that any differences detected following bisulphite modification were due to cytosine content.

The melt curves of the samples from each treatment group could be distinguished from the melt profile of the methylated control DNA, however, no significant difference in melting temperature between the 5-aza treated cells and the vehicle treated control cells was observed (Figure 3-5).

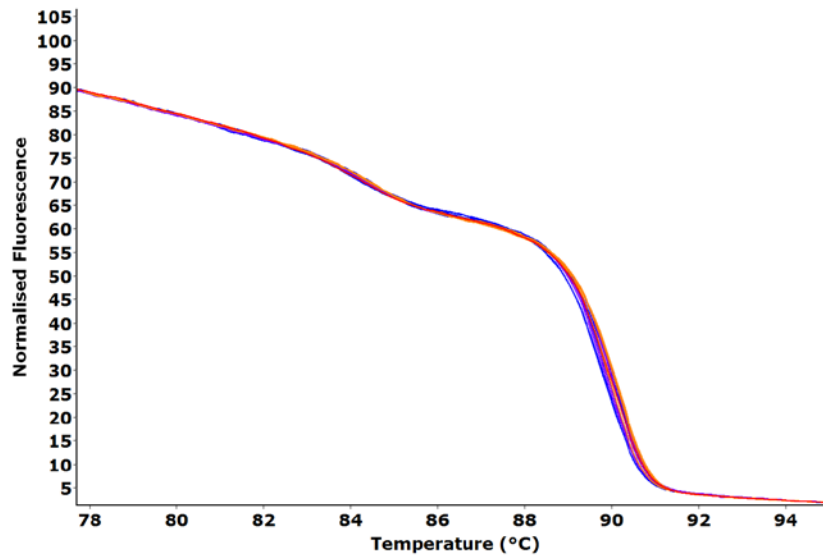


Figure 3-4: Melt curve analysis of unmodified genomic DNA.

Bisulphite unmodified gDNA (10 ng) from vehicle (blue), 0.125 μ M (purple) and 0.5 μ M (orange) 5-aza treated A11 cells (n = 3-5 samples per treatment group) was amplified with bisulphite unmodified-specific and unbiased for methylation status L1 primers and subjected to melt curve analysis. Unmodified methylated control gDNA is in red.

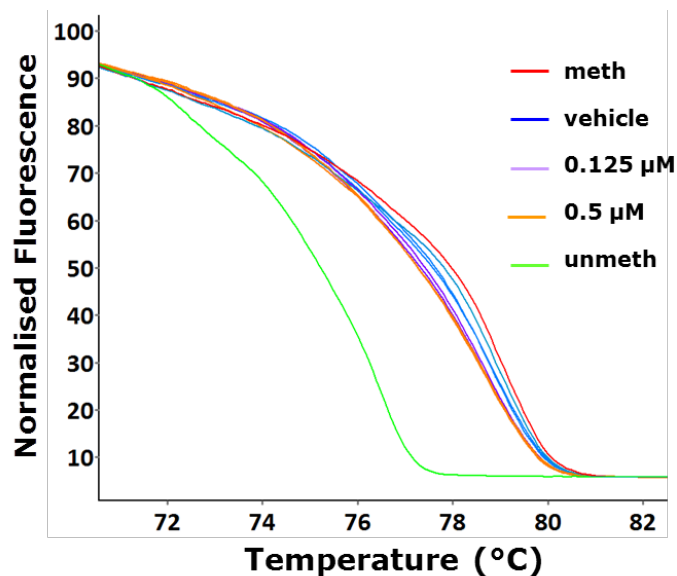


Figure 3-5: Detection of 5-aza induced partial demethylation of murine L1 elements in A11 cells using methylation-status unbiased L1 primers.

The normalised HRM melt curve (n = 5 samples per treatment group; n = 3 samples is displayed) for the vehicle control (DMSO) (blue), 0.125 μ M (purple) and 0.5 μ M (orange) 5-aza treated A11 cell line genomic DNA along with the methylated (red) and unmethylated (green) controls following bisulphite modification and amplification with the methylation-status unbiased L1 primers.

3.1.2.2 *Biasing of PCR primers to enhance sensitivity*

It has been proposed in several reports that PCR primers may need to enrich for methylated or unmethylated templates to increase sensitivity to detect small methylation/demethylation events within a large pool of heterogeneously methylated templates (Wojdacz and Hansen, 2006; Wojdacz and Dobrovic, 2007; Kristensen *et al.*, 2008). Using this approach, a new forward and reverse primer pair was designed to match the bisulphite-modified sequence of an unmethylated CpG dinucleotide at the 3' end of each oligonucleotide. Thus, the same region could now be amplified with a methylation-status unbiased primer pair (not selective for methylation status) or an unmethylated-biased primer pair (preferentially amplifying L1 sequences with both flanking CpG sites unmethylated). Using the unmethylated-biased primers, a distinct, dose-dependent difference in melt curves was observed (Figure 3-6A).

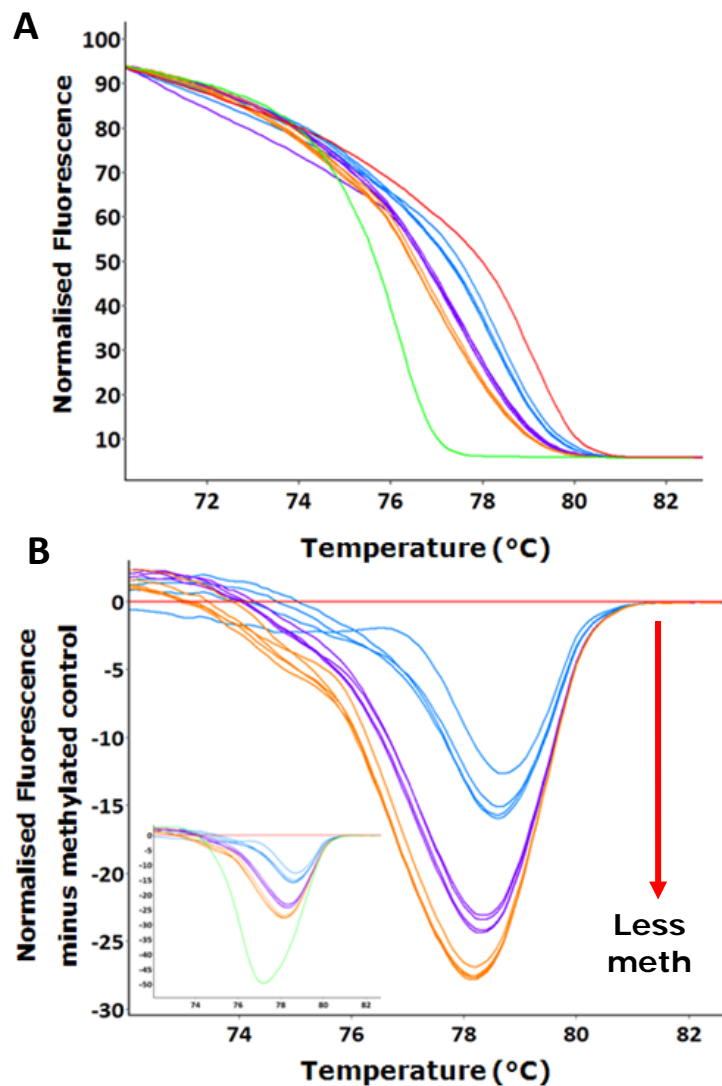


Figure 3-6: Detection of 5-aza induced partial demethylation of murine L1 elements in A11 cells using unmethylated-biased L1 primers.

(A) The normalised HRM melt curve and (B) the difference plot (inset is the difference graph with the unmethylated control included) for the vehicle control (DMSO) (blue), 0.125 μM (purple) and 0.5 μM (orange) 5-aza treated A11 cell line genomic DNA along with the methylated (red) and unmethylated (green) controls following bisulphite modification and amplification with the unmethylated-biased primers L1 (one PCR replicate for each of the n = 4-5 samples is displayed).

3.1.2.3 Statistical analysis of methylation differences between samples using the Net Temperature Shift

In order to statistically quantify the differences in melt curves observed, a means of deriving the methylation index of a sample based on the melting profile of the amplicons was devised. Within the Rotor-Gene Q software, normalised melt curves of all samples were generated. Following this, a control sample was selected (in this instance, the methylated control DNA) and a difference plot of the melt curves compared to the methylated control was generated (Figure 3-6B). The difference plot fluorescence value at each temperature point (0.1°C intervals from 74°C to 84°C for a total of 100 readings) within the melt curve was exported to Microsoft Excel. All values within the melt curve were summed and divided by 100 to give the Net Temperature Shift (NTS) value. A greater negative NTS value indicates a greater shift from the methylated control, and thus a less methylated sample. Using the NTS, a significant dose-dependent demethylation of the L1 elements for samples treated with 5-aza compared to the vehicle control ($P < 10^{-5}$) and between the two 5-aza doses ($P < 10^{-5}$) was observed (Figure 3-7).

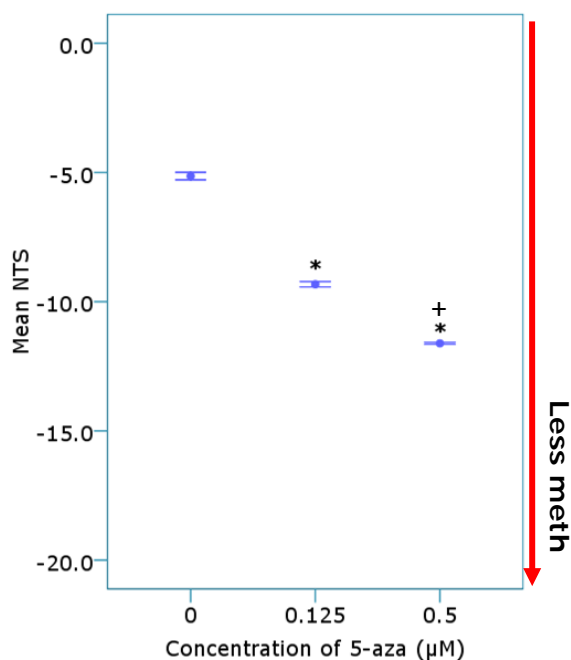


Figure 3-7: Quantitation of methylation differences using the Net Temperature Shift.

Based on the difference plot of normalised fluorescence from the methylated control, the normalised fluorescence at each temperature point on the melt curve was used to calculate the mean NTS of the 5-aza treated samples for the L1 elements ($n = 4-5$ samples per treatment group). * $P < 0.05$ compared to the vehicle control; + $P < 0.05$ compared to the 0.125 µM treated 5-aza samples. Error bars represent 1 SE.

3.1.3 Validation of L1-HRM assay

3.1.3.1 Pyrosequencing

The L1-HRM PCR products were pyrosequenced in order to determine if all CpGs within the L1-HRM amplicon in the 5-aza treated samples underwent demethylation in comparison to the vehicle control (Figure 3-8).

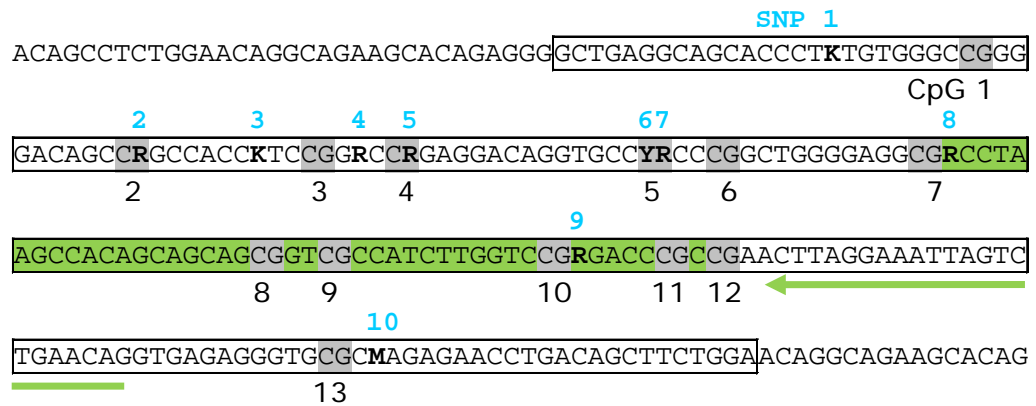


Figure 3-8: Schematic diagram of the L1 pyrosequencing target sequence.

The pyrosequencing primer is highlighted by the green arrow and the region pyrosequenced is shown in green. The location of sequence variants in the target L1 region (boxed region) in unmodified genomic DNA identified from both sequence analysis of L1-PCR products (amplified with *F_unmod_mLINE1* and *R_unmod_mLINE1*) and in silico PCR analysis are shown in bold, numbered 1-10 in blue and characterised as an R (A/G), K (T/G) or M (A/C). CpGs are shaded and numbered in black 1-13.

Pyrosequencing of CpGs 7 - 12 revealed that each of the six CpG sites in the DNA from the 0.125 μM and 0.5 μM 5-aza treated cells displayed significantly less L1 methylation than the vehicle control ($P < 0.05$), and that there was dose-dependent demethylation of each CpG ($P < 0.05$) (Figure 3-9A). The mean percent of L1 methylation across all six CpGs revealed a significant dose-dependent reduction in L1 methylation with increasing concentration of 5-aza and a significant difference between all treatments ($P < 10^{-5}$) (Figure 3-9B). Comparison of the 0.125 μM and 0.5 μM 5-aza treated samples demonstrated that CpG 9 had the greatest reduction in methylation compared to the other CpG sites analysed (1 - 28% loss of methylation; $P < 10^{-5}$), and in comparison with the CpGs from the vehicle control treated samples (30 - 40% loss of methylation; $P < 10^{-5}$). Between the 0.125 μM and 0.5 μM 5-aza

samples the biggest difference in methylation was observed for CpG 12 (11.4% difference; $P < 10^{-5}$).

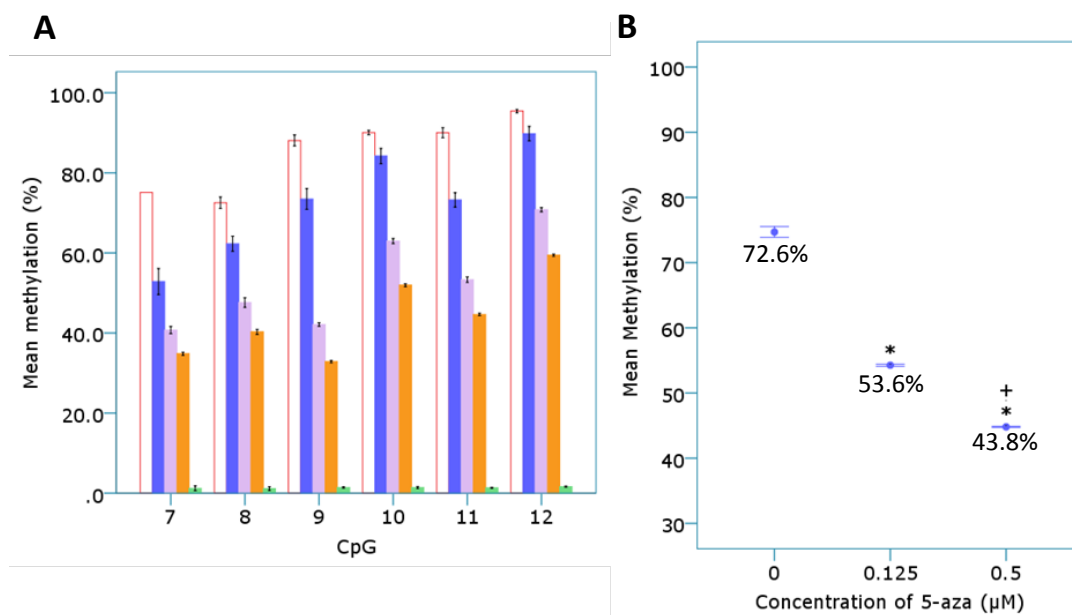


Figure 3-9: Pyrosequencing of 5-aza treated A11 cells L1-HRM PCR products.

(A) The percent methylation of each CpG was plotted for each 5-aza concentration (vehicle - blue, 0.125 μM - purple and 0.5 μM - orange) or control DNA status (red – methylated control, green – unmethylated control). (B) The mean methylation of all CpGs pyrosequenced (7-12) was plotted versus 5-aza concentration. * $P < 10^{-5}$ compared to the vehicle control; + $P < 0.05$ compared to the 0.125 μM treated 5-aza samples ($n = 4-5$ samples per treatment group). Error bars represent 1 SE.

3.1.3.2 Liquid chromatography-mass spectrometry

Liquid chromatography-mass spectrometry (LC-MS) was used to assess total genomic 5mdC content in the 5-aza treated A11 samples for comparison with the L1-HRM assay. A significant reduction in total genomic 5mdC content compared with the vehicle control for both 0.125 μM and 0.5 μM treated samples was observed ($P < 10^{-5}$) (Figure 3-10). Unlike the HRM assay and pyrosequencing, the LC-MS method was unable to distinguish differences in DNA methylation between the 0.125 μM and 0.5 μM 5-aza treated cells. Bivariate correlations with 5-aza dose for

the three assays showed equal and significant negative correlations ($P < 0.01$) for NTS vs. 5-aza dose (Pearson correlation coefficient: -0.952) and pyrosequencing mean methylation vs. 5-aza dose (Pearson correlation coefficient: -0.952), with a weaker but still significant negative correlation ($P < 0.01$) between LC-MS 5mdC content vs. 5-aza dose (Pearson correlation coefficient: -0.391). The NTS and pyrosequencing mean methylation levels were highly and significantly correlated with each other (Pearson correlation coefficient: 0.913; $P < 0.01$), while the 5mdC content by LC-MS, which is not specific for L1 methylation, showed less concordance with the other two methods (Pearson correlation coefficient: LC-MS and NTS, 0.387; LC-MS and pyrosequencing mean methylation, 0.377; $P < 0.01$).

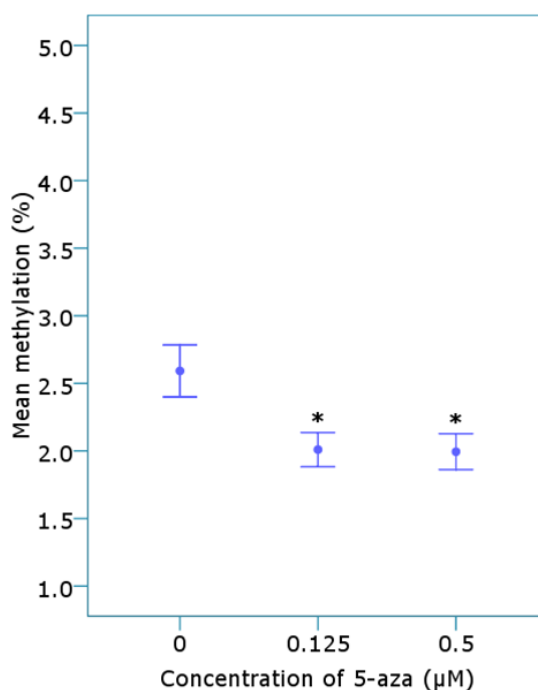


Figure 3-10: Analysis of total genomic 5mdC content in 5-aza treated A11 cells.

Genomic DNA samples ($n = 4-5$ per treatment group) were analysed by liquid chromatography – mass spectrometry (LC-MS) for total genomic 5mdC content and mean percent methylation (5mdC/dG ratio) for each treatment group plotted ($*P < 0.05$). Error bars represent 1 SE.

3.1.3.3 Sensitivity, reproducibility and linearity of the L1-HRM assay

The sensitivity, reproducibility and linearity of the L1-HRM assay were determined. Various ratios of genomic DNA from the 0.5 μ M 5-aza treated and vehicle treated samples were made (prior to bisulphite modification) to create heterogeneously methylated samples with predicted mean L1 methylation levels (based on pyrosequencing measurements) between 45.4 and 75.6%. These methylation values represented the highest and lowest methylation levels of the vehicle and 5-aza treated samples. Linear regression analysis on the standard curve indicated that the NTS was highly linear compared to the predicted L1 methylation levels of the samples ($P < 0.001$; $R^2 = 0.992$) (Figure 3-11). Bonferroni corrected *post-hoc* analysis revealed that with the number of replicates used here, an absolute difference of 3% mean L1 methylation or greater could be detected between two mixes of heterogeneously methylated DNA ($P < 0.05$). Comparison of these DNA mixtures by L1-HRM was performed for two separate bisulphite modification reactions and two HRM-PCR runs per modification (shown in Table 8) and revealed that neither bisulphite modification batch nor PCR run made a significant contribution to the overall variance (MANOVA, $P < 0.05$), with the variance largely explained by the predicted methylation levels of the various mixtures ($P < 0.01$).

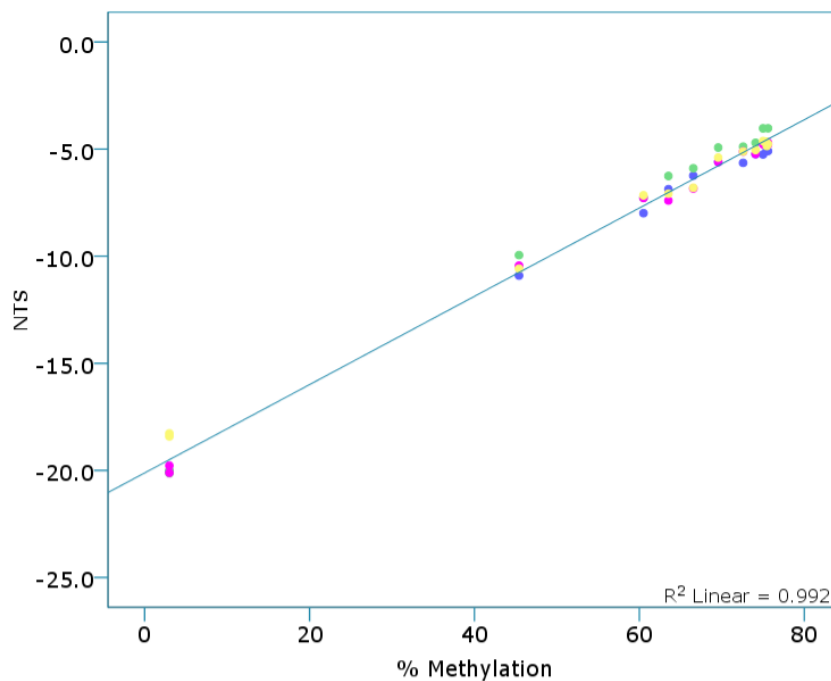


Figure 3-11: Linearity of L1-HRM assay.

Linear regression analysis was performed on the mean NTS for samples of a standard curve ($R^2 = 0.992$; $P < 0.001$). The standard curve was made from mixtures of the vehicle and 0.5 μM 5-aza treated A11 samples (75.6, 75.45, 75.3, 75, 74.09, 72.58, 69.56, 66.54, 63.52, 60.5 and 45.4% methylated) using the mean pyrosequencing values for the two samples. The unmethylated control DNA (~3% methylated) was also included in the L1-HRM PCR reactions. The samples underwent two separate bisulphite modifications and were amplified with the unmethylated-biased primers in two separate PCR reactions per bisulphite modification, prior to melt analysis.

Sample Mean Meth (%)	Bisulphite Modification Reaction #1						Bisulphite Modification Reaction #2						Mean NTS	SD		
	PCR 1			PCR 2			PCR 1			PCR 2					Mean NTS	SD
	NTS	SD	NTS	NTS	SD	NTS	NTS	SD	NTS	SD	NTS	SD				
45.40	-10.90	0.09	-9.95	0.25	-10.43	0.67	-10.44	0.06	-10.58	0.10	-10.51	0.10	-10.47	0.38		
60.50	-7.99	0.07	-7.27	0.11	-7.63	0.51	-7.28	0.08	-7.16	0.01	-7.22	0.08	-7.42	0.36		
63.52	-6.87	0.09	-6.26	0.01	-6.57	0.43	-7.40	0.05	-7.08	0.02	-7.24	0.23	-6.90	0.45		
66.54	-6.24	0.21	-5.89	0.13	-6.07	0.25	-6.84	0.34	-6.81	0.03	-6.83	0.02	-6.45	0.45		
69.56	-5.60	0.08	-4.93	0.00	-5.27	0.47	-5.60	0.06	-5.40	0.09	-5.50	0.14	-5.38	0.30		
72.58	-5.64	0.12	-4.89	0.21	-5.27	0.53	-5.11	0.00	-5.11	0.00	-5.11	0.00	-5.19	0.31		
74.09	-5.24	0.03	-4.70	0.00	-4.97	0.38	-5.23	0.09	-5.04	0.07	-5.14	0.13	-5.10	0.20		
75.00	-5.25	0.03	-4.03	1.01	-4.64	0.86	-4.78	0.05	-4.63	0.03	-4.71	0.11	-4.67	0.60		
75.30	-4.71	0.07	-4.68	0.13	-4.70	0.02	-4.74	0.03	-4.64	0.08	-4.69	0.07	-4.69	0.07		
75.45	-5.05	0.06	-4.67	0.01	-4.86	0.27	-4.73	0.04	-4.86	0.04	-4.80	0.09	-4.83	0.16		
75.60	-5.09	0.03	-4.03	0.72	-4.56	0.75	-4.70	0.06	-4.76	0.16	-4.73	0.04	-4.66	0.50		

Table 8: Analysis of variability of L1-HRM assay.

The 5-aza standard curve made from mixtures of the vehicle and 0.5 μM 5-aza treated A11 samples (75.6, 75.45, 75.3, 75, 74.09, 72.58, 69.56, 66.54, 63.52, 60.5 and 45.4% methylated) using the mean pyrosequencing values for the two samples, was used to assess intra- and inter-assay variability. Each sample underwent two separate bisulphite modifications and two separate HRM-PCR runs with two PCR reaction duplicates per HRM-PCR.

3.1.4 Application of the HRM methylation assay to other murine repeat elements

3.1.4.1 *SINE1 and IAP_LTR repeat elements*

As 5-aza is a general demethylating agent, the effect of the treatment at other repeat elements was investigated in the 5-aza treated A11 hybridoma cells. Primers specific for mouse B1 (Short Interspersed Elements; SINE family, Mm) and Intracisternal-A particle Long Terminal Repeat elements (IAP_LTR) (Lane *et al.*, 2003) were designed to be used in the HRM assay. Due to the small size and number of CpGs within the B1 repeat element (primers were located within the first 92 bp of the ~130 bp monomeric repeat unit), unmethylated-biased primers to enhance the sensitivity of detection were unable to be designed, and therefore primers were unbiased for methylation status. The IAP_LTR element primers were able to be biased for unmethylated CpGs to enhance sensitivity (IAP_LTR; located within the 5'LTR of the IAP promoter) (Figure 3-12). For both the B1 and IAP elements, there was a significant difference in the NTS of the 0.125 μ M and 0.5 μ M 5-aza treated samples compared with the vehicle control ($P < 10^{-5}$) (Figure 3-13). Both repeat elements showed strong correlation with the L1 elements ($P < 0.01$); with the IAP_LTR demonstrating greater correlation with the L1 elements than the B1 elements (Table 9).

A

AGCCGGGGCGTGGTGGCGCACGCCTTTAATCCCAGCACTCGGGAGGCAGAGGCAGG
 CCGATTTCTGAGTTCCAGGCCAGCCTGGTCTACAAAGTGAGCTCCAGGAC

B

TAATATGGGTGGCCTATTTGCTCTTATTAAAAGGAAAGGGGGAGATGTTGGGAGCC
 ACGCCACATTCGCCGTTACAAGATGGCGCTGACAGCTGTGTTCTAAGTGGTAAAC
 AAATAATCTGCGCATGTGCCGAGGGTGGTTCTCCACTCCATGTGCTCTGCCTTCCC
 CGTGACGWCAACTCGGCCGATGGGCTGCAGCCAATCAGGGAGTGACACCGTCTTAGG
 CGAAATATAACTCTCCTAAAAAAGGGACGGGGTTCTTTTCTCTCTCTCTTGCTTC

Figure 3-12: Murine B1 and Intracisternal-A-Particle Long Terminal Repeat element sequences.

The target consensus sequence of the (A) murine B1 and (B) murine IAP_LTR repeat elements (boxed region) are shown with the CpGs shaded in grey. Sequence polymorphisms are depicted as a W (A/T).

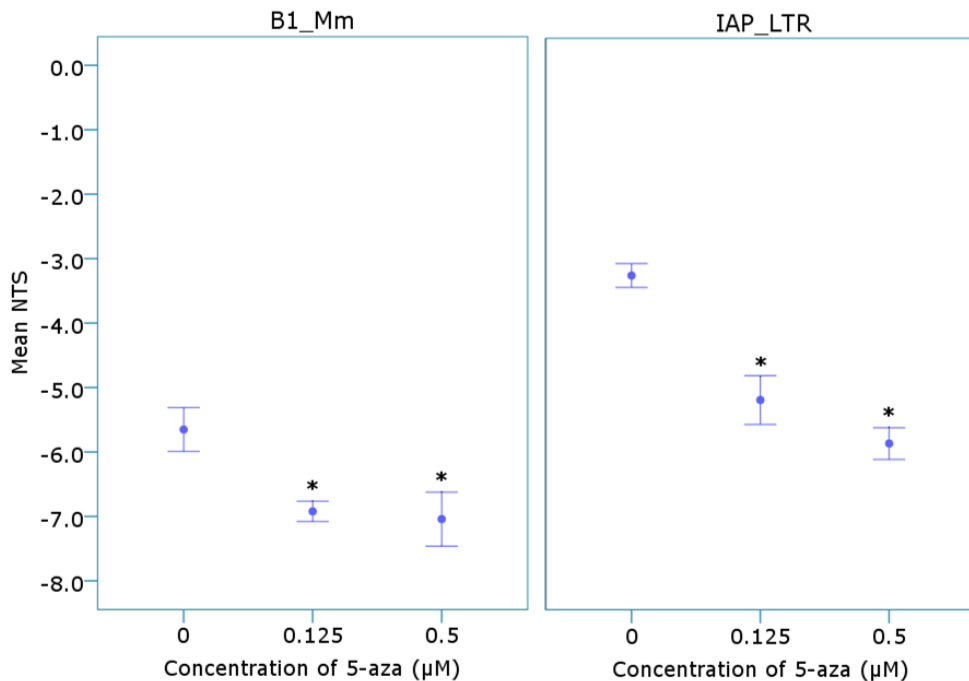


Figure 3-13: Demethylation of B1 and IAP_LTR repeat elements after 5-aza treatment.

The mean NTS of the 5-aza treated samples for murine B1 family Mm repeat element (B1_Mm) amplified with unbiased primers, and the Intracisternal- A-Particle Long Terminal Repeat (IAP_LTR) elements amplified with unmethylated-biased primers following bisulphite modification of genomic DNA (n = 4-5 samples per treatment group) (*P < 10⁻⁵ compared to the vehicle control). Error bars represent 1 SE.

Table 9: Pearson correlation of L1, B1 and IAP repeat element NTS values for the 5-aza treated A11 cell line samples.

	Pearson Correlation Coefficient			
	Treatment	LINE1	B1_Mm	IAP_LTR
Treatment (vehicle, 0.5 μ M, 0.125 μ M)	1	-0.937*	-0.482*	-0.750*
LINE1	-0.937*	1	0.672*	0.868*
B1_Mm	-0.482*	0.672*	1	0.801*
IAP_LTR	-0.750*	0.868*	0.801*	1

* $P < 0.01$

3.2 Discussion

Analysis of the methylation levels of L1 elements using HRM presents a challenge due to the number of CpGs within the CpG islands, and the abundance and sequence diversity of L1 elements throughout the genome. Methylation profiles will be heterogeneous and will produce complex melt curves that cannot be quantified by comparison to a standard curve of methylated/unmethylated DNA. The first aim of this thesis was to utilise HRM technology in order to detect small changes in DNA methylation to L1 elements throughout the genome that may result from perturbations to the homeostatic environment following both low and high dose radiation exposure.

3.2.1 Detection of demethylation using the L1-HRM assay

HRM analysis of bisulphite modified DNA templates is used to investigate DNA methylation, with various quantitative calculations of methylation levels employed.

These calculations range from comparing Cq values to a standard curve (Kristensen *et al.*, 2008; Stanzer *et al.*, 2010), a calculation based on the temperature at which half of the PCR products have melted (Smith *et al.*, 2009), measuring the height of the differential fluorescence melt peak from a nominated control (Malentacchi *et al.*, 2009), TaqMan™ probe technology (Eads *et al.*, 2000) and single dilutions of complex melt curves (Candiloro *et al.*, 2008). In these assays, the methylation of a sample is calculated by comparison to a standard curve that is generated using completely methylated and unmethylated control DNA (Eads *et al.*, 2000; Candiloro *et al.*, 2008; Kristensen *et al.*, 2008; Lorente *et al.*, 2008; Malentacchi *et al.*, 2009; Smith *et al.*, 2009; Stanzer *et al.*, 2010). With the exception of Stanzer *et al.* (2010), all assays were utilised to investigate gross changes in CpG methylation at single genomic loci in cancer samples. In this thesis, as a proof-of-principle, the chemical demethylating agent 5-aza was used to demonstrate the detection of L1 demethylation using HRM. Treatment with 5-aza causes significant reduction in total genomic 5mdC levels (Jüttermann *et al.*, 1994; Mund *et al.*, 2005). In this study, the doses of 5-aza used were 2-20 fold lower than doses reported in the literature that induce almost complete loss of DNA methylation (Jüttermann *et al.*, 1994; Mund *et al.*, 2005; Palii *et al.*, 2008; Smith *et al.*, 2009). Furthermore, the A11 cells underwent only one cell division. It was proposed that only one cell division following treatment with low concentrations of 5-aza treatment would cause partial demethylation resulting in increased heterogeneity across the L1 elements. Initial analysis of the resulting melt curves following amplification with primers unbiased for L1 methylation status demonstrated demethylation of the 5-aza treated cells compared with vehicle treated cells but no difference between the two 5-aza doses

(0.125 μM and 0.5 μM). To enhance the detection of small differences in methylation, primers were biased for unmethylated CpGs within the primer binding sites to enrich for the small proportion of samples that had undergone partial demethylation, hypothesising that CpGs within the target region would also have undergone some partial demethylation. When these primers were applied to the same 5-aza treated samples, a difference in the melt curves of the two different 5-aza doses was observed, indicating that the biased primers were capable of detecting changes in GC content of the L1 elements following bisulphite modification that were too small to be detected by the unbiased primers.

In order to quantify these differences, a novel means of measuring the difference in melt temperature between samples following PCR was devised – termed the Net Temperature Shift (NTS). The NTS quantifies changes in methylation (based on the GC content of the amplicons) compared to a control sample, rather than determining mean percent methylation of a target region, and incorporates all products that melt at each 0.1°C interval within the melt range for an amplified sample. By analysing the data obtained at all points within the melt curve, all products that are melting are included in the final index of methylation. This approach enables non-uniform melt profiles to be more accurately analysed in comparison to other reported methods for analysing HRM data, for example, the T50 (Smith *et al.*, 2009) or the differential fluorescence peak (Malentacchi *et al.*, 2009), where only a single point in the melt curve is measured.

3.2.2 Validation of HRM assay detection of methylation differences

It has been reported that 3' end primer biasing can introduce amplification-bias-induced false positive results, and can lead to the overestimation of the number of methylated or unmethylated samples (Wojdacz and Hansen, 2006; Wojdacz and Dobrovic, 2007; Wojdacz *et al.*, 2008a; Wojdacz *et al.*, 2008b). However, analysis of the L1-HRM PCR products by pyrosequencing confirmed that the L1 elements amplified by the biased primers were heterogeneously methylated and that primer biasing did not enrich for L1 elements that were completely unmethylated at all CpGs. The mean methylation of all CpGs within the L1 target region analysed by pyrosequencing confirmed that there was dose dependent demethylation with 5-aza treatment compared to vehicle treated control cells, however it also demonstrated that the level of demethylation induced by 5-aza was not uniform across all of the CpGs. The non-CpG sequence variation of the L1 elements restricted the pyrosequencing analysis to only 6 out of the 13 CpG dinucleotides. As HRM will detect non-CpG polymorphisms there is the potential for these non-CpG variants to influence the melting profiles of the amplified L1 elements. When the L1-HRM assay was applied to bisulphite-unmodified gDNA from the 5-aza treated A11 cells following amplification with bisulphite-unmodified and methylation status-unbiased specific L1 primers, there was no difference in the melt curves of the unmodified genomic DNA (gDNA). This demonstrated that differences in the melt curves of the bisulphite modified 5-aza treated samples were due CpG differences.

Application of the assay to two other murine repetitive DNA elements demonstrated that the assay design can also be applied to other repeat elements.

The number of CpGs available for analysis within the smaller B1 elements precluded the design and use of unmethylated-biased primers to enhance sensitivity of detection, while the IAP_LTR element primers were able to be biased for unmethylated CpGs to enhance sensitivity. Although not significant, the IAP_LTR elements appeared to display a greater NTS difference between the 0.125 μM and 0.5 μM treated 5-aza samples relative to the B1 elements. While this may provide further evidence that biasing can increase the sensitivity to detect small changes in cytosine content, it could also indicate that the number of CpGs within a target region influence sensitivity. Biasing of primers for these elements to investigate demethylation following 5-aza treatment has not been reported, with only two studies investigating demethylation of B1 (Jeong and Lee, 2005) and IAP_LTR (Brunmeir *et al.*, 2010) elements following 5-aza treatment with doses ranging from 0.2 -1 μM . In both of these reports, only 3 CpGs were analysed compared to the 7 that were analysed in this thesis, and primers were not biased.

While good correlation between the L1-HRM assay and the LC-MS data was observed, the HRM assay is specific for L1 methylation, and may not reflect changes in cytosine content occurring elsewhere. The demonstration of methylation differences between the two 5-aza doses using the L1 assay suggests that either there is a difference in GC content at the L1 elements that is not reflected in the total genomic 5mdC content, indicating that L1 elements are more sensitive to 5-aza induced demethylation, or, that the L1 assay has greater sensitivity to detect small changes in DNA methylation. L1 elements have been shown in other studies to be relatively resistant to 5-aza induced demethylation compared to other sequences in the genome (Bender *et al.*, 1998). This suggests that the L1 assay is a

sensitive assay capable of detecting changes in L1 DNA methylation across the genome.

3.2.3 Reproducibility, sensitivity and linearity of the L1-HRM assay

Irahara *et al* (2010) analysed the precision and reproducibility of pyrosequencing to detect methylation differences, which is reported to be one of the most sensitive methods for methylation analysis. They demonstrated that variability arising from bisulphite modification ranged from 1.2 – 4.2%, and run to run variation for the pyrosequencing reactions ranged from 1.9 – 3.8% of the detected mean CpG methylation. The L1 assay presented here was shown to be as sensitive as the gold standard methods, with a 3% difference in NTS between samples detected. The sensitive nature of the L1-HRM assay as a result of biasing the primers was further demonstrated by the strong correlation of the assay with the pyrosequencing results. Assessment of the effect of PCR and bisulphite modification reaction variability on detection of methylation differences confirmed that the differences detected between samples was not due to inherent PCR or bisulphite modification variability, but due to differences in cytosine content.

In their human LINE1 element specific HRM assay, Stanzer *et al* (2010) reported that although linear, their assay had a low dynamic range, i.e. smaller methylation differences between samples were more difficult to detect. They surmised that this could in part be due to sequence variation between individuals at CpGs that may have undergone evolutionary deamination with conversion of the CpG's to TpG, resulting in a higher "background noise". From analysis of the consensus L1

sequence presented here, it was shown that: 1) the sequence variants occurred at a low frequency; 2) there was no significant difference in the melt curves of non-bisulphite modified gDNA; and 3) there was good correlation of the HRM data with LC-MS. Compared with pyrosequencing, the L1 assay is not as limited by the presence of non-CpG sequence variants or the size of the target region. The target region of a pyrosequencing assay is restricted to ~30 nucleotides, whereas the L1 assay as designed in this thesis incorporates an entire CpG island consisting of 13 CpGs spanning 192 bp (of the ~6 kb L1 element).

Tse *et al* (2011) in their paper describe a human LINE1 HRM assay. In their assay, the linearity of the assay was examined using ratios of completely methylated and unmethylated control DNA samples, and demonstrated a strong correlation between the predicted methylation level and HRM generated methylation value. A similar result was reported by Stanzer *et al* (2010) for their human LINE1 HRM assay. However, unlike the assay described in this thesis, the ability of the assays described by Tse *et al* (2011) and Stanzer *et al* (2010) to detect differences in melting temperature between heterogeneously methylated samples was not investigated. The murine L1-HRM assay developed here demonstrated a strong correlation with predicted methylation levels, and demonstrated linear detection of heterogeneously methylated samples ranging from 45 – 75% methylated. Based on previous reports of L1 methylation changes, complete demethylation of the repeat elements would not be expected in response to exogenous and endogenous modulators of DNA methylation, but it would be likely that changes would be heterogeneous (Estecio *et al.*, 2007; Igarashi *et al.*, 2010; Irahara *et al.*, 2010; Stanzer *et al.*, 2010; Aporn Dewan *et al.*, 2011).

3.2.4 Conclusion

In summary, the murine L1-HRM assay provides the ability to quantitatively measure L1 DNA methylation changes where individual CpG methylation data or mean percent (%) methylation is not sought. The assay has been shown to be reproducible and has the ability to detect small changes in methylation between heterogeneously methylated samples, providing a useful assay for studying methylation changes at repeat elements in response to exogenous agents in a mouse model. In experiments where limited template is available, or many samples need to be screened, the L1 assay provides a high-throughput, reproducible, in-house technique to screen for changes in DNA methylation. In subsequent chapters, the L1-HRM assay has been utilised to investigate the L1 methylation changes in response to both high and low dose radiation exposure, in particular the temporal nature of DNA methylation changes (Chapter 4), and the response of L1 methylation in ageing animals that were exposed to a low dose of radiation in early life (Chapter 5).

4 ANALYSIS OF REPEAT ELEMENT DNA METHYLATION CHANGES IN MOUSE STRAINS WITH DIFFERING RADIATION SENSITIVITIES FOLLOWING EXPOSURE TO IONISING RADIATION

Studies have demonstrated that different inbred mouse strains respond differently to radiation exposure. The BALB/c, CBA and C57Bl/6 strains are the most commonly utilised mouse strains in radiation research, and are classified as radiation-sensitive (BALB/c and CBA) or radiation-resistant (C57Bl/6). Their differences in radiosensitivity have been determined by investigating end-points such as time to lethality (Grahn and Hamilton, 1957; Kallman, 1962; Roderick, 1963; Lindsay *et al.*, 2007), chromosomal aberrations (Ponnaiya *et al.*, 1997; Hamasaki *et al.*, 2007), deficiencies in DNA repair (Biedermann *et al.*, 1991; Okayasu *et al.*, 2000; Hamasaki *et al.*, 2007) and the development of radiation-induced malignancies (Storer, 1967; Giotopoulos *et al.*, 2006; Jackson *et al.*, 2011).

DNA methylation is generally a stably inherited modification to DNA that affects gene expression by influencing chromatin structure, and is considered to be a key player in maintaining genome stability. It has been proposed that modulation of DNA methylation, namely a loss of methylation, may be involved in the development of radiation-induced malignancies (Giotopoulos *et al.*, 2006).

A number of studies have been conducted to investigate DNA methylation responses following radiation exposure. The majority of research has been

conducted in the radioresistant C57Bl/6 mouse strain with variable results. Table 4 (Chapter 1; page 41) outlines the experiments published to date investigating modulation of DNA methylation following ionising radiation exposure *in vivo* using mouse models. In these studies the liver, thymus, muscle and testis all display increases and decreases in global DNA methylation levels following doses ranging from 0.5 to 10 Gy. It also appears that these changes occurred quite early (<6 h) following irradiation. Many of the tissues and time-points demonstrate no change; some show a gain of methylation, while other studies demonstrate that the changes are dependent on whether the animal is male or female. The various studies also used a range of methods (HPLC, cytosine extension assay, methylation-specific PCR) to analyse methylation levels. The different methods, time-points of analysis, radiation doses, dose-rate and tissues investigated makes it difficult to compare studies. Although the BALB/c, CBA and C57Bl/6 mouse strains have been compared for other markers of genomic stability (such as chromosomal aberrations) following irradiation based on radiation-sensitivity status, only one study has investigated whether radiation-sensitivity influences the modulation of DNA methylation. In comparing C57Bl/6 and CBA mouse strains, Giotopoulos *et al* (2006) demonstrated that there was no difference in the baseline genomic DNA methylation levels of the tissues investigated (spleen and bone marrow) using HPLC, with only the bone marrow from the CBA mice demonstrating a change (loss) of methylation following irradiation with 3 Gy X-rays. These results suggest that tissue-specific modulation of DNA methylation following ionising radiation exposure may be influenced by the radiosensitivity of the mice. The aim of this chapter was to further investigate if radiosensitivity influences the modulation of DNA methylation *in vivo* by directly

comparing three mouse strains that differ in their radiosensitivity. This study was performed using the L1-HRM assay described in Chapter 3. It was hypothesised that increased radiation-sensitivity would influence the modulation of L1 DNA methylation, with the more radiosensitive mice (BALB/c and CBA) exhibiting a greater loss of L1 DNA methylation compared to the radioresistant C57Bl/6 mice. The L1 methylation levels of the spleen, a radiosensitive organ that has been shown to exhibit differences between the strains for other experimental end-points, was investigated in male and female mice at various time-points following irradiation.

4.1 Results

4.1.1 L1 methylation levels in mouse spleen 6-7 days following 1 Gy X-irradiation

Changes in L1 methylation were investigated in the spleen tissues of radioresistant C57Bl/6 and radiosensitive BALB/c and CBA mice 6-7 days following whole body irradiation with sham (0 Gy) and 1 Gy X-rays. Both male and female BALB/c mice irradiated with 1 Gy demonstrated a marked increase in L1 methylation compared with sham-irradiated mice (male: $P < 10^{-5}$; female: $P = 0.040$) (Figure 4-1), as did female CBA mice ($P = 0.009$). The BALB/c and CBA experiment was conducted twice, with the same result observed for both experiments. Figure 4-1 shows the mean of the two irradiation experiments for the BALB/c and CBA mice. Neither the 1 Gy treated male CBA mice nor the male or female C57Bl/6 mice demonstrated significant changes in L1 methylation level compared with the sham-irradiated mice.

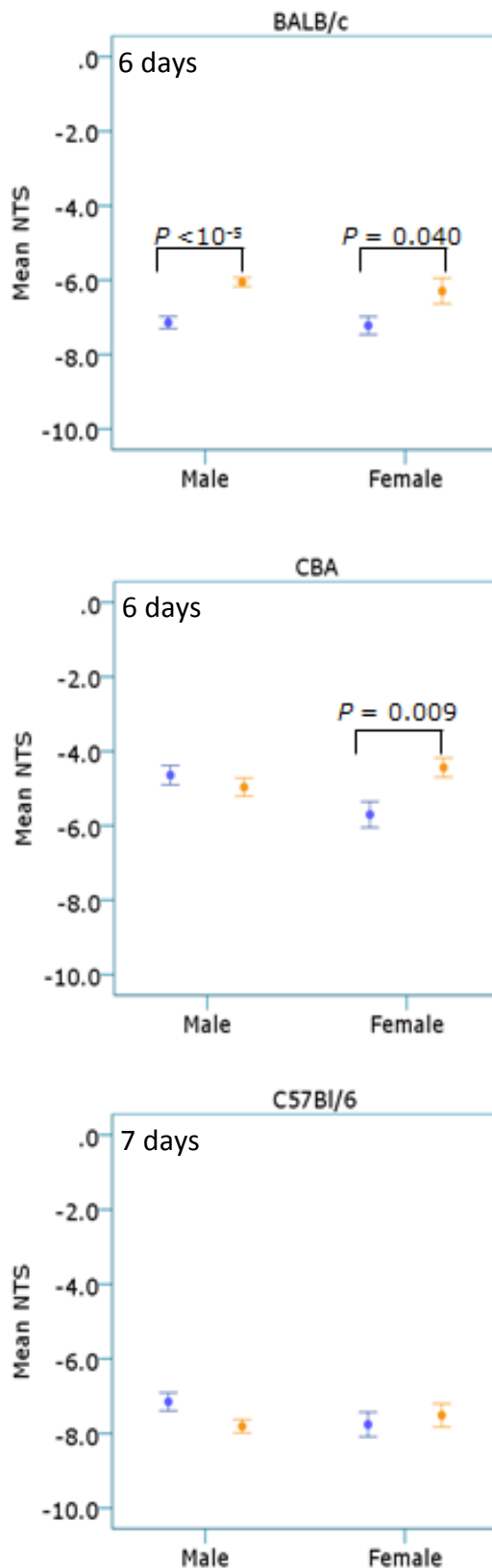


Figure 4-1: Spleen tissue L1 methylation in BALB/c, CBA and C57Bl/6 mice 6-7 days following irradiation with 1 Gy X-rays.

BALB/c, CBA and C57Bl/6 spleen tissue mean L1 NTS 6-7 days following sham (blue) or 1 Gy (orange) X-irradiation from male ($n = 4-5$ per treatment group) and female ($n = 5$ per treatment group) mice. L1 methylation was analysed following bisulphite modification of gDNA and amplification with L1 unmethylated-biased primers. The graphs for the BALB/c and CBA mice represent the mean of the results from two independent irradiation experiments. The effect of 1 Gy compared to sham-irradiation was analysed using the Independent Samples T-test, with significance achieved at $P < 0.05$. Error bars represent 1 SE.

4.1.1.1 Pyrosequencing analysis of spleen L1-HRM assay samples from male BALB/c and female CBA mice 6 days following 1 Gy X-irradiation

Pyrosequencing was used to determine the methylation levels at CpGs 7-12 of the L1-HRM PCR product target region in the male BALB/c and female CBA mice. The male BALB/c mice were analysed as these mice demonstrated the largest change in methylation following irradiation, while the female CBA mice were chosen as the male CBA mice did not demonstrate a change following irradiation. C57Bl/6 mice were not analysed as this strain did not demonstrate a change in L1 methylation levels following irradiation. Compared to sham-irradiated mice, male BALB/c mice treated with 1 Gy demonstrated significant increases in methylation at CpGs 7, 9, 10 and 12 (Table 10 and Figure 4-2A). The female CBA mice did not demonstrate significant differences between the treatment groups at any CpG, however they displayed a similar pattern of CpG methylation to that observed in the male BALB/c mice. For both the female CBA and male BALB/c mice, CpG 7 was the least methylated CpG and CpG 12 was the most methylated of the CpGs analysed. The mean methylation (Figure 4-2B) of all the CpGs analysed by pyrosequencing revealed a significant difference of 2.34% in methylation between the sham and 1 Gy irradiated male BALB/c mice ($P = 0.013$).

Table 10: L1 CpG methylation levels (%) for male BALB/c and female CBA mice 6 days following 1 Gy X-irradiation using pyrosequencing.

<i>CpG</i>	<i>Dose</i>			
	<i>0 Gy[#]</i>		<i>1 Gy[^]</i>	
	<i>Strain</i>		<i>Strain</i>	
	BALB/c	CBA	BALB/c	CBA
7	55.09	55.91	58.40	58.92
8	58.48	58.82	59.33	59.07
9	69.60	72.29	72.60	75.21
10	75.85	78.44	77.65	79.97
11	68.18	70.05	70.06	70.86
12	79.16	82.55	82.36	84.58
<i>Mean</i>	<i>67.73</i>	<i>69.68</i>	<i>70.07</i>	<i>71.44</i>
<i>SD</i>	<i>1.14</i>	<i>3.85</i>	<i>1.19</i>	<i>1.35</i>

[#]*n* = 4-5[^]*n* = 5

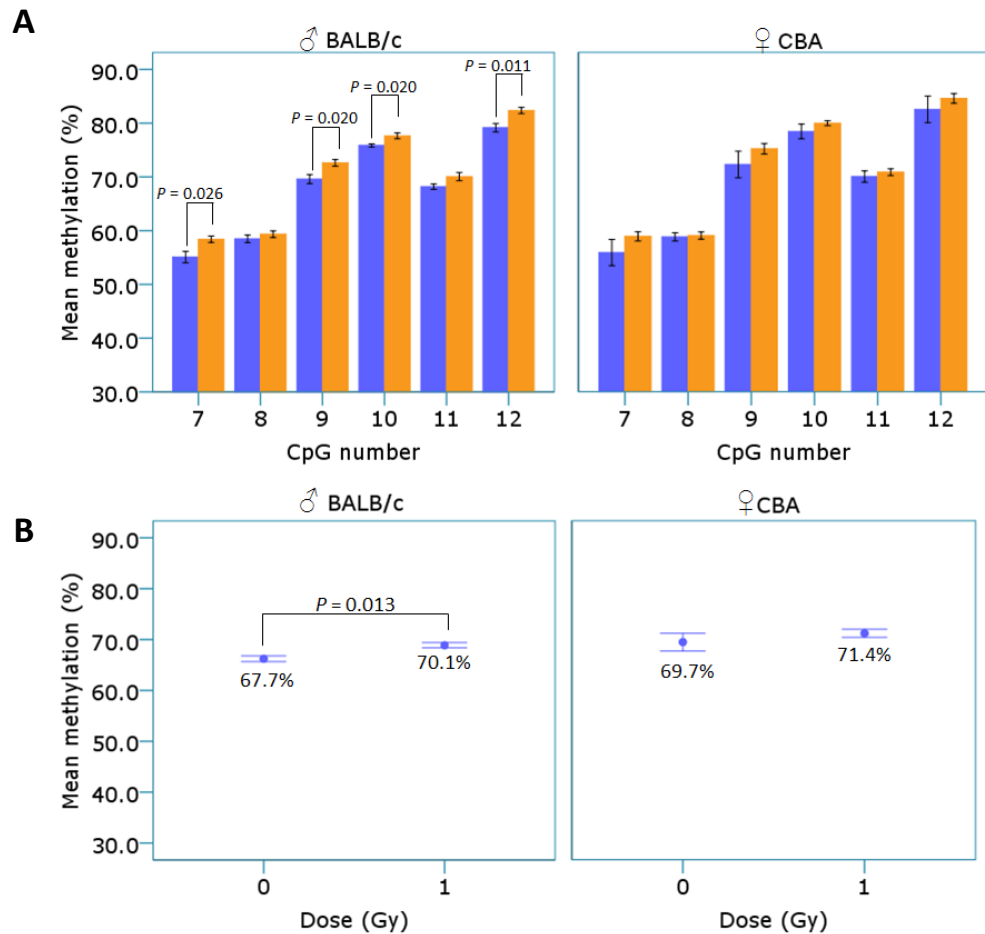


Figure 4-2: LC-MS and pyrosequencing analysis of spleen methylation levels in male BALB/c and female CBA mice 6 days following 1 Gy X-irradiation.

The effect of sham (0 Gy; blue) and 1 Gy (orange) X-irradiation on male BALB/c ($n = 4-5$ per treatment group) and female CBA mice ($n = 5$ per treatment group) spleen tissue DNA methylation at individual CpGs within the L1 element CpG island (CpGs 7-12) was analysed by pyrosequencing. (B) The mean methylation of all CpGs pyrosequenced in the sham and 1 Gy irradiated male BALB/c and female CBA mice. The effect of 1 Gy compared to 0 Gy was analysed using the Independent Samples T-test, with significance achieved at $P < 0.05$. Error bars represent 1 SE.

4.1.2 LC-MS analysis of male BALB/c and female CBA mouse spleen total genomic DNA methylation levels 6 days following 1 Gy X-irradiation

The total 5-methylcytosine (5mdC) content of splenic genomic DNA 6 days following 1 Gy and sham-irradiation was determined for the male BALB/c and female CBA mice using LC-MS (Figure 4-3). There was no significant difference in genomic 5mdC between the treatment groups for either strain.

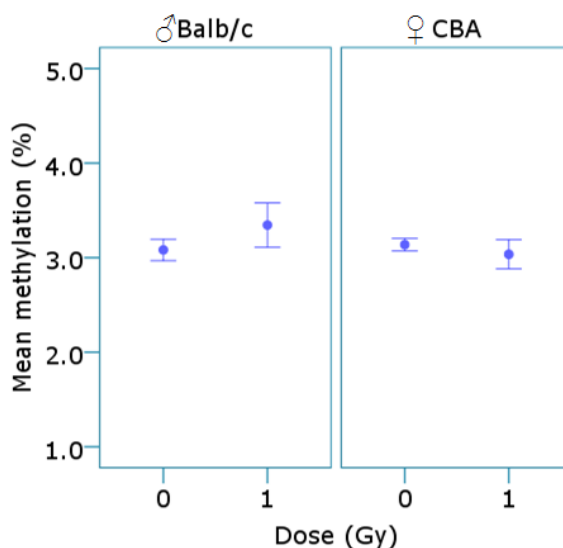


Figure 4-3: LC-MS analysis of total splenic genomic DNA methylation levels in male BALB/c and female CBA mice 6 days following 1 Gy X-irradiation.

Total genomic 5mdC content in spleen tissue of male BALB/c (n = 4-5 per treatment group) and female CBA mice (n = 5 per treatment group) 6 days following irradiation with sham or 1 Gy X-rays was analysed using LC-MS. Percent methylation was calculated as the ratio of 5mdC/dG. Error bars represent 1 SE.

4.1.3 B1 and IAP repeat element methylation levels of male and female BALB/c and CBA mouse spleen 6 days following 1 Gy X-irradiation

The mouse strains that demonstrated changes in L1 methylation were investigated for changes at other murine repeat elements. Spleen B1 and IAP_LTR element methylation changes in response to 1 Gy X-irradiation were also investigated in the BALB/c and CBA mice. The male BALB/c mice demonstrated a significant increase in B1 element methylation following 1 Gy irradiation ($P = 0.014$). A significant difference in B1 and IAP_LTR methylation for the female BALB/c mice and the male and female CBA mice was not detected (Figure 4-4).

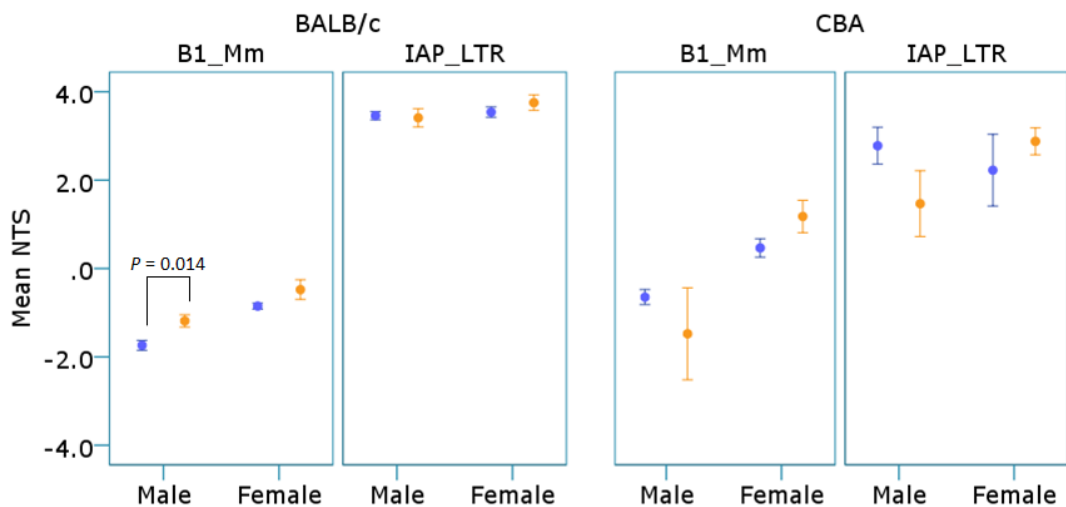


Figure 4-4: B1 and IAP repeat element methylation in spleen tissues from BALB/c and CBA mice 6 days following 1 Gy X-irradiation.

BALB/c and CBA spleen tissue mean NTS of B1 (B1_Mm) and Intracisternal-A-Particle Long Terminal Repeat (IAP_LTR) elements 6 days following sham (blue) or 1 Gy (orange) X-irradiation from male ($n = 4-5$ per treatment group) and female ($n = 5$ per treatment group) mice. B1 and IAP methylation was analysed following bisulphite modification of gDNA and amplification with methylation-status unbiased B1 or unmethylated-biased IAP_LTR primers. The effect of 1 Gy compared to sham-irradiation was analysed using the Independent Samples T-test, with significance achieved at $P < 0.05$. Error bars represent 1 SE.

4.1.4 Analysis of temporal spleen methylation changes in C57Bl/6 mice following 1 Gy X-irradiation

Previous studies have investigated the effect of high dose radiation exposure on total genomic 5mdC levels using the C57Bl/6 mouse strain (Table 1, page 41). These studies analysed methylation levels at time-points ranging from 6 hours to 4 weeks post- irradiation and demonstrated that methylation levels varied at the different time-points. As no change in L1 methylation levels was observed at 7 days post-irradiation in the C57Bl/6 mice, L1 methylation levels in the spleen were investigated at time-points ranging from 7 h to 14 days following irradiation with 1 Gy. Archival frozen tissues were utilised for these experiments. Each time-point represents an individual irradiation experiment with its own sham-irradiated control, this data were normalised to the mean of the sham-irradiated mice for each experiment.

A significant increase in L1 methylation was observed 1 day following irradiation with 1 Gy compared to sham-irradiated mice ($P = 0.048$) (Figure 4-5). By 3 days post- irradiation, L1 methylation levels had returned to that of the sham-irradiated mice. By 14 days post- irradiation, a significant loss in L1 methylation was detected for mice treated with 1 Gy ($P = 0.001$). Although there was an even distribution of male and female mice across the treatment groups for each time-point, there were not enough mice of each sex in each treatment group to analyse for sex differences.

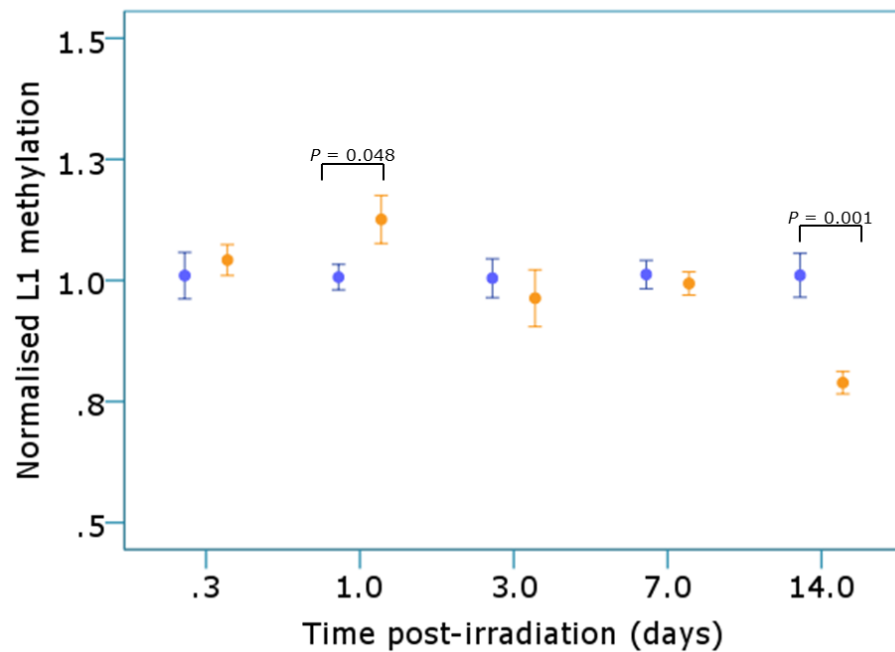


Figure 4-5: L1 methylation levels in C57Bl/6 spleen tissue up to 14 days following irradiation with 1 Gy X-rays.

C57Bl/6 mouse spleen tissue L1 methylation levels were analysed 0.3 days (7 h) to 14 days following sham-irradiation (blue) or irradiation with 1 Gy (orange) X-rays (n = 4-6 per treatment group) following bisulphite modification of gDNA and amplification with unmethylated-biased primers. Data were normalised to the mean NTS of the sham-irradiated mice at each time-point. The effect of 1 Gy compared to sham-treatment was analysed using an Independent Samples T-test, with significance achieved at $P < 0.05$. Error bars represent 1 SE.

4.1.4.1 Pyrosequencing analysis of spleen L1 methylation changes in C57Bl/6 mice 1 and 14 days following 1 Gy X-irradiation

Pyrosequencing revealed no difference between the treatment groups at 1 day post-irradiation at individual CpGs (CpGs 7-12) within the L1-HRM target region (Figure 4-6A). Regardless of radiation dose, CpG 12 had statistically greater methylation compared with all CpGs ($P < 10^{-5}$ vs. CpGs 7, 8 and 11; $P = 0.006$ vs. CpG9; $P = 0.027$ v CpG10; ANOVA with Bonferroni *post-hoc* analysis), while CpG 8 was the least methylated compared with all CpGs ($P < 10^{-5}$ vs. CpGs 9, 10 and 12; $P =$

0.001 vs. CpG7; $P = 0.006$ vs. CpG11; ANOVA with Bonferroni *post-hoc* analysis). At 14 days post-irradiation, there was a significant reduction in methylation at CpGs 7, 9 and 12 ($P = 0.009$, $P = 0.005$ and $P < 10^{-5}$ respectively) within the L1-HRM target region (Figure 4-6B). There was a significant reduction in the mean methylation of all CpGs pyrosequenced ($P < 10^{-5}$) for 1 Gy irradiated mice compared to sham-irradiated mice 14 days post-irradiation.

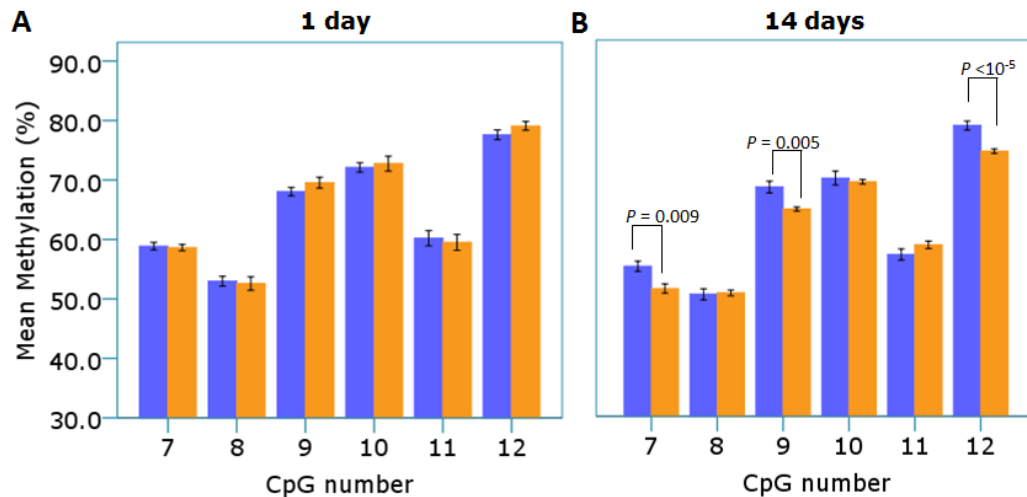


Figure 4-6: Pyrosequencing analysis of spleen methylation levels from C57Bl/6 mice 1 and 14 days following irradiation with 1 Gy X-rays.

The effect on the methylation of CpGs 7-12 within the L1 HRM-PCR target region (A) 1 day ($n = 5$ per treatment group) and (B) 14 days ($n = 6$ per treatment group) following sham (blue) and 1 Gy (orange) X-irradiation was analysed using pyrosequencing. The difference in methylation between sham and 1 Gy at each CpG was assessed using the Independent Samples T-test, with significance achieved at $P < 0.05$. Error bars represent 1 SE.

4.1.4.2 LC-MS analysis of spleen tissue genomic DNA from C57Bl/6 mice 1 and 14 days following 1 Gy X-irradiation

No change in 5mdC content was detected by LC-MS in the spleen tissues of C57Bl/6 mice 1 (Figure 4-7A) and 14 (Figure 4-7B) days following irradiation with sham and 1 Gy X-rays.

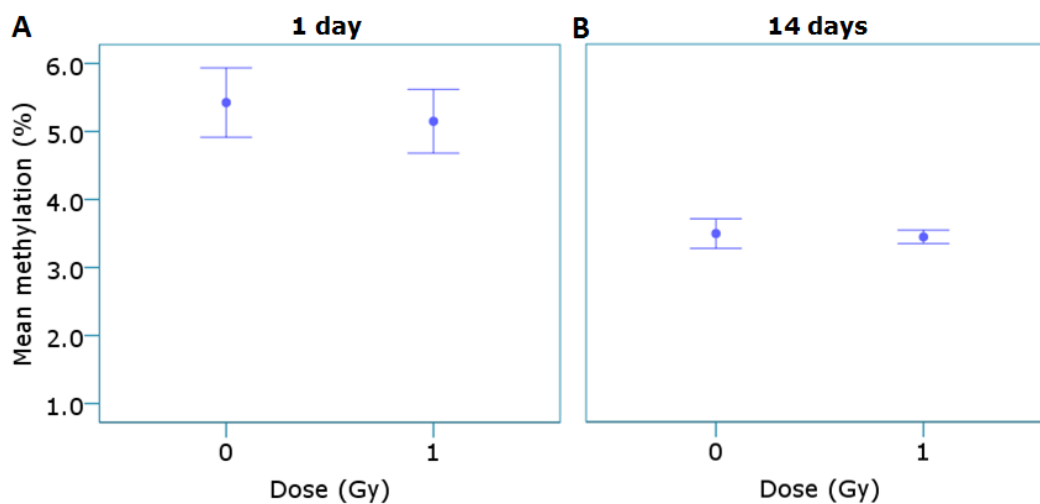


Figure 4-7: LC-MS analysis of spleen genomic 5mdC levels from C57Bl/6 mice 14 days following irradiation with 1 Gy X-rays.

Total genomic 5mdC levels in the spleen tissues of sham or 1 Gy X-irradiated C57Bl/6 mice (A) 1 day (n = 5 per treatment group) and (B) 14 days (n = 6 mice per treatment group) following irradiation was assessed using LC-MS. Error bars represent 1 SE.

4.1.4.3 Spleen B1 and IAP element methylation levels in C57Bl/6 mice 14 days following 1 Gy X-irradiation

The greatest difference in L1 NTS in the C57Bl/6 mice was observed between sham and 1 Gy irradiated mice at 14 days following irradiation. Therefore, the methylation levels of the B1 and IAP_LTR elements at this time-point were also analysed (Figure 4-8). A significant loss of methylation at the IAP_LTR elements was observed ($P = 0.003$). While not significant ($P = 0.059$), the B1 elements also showed a trend towards a loss of methylation.

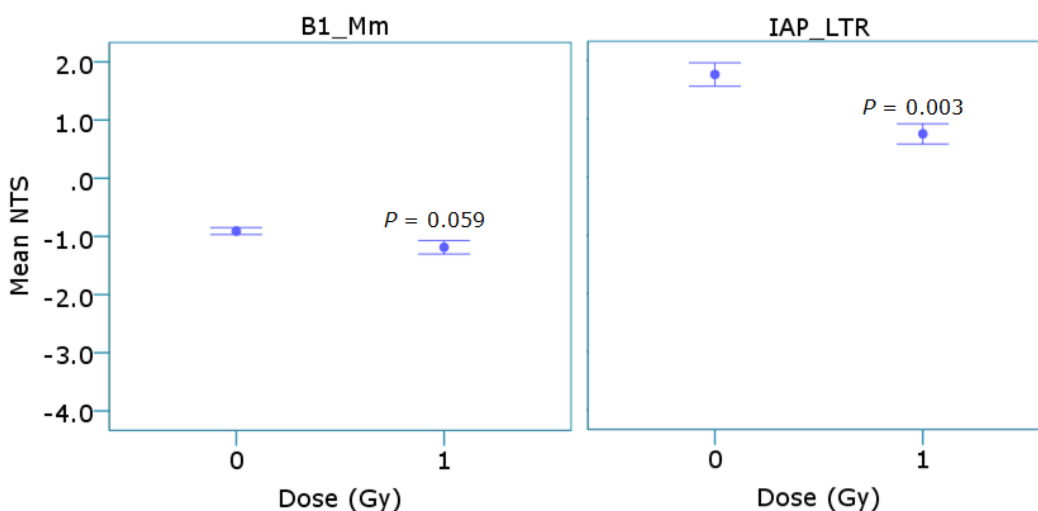


Figure 4-8: C57Bl/6 mouse spleen tissue B1 and IAP element methylation 14 days following irradiation with 1 Gy X-rays.

C57Bl/6 mouse spleen tissue mean NTS of B1 and IAP_LTR repeat elements 14 days following sham (0 Gy) or 1 Gy X-irradiation (n = 6 per treatment group) was analysed following bisulphite modification of gDNA and amplification with unbiased-B1 and unmethylated-biased IAP_LTR primers. The effect of 1 Gy compared to 0 Gy was analysed using an Independent Samples T-test, with significance achieved at $P < 0.05$. Error bars represent 1 SE.

4.1.4.4 Pyrosequencing analysis of the methylation changes at all CpGs within the L1-HRM assay target sequence in the spleens of C57Bl/6 mice 14 days following 1 Gy X-irradiation

Following the observation that the loss of methylation at CpGs 7-12 within the L1 target region was not uniform across all CpGs 14 days following 1 Gy X-irradiation, the methylation levels of CpGs 2-6 was assessed. However, the cluster of non-CpG SNPs at the 5' end of the L1-HRM target amplicon inhibited the design of a suitable assay that could pyrosequence CpGs 2-6 (see Section 3.1.3.1). Therefore, in order to assess the methylation levels of CpGs 2-6, the dispensation order of the pyrosequencing assay was altered so that the SNPs that occur at the beginning of the L1 amplicon were not included in the assay. Briefly, where a SNP occurred in the sequence, for example, in the case of an A/G, rather than an R being placed at the nucleotide position indicating to the pyrosequencing assay program (Pyro Q-CpG) that at that particular location within the target sequence there could be an A or a G (Figure 4-9A), the dominant SNP was placed first in the sequence followed by the less common base (Figure 4-9B). This proved to be a successful approach with all 11 CpGs (not including the CpGs located within the primer binding sites) being successfully pyrosequenced (Figure 4-10).

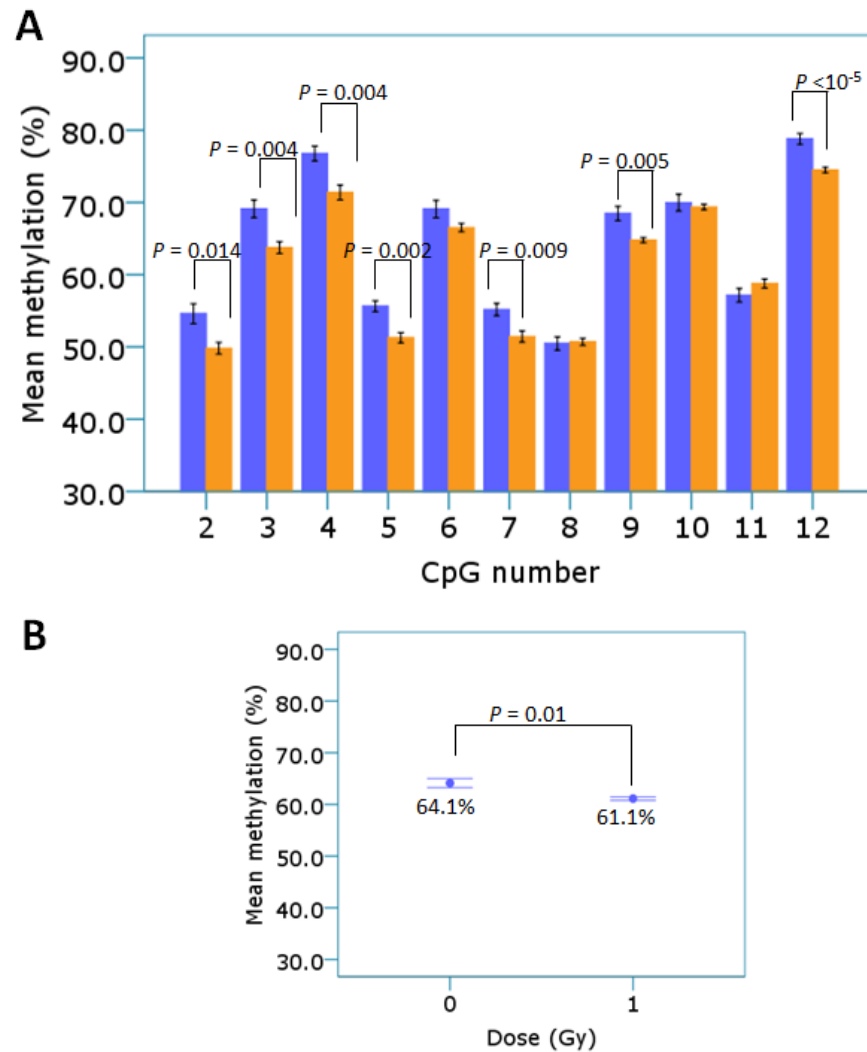


Figure 4-10: Pyrosequencing analysis of all CpGs within the L1 CpG island of spleen samples from C57Bl/6 mice 14 days following irradiation with 1 Gy X-rays.

(A) The effect of sham (0 Gy; blue) and 1 Gy (orange) X-irradiation on L1 methylation levels in the spleens of C57Bl/6 mice ($n = 6$ per treatment group) 14 days following irradiation was assessed by pyrosequencing CpGs 2-12 of the L1-HRM PCR products. (B) The mean methylation of all CpGs pyrosequenced was determined. The effect of 1 Gy compared to sham-treatment was analysed using an Independent Samples T-test, with significance achieved at $P < 0.05$. Error bars represent 1 SE.

4.1.4.5 L1 promoter analysis

Lee *et al* (2010b) reported that within the mouse L1 promoter, two transcription factor binding sites, Ying Yang-1 (YY1) and E2F, appear to be conserved. Athanikar *et al* (2004) reported that human L1 elements require YY1 for transcription. Analysis of the L1 consensus promoter from this study using TFSearch (<http://www.cbrc.jp/htbin/nph-tfsearch>) demonstrated the presence of several intact YY1 (CGGTCGCCATCTTGGT) and E2F (CAGAGAA) transcription factor binding sites. One YY1 binding site was located within the L1 amplicon sequence and incorporated CpGs 8 and 9 (Figure 4-11A). It has been reported that besides needing intact YY1 binding sites, the L1 promoter also needs to contain a minimum of 2 monomer repeat sequences (DeBerardinis and Kazazian, 1999). Comparison of the consensus L1 promoter sequence features (monomer positions and YY1 and E2F binding sites) with that reported by Lee *et al* (2010b) for mouse L1 promoters (Figure 4-11B and C) demonstrated that the L1 promoter sequence from this study has the same structure as the actively transcribed L1 elements described by Lee *et al* (2010b). Furthermore, the target L1 sequences amplified in this study are from the T family, reported to be the L1 elements most capable of being transcribed (DeBerardinis *et al.*, 1998; Naas *et al.*, 1998).

A

CpG 1 2 3 4 5 6 7

GCTGAGGCAGCACCCCTKTGTGGGCCGGGGACAGCCRGCCACCKTCCGGRCCRGAGGACAGGTGCCYRCCCGGCTGGGGAGGCCGRCTAAGCCA

8 9 10 11 12 13

CAGCAGCAGCGGTCCGCATCTTGGTCCGRGACCCGCCGAACCTAGGAAATTAGTCTGAACAGGTGAGAGGGTCCGCAGAGAACTTGACAGCT

TCTGGAACAGGCCGGAAGCACAGAGGCGCTGAGGCAGCACCCCTTTGTGGGCCGGGGACAGCCAGCCACCGTCCGGACCGGAGGACAGGTGCC

GCCCGGCTGGGGAGGCGGCCTAAGCCACAGCAGCAGCGGTCCACCATCTTGGTCCGAGACCCGCCGAACCTAGGAAATTAGTCTGAACAGGTGA

GAGGGTGCGCAGAGAACTTGACAGCTTCTGGAACAGGCAGAAGCACAGAGGCGCTGAGGCAGCACCCCTTTGTGGGCCGGGGACAGCCGGCCA

CCTTCCGGACCGGAGGACAGGTGCCACCCGGCTGGGGAGGCGGCCTAAGCCACAGCAGCAGCGGTCCGCATCTTGGTCCCGAGACTCCAAG

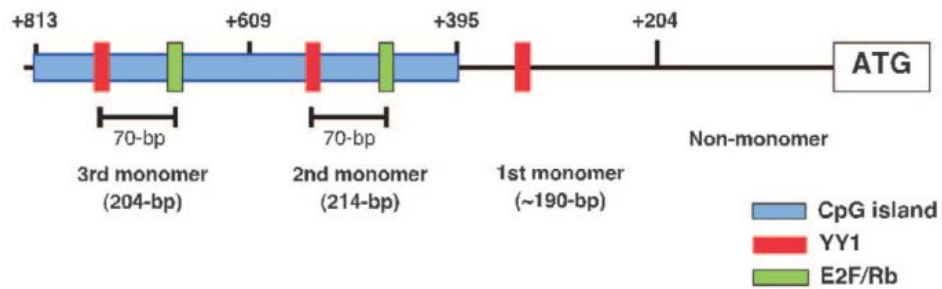
GAACCTAGGAAATTAGTCTGCTTAGGTGAGAGTCTGTACCACCTGGGAACTGCCAAAGCAACACAGTGTCTGAGAAAGGTCCTGTTTTGGGCC

ATCTTCTFCGCCAGGAGGAGGTCCAAATACAAGATATCTGCGCACCTTCCCTGTAAGAGAGCTTGCACAGAGAGTGTCTGAGCACTGAAA

CTCAGAGGAGAGAATCTGTCTCCAGGTCTGCTGATAGACGGTAACAGAATCACCAGAAGAACAATCTCTAAACAGAGTCAACTATAACTACTA

ACTCCAGAGATTACCAGATG

B



C

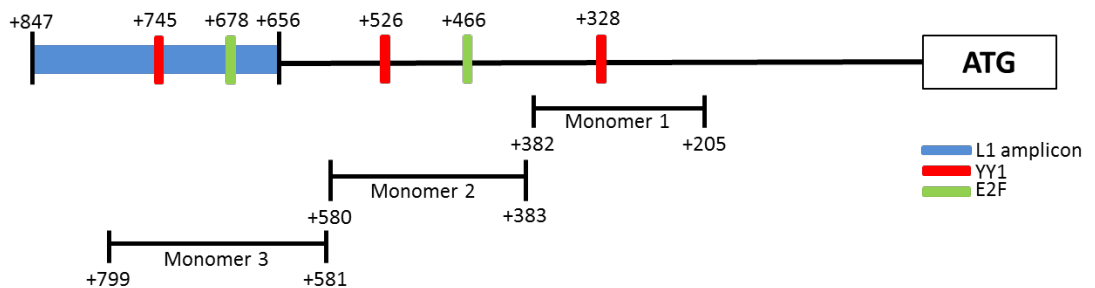


Figure 4-11: Analysis of the L1 promoter sequence.

The promoter sequence downstream of the L1 amplicon sequence was analysed for features reported to be associated with actively transcribed L1 elements. (A) The promoter sequence is shown with the L1 amplicon sequence highlighted in **bold** and the CpGs shaded grey and numbered 1 - 13. Transcription factors YY1 (solid red box) and E2F (solid green box) binding sites are shown within Monomers 3 (dark blue outline), 2 (light blue outline) and 1 (red outline). (B) The schematic of the mouse L1 promoter by Lee et al (2010b). The vertical lines indicate the position and numbering of repeat sequence monomers; the boxes represent the transcription factor binding sites, YY1 (solid red box) and E2F (solid green green). The corresponding position of the CpG island in relation to the transcription start site (ATG) is illustrated by the light blue box. (C) Schematic of the consensus L1 promoter from this study. The complete promoter sequence and ORFs 1 and 2 are in Appendix D.

Primers specific for the L1 open reading frame 1 (ORF1) and open reading frame 2 (ORF2) sequences were used to investigate the transcription of the L1 repeat elements (Muotri *et al.*, 2010) (see Appendix B for primer sequences and Appendix D for location within the L1-HRM assay promoter sequence). Gene expression studies require multiple stably expressed reference genes (RGs) for qPCR data normalisation (Bustin *et al.*, 2010). Therefore, 7 RGs were chosen based on previous use in our laboratory (*pol2rc*), historically used RGs (*Gapdh* and *Rn18s*), and genes selected using the program Genevestigator[®] (*Coch*, *Cpb-1*, *Pnlip* and *Spic-c*). Briefly, Genevestigator[®] is an open access program whereby researchers can deposit gene expression data and microarray studies. These studies are grouped by species, treatments, tissues and other variables. The program has been designed for the identification of genes that are unaffected by treatment and other experimental variables that may be suitable as RGs. A RG is one which remains unaffected by treatment and is expressed at similar levels to the target genes. Therefore, a spleen

cDNA sample was screened with all candidate RGs (data not shown). RGs were automatically excluded if they had poor amplification or failed to amplify at the T_m which was specific for the ORF primers. The ORF primers amplified very early compared with the RG primers. One RG (*Rn18s*) failed to amplify under the conditions which were specific for all of the other primers, while *Cpb-1* and *Pnlip* had poor/late amplification. For all L1 transcript experiments, the candidate RGs *Gapdh*, *Pol2rc*, *Coch* and *Spi-c* were included in the assay. The most stable RGs to which the data could be normalised were determined using geNorm, within the program qbase^{PLUS}.

Spleen tissue RNA from mice culled 14 days following irradiation with sham or 1 Gy was amplified for the four RGs (*Gapdh*, *Pol2rc*, *Coch*, and *Spi-c*). GeNorm analysis determined that *Coch* and *Pol2rc* were the two most stable RGs and thus all data were normalised to these genes (data not shown).

There was no significant change in the level of ORF1 or ORF2 transcripts observed following irradiation with 1 Gy (Figure 4-12). Samples were analysed in two separate reverse-transcription and qPCR experiments. The transcript levels did not correlate with the pyrosequencing mean methylation or LC-MS data (Table 11).

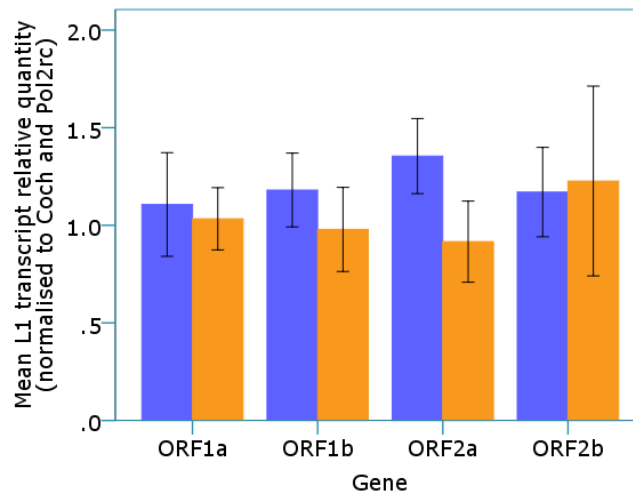


Figure 4-12: L1 transcript levels in the spleen tissues of C57Bl/6 mice 14 days following irradiation with sham or 1 Gy X-rays.

The relative L1 ORF 1 (primer sets a and b) and ORF2 (primer sets a and b) transcript levels were analysed in the spleens of C57Bl/6 mice (n = 4-5 mice per treatment group) 14 days following sham (blue) or 1 Gy (orange) X-irradiation. *qBase^{PLUS}* was used to normalise qPCR data values to the geometric mean of the reference genes Coch and Pol2rc (Hellemans et al., 2007). Error bars represent 1 SE.

Table 11: Correlation of L1 transcript levels with LC-MS and pyrosequencing mean methylation.

	<i>ORF1a</i>		<i>ORF1b</i>		<i>ORF2a</i>		<i>ORF2b</i>	
	correlation coefficient [#]	<i>P</i> -value						
LCMS	-0.286	0.493	0.071	0.867	0	1	0.048	0.911
Pyro*	0.317	0.406	0.517	0.154	0.517	0.154	0.217	0.579

[#]Spearman's rho non-parametric analysis

*Mean methylation of all CpGs pyrosequenced

To determine if a loss of methylation at the L1 promoter was associated with increased L1 transcription, 5-aza treated A11 cell line samples (see Section 3.1.2) were analysed. For all 7 RGs, an effect of 5-aza treatment was observed, and thus all 7 RGs were unsuitable for data normalisation. Therefore, expression data was normalised to RNA input using the Δ Ct method. Only one primer set for each L1-

ORF was analysed. The L1-ORF1 transcript levels were not significantly altered following treatment with 0.5 μM 5-aza. Although not significant ($P = 0.066$), there was a trend towards increased L1-ORF2 transcript levels following treatment with 0.5 μM 5-aza compared to the vehicle treated cells (Figure 4-13).

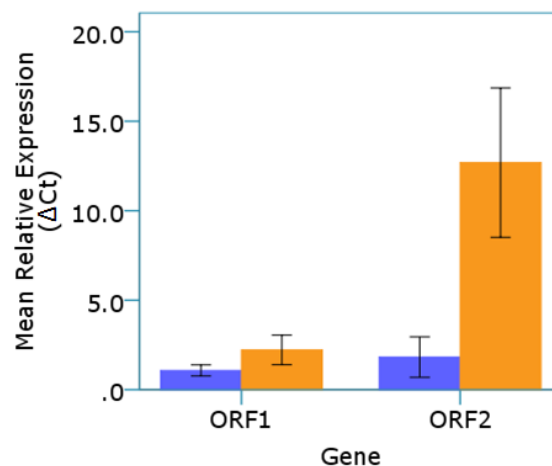


Figure 4-13: L1 transcript expression in 5-aza treated A11 cells.

The relative expression of ORF1 and ORF2 transcripts were analysed in A11 cells 24 h following treatment with vehicle control (DMSO – blue) or 0.5 μM 5-aza (orange) ($n = 3$). Relative quantification of L1 transcript quantity was calculated based on RNA input (ΔCt). Error bars represent 1 SE.

4.1.4.6 Analysis of histone H3 tri-methylation in the spleens of C57Bl/6 mice 14 days following 1 Gy X-irradiation

DNA methylation along with histone modifications influences chromatin structure. Heavily methylated regions of the genome are associated with repressive histone marks, such as the tri-methylation of histone H3 lysine 9 residue (H3me3K9). A preliminary experiment was performed to assess the relative abundance of H3me3K9, by Western Blot analysis in the C57Bl/6 mice 14 days following

irradiation with sham or 1 Gy (Figure 4-14A). In the mice treated with 1 Gy, there was a trend towards a loss of tri-methylation at lysine 9 ($P = 0.054$) (Figure 4-14B). However, the experiment needs to be repeated due to the uneven loading of sample, evident in the total histone H3 band (upper panel).

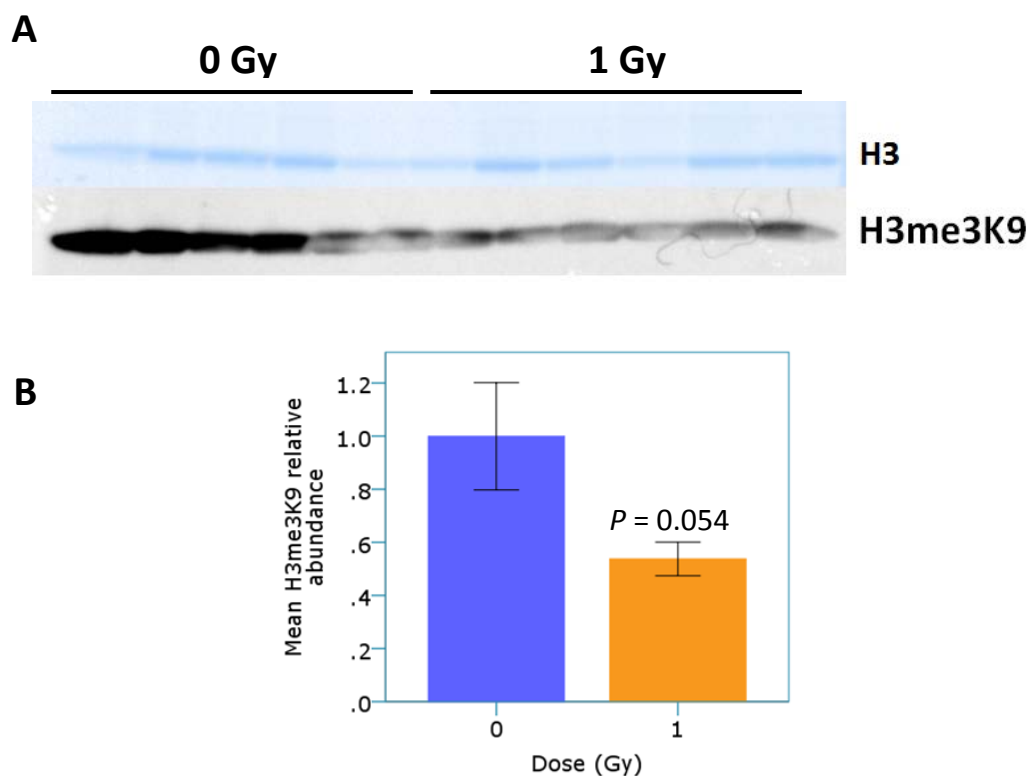


Figure 4-14: Analysis of histone H3 tri-methylation in spleen tissue of C57Bl/6 mice 14 days following 1 Gy X-irradiation.

The tri-methylation of histone H3 lysine 9 (H3me3K9) in C57Bl/6 mice 14 days following sham or 1 Gy X-irradiation ($n = 6$ per treatment group). (A) Histone proteins were acid extracted from three 25 μ M frozen spleen sections, quantitated and 10 μ g of lysate loaded onto a CriterionTMTGXTM Stain-Free pre-cast gel. Proteins were transferred to PVDF and probed with a rabbit anti-H3me3K9 antibody. The gel (top row) was imaged and total histone H3 protein was used as a loading control to normalise antibody band intensity (bottom row). (B) The H3me3K9 band intensity was normalised to the mean of the total H3 gel band and fold relative abundance of 1 Gy X-irradiated mice (orange) was normalised to the mean of the sham-irradiated mice (blue) of two western blot experiments. The effect of 1 Gy compared to sham-treatment was analysed using an Independent Samples T-test, with significance achieved at $P < 0.05$. Error bars represent 1 SE.

4.1.5 Analysis of spleen temporal L1 methylation changes in BALB/c and CBA mice following 1 Gy X-irradiation

Changes to spleen L1 methylation at a time-point prior to and after 6 days following sham or 1 Gy X-irradiation were analysed in the BALB/c and CBA mice for comparison with the results observed for the C57Bl/6 mice in Section 4.1.4, and to the data obtained at 6 days following irradiation observed for the BALB/c and CBA mice in Section 4.1.1.

At 1 day post-irradiation, female BALB/c and male CBA mice demonstrated a significant increase in L1 methylation following irradiation with 1 Gy (female BALB/c: $P < 10^{-5}$; male CBA: $P = 0.008$). The male BALB/c ($P = 0.106$) and the female CBA ($P = 0.256$) mice did not demonstrate a significant increase at 1 day following irradiation with 1 Gy. As discussed in Section 4.1.1, the male ($P < 10^{-5}$) and female ($P = 0.040$) BALB/c and the female CBA ($P = 0.009$) mice demonstrated a significant increase in methylation at 6 days post-irradiation with 1 Gy. The male CBA mice did not demonstrate a change following irradiation at 6 days ($P = 0.340$). By 14 days following irradiation with 1 Gy, there was no difference in L1 methylation levels compared to sham-irradiated mice in either strain (Figure 4-15).

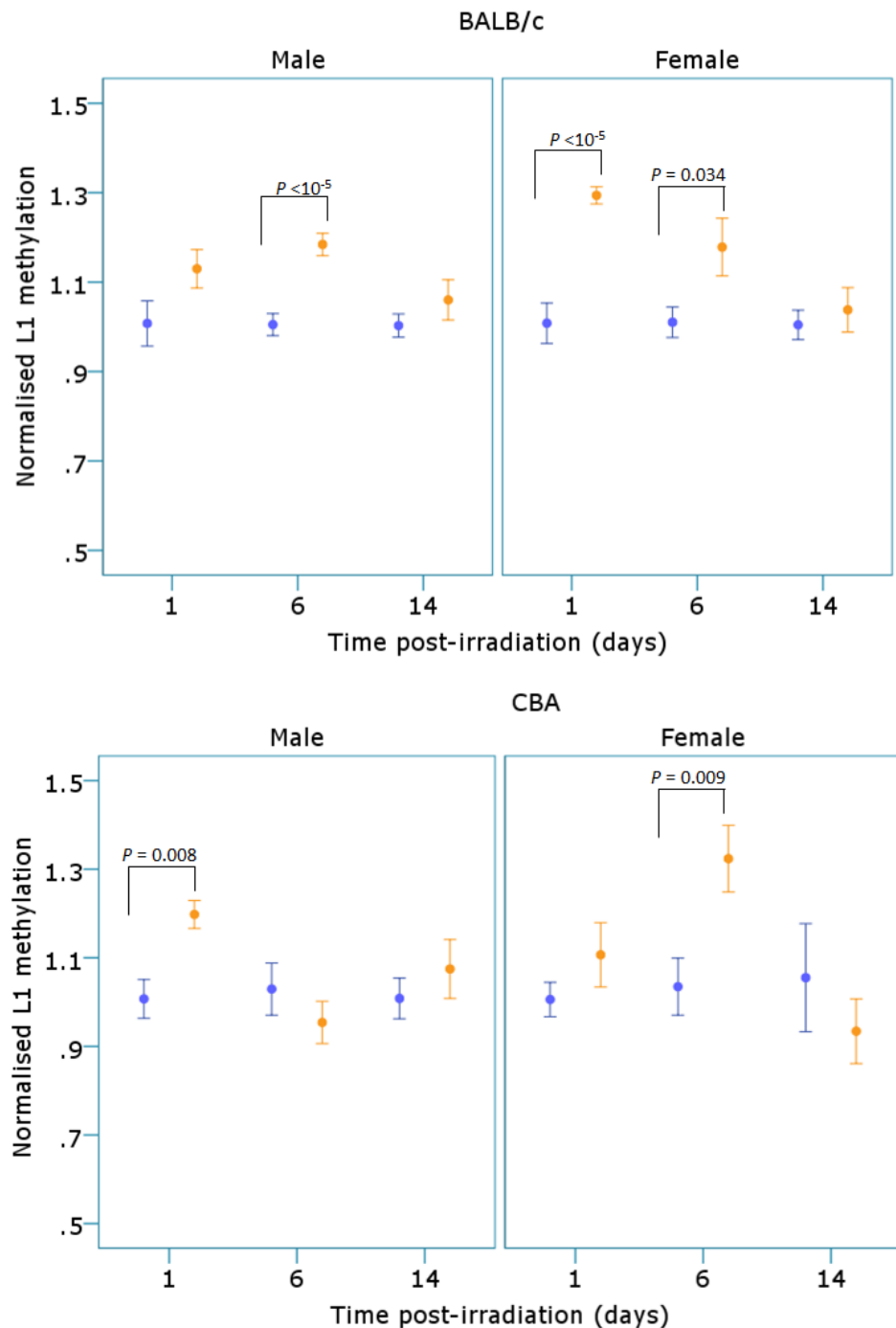


Figure 4-15: BALB/c and CBA L1 methylation levels 1, 6 and 14 days following irradiation with 1 Gy X-rays.

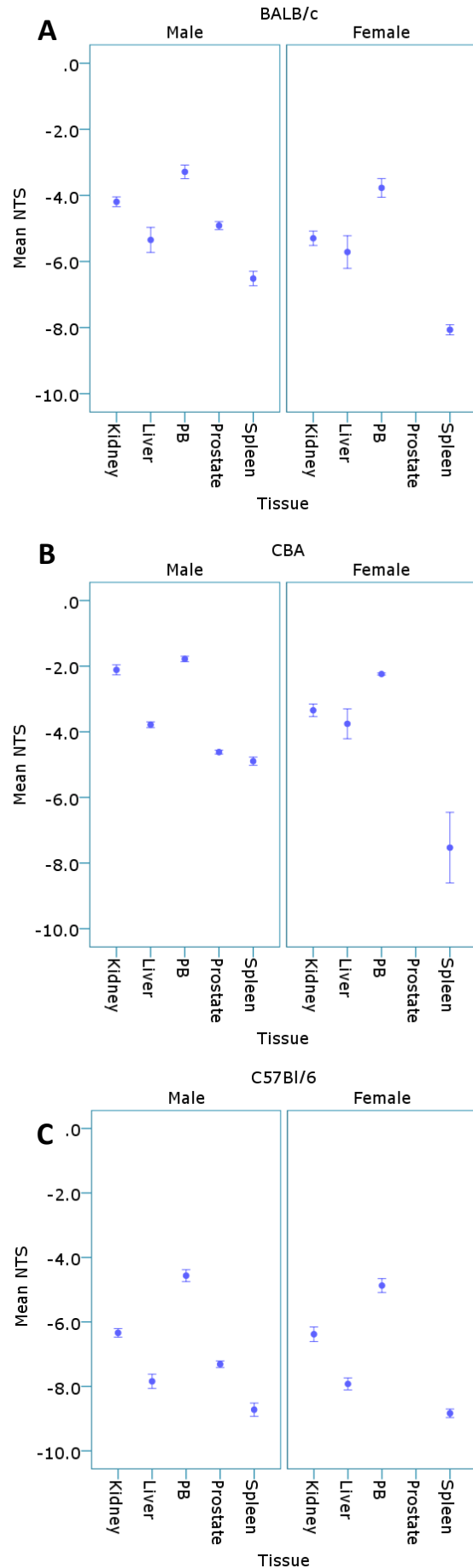
The spleen tissue L1 methylation levels of male ($n = 4-5$) and female ($n = 5$) BALB/c and CBA mice 1, 6 and 14 days following sham (blue) or 1 Gy (orange) X-irradiation was analysed following bisulphite modification and amplification of gDNA with unmethylated-biased primers. Data was normalised to the mean NTS for the sham-irradiated mice for each time-point. The effect of 1 Gy compared to sham-treatment was analysed using an Independent Samples T-test, with significance achieved at $P < 0.05$. The 6 days post-irradiation data is from Figure 4-1. Error bars represent 1 SE.

4.1.6 Tissue L1 methylation levels of untreated BALB/c, CBA and C57Bl/6 mice

Kidney, liver, peripheral blood (PB), prostate and spleen gDNA from 2-3 month old male and female BALB/c, CBA and C57Bl/6 mice were analysed using the unmethylated-biased L1 primers (Figure 4-16). Analysis of the NTS values revealed strain, tissue and gender differences in L1 methylation levels; with the PB samples displaying the highest L1 methylation and the spleen tissue the lowest L1 methylation for male and female mice from the three strains. In all mice, the order of L1 methylation from highest to lowest was as follows: PB > kidney ≥ liver ≥ prostate > spleen. For BALB/c mice, higher methylation was also observed in the male kidney ($P = 0.030$) and spleen ($P = 0.010$) tissues compared to the females, and for CBA mice, higher methylation was observed in the male kidney ($P = 0.010$), PB ($P = 0.010$) and spleen ($P = 0.028$) tissues relative to female mice ($P < 10^{-5}$, ANOVA with Bonferroni *post-hoc* analysis). For C57Bl/6 mice, there was no difference in L1 methylation levels in any of the tissues studied between the male and female mice. The female CBA mice demonstrated greater L1 methylation levels compared to both the BALB/c and C57Bl/6 female mice for all tissues except the spleen; while the male CBA mice demonstrated higher L1 methylation of the kidney, liver, PB and prostate tissues compared to both the BALB/c and C57Bl/6 male mice ($P < 10^{-5}$, ANOVA with Bonferroni *post-hoc* analysis). There was no difference in the spleen L1 methylation levels for the male and female mice from all three strains. Across the strains and for both male and female mice, the order of highest to the lowest L1 methylation levels for all tissues was CBA > BALB/c > C57Bl/6.

Figure 4-16: L1 methylation in various tissues from the BALB/c, CBA and C57Bl/6 mouse strains.

The L1 methylation levels in the kidney, liver, peripheral blood (PB), prostate and spleen tissues of untreated 2-3 month old male (n = 5) and female (n = 5) (A) BALB/c, (B) CBA and (C) C57Bl/6 mice was assessed following bisulphite modification and amplification with the unmethylated-biased primers. Error bars represent 1 SE.



A comparison of the methylation-status unbiased primers on the male BALB/c tissues showed hierarchy of tissue L1 methylation that correlated with the NTS for the unmethylated-biased primers (Figure 4-17; $P < 0.01$, Pearson correlation). However, the methylation-status unbiased primers did not demonstrate significant differences in L1 methylation between all tissues. For example, the spleen was less methylated at L1 elements compared with all other tissues when analysed with the unmethylated-biased primers (ANOVA, with Bonferroni *post-hoc*; $P < 0.05$); whereas the unbiased primers only demonstrated significant lower L1 methylation of the spleen when compared with the PB samples (ANOVA, with Bonferroni *post-hoc*; $P = 0.045$).

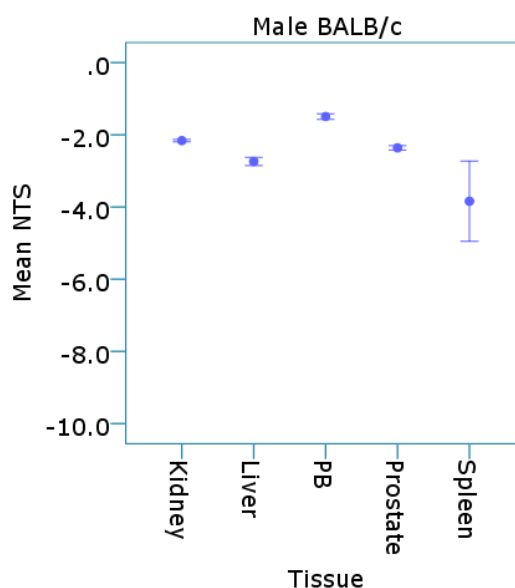


Figure 4-17: Analysis of male BALB/c tissue panel with methylation-status unbiased L1 primers.

The L1 methylation levels in the kidney, liver, peripheral blood (PB), prostate and spleen tissues of untreated 2-3 month old male ($n = 5$) BALB/c mice was assessed following bisulphite modification and amplification with the methylation-status unbiased primers. Error bars represent 1 SE.

4.1.7 Tissue responses 6 days following 1 Gy X-irradiation in male and female BALB/c and CBA mice

The L1 methylation levels of tissues other than the spleen in the BALB/c and CBA mice (kidney, liver, prostate and PB) were analysed to determine if there were changes in L1 methylation 6 days following 1 Gy X-irradiation similar to those observed previously in the spleen (Table 12). There was no significant difference in L1 methylation levels between the two treatment groups for these tissues. PB sampling was performed 3 days prior to irradiation to establish base line methylation levels and for comparison to the 6 day PB samples. There was no significant difference between the pre- and post-irradiation blood samples (Table 13). Archival spleen tissues were used for the C57Bl/6 study in Section 4.1.1 however other tissues from these mice were not available for analysis.

Table 12: Mean L1 NTS for tissues from BALB/c and CBA mice treated with 1 Gy X-rays.

Strain	Tissue	Male (n = 4-5)				Female (n = 5)			
		Dose (Gy) 0		1		0		1	
		Mean NTS	SD	Mean NTS	SD	Mean NTS	SD	Mean NTS	SD
BALB/c	Liver	-6.74	0.47	-6.36	0.4	-4.86	0.33	-5.41	0.61
	Kidney	-3.32	0.26	-3.61	0.51	-3.91	0.51	-3.43	0.25
	Prostate	-5.87	0.55	-5.67	0.97	n/a			
CBA	Liver	-3.67	0.24	-3.68	0.34	-3.45	0.64	-3.97	0.7
	Kidney	-2.14	0.55	-2.57	0.82	-3.18	0.47	-3.28	0.65
	Prostate	-4.27	0.62	-4.17	0.7	n/a			

NTS – net temperature shift

n/a – not applicable

Table 13: Mean L1 NTS for peripheral blood samples from BALB/c and CBA mice treated with 1 Gy X-rays.

Strain	Dose (Gy)	Male (n = 4-5)				Female (n = 5)			
		0		1		0		1	
		Mean NTS	SD	Mean NTS	SD	Mean NTS	SD	Mean NTS	SD
BALB/c	(-) 3 ^A	-2.90	1.36	-2.86	1.39	-2.79	1.35	-2.97	1.03
	(+) 6 ^B	-2.84	1.40	-2.58	1.23	-2.52	0.95	-2.55	1.14
CBA	(-) 3	-2.49	0.80	-2.32	1.01	-1.99	1.05	-1.84	1.23
	(+) 6	-2.41	1.33	-1.98	0.94	-2.08	0.86	-2.31	0.74

NTS – net temperature shift

^A PB sample taken 3 days prior to irradiation

^B PB sample taken 6 days following irradiation

4.1.8 Immunohistochemical analysis of spleen tissue cell populations

It was possible that the change in L1 methylation observed in the spleen tissues following 1 Gy X-irradiation was not the result of changes in CpG methylation, but due to a change in cell population of the spleen resulting in selection of cells with higher (or lower) L1 methylation levels. Therefore spleen sections from the male BALB/c and CBA mice 6 days following irradiation with 1 Gy were analysed with a pan-T cell (CD3 ϵ) marker. Figure 4-18 depicts an example of a positive staining T-cell area in the spleens of sham-irradiated BALB/c (Figure 4-18A and C) and CBA (Figure 4-18B and D) mice. Two spleen sections were cut and examined per mouse, with ten random fields per slide photographed. A CellProfiler™ pipeline (Lamprecht *et al.*, 2007) (see Appendix F) was created to determine T-cell stained areas (Figure 4-19). Firstly, non-DAPI stained nuclei areas were masked (Figure 4-19A-B (i)). Areas that demonstrated positive FITC/CD3 ϵ staining that also demonstrated DAPI

staining were highlighted as T-cell areas (Figure 4-19A-B (ii)), following which the intensity of the T-cell areas was determined (Figure 4-19A-B (iii)).

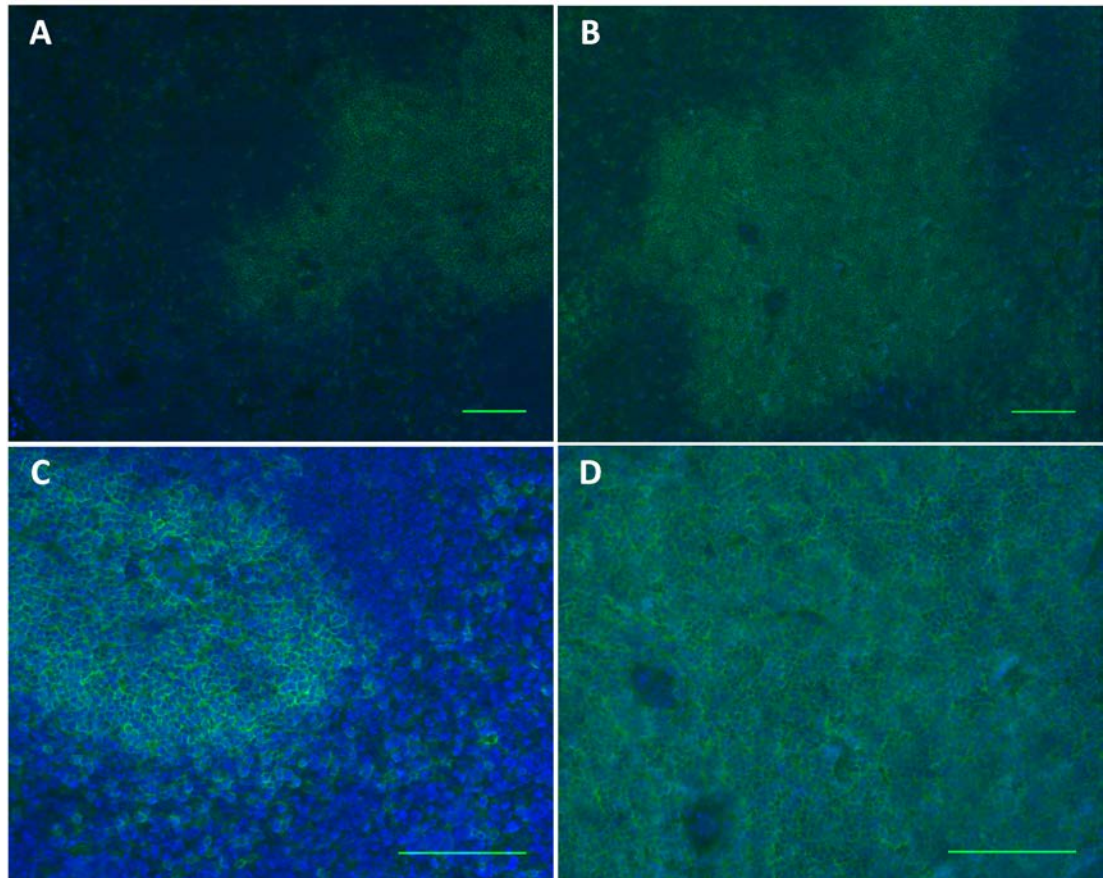


Figure 4-18: Detection of splenic T-cells in male BALB/c and CBA mice using immunohistochemistry.

Five μm frozen spleen sections were cut and stained with a pan-T-cell marker (CD3 ϵ ; FITC) and counterstained with DAPI to identify nuclei. Shown are merged images (DAPI – blue; T-cell – green/FITC) taken on a 10x objective lens for a (A) BALB/c and (B) CBA mouse; and merged images taken on a 20x objective lens for a (C) BALB/c and (D) CBA mouse. Scale bars represent 100 μm .

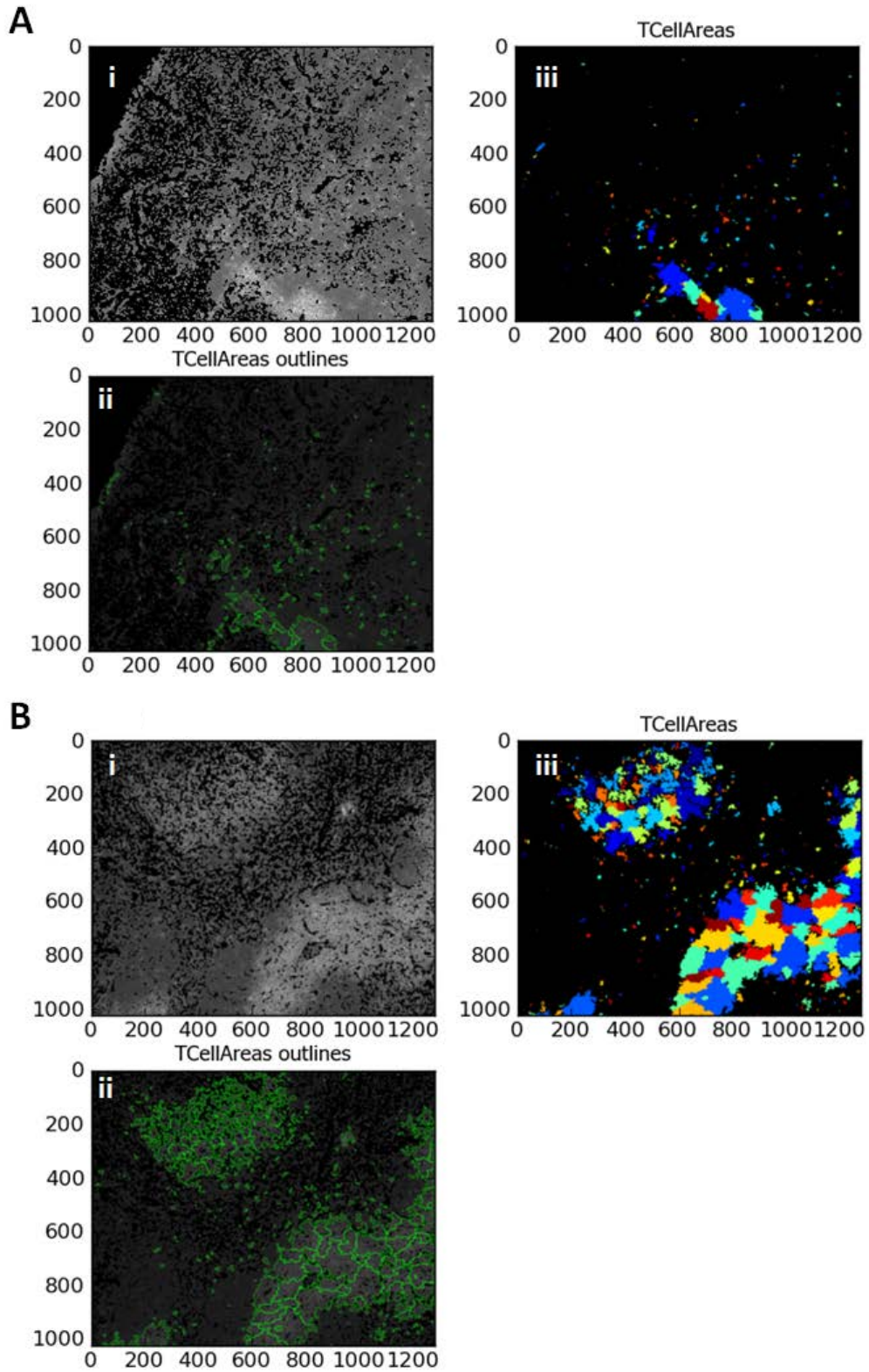


Figure 4-19: CellProfiler™ identification of splenic T-cells.

CellProfiler™ analysis of a (A) low intensity T-cell area and (B) a high intensity T-cell area. DAPI-stained nuclei were identified and non-stained areas masked (i) prior to identification of T-cell areas (ii – outlined in green). The intensity of the T-cell stained areas was then determined (iii). The colours represent different areas of cells identified as positive staining and are arbitrarily assigned to aid identification.

Analysis of the mean T-cell area of 1 to 10 random fields (roving mean) was performed to determine the number of fields required to obtain a stable and accurate T-cell frequency (Figure 4-20A). Comparison of the mean T-cell area of 6 fields versus 10 fields per spleen section indicated that a stable frequency was achieved with a minimum of 6 fields, with no statistical difference between the mean frequency of 6 fields and 10 fields per spleen section for each mouse ($P > 0.05$) (Figure 4-20B).

The mean T-cell area of spleen tissues from sham and 1 Gy treated male BALB/c and CBA mice was determined (Figure 4-21). There was no significant difference in the mean splenic T-cell area between the treatment groups for either strain. The CBA mice had significantly more splenic T-cells ($34 \pm 7\%$) compared to the BALB/c mice ($24 \pm 10\%$) ($P = 0.013$, Independent Samples T-test). A positive correlation between mean L1-NTS and the mean T-cell area was observed (Pearson correlation coefficient = 0.526; $P = 0.004$), indicating that mice with the highest L1 methylation had the highest T-cell areas (Figure 4-22).

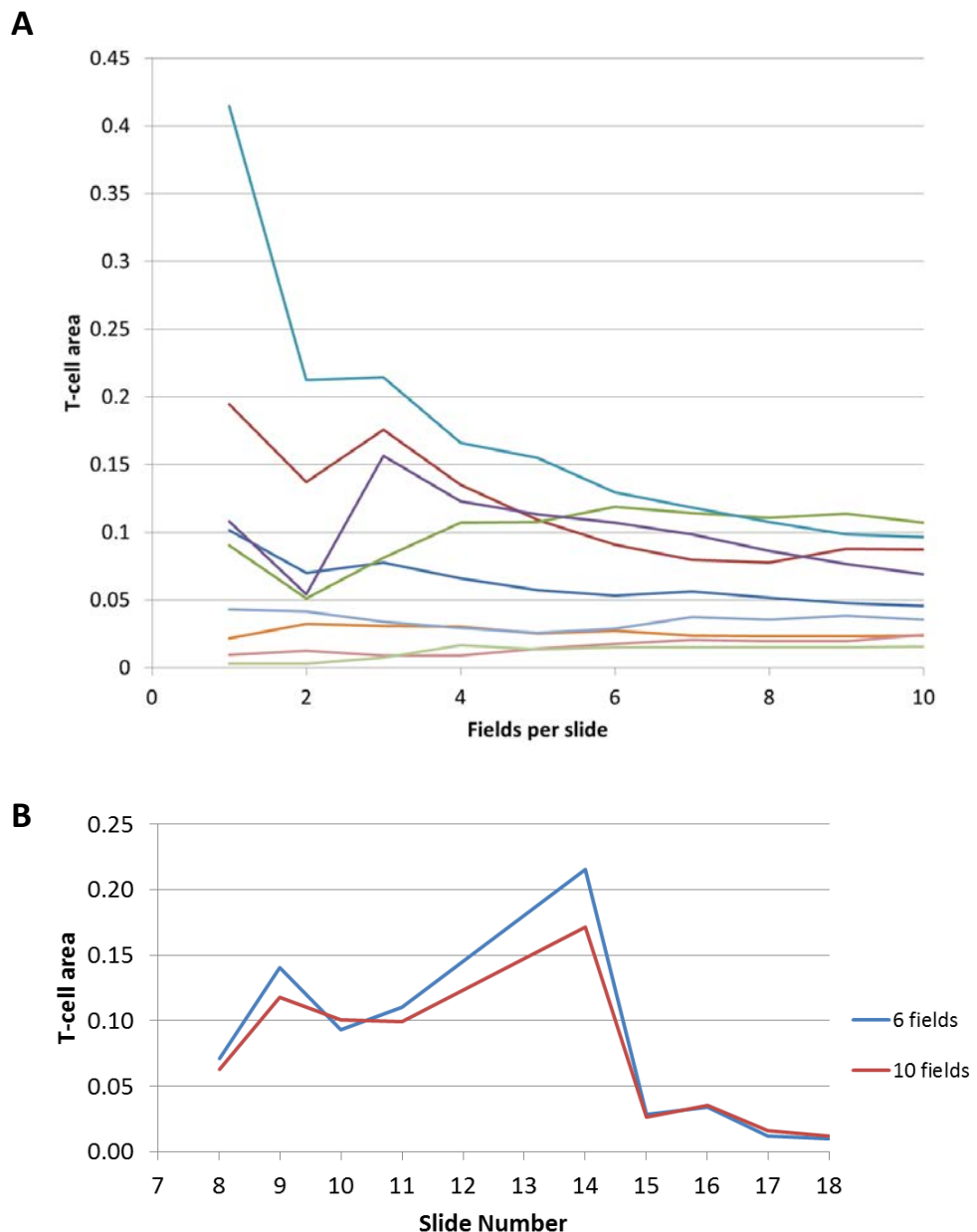


Figure 4-20: The roving mean of T-cell areas in BALB/c spleen.

(A) Ten random fields per slide were photographed on a 10x objective lens. The coloured lines represent the roving mean of T-cell frequency (T-cell area/ DAPI area) per field as determined by CellProfiler for an individual slide/mouse ($n = 9$ mice). (B) The roving mean of 6 and 10 fields per slide photographed on a 10 x objective lens were compared for 10 slides ($n = 5$ mice; 2 slides per mouse). There was no statistical difference in the mean T-cell frequency between 6 and 10 fields. Ten fields per slide were examined to ensure that the T-cell area frequency analysed represented a stable frequency.

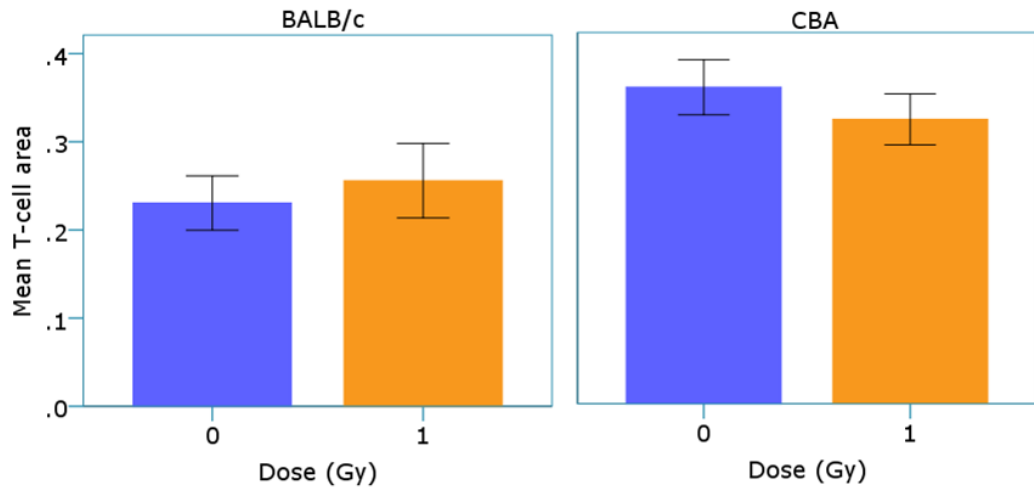


Figure 4-21: Mean splenic T-cell staining area frequency of male BALB/c and CBA mice.

Two 5 μm frozen spleen sections from male BALB/c ($n = 9$ per treatment group) and male CBA mice ($n = 5$ per treatment group) 6 days following sham (blue) and 1 Gy (orange) X-irradiation were cut and stained with a pan-T-cell marker (CD3 ϵ) and a DAPI counter stain. Ten random fields were photographed on a 10x objective lens and the T-cell area frequency (T-cell stained area/DAPI area) was determined. Error bars represent 1 SE.

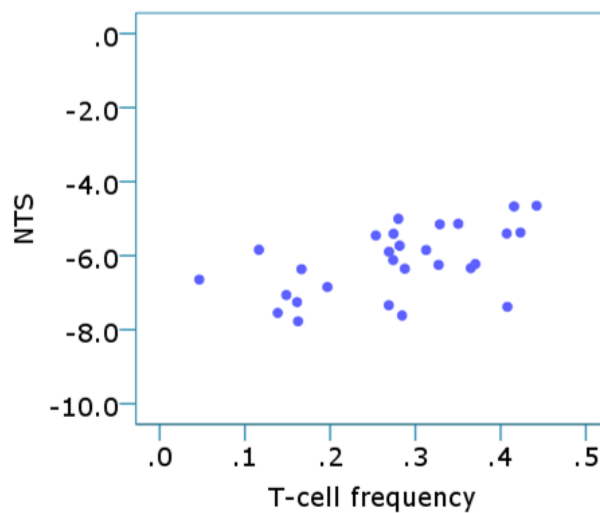


Figure 4-22: Correlation of NTS and splenic T-cell area frequency.

Pearson correlation was used to assess the relationship between mean L1 NTS and T-cell frequency for each of the male BALB/c ($n = 18$) and CBA ($n = 10$) mice 6 days following sham and 1 Gy X-irradiation.

4.2 Discussion

Radiation-sensitive mouse strains such as the BALB/c and CBA strains have been shown to exhibit persistent, radiation-induced DNA damage compared to the radiation-resistant C57Bl/6 strain. Furthermore, ionising radiation has been demonstrated to induce a loss of total genomic 5mdC in the radiosensitive CBA mice compared with the radioresistant C57Bl/6 mice. It was hypothesised here that the more radiosensitive strains would also exhibit a greater loss of L1 DNA methylation following radiation exposure.

4.2.1 Strain differences in response to irradiation

This is the first study to analyse the temporal L1 methylation response of three mouse strains with varying radiation sensitivity following high dose radiation exposure. A loss of L1 element DNA methylation is reported to induce genomic instability due to the transcription and transposition of the elements (Hagan *et al.*, 2003; Howard *et al.*, 2007). Here, it was demonstrated that there are strain and sex differences influencing the temporal modulation of spleen L1 DNA methylation following irradiation. All three strains exhibited an early increase (1 day) following the irradiation, which was also sex-specific. Radiation will cause a stress effect on the cells it interacts with. Genes involved in DNA repair are induced by both environmental and physiological stresses (Liebermann and Hoffman, 2008). It has been reported recently that rapid changes to the genome can occur following stress. Hunter *et al* (2009; 2013) reported increased methylation of histone H3 lysine 9 residues following the induction of restraint stress in rats as early as 2 hours

and persistent out to 7 days, and further examination revealed that the methylation was of histones associated with heterochromatin. This histone mark is associated with increased DNA methylation also. The increased methylation of L1 elements at 1 day following irradiation reported in this thesis may be a stress response to prevent increased DNA damage that could result from transposition of the repeat elements. Increases in methylation at a repeat element following irradiation have been reported for Agouti mice irradiated (with low dose radiation) *in utero*. It was proposed that the increased methylation, which resulted in the normal pseudoagouti phenotype, was a protective mechanism against the morbidities associated with the Agouti phenotype (Bernal *et al.*, 2012). However, it is likely that the increased methylation that was detected in all three strains is a temporary response to the irradiation as both the 1 Gy irradiated BALB/c and CBA mice exhibited no change in L1 methylation at 14 days in comparison to the sham-irradiated mice. The radioresistant C57Bl/6 mice demonstrated a reduction in methylation at 14 days. Of the C57Bl/6 mouse studies listed in Table 4 (Chapter 1, page 41), both increases and decreases in total genomic methylation levels have been demonstrated at early and late time-points following irradiation, however the temporal response of repeat element methylation has not been investigated. It is possible that the subsequent reduced methylation detected in the C57Bl/6 mice at day 14 could be the result of remaining, unrepaired DNA damage that is the result of a failure, or an inability to restore methyl groups to CpG sites. The latest time-point post-irradiation investigated previously to detect a loss of methylation was 4 weeks (Pogribny *et al.*, 2004; Koturbash *et al.*, 2005). In these studies, only thymus tissue exhibited a reduction in total genomic methylation, while spleen and liver

tissue did not. It is unclear, based on the literature as to whether the reduction in L1 methylation observed in the spleen tissue of the C57Bl/6 mice is permanent. Later time-points need to be investigated to determine if the reduction in L1 methylation persists, indicating a long-term effect of irradiation. While the study performed by Giotopoulos *et al* (2006) did not detect a change in splenic total 5mdC in CBA mice up to 42 days post-irradiation, long-term effects on spleen L1 methylation levels should also be investigated in the BALB/c and CBA mouse strains. When spleen samples from this study were analysed using a method for quantitating total genomic 5mdC (LC-MS), no change in total genomic 5mdC levels was observed in the spleen tissues of the 1 Gy treated mice, regardless of the strain, sex or time post-irradiation. As demonstrated in Chapter 3, the L1 assay can sensitively detect changes in methylation of the L1 elements that cannot be distinguished in overall 5mdC levels by LC-MS. While the changes in L1 methylation are likely to be at many sites across the genome, they may be relatively small in total and therefore not reflected in the total genomic 5mdC levels. Detection of changes in the B1 and IAP elements also confirms a more generalised effect of the irradiation on CpG methylation modulation.

Comparisons of the responses of the three strains for other endpoints following irradiation have been performed previously. It has been reported that different gene pathways are activated following irradiation with 200 mGy in C57Bl/6 and BALB/c strains, with chromatin remodelling and signal transduction pathways demonstrating the most diversity between the two strains (Mukherjee *et al.*, 2010). Furthermore, the three strains investigated in this thesis do exhibit differences in DNA repair following exposure to >100 mGy ionising radiation, such as reduced

levels and reactivity of repair proteins for the BALB/c mice compared with the C57Bl/6 mice (Ponnaiya *et al.*, 1997; Okayasu *et al.*, 2000; Hamasaki *et al.*, 2007).

The DNA methyltransferases have been shown to be linked with DNA repair processes (Gontijo *et al.*, 2003; Mortusewicz *et al.*, 2005; Li *et al.*, 2007; Valinluck and Sowers, 2007; Chiolo *et al.*, 2011; Ha *et al.*, 2011; Lee *et al.*, 2011; Armstrong *et al.*, 2012), however it has not been reported whether there are tissue and strain differences in the expression of the DNA methyltransferases following DNA damage. A comparison of the mRNA expression and protein levels of the DNMTs in different tissues and strains in irradiated and sham-irradiated mice would be informative. Investigation of DNMT protein levels by Western Blot analysis was attempted in this thesis, but was not successful. Further optimisation was required and could not be performed within the time-frame of this candidature. Analysis of the DNMT mRNA levels was also not investigated due to time constraints. There have been reports that have shown a relationship between p53 and the maintenance methyltransferase, DNMT1. It has been reported that p53 is involved in the control of DNMT1 activity, whereby up-regulation of p53 represses DNMT1 (Peterson *et al.*, 2003; Estève *et al.*, 2005; Park *et al.*, 2005). As mentioned in Section 1.2.1, the three strains investigated in this thesis exhibit differences in p53 function and expression levels (Feng *et al.*, 2007; Lindsay *et al.*, 2007), however a direct comparison has not been performed. It is possible that the methylation differences observed in this thesis could be due to the influence of p53 on the DNMTs, although a direct link is yet to be established.

Strain differences in normal *de novo* methylation activity has been demonstrated, with the *de novo* methylation occurring at different chromosomal locations for the strains investigated (Schumacher *et al.*, 2000). A role for the *de novo* methyltransferases in the modulation of radiation-induced DNA methylation changes has been shown, where a loss of DNA methylation in the testes of C57Bl/6 mice correlated with down regulation of DNMT3a but not DNMT1 following irradiation with 2.5 Gy (Filkowski *et al.*, 2010). Murine L1 elements have also been shown to exhibit strain-specific polymorphisms which are distributed non-randomly through the genome, contributing to strain genetic variation (Akagi *et al.*, 2008), and a recent study has also reported that both tissue type and genomic location of the L1 element influences its methylation level (Ekram *et al.*, 2012). Thus, the differences in L1 methylation responses observed here between the strains may be influenced by differences in both DNA methyltransferase activity linked with DNA repair, and differences in the chromosomal locations of the L1 elements affected by the radiation exposure.

In un-irradiated mice, differences between the three strains for baseline methylation levels in various tissues were demonstrated, with the C57Bl/6 strain displaying the lowest tissue L1 methylation levels compared to the BALB/c and CBA strains, while the CBA strain had the highest. The exception was the spleen, where there was no difference between the strains. It has previously been demonstrated that total genomic 5mdC levels in spleen are similar in CBA and C57Bl/6 mice (Giotopoulos *et al.*, 2006). This study is the first report of the methylation levels for a panel of tissues from more than one mouse strain, and the data correlates with the hierarchy of tissue 5mdC levels previously reported for the C57Bl/6 strain

(Vanyushin *et al.*, 1973; Gama-Sosa *et al.*, 1983; Tawa *et al.*, 1998; Giotopoulos *et al.*, 2006). These results suggest that the hierarchy of tissue L1 methylation is common across the mouse strains. This is the first report of the L1 methylation levels for a tissue panel from BALB/c, CBA and C57Bl/6 mice, and the first time peripheral blood (PB) methylation levels have been analysed. Using both the methylation-status unbiased and unmethylated-biased L1 primers, the PB was shown to be more methylated at L1 elements compared with other tissues. It was found that the PB samples demonstrated reduced and stochastic amplification with the unmethylated-biased L1 primers compared to amplification with the methylation-status unbiased L1 primers (data not shown). It was hypothesised that there were reduced target sites for the unmethylated-biased L1 primers due to the high methylation level of the PB, resulting in the stochastic amplification of technical and biological replicates. PB L1 methylation levels are commonly used in human studies to monitor the modulation of methylation by exogenous factors, and have been reported to be highly methylated (Estecio *et al.*, 2007; Bollati *et al.*, 2009; Irahara *et al.*, 2010; Jintaridh and Mutirangura, 2010; El-Maarri *et al.*, 2011; Woo and Kim, 2012; Wu *et al.*, 2012), as was observed for the murine samples used in this thesis. Only archival tissues from irradiated C57Bl/6 mice were used in this thesis, and tissues other than the spleen were not available to study. Analysis of a tissue panel from both male and female BALB/c and CBA mice irradiated with 1 Gy demonstrated no detectable effect on L1 methylation in any of the tissues 6 days post-irradiation. It is possible that the radiosensitivity of the spleen may influence the methylation responses observed. The spleen is a radiosensitive organ due to its high cellular turnover, the process of which has been demonstrated to influence the

radiation sensitivity of a tissue/organ (Dixon, 1985; Liu *et al.*, 2011a). Furthermore, it has been suggested that the high cellular turnover of a tissue influences its DNA methylation levels, with highly proliferative tissues exhibiting lower total genomic 5mC (Ehrlich *et al.*, 1982; Gama-Sosa *et al.*, 1983). It has also been shown that there are regions of the genome that are differentially methylated in different tissues, and that these regions respond differently to exogenous modulators of DNA methylation (Christensen *et al.*, 2009; Song *et al.*, 2009).

It is possible that dose-rate as well as the genetic background of the mice used in this study may have influenced the results observed, as the BALB/c and CBA mice were irradiated at a dose-rate of 1 Gy/ min, while the archival C57Bl/6 mice had received 1 Gy at a dose-rate of 179 mGy/ min. The methylation studies reported in the literature used doses ranging from 0.5 Gy to 10 Gy, as well as low-dose chronic irradiation to a total dose of 0.5 Gy; with dose-rates ranging from 2 mGy/ s to 5 Gy/ min (see Table 4, page 41). One study which compared the effect of dose-rate on time to lethality in the BALB/c and C57Bl/6 strains indicated that the C57Bl/6 mice were more affected by the dose-rate compared to the BALB/c mice (Kallman, 1962). The C57Bl/6 mice were more sensitive to a higher dose-rate, while the BALB/c mice demonstrated a similar LD₅₀ across the dose-rates investigated. Vesselinovitch *et al* (1971) demonstrated that the development of cancers in C57Bl/6 mice following irradiation was tissue specific at different doses. Liver tumours had reduced incidence at higher X-ray doses, while the rate of haematopoietic cancers such as leukaemia and lymphoma increased when dose was increased. Haematopoietic tissues were observed to be more sensitive to the radiation exposure. In the studies investigating the effect of irradiation on DNA methylation responses, there is no

consistency in the results showing an effect of dose-rate, except for the studies that demonstrated a loss of methylation, either a high dose (≥ 3 Gy) or high dose-rate (≥ 3 Gy/ min) was used. There is evidence showing that dose-rate can induce differences in the rate of DNA repair (reviewed in Vilenchik and Knudson, 2000). At a lower dose-rate, the time taken to deliver the dose increases, compared with the time of exposure for a higher dose-rate. However, for doses between 100 mGy/min and 1 Gy/min, the initial chemical processes in response to the radiation exposure, such as the generation of reactive oxygen species will occur, but the irradiation times to deliver a dose of 1 Gy are not considered long enough for the repair of DNA damage or any other processes to have begun (discussed by Steel, 1997). As the three mouse strains exhibit differences in sensitivity to dose-rate, experiments using 179 mGy/ min on the BALB/c and CBA mice, and 1 Gy/ min on the C57Bl/6 mice are needed to determine if the differences in L1 methylation modulation are influenced by the dose-rate used. In addition, the archival C57Bl/6 mouse spleen tissues analysed in this study were irradiated with X-ray energies ranging from 100 – 140 kVp, while the BALB/c and CBA mice were irradiated with 1 Gy using 6 MeV X-rays. It is unlikely that the energy of the X-rays used to deliver the 1 Gy would have had an effect on the results observed in this thesis, as it is generally accepted that all X-ray energies have the same relative biological effectiveness (E. Bezak, personal communication), and experimentally, it has been demonstrated that initial DNA damage is not different between X-ray energies for the same dose (Gomolka *et al.*, 2005).

Strain differences in splenic cell populations have been reported, with CBA mice demonstrating a greater T-cell:B-cell ratio compared to BALB/c mice, while C57Bl/6

mice have an equal ratio of T- and B-cells (Forni, 1988). It is possible that the increases in methylation observed following irradiation may not be due to *de novo* methylation of CpGs within the L1 elements of cells originally residing in the spleen, but instead due to changes in splenic cell populations resulting in a greater proportion of more highly methylated cells migrating into the spleen following irradiation. Comparison of the male BALB/c mice (which exhibited the greatest increase in methylation) and the male CBA mice (which exhibited no change in methylation) 6 days following irradiation was performed, with no difference in the proportion of T-cells in the spleen for either strain between sham and 1 Gy irradiated mice. The CBA mice exhibited more T-cell positive areas compared with the BALB/c mice which were consistent with the literature (Forni, 1988; de Haan *et al.*, 1997). Although there was no significant difference in T-cell frequency between the sham and 1 Gy treated mice, T-cell frequency did correlate with the L1 NTS, whereby those mice with higher L1 methylation had a higher frequency of T-cell areas. This indicates that L1 methylation levels in the spleen are influenced by differences in cell population. The influence of T-cell subtypes on methylation levels cannot be discounted as it is possible that there was a disproportionate increase in subtypes of T-cells following the radiation exposure. It has been shown in C57Bl/6 mice irradiated with 1 Gy that there were differences in T-cell subtype populations compared with the sham-irradiated mice (Harrington *et al.*, 1997). Meissner *et al.* (2008) reported that B-cells are more methylated (~17%) compared to T-cells (~11%), and as B-cell frequency was not investigated in this thesis, the increase in methylation due to B-cell frequency cannot be excluded. As L1 NTS did correlate with T-cell area, and T-cell sub-type and B-cell frequencies have not been

investigated, splenic cell population influences on DNA methylation levels cannot be excluded and warrants further investigation.

4.2.2 Sex differences in L1 methylation levels in response to X-irradiation

In the BALB/c and CBA mouse temporal studies, the male CBA mice exhibited early increases in L1 methylation following irradiation in comparison to female CBA mice. For the B1 elements, only the male BALB/c exhibited an increase following irradiation. Recently, it was shown that male offspring of dams irradiated with doses ranging from 7 – 760 mGy exhibited increased methylation of the IAP element upstream of the Agouti locus compared with female mice (Bernal *et al.*, 2012). Differences in global DNA methylation levels following irradiation between male and female C57Bl/6 mice have been reported (Kovalchuk *et al.*, 2004a; Kovalchuk *et al.*, 2004b; Pogribny *et al.*, 2004; Besplug *et al.*, 2005; Cassie *et al.*, 2006), but this is the first time different methylation responses between sexes in other mouse strains have been detected. It has previously been hypothesised that the methylation responses may be influenced by sex-hormones. In one animal study, it was observed that there were differences between ovariectomized and hormonally normal female C57Bl/6 mice for global DNA methylation and DNMT protein levels following 0.5 Gy X-irradiation. The ovariectomized female mice demonstrated similar liver DNA methylation levels and expression of the *de novo* DNMTs to that of male mice. Spleen methylation levels were unaffected by hormone levels, however male and female mice did display differences in spleen methylation levels following irradiation (Raiche *et al.*, 2004). Similarly, in humans it

was shown for PB that L1 methylation levels are different between males and females, however unlike the mouse study, did not appear to be affected by hormonal cycles and/or hormone levels (El-Maarri *et al.*, 2011). These studies suggest that the sex-based differences in spleen L1 methylation observed in this thesis may not be due to the influence of sex hormones. No effect of irradiation was observed in other tissues for both the male and female mice used in the study presented here, however there were baseline differences in L1 methylation levels between the sexes. This is the first report of differences in L1 methylation levels between male and female mice from across different mouse strains, and the first report of differences in the temporal modulation of L1 methylation following ionising radiation exposure.

4.2.3 Analysis of the effect of changes in methylation to the L1 promoter

Analysis of the L1-HRM assay consensus promoter sequence revealed that it displays the same structure as actively transcribed L1 promoters described by Lee *et al.* (2010b). The L1-HRM assay consensus promoter contains 3 monomeric repeats upstream of the start codon of ORF1, and within these repeats contains three Ying-Yang 1 (YY1) and two E2F transcription factor binding sites, with one YY1 and one E2F binding site found within the L1-HRM assay target sequence. YY1 has been shown to be necessary for human L1 transcription (Athanihar *et al.*, 2004). The proteins involved in driving murine L1 transcription are yet to be determined, however, as the murine L1 promoters contain intact YY1 binding sites, these are proposed to be the proteins involved in transcription. A 2.8% reduction in

methylation at 7 of the 11 CpGs located within the HRM assay L1 promoter, with one of the CpGs located within the YY1 binding site, was observed in C57Bl/6 mice 14 days post-irradiation with 1 Gy. However, no change in L1 transcript levels was detected in these mice. YY1 has been found to be methylation-sensitive in its binding to other repeat element promoters such as the IAP element (Satyamoorthy *et al.*, 1993). However, Hata and Sakaki (1997) reported that at human L1 promoter-reporter constructs, CpG methylation at the YY1 binding site has little effect on the binding of YY1, but that methylation of other CpGs within the promoter are critical for correct transcription and transposition. Furthermore, it has been demonstrated that a loss in methylation at a promoter does not always correspond to an increase in transcript levels. Howard *et al* (2007) observed that in DNMT1 null mice that exhibited genomic hypomethylation, there was no increase in the levels of the IAP element transcript until tumours had developed, with transcripts found only in the tumour tissue. Also, in another report, ~25% demethylation by 5-aza was demonstrated to result in an 80-fold increase of IAP transcripts *in vitro*, with only a 2-fold increase in B1 element transcripts and no change in L1 transcript levels (Brunmeir *et al.*, 2010). Four of the 11 CpGs within the HRM assay L1 promoter were unaffected by irradiation. It is possible that these CpGs are involved in the repression of transcription, and modulation of the methylation of these CpGs is critical. Evidence suggesting that all CpGs of the L1 promoter need to be modulated in order to affect transcription was demonstrated in the 0.5 μ M 5-aza treated A11 cells, where although not significant, there was an increase in ORF2 transcript levels that corresponded with an 18-40% loss of methylation at the 6 CpGs pyrosequenced, which reflected an overall ~30% loss of total 5mdC content (as

detected by LC-MS). The greatest loss of methylation was at the CpG located within the YY1 binding site (~40% compared with the vehicle control). The male BALB/c mice that demonstrated an increase in methylation 6 days following irradiation had increased methylation at 4 of the 6 CpGs pyrosequenced. Three of these CpGs were the same as those affected in the C57Bl/6 mice 14 days post-irradiation. This is the first report of the effect of radiation exposure on individual CpGs within a murine L1 promoter, and the first to demonstrate that between mouse strains, the same CpGs are resistant to, or affected by radiation exposure. As the CpG located within the YY1 binding site showed decreased methylation at 14 days post-irradiation, it would be interesting to determine if this reduction in methylation affects the binding of YY1 to the L1 promoter. It would also be of interest to pyrosequence the other time-points analysed for all strains. This would provide information regarding CpGs that are repeatedly affected by radiation exposure, and may lead to identifying crucial sequences within the L1 promoter. The region studied in this thesis is derived from one monomer of the L1 promoter, and therefore the other monomers of the L1 promoter should also be assessed using the HRM assay and pyrosequencing to understand the overall effect of the radiation exposure on the L1 promoter region. To the best of my knowledge, this has not been assessed before in any organism. Overall, the data suggests that a relatively small reduction in methylation at the L1 element promoter does not result in an immediate increase in L1 transcript levels.

It is possible that the radiation exposure altered the transcript levels of the B1 and IAP repeat elements. As mentioned, Brunmeir *et al* (2010) reported that following ~25% loss of methylation, L1 element transcript levels were unchanged, while B1

and IAP elements were increased. For the 14 days post-irradiation samples, a greater difference in NTS was observed for the IAP_LTR elements than the L1 and B1 elements following 1 Gy irradiation. This suggests that the IAP elements were more affected by the radiation exposure and thus it would be interesting to assess the transcript levels.

Changes in DNA methylation are associated with changes of other epigenetic modifiers such as histone proteins, which affect chromatin structure and ultimately, gene expression (Razin, 1998; Geiman and Robertson, 2002; Fraga *et al.*, 2005; Kondo *et al.*, 2007; Fan *et al.*, 2008; Sugimura *et al.*, 2010). The tri-methylation of lysine 9 on histone H3 (H3me3K9; known as a histone mark) is associated with tightly compacted heterochromatin, and is found at heavily methylated sequences of DNA such as L1 elements (Martens *et al.*, 2005; Peng and Karpen, 2009). Losses in DNA methylation have been associated with a reduction of this histone mark. When the levels of H3me3K9 were assessed in the spleens of the C57Bl/6 mice 14 days following irradiation with 1 Gy, reduced H3me3K9 levels were detected ($P = 0.054$). While this suggests that the 1 Gy radiation exposure is affecting heterochromatin structure, resulting in less compacted chromatin, this was a preliminary experiment that needs to be repeated to verify this observation. It is possible that if time-points later than 14 days post-irradiation had been analysed, an increase in L1 transcripts might have been detected due to relaxation of the chromatin surrounding the repeat elements and increased accessibility to transcription factors.

4.3 Conclusion

This is the first study to directly compare the modulation of repeat element methylation in three strains of laboratory mice that differ in their radiosensitivity.

The results did not support the hypothesis that the most radiosensitive strains would demonstrate the greatest loss of L1 element DNA methylation following ionising radiation exposure. However, it was demonstrated that both male and female mice from the radiosensitive BALB/c mice underwent modulation of L1 DNA methylation compared with the less radiosensitive CBA and the radioresistant C57Bl/6, suggesting that modulation of repeat element methylation may be influenced by radiation sensitivity. While the exact mechanism and biological outcome of the changes in DNA methylation observed are still to be elucidated, this study provides the first evidence that radiation exposure elicits time-dependent changes in repeat element methylation levels that are influenced by the genetic background and sex of the mice.

5 LONGITUDINAL STUDY OF REPEAT ELEMENT METHYLATION IN PERIPHERAL BLOOD IN RESPONSE TO LOW DOSE RADIATION

Age-associated changes in genomic stability are well documented for end-points such as the accumulation of unrepaired DNA lesions, reduced levels of proteins involved in maintaining genome integrity, changes in telomere length, and a loss of DNA methylation (reviewed by Calvanese *et al.*, 2009; reviewed by Gonzalo, 2010).

Telomere shortening is associated with ageing, whereby with each round of cell division, the telomere caps are replaced, but begin to lose fidelity until the telomeres are too short to prevent the degradation of DNA or the fusion of chromosomes, following which cells undergo cell cycle arrest, apoptosis or senescence. DNA methylation maintains genomic stability by preventing the expression of genes that can promote carcinogenesis (proto-oncogenes) as well as preventing the expression of transposable elements. In ageing mice, the gradual loss of DNA methylation has been shown to correlate with a gradual increase in transcription and subsequent retrotransposition of transposable elements such as L1, B1 and IAP (Maegawa *et al.*; Mays-Hoopers *et al.*, 1986; Gaubatz *et al.*, 1991; Barbot *et al.*, 2002). Human studies have shown that in older individuals (>60 years of age), there is also loss of methylation at these repeat elements (Bollati *et al.*, 2009; Calvanese *et al.*, 2009; Jintaridh and Mutirangura, 2010; Liu *et al.*, 2011b), and a strong correlation of a loss of LINE1 methylation with cancers such as colon

cancer, where an association between LINE1 hypomethylation and disease progression has been demonstrated (Fahrner *et al.*, 2002; Ogino *et al.*, 2008b; Christensen *et al.*, 2009; Daskalos *et al.*, 2009; Igarashi *et al.*, 2010; Saito *et al.*, 2010; Wolff *et al.*, 2010).

Shortened telomere length, DNA hypomethylation as well as increased cellular age can enhance radiation sensitivity to high dose radiation exposure, leading to increased radiation-induced damage that can ultimately result in either increased cell death or the initiation of cancer (Lindop and Rotblat, 1962; Sasaki, 1991; Gadhia, 1998; Beetstra *et al.*, 2005; Shuryak *et al.*, 2010; Drissi *et al.*, 2011; Kato *et al.*, 2011). In contrast, low doses of radiation (<100 mGy) can increase longevity in mice as well as suppress the development of cancers (Lorenz *et al.*, 1955; Mitchel *et al.*, 2003; Mitchel *et al.*, 2004; Ina *et al.*, 2005; Sakai *et al.*, 2006; Mitchel *et al.*, 2008), and reduce the level of endogenous DNA damage that accumulates with age (Zaichkina *et al.*, 2006). This is termed a low-dose radioadaptive response. In other studies, increased age at irradiation has been demonstrated to reduce the efficacy of the low-dose radioadaptive response (Gadhia, 1998; Miura *et al.*, 2002).

Given that the radioadaptive response has been shown to stimulate a long-term reduction in age-related accumulation of endogenous DNA damage as well as increase longevity, and that ageing is associated with a decline in repeat element DNA methylation, the aim of this chapter was to determine if the radioadaptive response could reduce or prevent the decline in L1 and B1 element DNA methylation associated with ageing, when the low dose of radiation was delivered to young mice. In order to investigate changes in the repeat element DNA

methylation levels over time following low dose irradiation, ageing mice were monitored using serial blood sampling. Telomere length in the ageing mice was also investigated to determine if the adaptive response could prevent age-related telomere shortening.

5.1 Results

5.1.1 Longitudinal study of repeat element DNA methylation in mice up to 299 days following 10 mGy X-irradiation (Longitudinal Study #1)

5.1.1.1 Outline of study

Changes in mouse PB L1 methylation levels over time following whole body irradiation with 0 mGy (sham) or 10 mGy X-rays were studied. Ten C57Bl/6 mice were allocated to each treatment group, and three days prior to irradiation, mice were weighed and a tail-vein peripheral blood (PB) sample was taken. Three days following irradiation, and at various time-points up to 299 days post-irradiation, mice were weighed and underwent PB sampling (outlined in Figure 5-1 and Table 14).

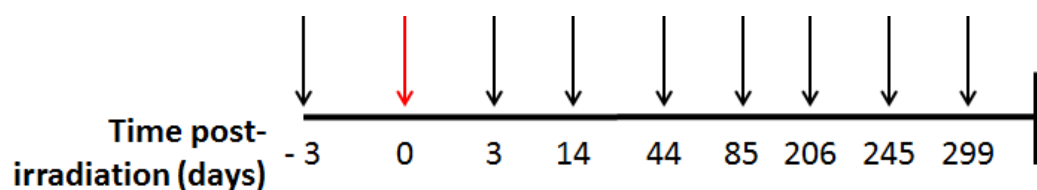


Figure 5-1: Outline of longitudinal study.

Twenty C57Bl/6 mice underwent tail-vein peripheral blood (PB) sampling three days prior to irradiation with sham or 10 mGy X-rays (red arrow; n = 10 per treatment group). PB samples were taken at various time-points following the irradiation (black arrows).

Table 14: Age of mice at PB sampling in longitudinal study (#1) up to 299 days post-irradiation with 10 mGy X-rays.

Time post-irradiation (d)		Dose (mGy)					
		0			10		
		<i>n</i>	Age (months)	<i>SD</i>	<i>n</i>	Age (months)	<i>SD</i>
-3	Male	5	4.36	0.41	5	3.95	0.75
	Female	5	4.05	0.34	5	4.40	0.46
3	Male	5	4.56	0.41	5	4.15	0.75
	Female	5	4.25	0.34	5	4.60	0.46
14	Male	5	4.92	0.41	5	4.51	0.75
	Female	5	4.61	0.34	5	4.96	0.46
44	Male	5	5.94	0.41	5	5.53	0.75
	Female	5	5.63	0.34	5	5.98	0.46
85	Male	3	7.04	0.49	5	6.77	0.75
	Female	5	6.88	0.34	5	7.23	0.46
206	Male	3	11.18	0.49	3	11.14	0.97
	Female	5	11.02	0.34	5	11.37	0.46
245	Male	2	12.22	0.60	3	12.32	0.97
	Female	5	12.20	0.34	5	12.55	0.46
299	Male	2	14.00	0.60	3	14.09	0.97
	Female	5	13.98	0.34	5	14.32	0.46

n = number of mice

5.1.1.2 Analysis of mouse weight and repeat element methylation changes following 10 mGy X- irradiation

At the final time-point of 299 days post-irradiation, the mean age of male and female mice was 14.05 (± 0.06) and 14.15 (± 0.24) months respectively. By 85 days post-irradiation, only three sham-irradiated male mice remained, and therefore male and female mice were not analysed separately. Repeated measures analysis of weight change over time revealed that there was a significant increase in weight for mice in both treatment groups ($P < 10^{-5}$), but no effect of irradiation on the weight changes over time ($P = 0.725$) (Figure 5-2).

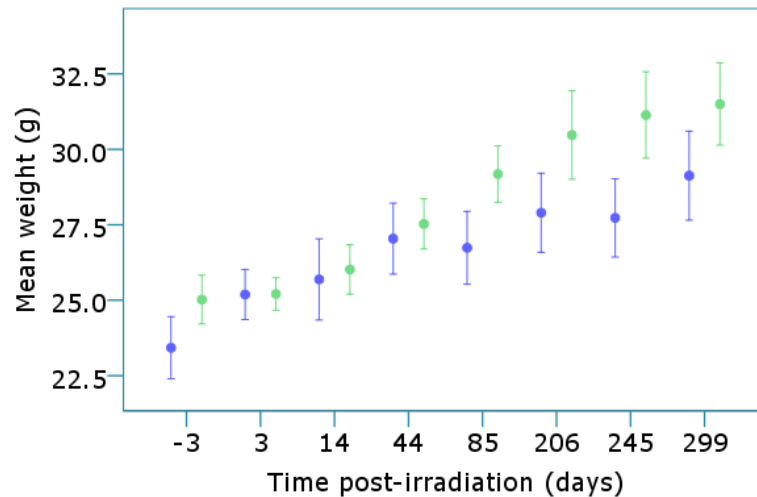


Figure 5-2: Mean weight over time of mice irradiated with sham and 10 mGy X-rays up to 299 days post-irradiation.

Twenty C57Bl/6 mice (n = 10 per treatment group) irradiated with sham (blue) or 10 mGy (green) X-rays were weighed 3 days prior to, and at various time-points following irradiation (7 ≤ n ≤ 10 per treatment group). Error bars represent 1 SE.

Due to the number of PB samples collected over the course of the study, it was not feasible to bisulphite modify all samples at the same time due to the equipment available and the time required. The samples were also unable to be run in the same HRM-PCR due to the size limitation of the PCR machine. Therefore, samples were randomly allocated to a bisulphite modification group and then re-distributed to a HRM-PCR group (Figure 5-3). This randomisation was necessary to remove any variation that could occur between different bisulphite modification reactions and PCRs.

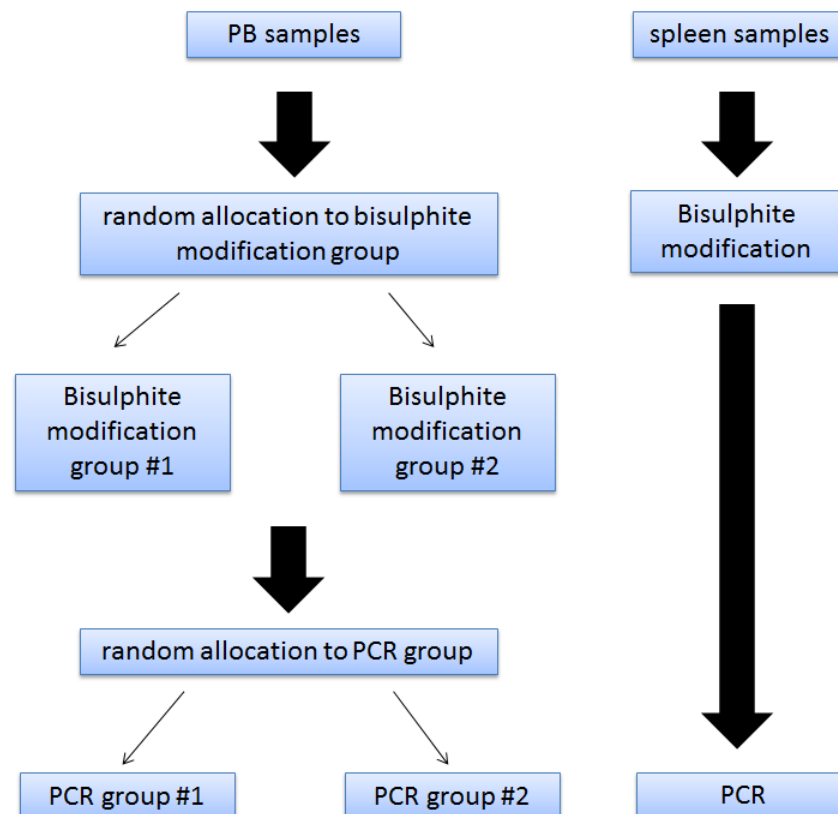


Figure 5-3: Outline of sample randomisation for HRM analysis.

PB gDNA samples were randomly allocated to a bisulphite modification group. Following bisulphite modification, samples were then randomly allocated to a PCR group prior to PCR and HRM analysis. Spleen samples were all bisulphite modified in the same reaction and underwent PCR and HRM analysis in the same PCR run.

Based on the logistics of analysing all samples up to 299 days post-irradiation, the L1 methylation of samples from time-points -3 to 85 days were initially analysed. An analysis of variance on the NTS data obtained demonstrated that there was variation in L1 NTS between samples due to PCR group allocation ($P < 10^{-5}$), but this was not the cause of the differences in NTS observed for an individual mouse over time. Multivariate analysis indicated that there was no significant difference in NTS of the pre- and post-irradiation bleeds up to 85 days post-irradiation ($P = 0.282$), nor was there an effect of irradiation on L1 NTS ($P = 0.656$) (Figure 5-4).

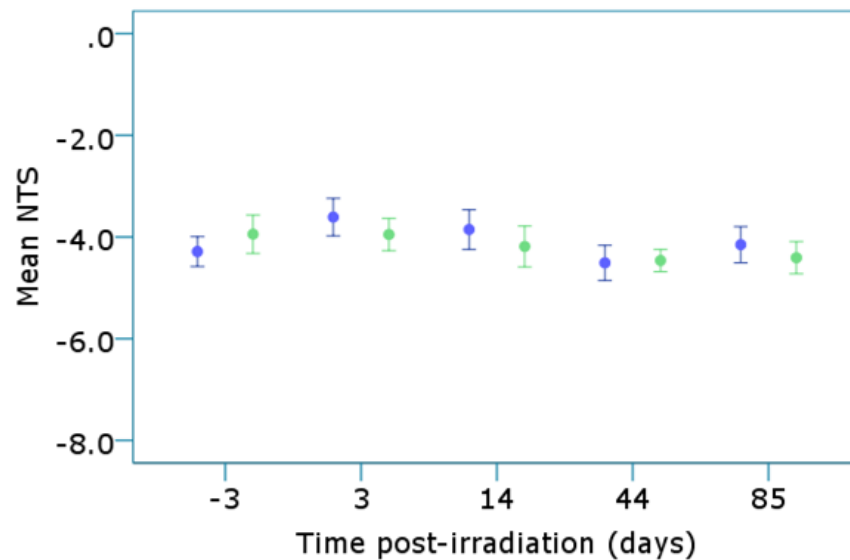


Figure 5-4: Mean PB L1 NTS of mice up to 85 days post-irradiation with 10 mGy X-rays.

C57Bl/6 mice had a tail-vein PB sample taken three days prior to and at time-points up to 85 days following irradiation ($7 \leq n \leq 10$ per treatment group) with sham (blue) or 10 mGy (green) X-rays. Following extraction and bisulphite modification, PB gDNA was amplified with unmethylated-biased L1 primers and the mean NTS was determined. Error bars represent 1 SE.

PB samples were taken at subsequent time-points of 206, 245 and 299 days post-irradiation (as outlined in Figure 5-1 and Table 14). As no effect on L1 methylation was observed at time-points prior to 85 days post-irradiation, analysis of both L1 and B1 element methylation levels were conducted on samples from -3, 85, 206, 245 and 299 days post-irradiation. Due to the small number of male mice remaining by 299 days post-irradiation, male and female mice were not analysed separately. Mouse-to-mouse variation in NTS for both L1 and B1 repeat elements at each time-point was detected, with increases and decreases in NTS observed for individual mice from both treatment groups ($P < 0.05$) (Figure 5-5). No significant effect of irradiation on the changes detected over time was observed ($P > 0.05$) (Table 15).

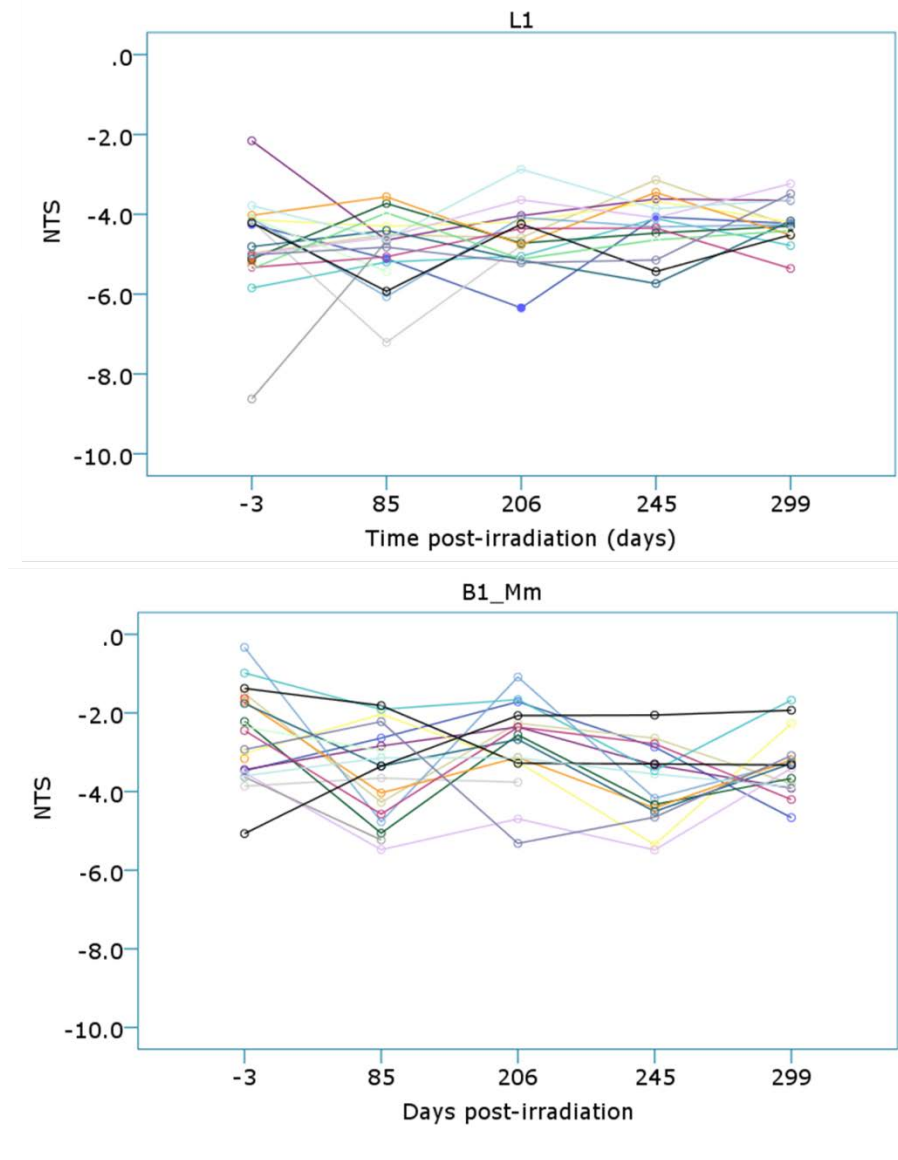


Figure 5-5: PB L1 and B1 element NTS of mice up to 299 days post-irradiation with sham or 10 mGy X-rays.

Three days prior to, and at various time-points following irradiation with sham or 10 mGy X-rays, C57Bl/6 mice ($7 \leq n \leq 10$ at each time-point) underwent tail-vein PB sampling. Following extraction and bisulphite modification, gDNA was amplified with L1 unmethylated-biased or methylation-status unbiased B1_Mm primers and mean NTS was determined. Coloured lines represent individual mice.

Table 15: Analysis of changes in PB L1 and B1 element NTS up to 299 days following irradiation with 10 mGy X-rays.

Changes in NTS over time	<i>P</i> -value	
	<i>L1</i>	<i>B1</i>
Individual mice	<10 ⁻⁵ *	<10 ⁻⁵ *
0 mGy	<10 ⁻⁵ *	<10 ⁻⁵ *
10 mGy	<10 ⁻⁵ *	<10 ⁻⁵ *
0 mGy vs. 10 mGy	0.933	0.350

*Repeated measures analysis; *P* <0.05

No significant difference between sham and 10 mGy irradiated mice was observed for mean L1 NTS at each time-point (*P* >0.05). For B1 elements, there was a significant difference in NTS between sham and 10 mGy irradiated mice at 299 days post-irradiation, with the 10 mGy mice showing less methylation (*P* = 0.032) (Figure 5-6). While the B1 NTS of the sham-irradiated mice at 299 days was not significantly different to the pre-irradiation samples, the mice irradiated with 10 mGy exhibited reduced methylation at 299 days compared with the pre-irradiation samples (*P* = 0.016; repeated measures analysis).

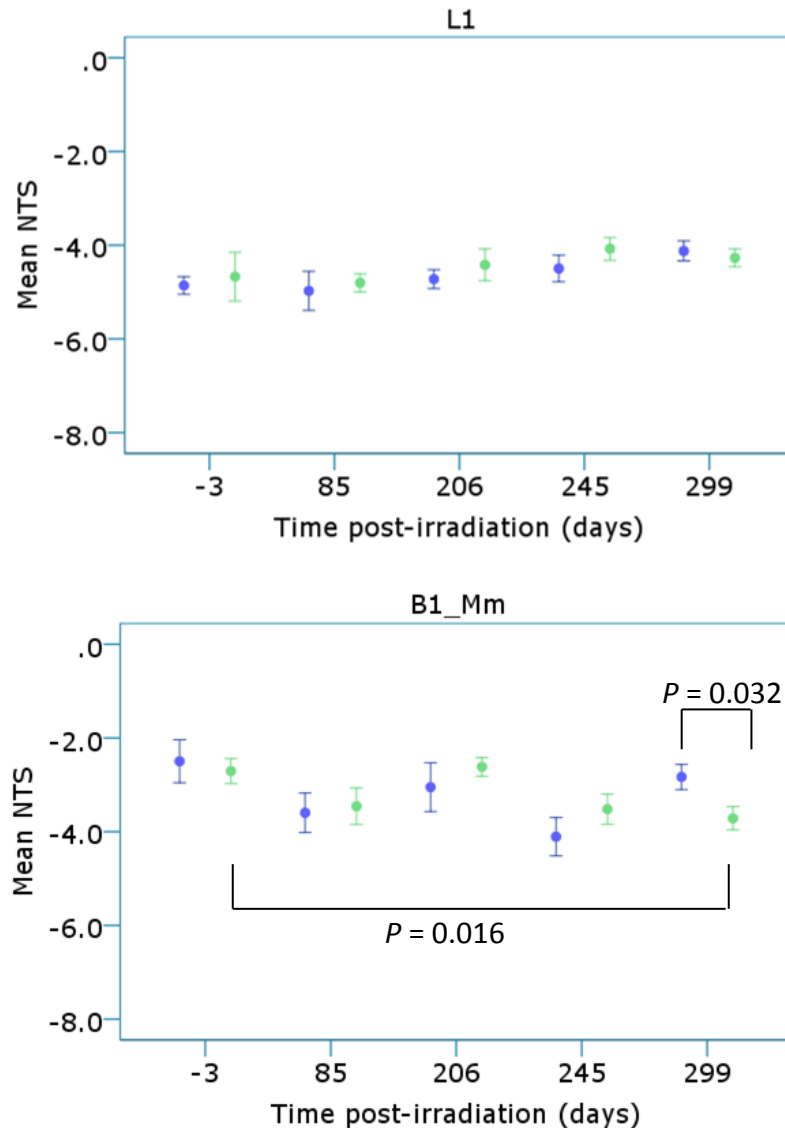


Figure 5-6: Mean L1 and B1 element NTS of PB samples up to 299 days following irradiation with sham or 10 mGy X-rays.

Three days prior to, and at various time-points following irradiation with sham (blue) or 10 mGy (green) X-rays, C57Bl/6 mice ($7 \leq n \leq 10$ per treatment group) underwent tail-vein PB sampling. Following extraction and bisulphite modification, gDNA was amplified with L1 unmethylated-biased or methylation-status unbiased B1_Mm primers and the mean NTS for samples at each time-point was determined. The difference in mean NTS between sham and 10 mGy irradiated mice at each time-point was analysed using the Independent Samples T-test. The difference in NTS between time-points was assessed using repeated measures analysis. Significance was achieved at $P < 0.05$. Error bars represent 1 SE.

The spleen NTS was analysed for the mice remaining at the end of the study (299 days post-irradiation). All samples were included in a single PCR experiment (as outlined in Figure 5-3). There was no significant NTS difference between sham and 10 mGy irradiated mice for both L1 ($P = 0.773$) and B1 elements ($P = 0.936$) (Figure 5-7).

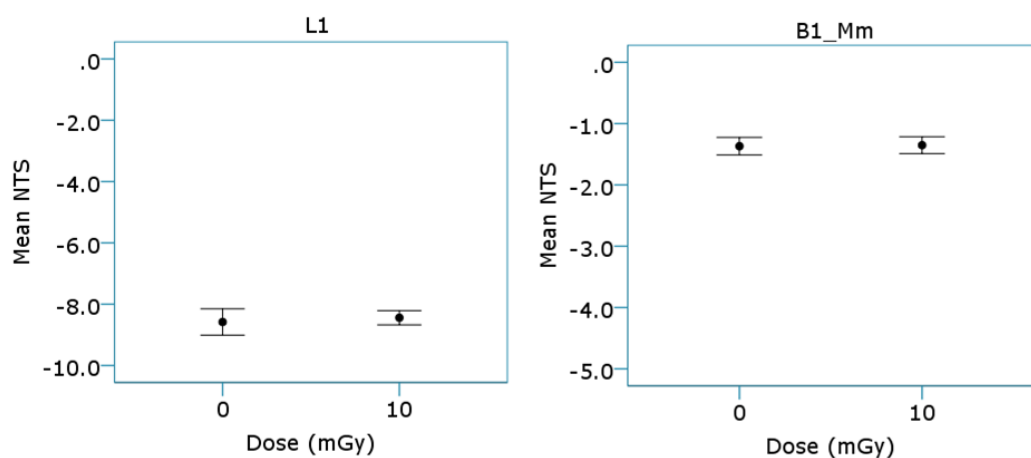


Figure 5-7: Spleen NTS of L1 and B1 elements from mice 299 days post-irradiation with sham and 10 mGy X-rays.

The mean NTS of spleen gDNA from C57Bl/6 mice 299 days following irradiation with sham (n = 7) or 10 mGy (n = 8) X-rays was determined following extraction, bisulphite modification and amplification with unmethylated-biased L1 and methylation-status unbiased B1_Mm primers. Error bars represent 1 SE.

The C57Bl/6 PB samples were more highly methylated in comparison with the other mouse tissues analysed (Figure 4-16). It was hypothesised that due to the greater level of methylation of the PB L1 elements, there were fewer targets for the unmethylated-biased primers to bind to, resulting in stochastic amplification and increased variability between technical and biological replicates. In this study, PB samples exhibited late amplification with the unmethylated-biased L1 primers

(mean Ct 24.8; SD = 1.35) in comparison to amplification with the methylation-status unbiased primers (mean Ct 18.8; SD = 1.8) (data not shown).

5.1.2 Longitudinal study of repeat element DNA methylation in mice up to 420 days following 10 mGy X-irradiation (Longitudinal Study #2)

5.1.2.1 Outline of longitudinal study #2

A second longitudinal study was conducted with the aim of analysing sham and 10 mGy irradiated mice at time-points greater than 299 days post-irradiation, through to old age (>18 months of age). Based on the final numbers of mice that remained by 299 days in longitudinal study #1, the number of sham and 10 mGy irradiated mice was increased to 20 per treatment group (10 males and 10 females per treatment group). As performed in the previous study, a PB sample was taken three days prior to irradiation. PB sampling and weight measurements were taken at the same time-points up to ~299 days (297 days) as for longitudinal study #1. The mice then had a final PB sample and weight measurement taken prior to euthanasia, at 420 days post-irradiation (Figure 5-8 and Table 16).

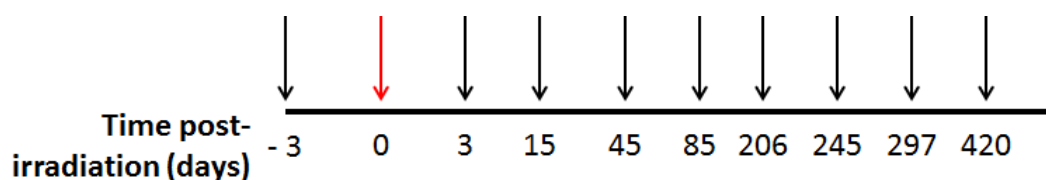


Figure 5-8: Outline of second longitudinal study.

Forty C57Bl/6 mice underwent tail-vein peripheral blood (PB) sampling three days prior to irradiation with sham (0 mGy) or 10 mGy X-rays (n = 20 per treatment group; red arrow). PB samples were taken at various time-points (black arrows) following the irradiation.

Table 16: Age of mice at PB sampling in longitudinal study (#2) up to 420 days post-irradiation with 10 mGy X-rays.

Time post-irradiation (d)		Dose (mGy)					
		0			10		
		<i>n</i>	Age (months)	<i>SD</i>	<i>n</i>	Age (months)	<i>SD</i>
-3	Male	10	4.94	0.89	10	4.66	1.05
	Female	10	4.27	0.87	10	4.19	0.72
3	Male	10	5.14	0.89	10	4.85	1.05
	Female	10	4.46	0.87	10	4.39	0.72
14	Male	10	5.53	0.89	10	5.25	1.05
	Female	10	4.86	0.87	10	4.78	0.72
45	Male	10	6.52	0.89	10	6.23	1.05
	Female	10	5.84	0.87	10	5.77	0.72
85	Male	10	7.83	0.89	10	7.55	1.05
	Female	10	7.16	0.87	10	7.08	0.72
206	Male	10	11.81	0.89	9	11.72	0.89
	Female	10	11.13	0.87	9	11.04	0.77
245	Male	8	13.20	0.86	8	13.01	0.95
	Female	10	12.42	0.87	9	12.32	0.77
297	Male	8	14.91	0.86	8	14.72	0.95
	Female	10	14.12	0.87	9	14.03	0.77
420	Male	8	18.95	0.86	6	18.61	1.05
	Female	9	18.11	0.90	9	18.07	0.77

5.1.2.2 Weight changes of male and female mice over time

At the end of the study, the mean age of both male and female mice was 18.53 (± 0.6) and 18.34 (± 0.4) months, respectively. There was no effect of irradiation on the changes in weight observed over time ($P > 0.05$; Table 17). Analysis of weight change over time revealed that there were significant differences in weight between mice ($P < 10^{-5}$). By 420 days post-irradiation, there was an increase in the mean weight of male mice (4.13 g) irrespective of treatment compared to the pre-irradiation mean weight ($P < 10^{-5}$). Female mice also exhibited an increase in mean weight (5.09 g) regardless of treatment group compared to the pre-irradiation mean weight ($P < 10^{-5}$) (Figure 5-9; Table 17).

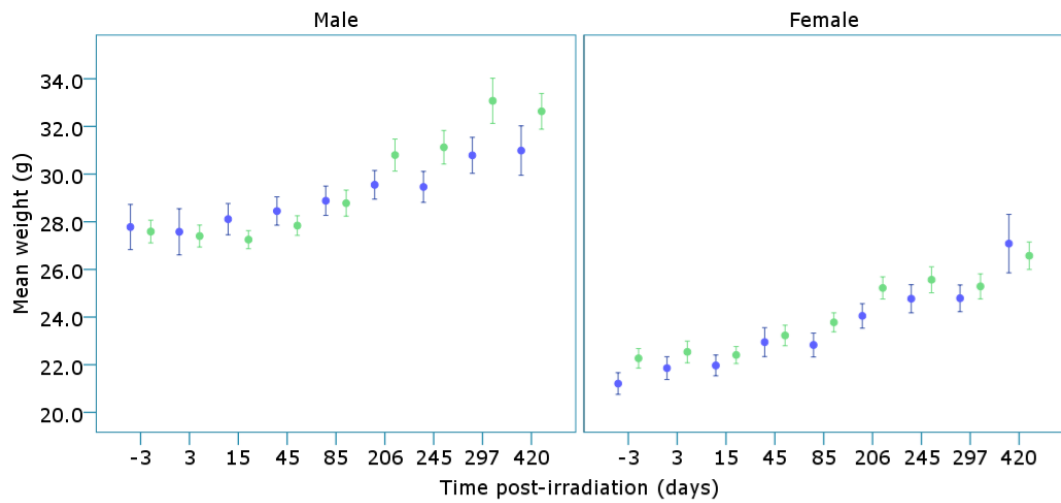


Figure 5-9: Mean weight over time for male and female mice irradiated with sham and 10 mGy X-rays.

Male ($6 \leq n \leq 10$ per treatment group) and female mice ($9 \leq n \leq 10$ per treatment group) irradiated with sham (blue) or 10 mGy (green) X-rays were weighed three days prior to, and at various time-points up to 420 days following irradiation.

Table 17: Analysis of changes in mouse weight up to 420 days post-irradiation with 10 mGy X-rays.

Changes in weight over time		P-value
Male	Individual mice	$<10^{-5}$ *
	0 mGy	0.049*
	10 mGy	$<10^{-5}$ *
	0 mGy vs. 10 mGy	0.370
Female	Individual mice	$<10^{-5}$ *
	0 mGy	$<10^{-5}$ *
	10 mGy	$<10^{-5}$ *
	0 mGy vs. 10 mGy	0.567
Male vs. Female		$<10^{-5}$ *

*Repeated measures analysis; $P < 0.05$

5.1.2.3 Analysis of the effect of irradiation and ageing on peripheral blood genomic DNA up to 420 days following irradiation with 10 mGy X-rays

5.1.2.3.1 Telomere length of peripheral blood genomic DNA

Mean length per telomere (kb) (MLT) was analysed for the pre-irradiation bleed (-3 days; 4.2 ± 0.8 months of age) and 420 days post-irradiation (18.2 ± 0.8 months of age) PB samples using a standard curve of known telomere lengths (Figure 5-10A) (O'Callaghan and Fenech, 2011). Only mice that were alive at the last PB sampling were analysed for both time-points ($n = 31^1$). Sixty-one percent (19/31) of the mice analysed had a significant difference in telomere length between the two time-points ($P < 10^{-5}$; repeated measures analysis) (Figure 5-10B). An effect of irradiation at either time-point was not detected for both male and female mice ($P > 0.05$) (Figure 5-11 and Table 24 in Appendix E). There was no significant difference in MLT between male and female mice ($P = 0.222$).

¹ The total number of mice remaining at the end of the study was $n = 32$, however one mouse was unable to be analysed due to limited DNA obtained

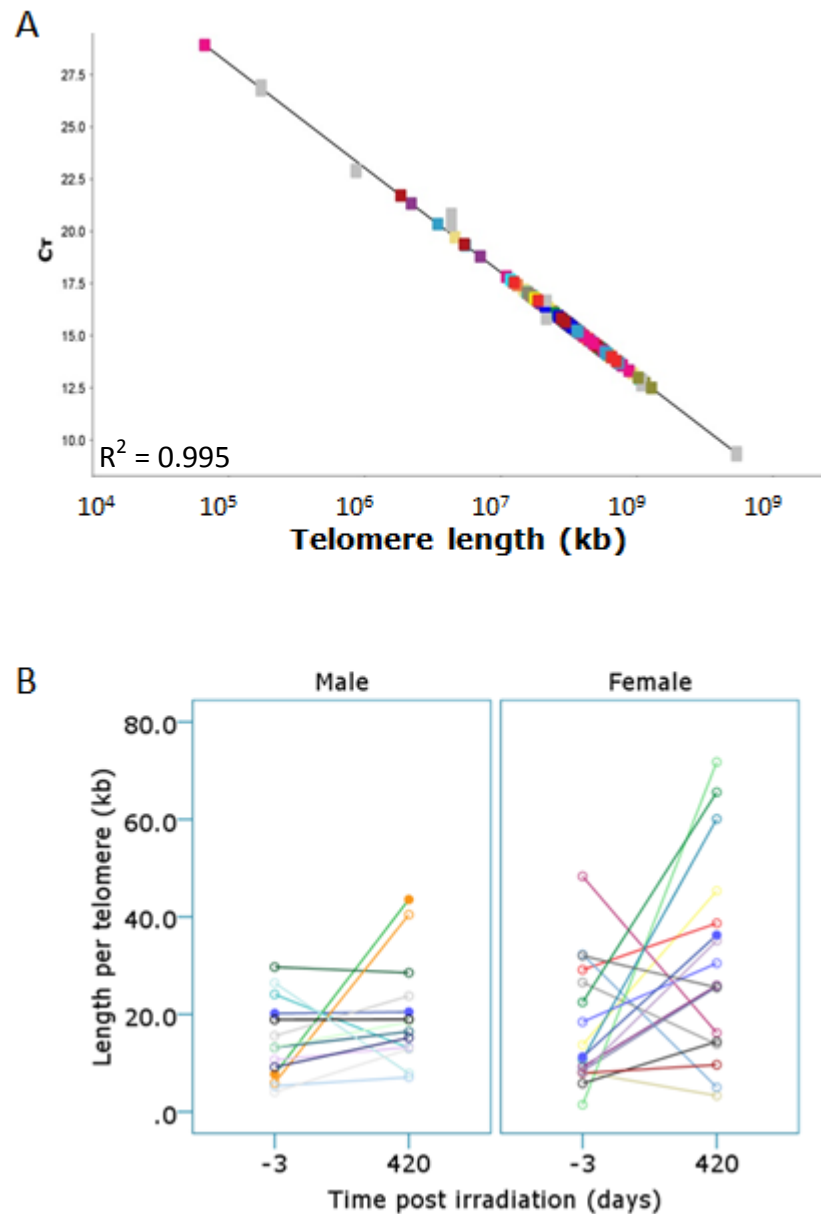


Figure 5-10: Telomere length of individual male and female mice pre- and post-irradiation with 10 mGy X-rays.

Following extraction, PB gDNA was amplified with murine telomere repeat sequence and 36B4 (for genome copy number determination) primers. (A) A representative standard curve used to calculate absolute telomere length per PCR. A synthesised oligonucleotide containing (TTAGG)₁₄ repeats was serially diluted 1/5 from 5.41 x 10⁸ to 6.92 x 10³ kb to create a standard curve of known total telomere length (see Appendix E). Adapted from O'Callaghan and Fenech (2011). Grey boxes represent standards, coloured boxes represent individual mice. (B) Length per telomere (kb) was calculated as a ratio of total telomere length and diploid genome copy number, divided by the total number of telomeres on 40 pairs of murine chromosomes for male (n = 6-8) and female (n = 9) mice three days prior to and 420 days post-irradiation with sham or 10 mGy X-rays. Coloured lines represent individual mice.

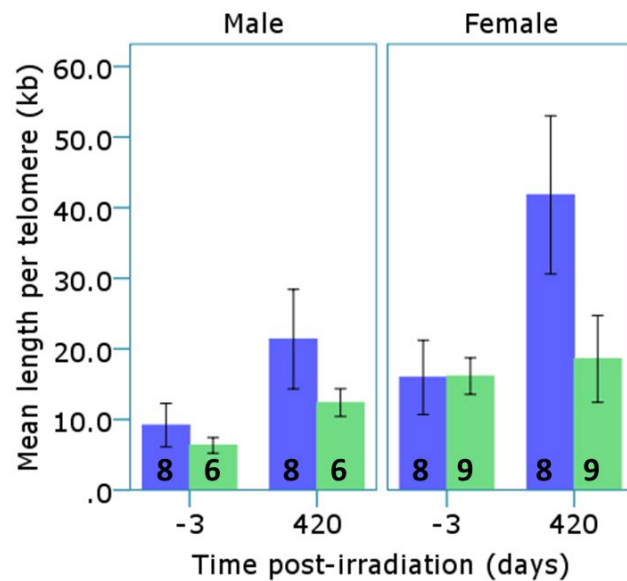


Figure 5-11: Mean telomere length of male and female mice pre- and post-irradiation with 10 mGy X-rays.

Following extraction, PB gDNA was amplified with murine telomere repeat sequence and 36B4 (for genome copy number determination) primers. Length per telomere (kb) was calculated as a ratio of total telomere length and diploid genome copy number, divided by the total number of telomeres on 40 pairs of murine chromosomes. Mean telomere length of sham (blue) and 10 mGy (green) irradiated mice three days (-3) prior and 420 days post irradiation divided by sex. Numbers in bold in each column indicates the number of mice (n). Error bars represent 1 SE.

5.1.2.3.2 Analysis of L1 and B1 element methylation changes up to 420 days post-irradiation with 10 mGy X-rays

As no significant change was detected in NTS between the pre-irradiation and samples for the time points up to 299 days post-irradiation in the first longitudinal study, only three time-points were chosen for the analysis of L1 and B1 element methylation changes in longitudinal study #2, -3 days (pre-irradiation bleed), 297 days (to compare with longitudinal study #1) and the final time-point of 420 days

post-irradiation. PB samples were randomly divided into different bisulphite modification groups and then randomly assigned to a HRM-PCR group (as was performed in longitudinal study #1). The samples in the second longitudinal study were amplified with the methylation-status unbiased L1 primers based on the low-level amplification observed with the unmethylated-biased L1 primers in longitudinal study #1. As there was a greater sample size of mice in this study, male and female mice were able to be analysed separately. For both L1 and B1 elements there were significant differences in NTS detected with time, with increases and decreases detected for, and between individual mice ($P < 0.05$; Table 18) (Figure 5-12A and B). No significant effect of irradiation on the L1 and B1 NTS changes over time was observed for either male or female mice, and there was no significant difference in NTS between male and female mice ($P > 0.05$; Table 18: Analysis of changes in PB L1 and B1 repeat element NTS in male and female mice up to 420 days post-irradiation with 10 mGy X-rays). Sham-irradiated female mice demonstrated increased B1 NTS at 297 days post-irradiation compared with 420 days post-irradiation ($P = 0.013$; Table 18) that was not observed for 10 mGy treated female mice.

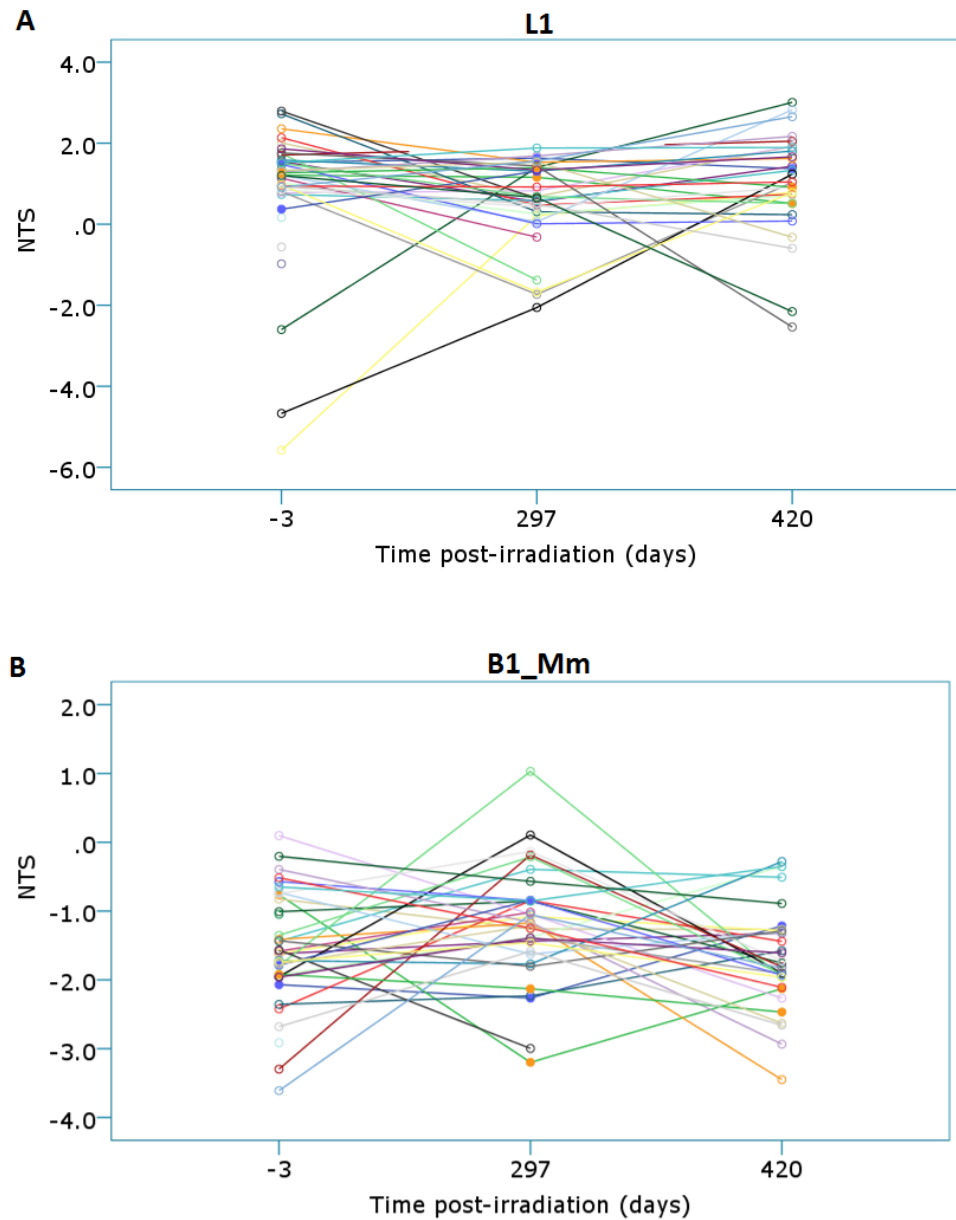


Figure 5-12: PB NTS for L1 and B1 elements for mice up to 420 days post-irradiation with sham or 10 mGy X-rays.

The NTS of PB gDNA from C57Bl/6 mice at -3, 297 and 420 days following irradiation with sham or 10 mGy X-rays ($15 \leq n \leq 20$ at each time-point) was assessed following extraction, bisulphite modification and amplification with methylation-status unbiased (A) L1 and (B) B1_Mm primers. Coloured lines represent individual mice.

Table 18: Analysis of changes in PB L1 and B1 repeat element NTS in male and female mice up to 420 days post-irradiation with 10 mGy X-rays.

Changes in NTS over time		P-value	
		L1	B1
Male	Individual mice	0.001*	<10 ⁻⁵ *
	0 mGy	0.519	0.825
	10 mGy	0.506	0.916
	0 mGy vs. 10 mGy	0.337	0.828
Female	Individual mice	<10 ⁻⁵ *	<10 ⁻⁵ *
	0 mGy	0.918	0.013*
	10 mGy	0.173	0.363
	0 mGy vs. 10 mGy	0.518	0.196
Male vs. Female		0.652	0.779

*Repeated measures analysis; $P < 0.05$

No difference in mean L1 and B1 NTS between sham and 10 mGy irradiated mice was detected at any time-point except for a decrease in L1 NTS of 10 mGy irradiated male mice at 420 days post irradiation ($P = 0.024$), however this group was not significantly different to the pre-bleed samples (Figure 5-13A and B). A significant, inverse correlation (Pearson correlation coefficient -0.206; $P = 0.033$) between L1 and B1 NTS for all PB samples analysed was observed (Figure 5-14). This indicated that mice that exhibited high L1 NTS had low B1 NTS and *vice versa*.

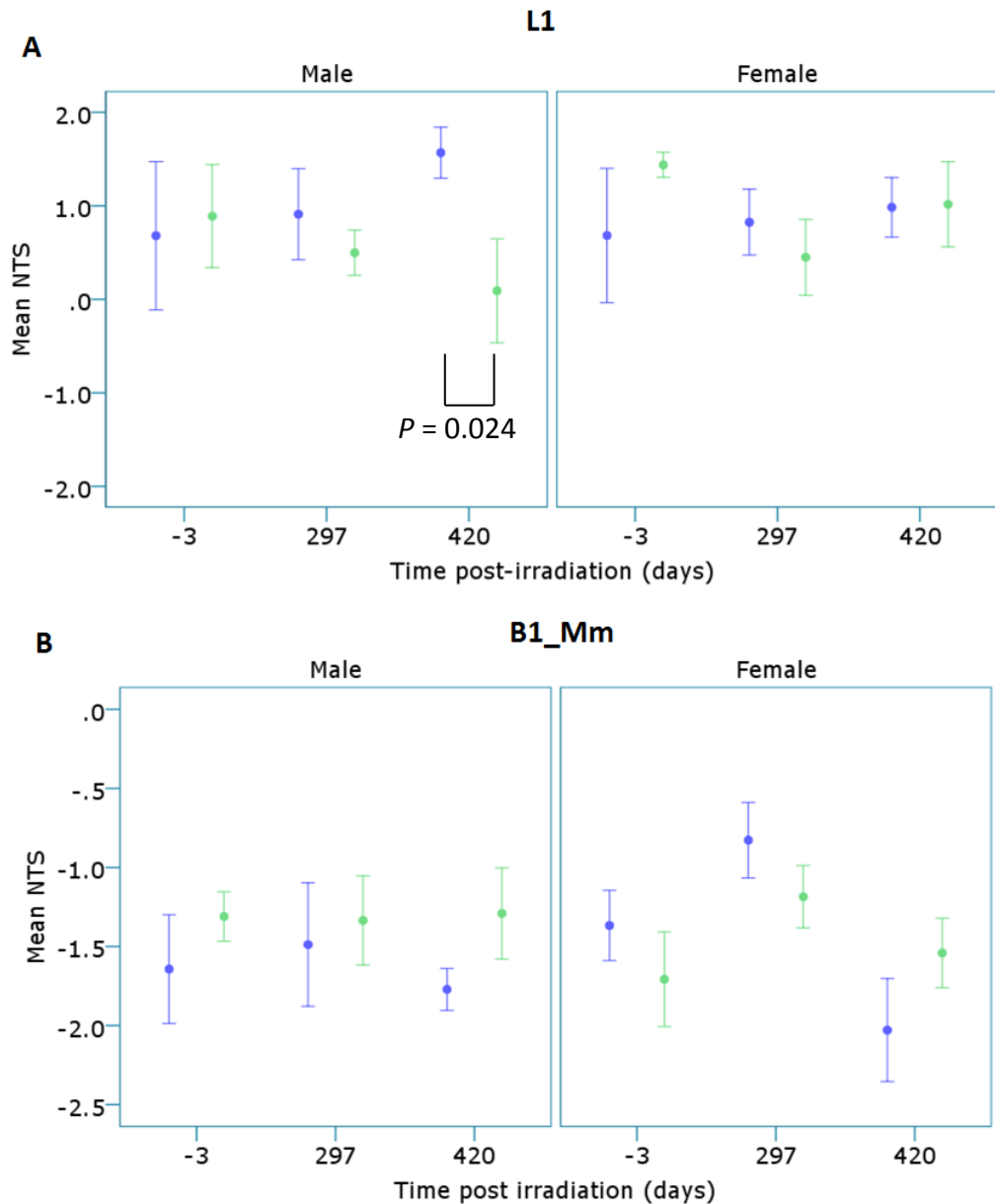


Figure 5-13: Mean PB NTS for L1 and B1 elements from mice up to 420 days post-irradiation with sham or 10 mGy X-rays.

The mean NTS of PB gDNA at -3, 297 and 420 days following irradiation with sham (blue) or 10 mGy (green) X-rays was assessed following extraction, bisulphite modification and amplification for male (n = 6-10) and female (n = 9-10) mice. (A) The mean L1 NTS (amplified with methylation-status unbiased primers), and (B) the mean NTS for B1_Mm repeat elements. The difference in NTS between sham and 10 mGy irradiated mice at each time-point was analysed using the Independent Samples T-test with significance achieved at $P < 0.05$. Error bars represent 1 SE.

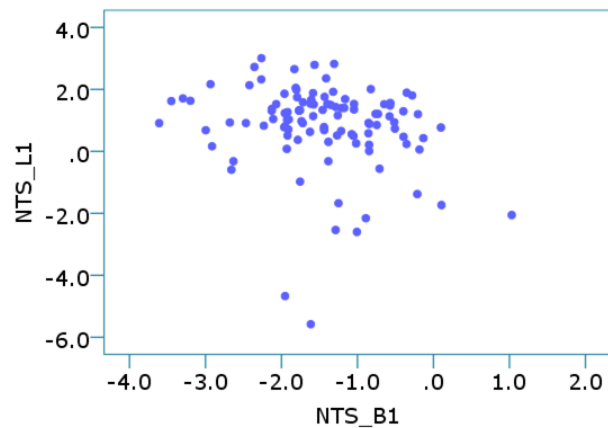


Figure 5-14: Correlation of L1 and B1 element NTS for PB.

Pearson correlation was used to assess the relationship between L1 (unbiased primers) and B1 (unbiased primers) element NTS for PB samples ($n = 107$) from sham and 10 mGy irradiated male and female mice at -3, 297 and 420 days post-irradiation.

5.1.2.4 Analysis of the effect of 10 mGy X-irradiation and ageing on spleen genomic DNA from mice at 420 days post-irradiation

5.1.2.4.1 Telomere length of spleen genomic DNA

The MTL of spleen gDNA from male and female mice ($n = 32$) at the end of the study (420 days post-irradiation; 18.2 ± 0.8 months of age) was analysed. There was no significant difference in MTL between male and female mice ($P = 0.125$). Irradiation had no effect on the MTL by 420 days post-irradiation for male and female mice (male mice: sham vs. 10 mGy; $P = 0.397$; female mice: sham vs. 10 mGy; $P = 0.193$). To assess the effect of age on spleen MTL, the MTL of the mice at the end of the study were compared to a cohort of young untreated 2 month old male and female mice ($n = 10$). There was no difference between the sham or 10 mGy irradiated mice and the young mice ($P > 0.05$; multivariate analysis of variance; see Table 25 in

Appendix E; Figure 5-15), although the older mice demonstrated greater variability for MTL compared with the younger mice.

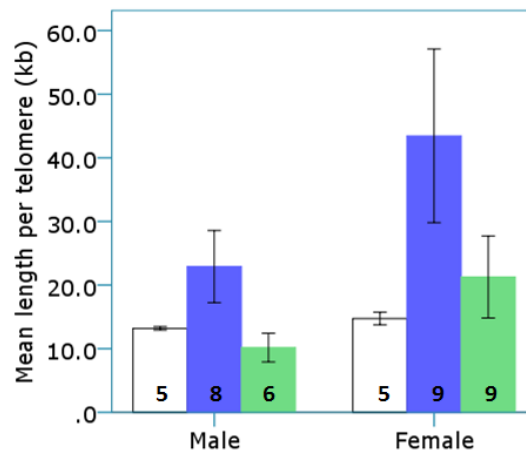


Figure 5-15: Analysis of spleen telomere length at 420 days post-irradiation with sham or 10 mGy X-rays compared to young untreated mice.

Following extraction, spleen gDNA was amplified with murine telomere repeat sequence and 36B4 (for genome copy number determination) primers. Length per telomere (kb) was calculated as a ratio of total telomere length and diploid genome copy number, divided by the total number of telomeres on 40 pairs of murine chromosomes. Mean telomere length of male and female mice 420 days post-irradiation with sham (blue) or 10 mGy (green) X-rays was compared to the mean telomere length of untreated 2 month old male and female mice (white). Numbers in bold indicate the number of mice (n). Error bars represent 1 SE.

5.1.2.4.2 Spleen tissue L1 and B1 element methylation 420 days following irradiation with 10 mGy X-rays

There was no significant difference between sham and 10 mGy irradiated mice for male and female spleen L1 and B1 NTS 420 days following irradiation ($P > 0.05$) (Figure 5-16). The L1 NTS of the spleens from the mice at the end of the study (420 days post-irradiation; ~18 months of age), were compared to the L1 NTS of the

young untreated mice (2 months of age). A significant increase ($P < 10^{-5}$) in L1 methylation was detected for the sham and 10 mGy irradiated mice compared with the untreated young mice. Due to time constraints, B1 element methylation levels of the young mice were not analysed.

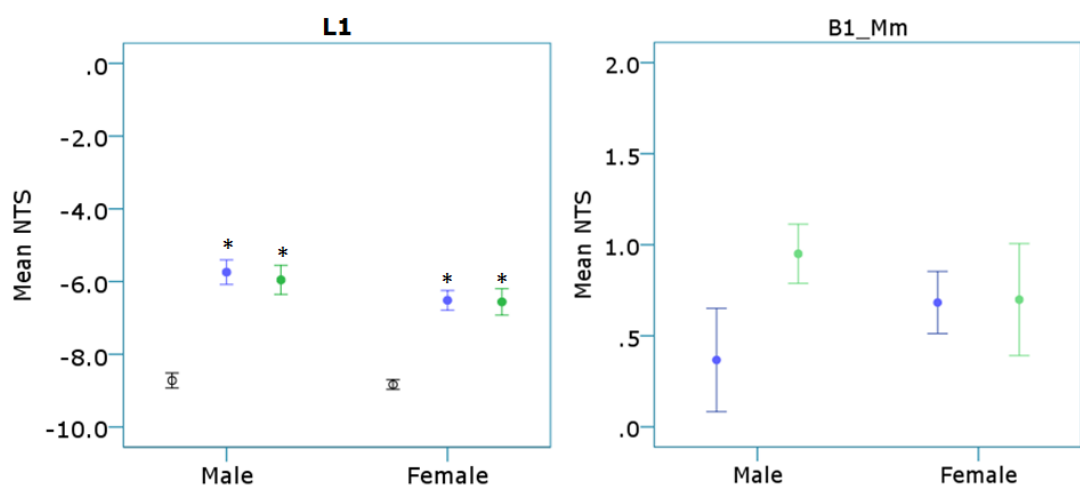


Figure 5-16: Spleen L1 NTS of mice 420 days post-irradiation compared with untreated young mice and analysis of B1 element NTS of mice 420 days post-irradiation with sham and 10 mGy X-rays.

*The mean L1 and B1 element NTS of sham (blue) irradiated male (n = 8) and female (n = 9), and 10 mGy (green) irradiated male (n = 6) and female (n = 9) mice 420 days following irradiation was analysed following extraction, bisulphite modification and amplification with unmethylated-biased L1 and unbiased B1_Mm primers. L1 NTS was compared to the mean NTS of untreated 2 month old (black) male (n = 5) and female (n = 5) mice. The difference between untreated, sham and 10 mGy irradiated mice was analysed using an ANOVA, with Games-Howell post-hoc analysis. Significance was achieved at $P < 0.05$. * $P < 10^{-5}$ compared with untreated mice. Error bars represent 1 SE.*

5.2 Discussion

The aim of this chapter was to use repeated PB sampling of mice in order to determine if a) there were age-associated changes in PB repeat element methylation levels and telomere lengths; and b) a low dose radiation exposure influenced the age-associated changes to the telomere lengths and methylation at the repeat elements.

5.2.1 Analysis of variation in NTS between PCRs

Initially, in longitudinal study #1, PB samples from the time-points -3 to 85 days post-irradiation were analysed in order to determine if there was an early effect of the irradiation, and to determine the variation that may have occurred due to the randomisation of the samples during bisulphite modification and PCR. Although a significant difference in NTS due to day-to-day PCR variation was detected between PCR groups (Table 19) which was also observed for repeat PCRs performed on the samples (data not shown), multivariate analysis demonstrated that the day-to-day variation in NTS between PCRs was not the cause of the changes in L1 NTS over time detected for individual mice. This indicated that any significant difference in NTS between the samples was greater than the PCR variation.

Table 19: Mean difference in L1 NTS between bisulphite modification and PCR groups for PB samples up to 85 days post-irradiation amplified with the unmethylated-biased primers.

	Group Number	<i>n</i>	Mean NTS	SE	Mean NTS difference between groups	<i>P</i> -value
Bisulphite modification	1	104	-4.18	0.146	0.07	0.736
	2	94	-4.11	0.153		
PCR	1	99 [^]	-4.90	0.085	1.51	<10 ^{-5*}
	2	99	-3.39	0.159		

[^]includes PCR controls

*Independent Samples T-test; with significance achieved at $P < 0.05$

In Chapter 3 it was shown that biasing the L1 primers for unmethylated CpGs within the primer binding sites enhanced the ability to detect small differences in NTS between samples. It was also observed that a significant change in L1 NTS between samples was reproducibly detected regardless of day-to-day variation in NTS values that occurs between different PCRs. However, it was found that the PB samples amplified later with the unmethylated-biased primers in comparison with amplification with the methylation-status unbiased L1 and B1 primers (Section 5.1.1.2, page 161). It has been reported that amplification of limited DNA sample/targets can result in stochastic fluctuation between the reaction replicates (Walsh *et al.*, 1992). It is possible that the reduced number of targets due to the high methylation level of the PB and the limited input DNA could have contributed to the late and variable amplification of the PB DNA samples observed with the unmethylated-biased primers. Despite reducing the sensitivity to detect small differences between samples, longitudinal study #2 was conducted with the methylation-status unbiased L1 primers as the number of target binding sites should be increased, improving amplification and reducing stochastic variation.

Differences in PB mean NTS between the randomly assigned PCR groups was also observed for the methylation-status unbiased L1 primers (Table 20). The difference in NTS between PCR groups amplified with the methylation-status unbiased primers was smaller than in longitudinal study #1, suggesting that there may have been less day-to-day PCR variation between PCRs conducted with the methylation-status unbiased L1 primers.

Table 20: Comparison of the mean L1 NTS for three PCR groups from longitudinal study #2 amplified with the methylation status-unbiased primers.

PCR group	n	Mean NTS	SE	PCR groups		Mean NTS difference		P-value
						between groups	SE	
1	33	0.77	0.171	1	2	0.536	0.328	0.315
2	34	1.30	0.188	1	3	0.266	0.325	1
3	35	0.50	0.300	2	3	0.802	0.323	0.044*

*ANOVA with Bonferroni *post-hoc* analysis; significance achieved at $P < 0.05$

While there were differences between the two longitudinal studies due to the number of mice used, the L1 primers used to analyse the samples and the final time-point of analysis, the same dose and dose-rate was used for both studies and the mice were from the same breeding colony and housed under the same conditions. Therefore, DNA samples from both studies could be compared in future experiments.

This is the first study to monitor changes in repeat element methylation within individual animals by repeated blood sampling. Other studies have compared cohorts of mice from different age groups in order to determine differences in

methylation in tissues such as the liver (Singhal *et al.*, 1987; Wilson *et al.*, 1987; Barbot *et al.*, 2002; Cherif *et al.*, 2003; Sauer *et al.*, 2010). While syngeneic, individual mice can respond differently following exposure to an exogenous modulator. For example, following maternal supplementation with folate, Agouti mice littermates can display a spectrum of the Agouti phenotype (Cropley *et al.*, 2010). The discordant changes between animals may occur at different time-points, and a cross-sectional study such as comparing two cohorts from a single time-point may miss this information, whereas longitudinal studies such as that performed here will be more likely to detect such changes. A limiting factor for a longitudinal study, such as the one reported in this thesis, is the number of samples that can be analysed in any one PCR. Ideally, a platform that can analyse >100 samples would be needed so that all samples are amplified in the same PCR to reduce PCR variation.

5.2.2 The longitudinal effect of 10 mGy X-irradiation on telomere length and repeat element methylation in spleen and peripheral blood up to 420 days post-irradiation

Gross physiological effects of the irradiation on the young mice were not apparent, and the weight changes/range were consistent with previous reports of ageing C57Bl/6 mice (Rowlatt *et al.*, 1976). PB samples exhibited intra-and inter-animal variation in NTS for both L1 and B1 elements methylation and telomere length. Telomere shortening has been reported to be an age-related phenomenon. At the

end of this study mice were in early old-age (~18 months; the age range for old-age is 17-24 months), and an age-related decline in telomere length was not detected. It was observed that female mice had greater variability in telomere length compared with male mice, with the trend of increased telomere length at old age (see Table 24 in Appendix E). While differences in telomere length between male and female inbred mice in normal ageing tissues has not been reported, some wild mouse strains with similar telomere lengths to humans exhibit gender differences in telomere lengths with ageing, with longer telomeres detected in female mice compared with male mice (Coviello-McLaughlin and Prowse, 1997). In rats, 15-month old males have been shown to have shorter telomeres in the kidney and liver than females (Cherif *et al.*, 2003). Variation in telomere length with ageing of up to 100 kb in genetically identical inbred animals including mice, has been previously reported, supporting the increased variation reported in this thesis (Starling *et al.*, 1990; Coviello-McLaughlin and Prowse, 1997; Cherif *et al.*, 2003; Roberts *et al.*, 2011). Human PB telomere lengthening with age has been observed in individuals ranging from 30-70 years of age, where sampling occurred 10 years apart, although the mean change in telomere length was a reduction of length, and there was no difference between males and females (Nordfjäll *et al.*, 2009). While telomere shortening with age is well established in humans, it has not been conclusively shown for inbred mice, as was reported in this thesis. It has been proposed that this is due to the longer length of murine telomeres (<150 kb) compared with human telomeres (<100 kb), and thus shortening of the telomeres is not easily detected (Coviello-McLaughlin and Prowse, 1997; Cherif *et al.*, 2003). A lack of telomere shortening in the aging mice might also be attributed to the observation that mice

express high levels of telomerase and can therefore restore telomere lengths to a greater extent than humans, who express relatively low levels of telomerase (Prowse and Greider, 1995). It would be of interest to determine if there is up-regulation of telomerase in the ageing mice or following irradiation from the study performed here. This is the first report of PB telomere length changes over time within individual mice. Studies of mouse cells *in vitro* have shown that cells with shorter telomeres exhibit increased sensitivity to high dose radiation exposure (Drissi *et al.*, 2011), while studies utilising mice deficient in telomerase reported radiation sensitivity only occurred following several generations, when telomeres were sufficiently shorter compared to wild type mice (Goytisolo *et al.*, 2000; Wong *et al.*, 2000). There are no comparative studies to that reported in this thesis investigating the effect of low dose radiation exposure and alteration of telomere length.

The effect of a low dose of ionising radiation or the effect of ageing on murine PB L1 methylation levels has not been previously reported. No effect of irradiation on PB L1 methylation levels was observed at any time-point. The repeated PB sampling performed in this thesis provides the first murine experiment that reports age-associated intra-individual variation in repeat element methylation. Human studies have shown intra-individual variation in PB repeat element methylation levels, with both losses and gains in methylation with age or in response to exogenous modulators (Bollati *et al.*, 2009; Jintaridth and Mutirangura, 2010; El-Maarri *et al.*, 2011; Woo and Kim, 2012; Wu *et al.*, 2012), as was observed for low dose ionising

radiation exposure here. A recent report has demonstrated that inter- and-intra individual variation exists for specific L1 element sequences located within the promoters of various genes. It was observed that tissues with high levels of transcriptional activity, such as the liver, exhibited more variable DNA methylation levels of the repeat elements, which were more obvious in adult mice compared with 1-week old pups (Ekram *et al.*, 2012). These observations provide support that the variation detected in PB L1 and B1 element NTS between animals with ageing, and suggest that the intra- and inter-animal fluctuation could be influenced by the location of the L1 and B1 elements. However, this is the first murine longitudinal study of methylation levels and thus there are no comparative studies.

In longitudinal study #1, a significant reduction in B1 NTS was detected in mice irradiated with 10 mGy compared with sham-irradiated mice at 299 days post-irradiation. No difference in NTS was detected between the pre-irradiation and 299 days post-irradiation PB samples for the sham-irradiated mice, however the 10 mGy irradiated mice exhibited reduced B1 methylation at 299 days post-irradiation compared to the pre-irradiation PB samples (Figure 5-6). This was not observed for longitudinal study #2. It is possible that the smaller samples size of longitudinal study #1 contributed to the difference in mean NTS between the treatment groups. A significant reduction in the L1 NTS of male mice irradiated with 10 mGy compared with sham-irradiated mice at 420 days post-irradiation was detected in longitudinal study #2 (Figure 5-13A). It is possible that the difference between the treatment groups may have increased if the study had continued past 18 months of age. Neither group was significantly different to the pre-irradiation bleeds, indicating

that while there was no overall decline in L1 methylation by 420 days, the two groups were exhibiting different trends of the repeat element methylation.

There are no comparative mouse studies investigating PB repeat element methylation levels or the effect of a low dose radiation exposure. The NTS values for the L1 elements of all PB samples, regardless of PCR group, demonstrated an inverse correlation with the NTS values of the B1 elements. This indicated that even with the observed PCR variation between the PCR groups, changes were occurring at two different types of repeat elements in different chromosomal locations that were amplified in different PCRs. These changes displayed trends for each mouse, with mice with high L1 methylation displaying low B1 methylation and *vice versa*, indicating that the results observed for individual mice were not due to technical variability, but due to a biological response. There is no comparative data in the literature to suggest why there would be an inverse relationship between L1 and B1 methylation levels in the PB samples, however it has been found that the proximity of the human B1 homologue, Alu, to L1 elements can influence the methylation status of the L1 elements (Kang *et al.*, 2006). One hypothesis for the inverse correlation is that while the B1 elements on their own are unable to transpose, they can utilise the L1 machinery, and are found to move more easily through the genome than L1 elements (Ostertag, 2001). Thus, tightening control of the L1 elements through methylation could result in less of a need to methylate the B1 element promoters. This correlation of the repeat element methylation levels requires further investigation. It would be informative to perform bisulphite sequencing in order to analyse individual repeat element sequences for mapping in order to determine the location of the repeat elements.

The majority of the murine ageing studies have demonstrated a loss of methylation in the liver with age, occurring around 24 months of age, and these studies have been cross-sectional. In this thesis, a cross-sectional study of spleen L1 NTS of young and old mice was conducted, where increased L1 methylation with age was observed for the mice at the final time-point of 420 days post-irradiation (~18 months of age). Increases in total genomic and repeat element methylation levels with ageing have been reported previously. In mice, Singhal *et al* (1987) observed a decrease in liver 5mdC levels (by HPLC) by 24 months of age, which was then followed by an increase that persisted until the end of the study (30 months of age). A human study reported that CpG island-rich regions, such as L1 repeat elements, exhibited increased methylation with age compared with CpG island-poor regions (Christensen *et al.*, 2009). Due to time-constraints, other tissues such as the liver were not able to be analysed for comparison with the other mouse studies, nor were the mice able to be analysed past ~18 months of age. It would be of interest to investigate the methylation levels of other tissues such as the liver, from the old mice remaining at the final time-point in this thesis to determine if there are tissue differences in response to both ageing and the irradiation. It would also be informative to analyse the methylation levels of the livers using LC-MS, and as a control for age-related methylation decline, investigate loci reported to undergo age-related losses in methylation as well as other repeat elements such as the IAP elements, which have been reported to undergo a loss of methylation and increased transcription in ageing animals (Barbot *et al.*, 2002). These experiments would indicate if there is an age-threshold for when a decline in methylation occurs.

As mentioned previously, a significant change in PB methylation levels was not detected by the end of the study, although fluctuation in the NTS was detected over time. It is not known whether the fluctuations in NTS are due to changes in white blood cell population. Retrospectively, it would have been useful to perform blood-smear histology at each PB sampling in order to determine if there had been gross changes in the white blood cell (WBC) population over time. It has been reported that in mice following low dose irradiation (75 mGy), an increase in WBC population at 48 hours post-irradiation was detected, but lower doses of 25 mGy and 50 mGy did not induce a change in cell population (Wang and Cai, 2000; Li *et al.*, 2004). Furthermore, a study on WBC populations in ageing mice (>24 months of age) did not detect a significant change in total WBC with age, however a modest increase in lymphocyte population was observed in the oldest mice (Silini and Andreozzi, 1974). Several studies have shown that baseline PB methylation levels are influenced by the population of cells in blood samples in humans (e.g. granulocytes vs. white blood cells) (Wu *et al.*, 2011; 2012). Flow cytometry for WBC types would have been useful to confirm if there had been changes in cell population that may have influenced methylation levels, but would have been difficult due to limited blood samples.

Dose-rate has been demonstrated to have an influence on endpoints such as chromosomal aberrations and the resulting DNA repair (Vilenchik and Knudson, 2000; Loucas *et al.*, 2004; Tubiana *et al.*, 2006). High dose radiation DNA methylation studies (as discussed in Section 1.4) have also reported different effects

on DNA methylation in different tissues depending on dose-rate. The one ageing study that demonstrated that a single low dose exposure could prevent ageing-associated increases in endogenous DNA damage used a dose of 100 mGy (Zaichkina *et al.*, 2006). The dose of 10 mGy used in this thesis has been demonstrated in the literature to induce an adaptive response *in vivo* for other endpoints, and is similar to doses received from CT scans. It is possible that a low dose of 10 mGy does not have any long term effects on either DNA methylation or telomere length. Alternatively, it is possible that the mice were not old enough for large changes in DNA methylation to be detected, and that an adaptive response may have been observed if the mice had been older than 18-months of age. While there are no comparative human studies investigating the effects of low dose radiation exposure on PB repeat element methylation, reports have demonstrated that exposure to low-level environmental pollutants induced <1% reduction in methylation at both the L1 and Alu repeat elements 180 days following exposure. In the human study, only 3 CpGs were analysed for the repeat elements in comparison to the 13 CpGs sites interrogated for the L1 elements and the 7 for the B1 elements presented in this thesis (Madrigano *et al.*, 2011). It is yet to be determined what the biological consequence of a <1% loss of repeat element methylation is.

5.3 Conclusion

There is much concern about the long term effects that may arise from the exposure to low doses of radiation, such as the 10 mGy used here (Valentin, 2007). Overall, an age-associated decline in repeat element methylation was not observed

at 18 months of age, while increased L1 methylation was observed in the spleens of the male and female mice irrespective of treatment, at the end of the study compared to young mice. Furthermore, no effect of the low dose radiation exposure was detected for either the repeat element methylation levels or telomere lengths. This is also the first report of murine PB telomere length changes in ageing animals and demonstrated there is also increased intra-individual variation in PB telomere length similar to that observed in human studies. This is the first study to longitudinally analyse age-associated changes and the effect that a low dose of 10 mGy has on repeat element methylation levels of murine PB samples, with the results indicating that a low dose ionising radiation exposure does not induce permanent changes in repeat element methylation levels.

6 GENERAL DISCUSSION

Ionising radiation induces DNA damage by direct ionisation of nucleotide bases and sugars or indirectly by generating reactive oxygen species, both potentially resulting in DNA strand breaks. However it has been shown that DNA damage can also occur in the form of the modulation of DNA methylation, a modification of cytosine that is involved in chromatin structure stability and the control of gene expression. Ionising radiation can affect DNA methylation by direct ionisation of the cytosine residue resulting in deamination, by the failure of a methyl group to be replaced following DNA repair due to mutation of the cytosine to a thymidine, and through 8-hydroxyguanine adducts and other DNA lesions inhibiting the activity of the DNA methyltransferases (DNMTs) (Riley, 1994; Turk *et al.*, 1995; Krivokapic *et al.*, 2008). These effects of ionising radiation on DNA methylation can be enhanced by the location of the DNA i.e. heterochromatin vs. euchromatin, the proliferative state of the tissue, and the tissue type. Aberrant DNA methylation has been shown to be involved in the tumour initiating processes for some cancers in both mouse and human studies (Bender *et al.*, 1998; Gaudet *et al.*, 2003; Tryndyak *et al.*, 2006; Ogino *et al.*, 2008a; Daskalos *et al.*, 2009; Igarashi *et al.*, 2010; Aporn Dewan *et al.*, 2011). However, it is less clear whether the modulation of DNA methylation is the cause of the radiation-induced genomic instability that can result in carcinogenesis. Certainly, tumour growth is successfully retarded when 5-aza induced demethylation renders the cancer cells more susceptible to radiation therapy, indicating that a loss of methylation is involved in the radiation-induced cell death (Dote *et al.*, 2005).

A hallmark of cancer is the hypermethylation of tumour suppressor genes, but an overall loss in genomic 5mdC content (as reviewed by Baylin *et al.*, 2001). The time required between the hypermethylation of loci and the initiation of cancer following radiation exposure is still unclear, but it must involve a cascade of events including histone modifications and the recruitment of methyl-binding proteins and methyltransferases, and it is likely that the hypermethylation of these loci occurs at a later time-point than the immediate DNA repair processes that occur following the irradiation. In this thesis, high dose ionising radiation (1 Gy) was demonstrated to modulate the CpG methylation levels of repetitive DNA elements located throughout the genome, and the modulation was demonstrated to be temporal. Investigation of total genomic 5mdC using LC-MS indicated that the radiation did not cause a change to the overall global DNA methylation levels, and suggests that the modulation of the L1, B1 and IAP element methylation represents a change in the distribution of the CpGs that are methylated, and may reflect small, localised changes in CpG methylation. It is likely that these localised changes are linked to the DNA repair responses at the repeat elements. There is mounting *in vitro* evidence indicating that the DNMTs play a crucial role in, and are affected by, the repair processes that occur following DNA damage, particularly for DNA DSBs, and that the resulting methylation changes are transient (Mortusewicz *et al.*, 2005; Barreto *et al.*, 2007; Li *et al.*, 2007; Damiani *et al.*, 2008; O'Hagan *et al.*, 2008; Ha *et al.*, 2011; Lee *et al.*, 2011; O'Hagan *et al.*, 2011; Sharma *et al.*, 2011; Wong *et al.*, 2011).

The pyrosequencing data from Figure 4-10A may suggest a potential mechanism for the modulation of CpG methylation at the L1 elements that was observed in this thesis. The majority of the loss of methylation 14 days following irradiation was

found to occur within the 5' end of the L1 CpG island. This region incorporates 5 CpGs and also contains the majority of the non-CpG SNPs. It is possible that CpG sites have been altered due to: C>T deamination; the less common nucleotide of the SNP being replaced in the repaired strand resulting in a failure of the DNMTs to recognise the site; or a DNA lesion (such as an adduct) inhibiting the activity of the DNMTs to restore the methyl group (Turk *et al.*, 1995; Valinluck and Sowers, 2007; O'Hagan *et al.*, 2011). There is evidence also, that implicates hemi-methylation states influencing the repair process. During repair, one strand remains methylated to act as a template for the newly synthesised strand. If mutations have occurred, the new strand may not be re-methylated (Liang *et al.*, 2002; Jeong *et al.*, 2009; Lee *et al.*, 2011). Alternatively, it has been suggested that increases in methylation following repair are the result of previously hemi-methylated regions undergoing full methylation (James *et al.*, 2003; Cuozzo *et al.*, 2007; O'Hagan *et al.*, 2008; Lee *et al.*, 2010a), and could be a possible mechanism for the transient increased methylation observed in this thesis. The transience in methylation levels that was observed in Chapter 4 may also be due to the *de novo* DNMTs associating with base-excision repair proteins and methylating CpGs – which are later recognised as incorrectly methylated following which the methyl group is removed. There is evidence in the literature demonstrating that this can occur (Li *et al.*, 2007; Shen *et al.*, 2010). However, the increase in L1 methylation observed in some mice was also detected at 6 days post-irradiation, and may indicate that some *de novo* methylation remained following repair. Re-methylation of repeat elements has also been linked with “methylation-spread”, where the restoration of methyl groups or

de novo methylation triggers the spread of methylation to neighbouring regions resulting in increased methylation levels (Woodcock *et al.*, 1997; Zhang *et al.*, 2012).

The LC-MS and L1-HRM assays used here to detect changes in CpG methylation are detecting different methylation events. LC-MS provides an overall measure of genomic methylation levels but does not give the location and distribution of the CpGs in relation to transcription start sites and gene loci which can influence, and be influenced, by DNA repair and methylation spread. While the L1-HRM assay was demonstrated to be more sensitive in detecting changes in methylation not detected by LC-MS, the assay also does not give an indication as to the chromosomal locations of the L1 elements undergoing changes in methylation. Therefore, it would be useful to utilise next generation sequencing platforms or bisulphite sequencing in order to determine if there are chromosomal locations or specific sub-families of the L1 elements that are affected by the irradiation.

It has been proposed that the gradual loss of methylation in ageing cells is due to the accumulation of increased damage from normal metabolic processes and reduced fidelity of repair. It is plausible that the fluctuations in PB L1 methylation levels over time detected by the L1-HRM assay described in this thesis were the result of normal DNA repair mechanisms resulting from endogenous oxidative damage, or DNMT activity linked to the cell cycle. Future studies could utilise flow cytometry to assess the cell cycle stage in splenic cells prior to genomic DNA extraction and assessment of L1 methylation levels using the L1-HRM assay. It has been shown that a low dose irradiation can induce an adaptive response and stimulate DNA repair mechanisms; however an adaptive response has not been

demonstrated for the modulation of DNA methylation. This study did not observe an effect of the 10 mGy irradiation on L1 or B1 methylation levels over time. It is possible that the up-regulation of the repair machinery by the low dose irradiation does not impact DNA methylation regulation, or that the changes in methylation were not large enough for an adaptive response to be observed. This is, however, the first report demonstrating that a low dose of 10 mGy does not elicit a detectable effect on repeat element methylation levels in ageing animals.

The increases in methylation observed in Chapter 4 may therefore represent transient up-regulation of normal processes that have little or no impact on L1 repression. This normal fluctuation in methylation levels may explain why a change in L1 transcript levels was not observed in the mice demonstrating a loss of CpG methylation following irradiation. Based on the literature, it was proposed that following high dose radiation exposure, a loss of methylation would be observed at the L1 elements. In this study it was demonstrated that the changes were transient, influenced by the genetic background, gender of the mice and the tissues investigated. Even so, the long term effects of high dose radiation exposure and the effect of dose-rate on DNA methylation are still largely unknown. Furthermore, while there is some evidence linking the modulation of DNA methylation to the DNA repair pathways, *in vivo* mechanisms are yet to be determined. It has not been demonstrated if the CBA, BALB/c and C57Bl/6 mouse strains exhibit differences in DNMT expression and activity, and would be of interest to investigate if the changes in methylation are associated with *de novo* DNA methyltransferase activity. Also, chromatin-immunoprecipitation (ChIP) experiments would provide information on the proteins, such as the DNMTs, DNA repair-associated proteins and the

transcription factor YY1, that are associating at the L1 elements. CHIP-sequencing could also be performed, which would give a detailed analysis of the sequence and chromosomal locations of the L1 elements that are undergoing methylation changes, and data on specific sequences within the L1 promoter that the proteins bind to. The temporal studies performed in this thesis demonstrated short-term effects of high dose radiation exposure. Therefore, similar studies should be conducted investigating longer times post-irradiation to understand if the transient changes in methylation that occurred within 14 days following the irradiation exposure are maintained for a limited period of time, or if a more permanent change to the methylation levels occurs. There is emerging evidence that the modulation of DNA methylation is also influenced by other epigenetic mechanisms such as histone protein marks and non-coding RNAs (ncRNAs). It has been demonstrated that repeat elements can produce ncRNA transcripts (such as long-ncRNAs and piwi-RNAs) that regulate the methylation of the L1 promoters as well as surrounding areas (Reuter *et al.*, 2011; Blackwell *et al.*, 2012). At present, the effect of irradiation on ncRNAs is unknown, although ncRNAs have been demonstrated to be associated with DNA repair machinery. A recent investigation of Alu repeat element ncRNAs found that the ncRNAs bound and interacted with DNA repair proteins such as DDB1 and PARP, as well as chromatin modifying proteins such as SOX6 and INO80 (Blackwell *et al.*, 2012). However, most of these associations have been demonstrated in embryonic cells and it is unclear whether the same processes occur in adult somatic tissues.

The studies described in this thesis demonstrate the importance of timing of analysis in methylation studies. They also highlight that a high dose of 1 Gy can induce transient changes in the methylation levels of transcriptionally repressed DNA elements, despite the accepted dogma that a high dose of radiation will cause a permanent loss of DNA methylation, and indicate that the dose of radiation also needs to be considered in DNA methylation studies. Furthermore, this is the first report to show that a low dose radiation exposure (10 mGy) does not permanently alter repeat element DNA methylation levels or telomere lengths in ageing mice, changes which have been associated with age-related genomic instability and increased cancer risk. Also, this thesis describes the first murine longitudinal study to utilise PB sampling to monitor changes in DNA methylation in ageing mice.

The results from this thesis have expanded the knowledge in the relatively small field of radiation effects on DNA methylation, exemplifying the complex nature of methylation responses at repetitive DNA elements. The studies described in this thesis highlight that further work is required to understand the link between DNA methylation modulation and the response to ionising radiation.

REFERENCES

Akagi, K., Li, J., Stephens, R. M., Volfovsky, N., Symer, D. E. (2008). Extensive variation between inbred mouse strains due to endogenous L1 retrotransposition. *Genome Research* **18** (6): 869-880.

Aldridge, G. M., Podrebarac, D. M., Greenough, W. T., Weiler, I. J. (2008). The use of total protein stains as loading controls: an alternative to high-abundance single-protein controls in semi-quantitative immunoblotting. *Journal of Neuroscience Methods* **172** (2): 250-254.

Aporntewan, C., Phokaew, C., Piriyaongsa, J., Ngamphiw, C., Ittiwut, C., Tongsimma, S., Mutirangura, A. (2011). Hypomethylation of Intragenic LINE-1 Represses Transcription in Cancer Cells through AGO2. *PLoS ONE* **6** (3): e17934.

Armstrong, C. A., Jones, G. D., Anderson, R., Iyer, P., Narayanan, D., Sandhu, J., Singh, R., Talbot, C. J., Tufarelli, C. (2012). DNMTs are required for delayed genome instability caused by radiation. *Epigenetics* **7** (8): 0--1.

Athanikar, J. N., Badge, R. M., Moran, J. V. (2004). A YY1-binding site is required for accurate human LINE-1 transcription initiation. *Nucleic Acids Research* **32** (13): 3846-3855.

Aukett, R., Burns, J., Greener, A., Harrison, R., Moretti, C., Nahum, A., Rosser, K. (2005). Addendum to the IPEMB code of practice for the determination of absorbed dose for x-rays below 300 kV generating potential (0.035 mm Al-4 mm Cu HVL). *Physics in Medicine and Biology* **50** 2739.

Aukett, R., Harrison, R., Moretti, C., Nahum, A., Rosser, K. (1996). The IPEMB code of practice for the determination of absorbed dose for x-rays below 300 kV generating

potential (0.035 mm Al-4 mm Cu HVL; 10-300 kV generating potential). *Physics in Medicine and Biology* **41** 2605.

Aypar, U., Morgan, W. F., Baulch, J. E. (2011). Radiation-induced epigenetic alterations after low and high LET irradiations. *Mutation Research/Fundamental and Molecular Mechanisms of Mutagenesis* **707** (1-2): 24-33.

Azzam, E., De Toledo, S., Raaphorst, G., Mitchel, R. (1996). Low-dose ionizing radiation decreases the frequency of neoplastic transformation to a level below the spontaneous rate in C3H 10T1/2 cells. *Radiation Research* **146** (4): 369-373.

Azzam, E., Raaphorst, G., Mitchel, R. (1994). Radiation-induced adaptive response for protection against micronucleus formation and neoplastic transformation in C3H 10T1/2 mouse embryo cells. *Radiation Research* **138** (1): 28-31.

Baccarelli, A., Wright, R. O., Bollati, V., Tarantini, L., Litonjua, A. A., Suh, H. H., Zanobetti, A., Sparrow, D., Vokonas, P. S., Schwartz, J. (2009). Rapid DNA Methylation Changes after Exposure to Traffic Particles. *American Journal of Respiratory and Critical Care Medicine* **179** (7): 572-578.

Barber, R., Hickenbotham, P., Hatch, T., Kelly, D., Topchiy, N., Almeida, G., Jones, G., Johnson, G., Parry, J., Rothkamm, K. (2006). Radiation-induced transgenerational alterations in genome stability and DNA damage. *Oncogene* **25** (56): 7336-7342.

Barber, R., Plumb, M. A., Boulton, E., Roux, I., Dubrova, Y. E. (2002). Elevated mutation rates in the germ line of first- and second-generation offspring of irradiated male mice. *Proceedings of the National Academy of Sciences* **99** (10): 6877-6882.

Barbot, W., Dupressoir, A., Lazar, V., Heidmann, T. (2002). Epigenetic regulation of an IAP retrotransposon in the aging mouse: progressive demethylation and de-

silencing of the element by its repetitive induction. *Nucleic Acids Research* **30** (11): 2365.

Barreto, G., Schäfer, A., Marhold, J., Stach, D., Swaminathan, S. K., Handa, V., Döderlein, G., Maltry, N., Wu, W., Lyko, F., Niehrs, C. (2007). Gadd45a promotes epigenetic gene activation by repair-mediated DNA demethylation. *Nature* **445** (7128): 671-675.

Batzler, M. A., Deininger, P. L. (2002). Alu repeats and human genomic diversity. *Nature Reviews Genetics* **3** (5): 370-379.

Baylin, S. B., Esteller, M., Rountree, M. R., Bachman, K. E., Schuebel, K., Herman, J. G. (2001). Aberrant patterns of DNA methylation, chromatin formation and gene expression in cancer. *Human Molecular Genetics* **10** (7): 687-92.

Beetstra, S., Thomas, P., Salisbury, C., Turner, J., Fenech, M. (2005). Folic acid deficiency increases chromosomal instability, chromosome 21 aneuploidy and sensitivity to radiation-induced micronuclei. *Mutation Research/Fundamental and Molecular Mechanisms of Mutagenesis* **578** (1-2): 317-326.

Bender, C. M., Pao, M. M., Jones, P. A. (1998). Inhibition of DNA Methylation by 5-Aza-2'-deoxycytidine Suppresses the Growth of Human Tumor Cell Lines. *Cancer Research* **58** (1): 95-101.

Bernal, A. J., Dolinoy, D. C., Huang, D., Skaar, D. A., Weinhouse, C., Jirtle, R. L. (2012) Adaptive radiation-induced epigenetic alterations mitigated by antioxidants. *The FASEB Journal*:**27** 10.1096/fj.12-220350 November 1, 2012.

Besplug, J., Burke, P., Ponton, A., Filkowski, J., Titov, V., Kovalchuk, I., Kovalchuk, O. (2005). Sex and tissue-specific differences in low-dose radiation-induced oncogenic signaling. *International Journal of Radiation Biology* **81** (2): 157-68.

Biedermann, K. A., Sun, J. R., Giaccia, A. J., Tosto, L. M., Brown, J. M. (1991). *scid* mutation in mice confers hypersensitivity to ionizing radiation and a deficiency in DNA double-strand break repair. *Proceedings of the National Academy of Sciences of the United States of America* **88** (4): 1394-1397.

Blackwell, B. J., Lopez, M. F., Wang, J., Krastins, B., Sarracino, D., Tollervey, J. R., Dobke, M., Jordan, I. K., Lunyak, V. V. (2012). Protein interactions with piALU RNA indicates putative participation of retroRNA in the cell cycle, DNA repair and chromatin assembly. *Mobile Genetic Elements* **2** (1): 26-35.

Bollati, V., Schwartz, J., Wright, R., Litonjua, A., Tarantini, L., Suh, H., Sparrow, D., Vokonas, P., Baccarelli, A. (2009). Decline in genomic DNA methylation through aging in a cohort of elderly subjects. *Mechanisms of Ageing and Development* **130** (4): 234-9.

Boulton, E., Cole, C., Knight, A., Cleary, H., Snowden, R., Plumb, M. (2003). Low-penetrance genetic susceptibility and resistance loci implicated in the relative risk for radiation-induced acute myeloid leukemia in mice. *Blood* **101** (6): 2349-2354.

Boulton, H. C., D. Papworth, M. Plumb, E. (2001). Susceptibility to radiation-induced leukaemia/lymphoma is genetically separable from sensitivity to radiation-induced genomic instability. *International Journal of Radiation Biology* **77** (1): 21-29.

Broome, E. J., Brown, D. L., Mitchel, R. E. (2002). Dose responses for adaption to low doses of ⁶⁰Co gamma rays and ³H beta particles in normal human fibroblasts. *Radiation Research* **158** (2): 181-6.

Brunmeir, R., Lagger, S., Simboeck, E., Sawicka, A., Egger, G., Hagelkruys, A., Zhang, Y., Matthias, P., Miller, W. J., Seiser, C. (2010). Epigenetic regulation of a murine retrotransposon by a dual histone modification mark. *PLoS Genetics* **6** (4): e1000927.

Bustin, S., Beaulieu, J. F., Huggett, J., Jaggi, R., Kibenge, F., Olsvik, P., Penning, L., Toegel, S. (2010). MIQE precis: Practical implementation of minimum standard guidelines for fluorescence-based quantitative real-time PCR experiments. *BMC Molecular Biology* **11** (1): 74.

Calvanese, V., Lara, E., Kahn, A., Fraga, M. F. (2009). The role of epigenetics in aging and age-related diseases. *Ageing Research Reviews* **8** (4): 268-276.

Candiloro, I. L., Mikeska, T., Hokland, P., Dobrovic, A. (2008). Rapid analysis of heterogeneously methylated DNA using digital methylation-sensitive high resolution melting: application to the CDKN2B (p15) gene. *Epigenetics and Chromatin* **1** (1): 7.

Carpenter, A. E., Jones, T. R., Lamprecht, M. R., Clarke, C., Kang, I. H., Friman, O., Guertin, D. A., Chang, J. H., Lindquist, R. A., Moffat, J. (2006). CellProfiler: image analysis software for identifying and quantifying cell phenotypes. *Genome Biology* **7** (10): R100.

Cassie, S., Koturbash, I., Hudson, D., Baker, M., Ilnytskyy, Y., Rodriguez-Juarez, R., Weber, E., Kovalchuk, O. (2006). Novel retinoblastoma binding protein RBBP9 modulates sex-specific radiation responses in vivo. *Carcinogenesis* **27** (3): 465-74.

Charlton, D., Nikjoo, H., Humm, J. (1989). Calculation of initial yields of single- and double-strand breaks in cell nuclei from electrons, protons and alpha particles. *International Journal of Radiation Biology* **56** (1): 1-19.

Cheda, A., Wrembel-Wargocka, J., Lisiak, E., Nowosielska, E., Marciniak, M., Janiak, M. (2004). Single low doses of X rays inhibit the development of experimental tumor metastases and trigger the activities of NK cells in mice. *Radiation Research* **161** (3): 335-340.

- Chen, C. C., Carson, J. J., Feser, J., Tamburini, B., Zabaronick, S., Linger, J., Tyler, J. K. (2008). Acetylated lysine 56 on histone H3 drives chromatin assembly after repair and signals for the completion of repair. *Cell* **134** (2): 231-243.
- Chen, H., Shaw, B. R. (1993). Kinetics of bisulfite-induced cytosine deamination in single-stranded DNA. *Biochemistry* **32** (14): 3535-9.
- Cherif, H., Tarry, J., Ozanne, S., Hales, C. (2003). Ageing and telomeres: A study into organ-and gender-specific telomere shortening. *Nucleic Acids Research* **31** (5): 1576-1583.
- Chiolo, I., Minoda, A., Colmenares, S. U., Polyzos, A., Costes, S. V., Karpen, G. H. (2011). Double-Strand Breaks in Heterochromatin Move Outside of a Dynamic HP1a Domain to Complete Recombinational Repair. *Cell* **144** (5): 732-744.
- Christensen, B. C., Houseman, E. A., Marsit, C. J., Zheng, S., Wrensch, M. R., Wiemels, J. L., Nelson, H. H., Karagas, M. R., Padbury, J. F., Bueno, R., Sugarbaker, D. J., Yeh, R. F., Wiencke, J. K., Kelsey, K. T. (2009). Aging and environmental exposures alter tissue-specific DNA methylation dependent upon CpG island context. *PLoS Genetics* **5** (8): e1000602.
- Cooney, C. A., Dave, A. A., Wolff, G. L. (2002). Maternal methyl supplements in mice affect epigenetic variation and DNA methylation of offspring. *The Journal of Nutrition* **132** (8): 2393S-2400S.
- Costello, J. F., Plass, C. (2001). Methylation matters. *Journal of Medical Genetics* **38** (5): 285-303.
- Coviello-McLaughlin, G. M., Prowse, K. R. (1997). Telomere length regulation during postnatal development and ageing in *Mus spretus*. *Nucleic Acids Research* **25** (15): 3051-3058.

- Cowell, I. G., Sunter, N. J., Singh, P. B., Austin, C. A., Durkacz, B. W., Tilby, M. J. (2007). gamma-H2AX Foci Form Preferentially in Euchromatin after Ionising-Radiation. *PLoS ONE* **2** (10): e1057.
- Cropley, J. E., Suter, C. M., Beckman, K. B., Martin, D. I. (2010). CpG methylation of a silent controlling element in the murine Avy allele is incomplete and unresponsive to methyl donor supplementation. *PLoS ONE* **5** (2): e9055.
- Cuozzo, C., Porcellini, A., Angrisano, T., Morano, A., Lee, B., Di Pardo, A., Messina, S., Iuliano, R., Fusco, A., Santillo, M. R. (2007). DNA damage, homology-directed repair, and DNA methylation. *PLoS Genetics* **3** (7): e110.
- Curradi, M., Izzo, A., Badaracco, G., Landsberger, N. (2002). Molecular mechanisms of gene silencing mediated by DNA methylation. *Molecular and Cellular Biology* **22** (9): 3157-73.
- Damiani, L. A., Yingling, C. M., Leng, S., Romo, P. E., Nakamura, J., Belinsky, S. A. (2008). Carcinogen-Induced Gene Promoter Hypermethylation Is Mediated by DNMT1 and Causal for Transformation of Immortalized Bronchial Epithelial Cells. *Cancer Research* **68** (21): 9005-9014.
- Daskalos, A., Nikolaidis, G., Xinarianos, G., Savvari, P., Cassidy, A., Zakopoulou, R., Kotsinas, A., Gorgoulis, V., Field, J. K., Liloglou, T. (2009). Hypomethylation of retrotransposable elements correlates with genomic instability in non-small cell lung cancer. *International Journal of Cancer* **124** (1): 81-87.
- Dauer, L. T., Brooks, A. L., Hoel, D. G., Morgan, W. F., Stram, D., Tran, P. (2010) Review and evaluation of updated research on the health effects associated with low-dose ionising radiation. *Radiation Protection Dosimetry*: 10.1093/rpd/ncq141.
- Day, T., Zeng, G., Hooker, A., Bhat, M., Scott, B., Turner, D., Sykes, P. (2006). Extremely low priming doses of X radiation induce an adaptive response for

chromosomal inversions in pKZ1 mouse prostate. *Radiation Research* **166** (5): 757-766.

Day, T. K. (2006) Low dose X-radiation induced adaptive responses, PhD thesis, Department of Haematology and Genetic Pathology, Flinders University, Adelaide.

Day, T. K., Hooker, A. M., Zeng, G., Sykes, P. J. (2007a). Low dose X-radiation adaptive response in spleen and prostate of Atm knockout heterozygous mice. *International Journal of Radiation Biology* **83** (8): 523-34.

Day, T. K., Zeng, G., Hooker, A. M., Bhat, M., Scott, B. R., Turner, D. R., Sykes, P. J. (2007b). Adaptive response for chromosomal inversions in pKZ1 mouse prostate induced by low doses of X radiation delivered after a high dose. *Radiation Research* **167** (6): 682-92.

de Andrade, A., Wang, M., Bonaldo, M. F., Xie, H., Soares, M. B. (2011). Genetic and epigenetic variations contributed by Alu retrotransposition. *BMC Genomics* **12** (1): 617.

de Haan, G., Nijhof, W., Van Zant, G. (1997). Mouse Strain-Dependent Changes in Frequency and Proliferation of Hematopoietic Stem Cells During Aging: Correlation Between Lifespan and Cycling Activity. *Blood* **89** (5): 1543-1550.

DeAngelis, J. T., Farrington, W. J., Tollefsbol, T. O. (2008). An overview of epigenetic assays. *Molecular Biotechnology* **38** (2): 179-83.

DeBerardinis, R. J., Goodier, J. L., Ostertag, E. M., Kazazian, H. H. (1998). Rapid amplification of a retrotransposon subfamily is evolving the mouse genome. *Nature Genetics* **20** (3): 288-290.

DeBerardinis, R. J., Kazazian, H. H. (1999). Analysis of the promoter from an expanding mouse retrotransposon subfamily. *Genomics* **56** (3): 317-323.

Dewannieux, M., Dupressoir, A., Harper, F., Pierron, G., Heidmann, T. (2004). Identification of autonomous IAP LTR retrotransposons mobile in mammalian cells. *Nature Genetics* **36** (5): 534-539.

Dixon, B. (1985). The biological and clinical effects of acute whole or partial body irradiation. *Journal of the Society for Radiological Protection* **5** 121.

Dolinoy, D. C., Huang, D., Jirtle, R. L. (2007). Maternal nutrient supplementation counteracts bisphenol A-induced DNA hypomethylation in early development. *Proceedings of the National Academy of Sciences* **104** (32): 13056-13061.

Dote, H., Cerna, D., Burgan, W. E., Carter, D. J., Cerra, M. A., Hollingshead, M. G., Camphausen, K., Tofilon, P. J. (2005). Enhancement of in vitro and in vivo tumor cell radiosensitivity by the DNA methylation inhibitor zebularine. *Clinical Cancer Research* **11** (12): 4571-4579.

Drissi, R., Wu, J., Hu, Y., Bockhold, C., Dome, J. S. (2011). Telomere Shortening Alters the Kinetics of the DNA Damage Response after Ionizing Radiation in Human Cells. *Cancer Prevention Research* **4** (12): 1973-1981.

Eads, C. A., Danenberg, K. D., Kawakami, K., Saltz, L. B., Blake, C., Shibata, D., Danenberg, P. V., Laird, P. W. (2000). MethyLight: a high-throughput assay to measure DNA methylation. *Nucleic Acids Research* **28** (8): e32-00.

Edwards, A., Lloyd, D. (1998). Risks from ionising radiation: deterministic effects. *Journal of Radiological Protection* **18** (3): 175.

Edwards, L. J. (2000). Modern statistical techniques for the analysis of longitudinal data in biomedical research. *Pediatric Pulmonology* **30** (4): 330-344.

- Ehrlich, M., Gama-Sosa, M. A., Huang, L.-H., Midgett, R. M., Kuo, K. C., McCune, R. A., Gehrke, C. (1982). Amount and distribution of 5-methylcytosine in human DNA from different types of tissues or cells. *Nucleic Acids Research* **10** (8): 2709-2721.
- Ekram, M. B., Kang, K., Kim, H., Kim, J. (2012). Retrotransposons as a major source of epigenetic variations in the mammalian genome. *Epigenetics* **7** (4): 0--1.
- El-Maarri, O., Walier, M., Behne, F., van Üüm, J., Singer, H., Diaz-Lacava, A., Nüsgen, N., Niemann, B., Watzka, M., Reinsberg, J., van der Ven, H., Wienker, T., Stoffel-Wagner, B., Schwaab, R., Oldenburg, J. (2011). Methylation at global LINE-1 repeats in human blood are affected by gender but not by age or natural hormone cycles. *PLoS ONE* **6** (1): e16252.
- Elmore, E., Lao, X. Y., Kapadia, R., Giedzinski, E., Limoli, C., Redpath, J. L. (2008). Low doses of very low-dose-rate low-LET radiation suppress radiation-induced neoplastic transformation in vitro and induce an adaptive response. *Radiation Research* **169** (3): 311-8.
- Estecio, M. R., Gharibyan, V., Shen, L., Ibrahim, A. E., Doshi, K., He, R., Jelinek, J., Yang, A. S., Yan, P. S., Huang, T. H., Tajara, E. H., Issa, J. P. (2007). LINE-1 hypomethylation in cancer is highly variable and inversely correlated with microsatellite instability. *PLoS ONE* **2** (5): e399.
- Estecio, M. R. H., Gallegos, J., Vallot, C., Castoro, R. J., Chung, W., Maegawa, S., Oki, Y., Kondo, Y., Jelinek, J., Shen, L., Hartung, H., Aplan, P. D., Czerniak, B. A., Liang, S., Issa, J.-P. J. (2010). Genome architecture marked by retrotransposons modulates predisposition to DNA methylation in cancer. *Genome Research* **20** (10): 1369-1382.
- Estève, P.-O., Chin, H. G., Pradhan, S. (2005). Human maintenance DNA (cytosine-5)-methyltransferase and p53 modulate expression of p53-repressed promoters. *Proceedings of the National Academy of Sciences of the United States of America* **102** (4): 1000-1005.

- Fahrner, J. A., Eguchi, S., Herman, J. G., Baylin, S. B. (2002). Dependence of Histone Modifications and Gene Expression on DNA Hypermethylation in Cancer. *Cancer Research* **62** (24): 7213-7218.
- Fan, S., Zhang, M. Q., Zhang, X. (2008). Histone methylation marks play important roles in predicting the methylation status of CpG islands. *Biochemical and Biophysical Research Communications* **374** (3): 559-64.
- Fandy, T. E., Herman, J. G., Kerns, P., Jiemjit, A., Sugar, E. A., Choi, S.-H., Yang, A. S., Aucott, T., Dausies, T., Odchimar-Reissig, R., Licht, J., McConnell, M. J., Nasrallah, C., Kim, M. K. H., Zhang, W., Sun, Y., Murgu, A., Espinoza-Delgado, I., Oteiza, K., Owoeye, I., Silverman, L. R., Gore, S. D., Carraway, H. E. (2009). Early epigenetic changes and DNA damage do not predict clinical response in an overlapping schedule of 5-azacytidine and entinostat in patients with myeloid malignancies. *Blood* **114** (13): 2764-2773.
- Farkash, E. A., Kao, G. D., Horman, S. R., Prak, E. T. L. (2006). Gamma radiation increases endonuclease-dependent L1 retrotransposition in a cultured cell assay. *Nucleic Acids Research* **34** (4): 1196-1204.
- Farkash, E. A., Prak, E. T. (2006). DNA damage and L1 retrotransposition. *Journal of Biomedicine and Biotechnology* **2006** (1): 37285.
- Faulkner, G. J., Kimura, Y., Daub, C. O., Wani, S., Plessy, C., Irvine, K. M., Schroder, K., Cloonan, N., Steptoe, A. L., Lassmann, T., Waki, K., Hornig, N., Arakawa, T., Takahashi, H., Kawai, J., Forrest, A. R. R., Suzuki, H., Hayashizaki, Y., Hume, D. A., Orlando, V., Grimmond, S. M., Carninci, P. (2009). The regulated retrotransposon transcriptome of mammalian cells. *Nature Genetics* **41** (5): 563-571.

Faure, E., Emanoil-Ravier, R., Champion, S. (1997). Induction of transcription from the long terminal repeat of the intracisternal particles type A (IAP) by X-irradiation. *Archives of Physiology and Biochemistry* **105** (2): 183-189.

Fedorov, A. (2009). Regulation of mammalian LINE1 retrotransposon transcription. *Cell and Tissue Biology* **3** (1): 1-13.

Feng, Z., Hu, W., Teresky, A. K., Hernando, E., Cordon-Cardo, C., Levine, A. J. (2007). Declining p53 function in the aging process: a possible mechanism for the increased tumor incidence in older populations. *Proceedings of the National Academy of Sciences* **104** (42): 16633-16638.

Filkowski, J. N., Ilnytsky, Y., Tamminga, J., Koturbash, I., Golubov, A., Bagnyukova, T., Pogribny, I. P., Kovalchuk, O. (2010). Hypomethylation and genome instability in the germline of exposed parents and their progeny is associated with altered miRNA expression. *Carcinogenesis* **31** (6): 1110-1115.

Finnell, R. H., Spiegelstein, O., Wlodarczyk, B., Triplett, A., Pogribny, I. P., Melnyk, S., James, J. S. (2002). DNA methylation in Folbp1 knockout mice supplemented with folic acid during gestation. *Journal of Nutrition* **132** (8 Suppl): 2457S-2461S.

Forni, L. (1988). Strain differences in the postnatal development of the mouse splenic lymphoid system. *Annales de l'Institut Pasteur / Immunologie* **139** (3): 257-266.

Fraga, M. F., Ballestar, E., Villar-Garea, A., Boix-Chornet, M., Espada, J., Schotta, G., Bonaldi, T., Haydon, C., Ropero, S., Petrie, K., Iyer, N. G., Perez-Rosado, A., Calvo, E., Lopez, J. A., Cano, A., Calasanz, M. J., Colomer, D., Piris, M. A., Ahn, N., Imhof, A., Caldas, C., Jenuwein, T., Esteller, M. (2005). Loss of acetylation at Lys16 and trimethylation at Lys20 of histone H4 is a common hallmark of human cancer. *Nature Genetics* **37** (4): 391-400.

- Frommer, M., McDonald, L. E., Millar, D. S., Collis, C. M., Watt, F., Grigg, G. W., Molloy, P. L., Paul, C. L. (1992). A genomic sequencing protocol that yields a positive display of 5-methylcytosine residues in individual DNA strands. *Proceedings of the National Academy of Sciences of the United States of America* **89** (5): 1827-31.
- Fulop, G., Phillips, R. (1990). The scid mutation in mice causes a general defect in DNA repair. *Nature* **347** (6292): 479-482.
- Furano, A. V., Robb, S. M., Robb, F. T. (1988). The structure of the regulatory region of the rat L1 (L1Rn, long interspersed repeated) DNA family of transposable elements. *Nucleic Acids Research* **16** (19): 9215.
- Gadhia, P. K. (1998). Possible age-dependent adaptive response to a low dose of X-rays in human lymphocytes. *Mutagenesis* **13** (2): 151-2.
- Gama-Sosa, M. A., Midgett, R. M., Slagel, V. A., Githens, S., Kuo, K. C., Gehrke, C. W., Ehrlich, M. (1983). Tissue-specific differences in DNA methylation in various mammals. *Biochimica et Biophysica Acta (BBA) - Gene Structure and Expression* **740** (2): 212-219.
- Gaubatz, J. W., Arcement, B., Cutler, R. G. (1991). Gene expression of an endogenous retrovirus-like element during murine development and aging. *Mechanisms of Ageing and Development* **57** (1): 71-85.
- Gaudet, F. o., Hodgson, J. G., Eden, A., Jackson-Grusby, L., Dausman, J., Gray, J. W., Leonhardt, H., Jaenisch, R. (2003). Induction of tumors in mice by genomic hypomethylation. *Science* **300** (5618): 489-492.
- Gebhard, C., Benner, C., Ehrlich, M., Schwarzfischer, L., Schilling, E., Klug, M., Dietmaier, W., Thiede, C., Holler, E., Andreesen, R. (2010). General transcription factor binding at CpG islands in normal cells correlates with resistance to de novo DNA methylation in cancer cells. *Cancer Research* **70** (4): 1398.

Geiman, T. M., Robertson, K. D. (2002). Chromatin remodeling, histone modifications, and DNA methylation-how does it all fit together? *Journal of Cellular Biochemistry* **87** (2): 117-25.

Giotopoulos, G., McCormick, C., Cole, C., Zanker, A., Jawad, M., Brown, R., Plumb, M. (2006). DNA methylation during mouse hemopoietic differentiation and radiation-induced leukemia. *Experimental Hematology* **34** (11): 1462-70.

Goetz, W., Morgan, M. N. M., Baulch, J. E. (2011). The Effect of Radiation Quality on Genomic DNA Methylation Profiles in Irradiated Human Cell Lines. *Radiation Research* **175** (5): 575-587.

Gomolka, M., Rössler, U., Hornhardt, S., Walsh, L., Panzer, W., Schmid, E. (2005). Measurement of the Initial Levels of DNA Damage in Human Lymphocytes Induced by 29 kV X Rays (Mammography X Rays) Relative to 220 kV X Rays and γ Rays. *Radiation Research* **163** (5): 510-519.

Gontijo, A. M. d. M. C., Green, C. M., Almouzni, G. (2003). Repairing DNA damage in chromatin. *Biochimie* **85** (11): 1133-1147.

Gonzalo, S. (2010). Epigenetic alterations in aging. *Journal of Applied Physiology: Respiratory, Environmental and Exercise Physiology* **109** (2): 586-597.

Gonzalo, S., Jaco, I., Fraga, M. F., Chen, T., Li, E., Esteller, M., Blasco, M. A. (2006). DNA methyltransferases control telomere length and telomere recombination in mammalian cells. *Nature Cell Biology* **8** (4): 416-424.

Goodarzi, A. A., Noon, A. T., Deckbar, D., Ziv, Y., Shiloh, Y., Lobrich, M., Jeggo, P. A. (2008). ATM signaling facilitates repair of DNA double-strand breaks associated with heterochromatin. *Molecular Cell* **31** (2): 167-177.

Goodhead, D. (1994). Initial events in the cellular effects of ionizing radiations: clustered damage in DNA. *International Journal of Radiation Biology* **65** (1): 7-17.

Goodhead, D. (2009). Understanding and characterisation of the risks to human health from exposure to low levels of radiation. *Radiation Protection Dosimetry* **137** (1-2): 109.

Goodhead, D. T. (1989). The initial physical damage produced by ionizing radiations. *International Journal of Radiation Biology* **56** (5): 623.

Gorbunova, V., Seluanov, A., Mao, Z., Hine, C. (2007). Changes in DNA repair during aging. *Nucleic Acids Research*.

Goytisolo, F. A., Samper, E., Martín-Caballero, J., Finnon, P., Herrera, E., Flores, J. M., Bouffler, S. D., Blasco, M. A. (2000). Short telomeres result in organismal hypersensitivity to ionizing radiation in mammals. *The Journal of Experimental Medicine* **192** (11): 1625-1636.

Grahn, D., Hamilton, K. F. (1957). Genetic variation in the acute lethal response of four inbred mouse strains to whole body X-irradiation. *Genetics* **42** (3): 189-198.

Green, E. L. (ed.) (1966) *Biology of the laboratory mouse*. Dover Publications: New York, 427-443.

Gronbaek, K., Hother, C., Jones, P. A. (2007). Epigenetic changes in cancer. *APMIS* **115** (10): 1039-59.

Ha, K., Lee, G. E., Pali, S. S., Brown, K. D., Takeda, Y., Liu, K., Bhalla, K. N., Robertson, K. D. (2011). Rapid and transient recruitment of DNMT1 to DNA double-strand breaks is mediated by its interaction with multiple components of the DNA damage response machinery. *Human Molecular Genetics* **20** (1): 126-140.

- Hagan, C. R., Sheffield, R. F., Rudin, C. M. (2003). Human Alu element retrotransposition induced by genotoxic stress. *Nature Genetics* **35** (3): 219-20.
- Hamasaki, K., Imai, K., Hayashi, T., Nakachi, K., Kusunoki, Y. (2007). Radiation sensitivity and genomic instability in the hematopoietic system: Frequencies of micronucleated reticulocytes in whole-body X-irradiated BALB/c and C57BL/6 mice. *Cancer Science* **98** (12): 1840-4.
- Harrington, N., Chambers, K., Ross, W., Fillion, L. (1997). Radiation damage and immune suppression in splenic mononuclear cell populations. *Clinical and Experimental Immunology* **107** (2): 417-424.
- Hashimoto, S., Shirato, H., Hosokawa, M., Nishioka, T., Kuramitsu, Y., Matushita, K., Kobayashi, M., Miyasaka, K. (1999). The suppression of metastases and the change in host immune response after low-dose total-body irradiation in tumor-bearing rats. *Radiation Research* **151** (6): 717-724.
- Hata, K., Sakaki, Y. (1997). Identification of critical CpG sites for repression of L1 transcription by DNA methylation. *Gene* **189** (2): 227-234.
- Hellemans, J., Mortier, G., De Paepe, A., Speleman, F., Vandesompele, J. (2007). qBase relative quantification framework and software for management and automated analysis of real-time quantitative PCR data. *Genome Biology* **8** (2): R19.
- Hooker, A., Bhat, M., Day, T., Lane, J., Swinburne, S., Morley, A., Sykes, P. (2004). The linear no-threshold model does not hold for low-dose ionizing radiation. *Radiation Research* **162** (4): 447-452.
- Hooker, A., Home, R., Morley, A., Sykes, P. (2002). Dose-dependent increase or decrease of somatic intrachromosomal recombination produced by etoposide. *Mutation Research/Fundamental and Molecular Mechanisms of Mutagenesis* **500** (1-2): 117-124.

Howard, G., Eiges, R., Gaudet, F., Jaenisch, R., Eden, A. (2007). Activation and transposition of endogenous retroviral elements in hypomethylation induced tumors in mice. *Oncogene* **27** (3): 404-408.

Hruz, T., Laule, O., Szabo, G., Wessendorp, F., Bleuler, S., Oertle, L., Widmayer, P., Gruissem, W., Zimmermann, P. (2008). Genevestigator V3: a reference expression database for the meta-analysis of transcriptomes. *Advances in Bioinformatics* **2008**.

Hunter, R. G., McCarthy, K. J., Milne, T. A., Pfaff, D. W., McEwen, B. S. (2009). Regulation of hippocampal H3 histone methylation by acute and chronic stress. *Proceedings of the National Academy of Sciences* **106** (49): 20912-20917.

Hunter, R. G., McEwen, B. S., Pfaff, D. W. (2013). Environmental stress and transposon transcription in the mammalian brain. *Mobile Genetic Elements* **3** (2): e24555.

Igarashi, S., Suzuki, H., Niinuma, T., Shimizu, H., Nojima, M., Iwaki, H., Nobuoka, T., Nishida, T., Miyazaki, Y., Takamaru, H., Yamamoto, E., Yamamoto, H., Tokino, T., Hasegawa, T., Hirata, K., Imai, K., Toyota, M., Shinomura, Y. (2010). A novel correlation between LINE-1 hypomethylation and the malignancy of gastrointestinal stromal tumors. *Clinical Cancer Research* **16** (21): 5114-5123.

Ina, Y., Tanooka, H., Yamada, T., Sakai, K. (2005). Suppression of thymic lymphoma induction by life-long low-dose-rate irradiation accompanied by immune activation in C57BL/6 mice. *Radiation Research* **163** (2): 153-158.

International Atomic Energy Agency (2000). Technical Report Series 398. *Absorbed dose determination in external beam radiotherapy: An International Code of Practice for Dosimetry based on standards of absorbed dose to water*.

Irahara, N., Noshō, K., Baba, Y., Shima, K., Lindeman, N., Hazra, A., Schernhammer, E., Hunter, D., Fuchs, C., Ogino, S. (2010). Precision of pyrosequencing assay to measure LINE-1 methylation in colon cancer, normal colonic mucosa, and peripheral blood cells. *Journal of Molecular Diagnostics* **12** (2): 177.

Ishii, K., Hosoi, Y., Yamada, S., Ono, T., Sakamoto, K. (1996). Decreased incidence of thymic lymphoma in AKR mice as a result of chronic, fractionated low-dose total-body X irradiation. *Radiation Research* **146** (5): 582-585.

Jackson, I. L., Vujaskovic, Z., Down, J. D. (2011). A Further Comparison of Pathologies after Thoracic Irradiation among Different Mouse Strains: Finding the Best Preclinical Model for Evaluating Therapies Directed Against Radiation-Induced Lung Damage. *Radiation Research*.

Jakob, B., Splinter, J., Conrad, S., Voss, K.-O., Zink, D., Durante, M., Löbrich, M., Taucher-Scholz, G. (2011). DNA double-strand breaks in heterochromatin elicit fast repair protein recruitment, histone H2AX phosphorylation and relocation to euchromatin. *Nucleic Acids Research*.

James, S. J., Pogribny, I. P., Pogribna, M., Miller, B. J., Jernigan, S., Melnyk, S. (2003). Mechanisms of DNA Damage, DNA Hypomethylation, and Tumor Progression in the Folate/Methyl-Deficient Rat Model of Hepatocarcinogenesis. *The Journal of Nutrition* **133** (11): 3740S-3747S.

Jeong, K.-S., Lee, S. (2005). Estimating the total mouse DNA methylation according to the B1 repetitive elements. *Biochemical and Biophysical Research Communications* **335** (4): 1211-1216.

Jeong, S., Liang, G., Sharma, S., Lin, J. C., Choi, S. H., Han, H., Yoo, C. B., Egger, G., Yang, A. S., Jones, P. A. (2009). Selective Anchoring of DNA Methyltransferases 3A/3B to Nucleosomes Containing Methylated DNA. *Molecular and Cellular Biology*.

- Jiang, H., Li, W., Li, X., Cai, L., Wang, G. (2008). Low-dose radiation induces adaptive response in normal cells, but not in tumor cells: in vitro and in vivo studies. *Journal of Radiation Research* **49** (3): 219-30.
- Jintaridith, P., Mutirangura, A. (2010). Distinctive patterns of age-dependent hypomethylation in interspersed repetitive sequences. *Physiological Genomics* 00146.2009.
- Jüttermann, R., Li, E., Jaenisch, R. (1994). Toxicity of 5-aza-2'-deoxycytidine to mammalian cells is mediated primarily by covalent trapping of DNA methyltransferase rather than DNA demethylation. *Proceedings of the National Academy of Sciences* **91** (25): 11797-11801.
- Kalinich, J., Catravas, G., Snyder, S. (1989). The effect of radiation on DNA methylation. *Radiation Research* **117** (2): 185-197.
- Kallman, R. F. (1962). The Effect of Dose Rate on Mode of Acute Radiation Death of C57BL and BALB/c Mice. *Radiation Research* **16** (6): 796-810.
- Kang, M.-I., Rhyu, M.-G., Kim, Y.-H., Jung, Y.-C., Hong, S.-J., Cho, C.-S., Kim, H.-S. (2006). The length of CpG islands is associated with the distribution of Alu and L1 retroelements. *Genomics* **87** (5): 580-590.
- Kaplan, H. S., Brown, M. (1952). A quantitative dose-response study of lymphoid-tumor development in irradiated C 57 black mice. *Journal of the National Cancer Institute* **13** (1): 185.
- Kato, K., Kuwabara, M., Kashiwakura, I. (2011). The Influence of Gender-and Age-related Differences in the Radiosensitivity of Hematopoietic Progenitor Cells Detected in Steady-state Human Peripheral Blood. *Journal of Radiation Research* (0): 1103300199.

Kato, Y., Kaneda, M., Hata, K., Kumaki, K., Hisano, M., Kohara, Y., Okano, M., Li, E., Nozaki, M., Sasaki, H. (2007). Role of the Dnmt3 family in de novo methylation of imprinted and repetitive sequences during male germ cell development in the mouse. *Human Molecular Genetics* **16** (19): 2272-80.

Kaup, S., Grandjean, V., Mukherjee, R., Kapoor, A., Keyes, E., Seymour, C. B., Mothersill, C. E., Schofield, P. N. (2006). Radiation-induced genomic instability is associated with DNA methylation changes in cultured human keratinocytes. *Mutation Research/Fundamental and Molecular Mechanisms of Mutagenesis* **597** (1-2): 87-97.

Koito, A., Ikeda, T. (2012). Apolipoprotein B mRNA-editing, catalytic polypeptide cytidine deaminases and retroviral restriction. *Wiley Interdisciplinary Reviews: RNA* **3** (4): 529-541.

Kondo, Y., Shen, L., Suzuki, S., Kurokawa, T., Masuko, K., Tanaka, Y., Kato, H., Mizuno, Y., Yokoe, M., Sugauchi, F., Hirashima, N., Orito, E., Osada, H., Ueda, R., Guo, Y., Chen, X., Issa, J. P., Sekido, Y. (2007). Alterations of DNA methylation and histone modifications contribute to gene silencing in hepatocellular carcinomas. *Hepatology Research* **37** (11): 974-83.

Kongruttanachok, N., Phuangphairoj, C., Thongnak, A., Ponyeam, W., Rattanatanyong, P., Pornthanakasem, W., Mutirangura, A. (2010). Replication independent DNA double-strand break retention may prevent genomic instability. *Molecular Cancer* **9** 70.

Koturbash, I., Baker, M., Loree, J., Kutanzi, K., Hudson, D., Pogribny, I., Sedelnikova, O., Bonner, W., Kovalchuk, O. (2006). Epigenetic dysregulation underlies radiation-induced transgenerational genome instability in vivo. *International Journal of Radiation Oncology, Biology, Physics* **66** (2): 327-30.

Koturbash, I., Pogribny, I., Kovalchuk, O. (2005). Stable loss of global DNA methylation in the radiation-target tissue--a possible mechanism contributing to radiation carcinogenesis? *Biochemical and Biophysical Research Communications* **337** (2): 526-33.

Koturbash, I., Scherhag, A., Sorrentino, J., Sexton, K., Bodnar, W., Swenberg, J. A., Beland, F. A., Pardo-Manuel deVillena, F., Rusyn, I., Pogribny, I. P. (2011). Epigenetic mechanisms of mouse interstrain variability in genotoxicity of the environmental toxicant 1,3-Butadiene. *Toxicological Sciences* **122** (2): 448-456.

Kovalchuk, O., Burke, P., Besplug, J., Slovack, M., Filkowski, J., Pogribny, I. (2004a). Methylation changes in muscle and liver tissues of male and female mice exposed to acute and chronic low-dose X-ray-irradiation. *Mutation Research* **548** (1-2): 75-84.

Kovalchuk, O., Ponton, A., Filkowski, J., Kovalchuk, I. (2004b). Dissimilar genome response to acute and chronic low-dose radiation in male and female mice. *Mutation Research* **550** (1-2): 59-72.

Kristensen, L. S., Mikeska, T., Krypuy, M., Dobrovic, A. (2008). Sensitive melting analysis after real time-methylation specific PCR (SMART-MSP): high-throughput and probe-free quantitative DNA methylation detection. *Nucleic Acids Research* **36** (7): e42.

Krivokapic, A., Øhman, K., Hole, E., Nelson, W., Sagstuen, E. (2008). Primary Oxidation Radical in X-irradiated 5-Methylcytosine, a Mutagenic Hotspot in DNA. *Radioprotection* **43** (5).

Kuff, E. L., Lueders, K. K. (1988). The intracisternal A-particle gene family: structure and functional aspects. *Advances in Cancer Research* **51** 183-276.

- Kulkarni, A., Wilson, D. M., 3rd (2008). The involvement of DNA-damage and -repair defects in neurological dysfunction. *American Journal of Human Genetics* **82** (3): 539-66.
- Lamprecht, M. R., Sabatini, D. M., Carpenter, A. E. (2007). CellProfiler™: free, versatile software for automated biological image analysis. *Biotechniques* **42** (1): 71.
- Lander, E. S., Linton, L. M., Birren, B., Nusbaum, C., Zody, M. C., Baldwin, J., Devon, K., Dewar, K., Doyle, M., FitzHugh, W. (2001). Initial sequencing and analysis of the human genome. *Nature* **409** (6822): 860-921.
- Lane, N., Dean, W., Erhardt, S., Hajkova, P., Surani, A., Walter, J., Reik, W. (2003). Resistance of IAPs to methylation reprogramming may provide a mechanism for epigenetic inheritance in the mouse. *Genesis* **35** (2): 88-93.
- Lee, B., Morano, A., Porcellini, A., Muller, M. T. (2011). GADD45 α inhibition of DNMT1 dependent DNA methylation during homology directed DNA repair. *Nucleic Acids Research*.
- Lee, G. E., Kim, J. H., Taylor, M., Muller, M. T. (2010a). DNA methyltransferase 1-associated protein (DMAP1) is a co-repressor that stimulates DNA methylation globally and locally at sites of double strand break repair. *Journal of Biological Chemistry* **285** (48): 37630-37640.
- Lee, J. Y., Lee, T.-H. (2011). Effects of DNA Methylation on the Structure of Nucleosomes. *Journal of the American Chemical Society* **134** (1): 173-175.
- Lee, S.-H., Cho, S.-Y., Shannon, M. F., Fan, J., Rangasamy, D. (2010b). The Impact of CpG Island on Defining Transcriptional Activation of the Mouse L1 Retrotransposable Elements. *PLoS ONE* **5** (6): e11353.

- Li, L.-C., Dahiya, R. (2002). MethPrimer: designing primers for methylation PCRs. *Bioinformatics* **18** (11): 1427-1431.
- Li, W., Wang, G., Cui, J., Xue, L., Cai, L. (2004). Low-dose radiation (LDR) induces hematopoietic hormesis: LDR-induced mobilization of hematopoietic progenitor cells into peripheral blood circulation. *Experimental Hematology* **32** (11): 1088-1096.
- Li, Y.-Q., Zhou, P.-Z., Zheng, X.-D., Walsh, C. P., Xu, G.-L. (2007). Association of Dnmt3a and thymine DNA glycosylase links DNA methylation with base-excision repair. *Nucleic Acids Research* **35** (2): 390-400.
- Liang, G., Chan, M. F., Tomigahara, Y., Tsai, Y. C., Gonzales, F. A., Li, E., Laird, P. W., Jones, P. A. (2002). Cooperativity between DNA methyltransferases in the maintenance methylation of repetitive elements. *Molecular and Cellular Biology* **22** (2): 480-91.
- Liebermann, D. A., Hoffman, B. (2008). Gadd45 in stress signaling. *Journal of Molecular Signaling* **3** (1): 15.
- Lindop, P. J., Rotblat, J. (1962). The Age Factor in Radiation Sensitivity in Mice. *British Journal of Radiology* **35** (409): 23-31.
- Lindsay, K. J., Coates, P. J., Lorimore, S. A., Wright, E. G. (2007). The genetic basis of tissue responses to ionizing radiation. *British Journal of Radiology* **80** (Special_Issue_1): S2-6.
- Liu, C., Zhou, C., Gao, F., Cai, S., Zhang, C., Zhao, L., Zhao, F., Cao, F., Lin, J., Yang, Y. (2011a). MiR-34a in Age and Tissue Related Radio-Sensitivity and Serum miR-34a as a Novel Indicator of Radiation Injury. *International Journal of Biological Sciences* **7** (2): 221.

Liu, L., van Groen, T., Kadish, I., Li, Y., Wang, D., James, S., Karpf, A., Tollefsbol, T. (2011b). Insufficient DNA methylation affects healthy aging and promotes age-related health problems. *Clinical Epigenetics* **2** (2): 349-360.

Liu, S. (2010). Biological effects of low level exposures to ionizing radiation: Theory and practice. *Human and Experimental Toxicology* **29** (4): 275.

Lorente, A., Mueller, W., Urdangarín, E., Lázcoz, P., Von Deimling, A., Castresana, J. (2008). Detection of methylation in promoter sequences by melting curve analysis-based semiquantitative real time PCR. *BMC Cancer* **8** (1): 61.

Lorenz, E., Hollcroft, J. W., Miller, E., Congdon, C. C., Schweisthal, R. (1955). Long-Term Effects of Acute and Chronic Irradiation in Mice. I. Survival and Tumor Incidence Following Chronic Irradiation of 0.11 r Per Day. *Journal of the National Cancer Institute* **15** (4): 1049-1058.

Loucas, B. D., Eberle, R., Bailey, S. M., Cornforth, M. N. (2004). Influence of dose rate on the induction of simple and complex chromosome exchanges by gamma rays. *Radiation Research* **162** (4): 339-349.

Madrigano, J., Baccarelli, A., Mittleman, M. A., Wright, R. O., Sparrow, D., Vokonas, P. S., Tarantini, L., Schwartz, J. (2011). Prolonged exposure to particulate pollution, genes associated with glutathione pathways, and DNA methylation in a cohort of older men. *Environmental Health Perspectives* **119** (7): 977.

Maegawa, S., Hinkal, G., Kim, H., Shen, L., Zhang, L., Zhang, J., Zhang, N., Liang, S., Donehower, L., Issa, J. Widespread and tissue specific age-related DNA methylation changes in mice. *Genome Research*.

Malentacchi, F., Forni, G., Vinci, S., Orlando, C. (2009). Quantitative evaluation of DNA methylation by optimization of a differential-high resolution melt analysis protocol. *Nucleic Acids Research* **37** (12): e86.

Martens, J. H., O'Sullivan, R. J., Braunschweig, U., Opravil, S., Radolf, M., Steinlein, P., Jenuwein, T. (2005). The profile of repeat-associated histone lysine methylation states in the mouse epigenome. *EMBO Journal* **24** (4): 800-12.

Masutomi, K., Possemato, R., Wong, J. M. Y., Currier, J. L., Tothova, Z., Manola, J. B., Ganesan, S., Lansdorp, P. M., Collins, K., Hahn, W. C. (2005). The telomerase reverse transcriptase regulates chromatin state and DNA damage responses. *Proceedings of the National Academy of Sciences of the United States of America* **102** (23): 8222.

Matsubara, J., Turcanu, V., Poindron, P., Ina, Y. (2000). Immune effects of low-dose radiation: Short-term induction of thymocyte apoptosis and long-term augmentation of T-cell-dependent immune responses. *Radiation Research* **153** (3): 332-338.

Matsuoka, M., Nagawa, F., Okazaki, K., Kingsbury, L., Yoshida, K., Muller, U., Larue, D., Winer, J., Sakano, H. (1991). Detection of somatic DNA recombination in the transgenic mouse brain. *Science* **254** (5028): 81.

Mays-Hoopers, L., Chao, W., Butcher, H. C., Huang, R. C. C. (1986). Decreased methylation of the major mouse long interspersed repeated DNA during aging and in myeloma cells. *Developmental Genetics* **7** (2): 65-73.

McCarthy, E. M., McDonald, J. F. (2004). Long terminal repeat retrotransposons of *Mus musculus*. *Genome Biology* **5** (3): 14-14.

Meissner, A., Mikkelsen, T. S., Gu, H., Wernig, M., Hanna, J., Sivachenko, A., Zhang, X., Bernstein, B. E., Nusbaum, C., Jaffe, D. B. (2008). Genome-scale DNA methylation maps of pluripotent and differentiated cells. *Nature* **454** (7205): 766-770.

Mietz, J. A., Grossman, Z., Lueders, K., Kuff, E. L. (1987). Nucleotide sequence of a complete mouse intracisternal A-particle genome: relationship to known aspects of particle assembly and function. *Journal of Virology* **61** (10): 3020-3029.

Mitchel, R. E. (2007). Cancer and low dose responses in vivo: implications for radiation protection. *Dose Response* **5** (4): 284-91.

Mitchel, R. E., Burchart, P., Wyatt, H. (2008). A lower dose threshold for the in vivo protective adaptive response to radiation. Tumorigenesis in chronically exposed normal and Trp53 heterozygous C57BL/6 mice. *Radiation Research* **170** (6): 765-75.

Mitchel, R. E., Jackson, J. S., Carlisle, S. M. (2004). Upper dose thresholds for radiation-induced adaptive response against cancer in high-dose-exposed, cancer-prone, radiation-sensitive Trp53 heterozygous mice. *Radiation Research* **162** (1): 20-30.

Mitchel, R. E., Jackson, J. S., Morrison, D. P., Carlisle, S. M. (2003). Low doses of radiation increase the latency of spontaneous lymphomas and spinal osteosarcomas in cancer-prone, radiation-sensitive Trp53 heterozygous mice. *Radiation Research* **159** (3): 320-7.

Mitchel, R. E. J. (2006). Low doses of radiation are protective in vitro and in vivo: Evolutionary origins. *Dose Response* **4** (2): 75-90.

Miura, Y., Abe, K., Urano, S., Furuse, T., Noda, Y., Tatsumi, K., Suzuki, S. (2002). Adaptive response and the influence of ageing: effects of low-dose irradiation on cell growth of cultured glial cells. *International Journal of Radiation Biology* **78** (10): 913-21.

Morgan, H. D., Sutherland, H. G. E., Martin, D. I. K., Whitelaw, E. (1999). Epigenetic inheritance at the agouti locus in the mouse. *Nature Genetics* **23** 314-318.

- Mortusewicz, O., Schermelleh, L., Walter, J., Cardoso, M. C., Leonhardt, H. (2005). Recruitment of DNA methyltransferase I to DNA repair sites. *Proceedings of the National Academy of Sciences of the United States of America* **102** (25): 8905-9.
- Mukherjee, S., Sainis, K. B., Deobagkar, D. D. (2010). Comparative analysis of gene expression profiles in BALB/c and C57BL/6 strains of mice in response to low-dose ionising radiation using microarray. *International Journal of Low Radiation* **7** (4): 306-323.
- Mund, C., Hackanson, B., Stresemann, C., Lübbert, M., Lyko, F. (2005). Characterization of DNA demethylation effects induced by 5-aza-2'-deoxycytidine in patients with myelodysplastic syndrome. *Cancer Research* **65** (16): 7086.
- Muotri, A., Marchetto, M., Coufal, N., Oefner, R., Yeo, G., Nakashima, K., Gage, F. (2010). L1 retrotransposition in neurons is modulated by MeCP2. *Nature* **468** (7322): 443-446.
- Naas, T. P., DeBerardinis, R. J., Moran, J. V., Ostertag, E. M., Kingsmore, S. F., Seldin, M. F., Hayashizaki, Y., Martin, S. L., Kazazian, H. H. (1998). An actively retrotransposing, novel subfamily of mouse L1 elements. *EMBO Journal* **17** (2): 590-597.
- Ng, L. J., Copley, J. E., Pickett, H. A., Reddel, R. R., Suter, C. M. (2009). Telomerase activity is associated with an increase in DNA methylation at the proximal subtelomere and a reduction in telomeric transcription. *Nucleic Acids Research* **37** (4): 1152-1159.
- Nguyen, C. T., Weisenberger, D. J., Velicescu, M., Gonzales, F. A., Lin, J. C. Y., Liang, G., Jones, P. A. (2002). Histone H3-lysine 9 methylation is associated with aberrant gene silencing in cancer cells and is rapidly reversed by 5-aza-2'-deoxycytidine. *Cancer Research* **62** (22): 6456.

- Nordfjäll, K., Svenson, U., Norrback, K. F., Adolfsson, R., Lenner, P., Roos, G. (2009). The individual blood cell telomere attrition rate is telomere length dependent. *PLoS Genetics* **5** (2): e1000375.
- O'Callaghan, N. J., Fenech, M. (2011). A quantitative PCR method for measuring absolute telomere length. *Biological Procedures Online* **13** 3.
- O'Hagan, H. M., Mohammad, H. P., Baylin, S. B. (2008). Double Strand Breaks Can Initiate Gene Silencing and SIRT1-Dependent Onset of DNA Methylation in an Exogenous Promoter CpG Island. *PLoS Genetics* **4** (8): e1000155.
- O'Hagan, H. M., Wang, W., Sen, S., DeStefano Shields, C., Lee, S. S., Zhang, Y. W., Clements, E. G., Cai, Y., Van Neste, L., Easwaran, H. (2011). Oxidative Damage Targets Complexes Containing DNA Methyltransferases, SIRT1, and Polycomb Members to Promoter CpG Islands. *Cancer Cell* **20** (5): 606-619.
- O'Sullivan, R. J., Karlseder, J. (2010). Telomeres: protecting chromosomes against genome instability. *Nature Reviews Molecular Cell Biology* **11** (3): 171-81.
- Ogino, S., Kawasaki, T., Noshio, K., Ohnishi, M., Suemoto, Y., Kirkner, G. J., Fuchs, C. S. (2008a). LINE-1 hypomethylation is inversely associated with microsatellite instability and CpG island methylator phenotype in colorectal cancer. *International Journal of Cancer* **122** (12): 2767-73.
- Ogino, S., Noshio, K., Kirkner, G. J., Kawasaki, T., Chan, A. T., Schernhammer, E. S., Giovannucci, E. L., Fuchs, C. S. (2008b). A cohort study of tumoral LINE-1 hypomethylation and prognosis in colon cancer. *Journal of the National Cancer Institute* **100** (23): 1734-1738.
- Okayasu, R., Suetomi, K., Yu, Y., Silver, A., Bedford, J. S., Cox, R., Ullrich, R. L. (2000). A Deficiency in DNA Repair and DNA-PKcs Expression in the Radiosensitive BALB/c Mouse. *Cancer Research* **60** (16): 4342-4345.

Olivieri, G., Bodycote, J., Wolff, S. (1984). Adaptive response of human lymphocytes to low concentrations of radioactive thymidine. *Science* **223** (4636): 594.

Ostertag, E. M. (2001). Biology of Mammalian L1 Retrotransposons. *Annual Review of Genetics* **35** (1): 501.

Palii, S., Van Emburgh, B., Sankpal, U., Brown, K., Robertson, K. (2008). DNA Methylation Inhibitor 5-Aza-2'-Deoxycytidine Induces Reversible Genome-Wide DNA Damage That Is Distinctly Influenced by DNA Methyltransferases 1 and 3B. *Molecular and Cellular Biology* **28** (2): 752.

Park, I. Y., Sohn, B. H., Choo, J. H., Joe, C. O., Seong, J. K., Lee, Y. I., Chung, J. H. (2005). Deregulation of DNA methyltransferases and loss of parental methylation at the insulin-like growth factor II (Igf2)/H19 loci in p53 knockout mice prior to tumor development. *Journal of Cellular Biochemistry* **94** (3): 585-596.

Peng, J. C., Karpen, G. H. (2009). Heterochromatic Genome Stability Requires Regulators of Histone H3 K9 Methylation. *PLoS Genetics* **5** (3): e1000435.

Peterson, E. J., Böglér, O., Taylor, S. M. (2003). p53-mediated repression of DNA methyltransferase 1 expression by specific DNA binding. *Cancer Research* **63** (20): 6579-6582.

Plumb, M. (1998). Genetic instability in radiation-induced leukaemias: mouse models. *International Journal of Radiation Biology* **74** (6): 711 - 720.

Pogribny, I., Koturbash, I., Tryndyak, V., Hudson, D., Stevenson, S. M., Sedelnikova, O., Bonner, W., Kovalchuk, O. (2005). Fractionated low-dose radiation exposure leads to accumulation of DNA damage and profound alterations in DNA and histone methylation in the murine thymus. *Molecular Cancer Research* **3** (10): 553-61.

Pogribny, I., Raiche, J., Slovack, M., Kovalchuk, O. (2004). Dose-dependence, sex- and tissue-specificity, and persistence of radiation-induced genomic DNA methylation changes. *Biochemical and Biophysical Research Communications* **320** (4): 1253-61.

Pogribny, I., Yi, P., James, S. J. (1999). A sensitive new method for rapid detection of abnormal methylation patterns in global DNA and within CpG islands. *Biochemical and Biophysical Research Communications* **262** (3): 624-8.

Ponnaiya, B., Cornforth, M., Ullrich, R. (1997). Radiation-induced chromosomal instability in BALB/c and C57BL/6 mice: The difference is as clear as black and white. *Radiation Research* **147** (2): 121-125.

Popp, C., Dean, W., Feng, S., Cokus, S. J., Andrews, S., Pellegrini, M., Jacobsen, S. E., Reik, W. (2010). Genome-wide erasure of DNA methylation in mouse primordial germ cells is affected by AID deficiency. *Nature* **463** (7284): 1101-1105.

Portess, D. I., Bauer, G., Hill, M. A., O'Neill, P. (2007). Low-Dose Irradiation of Nontransformed Cells Stimulates the Selective Removal of Precancerous Cells via Intercellular Induction of Apoptosis. *Cancer Research* **67** (3): 1246-1253.

Prowse, K. R., Greider, C. W. (1995). Developmental and tissue-specific regulation of mouse telomerase and telomere length. *Proceedings of the National Academy of Sciences* **92** (11): 4818-4822.

Puntschart, A., Vogt, M. (1998). A stochastic PCR approach for RNA quantification in multiple samples. *Methods in Molecular Medicine: Quantitative PCR Protocols* **26** 277-287.

Raabe, O. (2012). Ionizing radiation carcinogenesis. *Current Topics in Ionizing Radiation Research*. Neno, M (ed). InTech.

<http://www.intechopen.com/books/current-topics-in-ionizing-radiation-research/ionizing-radiation-carcinogenesis>.

Raiche, J., Rodriguez-Juarez, R., Pogribny, I., Kovalchuk, O. (2004). Sex- and tissue-specific expression of maintenance and de novo DNA methyltransferases upon low dose X-irradiation in mice. *Biochemical and Biophysical Research Communications* **325** (1): 39-47.

Rand, K., Molloy, P. (2010). Sensitive measurement of unmethylated repeat DNA sequences by end-specific PCR. *Biotechniques* **49** (4).

Ray, D., Wu, A., Wilkinson, J. E., Murphy, H. S., Lu, Q., Kluge-Beckerman, B., Liepnieks, J. J., Benson, M., Yung, R., Richardson, B. (2006). Aging in Heterozygous Dnmt1-Deficient Mice: Effects on Survival, the DNA Methylation Genes, and the Development of Amyloidosis. *Journals of Gerontology Series A, Biological Sciences and Medical Sciences* **61** (2): 115-124.

Razin, A. (1998). CpG methylation, chromatin structure and gene silencing—a three-way connection. *EMBO Journal* **17** (17): 4905-8.

Redpath, J., Liang, D., Taylor, T., Christie, C., Elmore, E. (2001). The shape of the dose-response curve for radiation-induced neoplastic transformation in vitro: Evidence for an adaptive response against neoplastic transformation at low doses of low-LET radiation. *Radiation Research* **156** (6): 700-707.

Reuter, M., Berninger, P., Chuma, S., Shah, H., Hosokawa, M., Funaya, C., Antony, C., Sachidanandam, R., Pillai, R. S. (2011). Miwi catalysis is required for piRNA amplification-independent LINE1 transposon silencing. *Nature* **480** (7376): 264-267.

Riley, P. (1994). Free radicals in biology: oxidative stress and the effects of ionizing radiation. *International Journal of Radiation Biology* **65** (1): 27-33.

- Ririe, K., Rasmussen, R., Wittwer, C. (1997). Product differentiation by analysis of DNA melting curves during the polymerase chain reaction. *Analytical Biochemistry* **245** (2): 154-160.
- Rithidech, K. N., Cronkite, E., Bond, V. (1999). Advantages of the CBA mouse in leukemogenesis research. *Blood Cells Molecules and Diseases* **25** 38-46.
- Roberts, A., Blewitt, M., Youngson, N., Whitelaw, E., Chong, S. (2011). Reduced dosage of the modifiers of epigenetic reprogramming Dnmt1, Dnmt3L, SmcHD1 and Foxo3a has no detectable effect on mouse telomere length in vivo. *Chromosoma* **120** (4): 377-385.
- Roderick, T. H. (1963). The Response of Twenty-Seven Inbred Strains of Mice to Daily Doses of Whole-Body X-Irradiation. *Radiation Research* **20** (4): 631-639.
- Rowlatt, C., Chesterman, F., Sheriff, M. (1976). Lifespan, age changes and tumour incidence in an ageing C57BL mouse colony. *Laboratory Animals* **10** (4): 419-442.
- Rudin, C. M., Thompson, C. B. (2001). Transcriptional activation of short interspersed elements by DNA-damaging agents. *Genes, Chromosomes and Cancer* **30** (1): 64-71.
- Ryu, S. H., Kang, K., Yoo, T., Joe, C. O., Chung, J. H. (2011). Transcriptional repression of repeat-derived transcripts correlates with histone hypoacetylation at repetitive DNA elements in aged mice brain. *Experimental Gerontology* **46** (10): 811-818.
- Saito, K., Kawakami, K., Matsumoto, I., Oda, M., Watanabe, G., Minamoto, T. (2010). Long interspersed nuclear element 1 hypomethylation is a marker of poor prognosis in stage IA non-small cell lung cancer. *Clinical Cancer Research* **16** (8): 2418-2426.
- Sakai, K., Nomura, T., Ina, Y. (2006). Enhancement of bio-protective functions by low dose/dose-rate radiation. *Dose Response* **4** (4): 327-332.

Sasaki, S. (1991). Influence of the age of mice at exposure to radiation on life-shortening and carcinogenesis. *Journal of Radiation Research* **32** 73.

Satyamoorthy, K., Park, K., Atchison, M. L., Howe, C. C. (1993). The intracisternal A-particle upstream element interacts with transcription factor YY1 to activate transcription: pleiotropic effects of YY1 on distinct DNA promoter elements. *Molecular and Cellular Biology* **13** (11): 6621-6628.

Sauer, J., Jang, H., Zimmerly, E. M., Kim, K.-c., Liu, Z., Chanson, A., Smith, D. E., Mason, J. B., Friso, S., Choi, S.-W. (2010). Ageing, chronic alcohol consumption and folate are determinants of genomic DNA methylation, p16 promoter methylation and the expression of p16 in the mouse colon. *British Journal of Nutrition* **104** (1): 1-7.

Schumacher, A., Koetsier, P. A., Hertz, J., Doerfler, W. (2000). Epigenetic and Genotype-specific Effects on the Stability of de Novo Imposed Methylation Patterns in Transgenic Mice. *Journal of Biological Chemistry* **275** (48): 37915-37921.

Scott, A. F., Schmeckpeper, B. J., Abdelrazik, M., Comey, C. T., O'Hara, B., Rossiter, J. P., Cooley, T., Heath, P., Smith, K. D., Margolet, L. (1987). Origin of the human L1 elements: Proposed progenitor genes deduced from a consensus DNA sequence. *Genomics* **1** (2): 113-125.

Sedelnikova, O. A. (2004). Senescing human cells and ageing mice accumulate DNA lesions with unreparable double-strand breaks. *Nature Cell Biology* **6** (2): 168.

Sharma, S., De Carvalho, D. D., Jeong, S., Jones, P. A., Liang, G. (2011). Nucleosomes Containing Methylated DNA Stabilize DNA Methyltransferases 3A/3B and Ensure Faithful Epigenetic Inheritance. *PLoS Genetics* **7** (2): e1001286.

- Shen, L., Gao, G., Zhang, Y., Zhang, H., Ye, Z., Huang, S., Huang, J., Kang, J. (2010). A single amino acid substitution confers enhanced methylation activity of mammalian Dnmt3b on chromatin DNA. *Nucleic Acids Research* **38** (18): 6054-6064.
- Shuryak, I., Sachs, R., Brenner, D. (2010). Cancer risks after radiation exposure in middle age. *Journal of the National Cancer Institute* **102** (21): 1628.
- Silini, G., Andreozzi, U. (1974). Haematological changes in the ageing mouse. *Experimental Gerontology* **9** (3): 99-108.
- Singhal, R. P., Mays-Hoopers, L. L., Eichhorn, G. L. (1987). DNA methylation in aging of mice. *Mechanisms of Ageing and Development* **41** (3): 199-210.
- Slupphaug, G., Kavli, B., Krokan, H. E. (2003). The interacting pathways for prevention and repair of oxidative DNA damage. *Mutation Research* **531** (1-2): 231-251.
- Smith, E., Jones, M. E., Drew, P. A. (2009). Quantitation of DNA methylation by melt curve analysis. *BMC Cancer* **9** 123.
- Song, F., Mahmood, S., Ghosh, S., Liang, P., Smiraglia, D. J., Nagase, H., Held, W. A. (2009). Tissue specific differentially methylated regions (TDMR): Changes in DNA methylation during development. *Genomics* **93** (2): 130-139.
- Song, L., James, S., Kazim, L., Karpf, A. (2005). Specific method for the determination of genomic DNA methylation by liquid chromatography-electrospray ionization tandem mass spectrometry. *Analytical Chemistry* **77** (2): 504-510.
- Stanzer, S., Balic, M., Strutz, J., Heitzer, E., Obermair, F., Hauser-Kronberger, C., Samonigg, H., Dandachi, N. (2010). Rapid and reliable detection of LINE-1 hypomethylation using high resolution melting analysis. *Clinical Biochemistry* **143** (18): 1443-1448.

- Starling, J. A., Maule, J., Hastie, N. D., Allshire, R. C. (1990). Extensive telomere repeat arrays in mouse are hypervariable. *Nucleic Acids Research* **18** (23): 6881-6888.
- Steel, G. G. (1997). The dose-rate effect:brachytherapy. In: Steel, GG (ed). *Basic Clinical Radiobiology*. Arnold Publishing.
- Stoilov, L., Mullenders, L., Darroudi, F., Natarajan, A. (2007). Adaptive response to DNA and chromosomal damage induced by X-rays in human blood lymphocytes. *Mutagenesis* **22** (2): 117-122.
- Storer, J. B. (1967). On the Relationship between Genetic and Somatic Sensitivity to Radiation Damage in Inbred Mouse Strains. *Radiation Research* **31** (4): 699-705.
- Storer, J. B., Mitchell, T., Fry, R. (1988). Extrapolation of the relative risk of radiogenic neoplasms across mouse strains and to man. *Radiation Research* **114** (2): 331-353.
- Sugimura, K., Fukushima, Y., Ishida, M., Ito, S., Nakamura, M., Mori, Y., Okumura, K. (2010). Cell cycle-dependent accumulation of histone H3.3 and euchromatic histone modifications in pericentromeric heterochromatin in response to a decrease in DNA methylation levels. *Experimental Cell Research* **316** (17): 2731-2746.
- Suzuki, S., Ono, R., Narita, T., Pask, A. J., Shaw, G., Wang, C., Kohda, T., Alsop, A. E., Marshall Graves, J. A., Kohara, Y., Ishino, F., Renfree, M. B., Kaneko-Ishino, T. (2007). Retrotransposon silencing by DNA methylation can drive mammalian genomic imprinting. *PLoS Genetics* **3** (4): e55.
- Tawa, R., Kimura, Y., Komura, J., Miyamura, Y., Kurishita, A., Sasaki, M. S., Sakurai, H., Ono, T. (1998). Effects of X-ray irradiation on genomic DNA methylation levels in mouse tissues. *Journal of Radiation Research* **39** (4): 271-8.

Trasler, J., Deng, L., Melnyk, S., Pogribny, I., Hiou-Tim, F., Sibani, S., Oakes, C., Li, E., James, S. J., Rozen, R. (2003). Impact of Dnmt1 deficiency, with and without low folate diets, on tumor numbers and DNA methylation in Min mice. *Carcinogenesis* **24** (1): 39-45.

Tryndyak, V. P., Kovalchuk, O., Pogribny, I. P. (2006). Loss of DNA methylation and histone H4 lysine 20 trimethylation in human breast cancer cells is associated with aberrant expression of DNA methyltransferase 1, Suv4-20h2 histone methyltransferase and methyl-binding proteins. *Cancer Biology and Therapy* **5** (1): 65-70.

Tse, M. Y., Ashbury, J. E., Zwingerman, N., King, W. D., Taylor, S. A. M., Pang, S. C. (2011). A refined, rapid and reproducible high resolution melt (HRM)-based method suitable for quantification of global LINE-1 repetitive element methylation. *BMC Research Notes* **4** (1): 565.

Tubiana, M., Aurengo, A., Averbek, D., Masse, R. (2006). Recent reports on the effect of low doses of ionizing radiation and its dose-effect relationship. *Radiation and Environmental Biophysics* **44** (4): 245-51.

Tubiana, M., Feinendegen, L. E., Yang, C., Kaminski, J. M. (2009). The Linear No-Threshold Relationship Is Inconsistent with Radiation Biologic and Experimental Data. *Radiology* **251** (1): 13-22.

Turk, P. W., Laayoun, A., Smith, S. S., Weitzman, S. A. (1995). DNA adduct 8-hydroxyl-2'-deoxyguanosine (8-hydroxyguanine) affects function of human DNA methyltransferase. *Carcinogenesis* **16** (5): 1253-5.

U.S. Environmental Protection Agency (2007b). *Ionizing Radiation Fact Book*. <http://www.epa.gov/radiation/docs/402-f-06-061.pdf>; 11 April 2010.

- U.S. Environmental Protection Agency (2007a). *Radiation Risks and Realities*. <http://www.epa.gov/radiation/docs/402-k-07-006.pdf>; 11 April 2010.
- Valentin, J. (ed.) (2007) *The 2007 Recommendations of the International Commission on Radiological Protection*. Elsevier.
- Valinluck, V., Sowers, L. C. (2007). Endogenous Cytosine Damage Products Alter the Site Selectivity of Human DNA Maintenance Methyltransferase DNMT1. *Cancer Research* **67** (3): 946-950.
- van Gent, D., Hoeijmakers, J., Kanaar, R. (2001). Chromosomal stability and the DNA double-stranded break connection. *Nature Reviews Genetics* **2** (3): 196-206.
- Vandesompele, J., De Preter, K., Pattyn, F., Poppe, B., Van Roy, N., De Paepe, A., Speleman, F. (2002). Accurate normalization of real-time quantitative RT-PCR data by geometric averaging of multiple internal control genes. *Genome Biology* **3** (7): research0034.
- Vanhees, K., Coort, S., Ruijters, E. J. B., Godschalk, R. W. L., van Schooten, F. J., van Doorn-Khosrovani, S. B. v. W. (2011). Epigenetics: prenatal exposure to genistein leaves a permanent signature on the hematopoietic lineage. *The FASEB Journal* **25** (2): 797-807.
- Vanyushin, B. F., Mazin, A. L., Vasilyev, V. K., Belozersky, A. N. (1973). The content of 5-methylcytosine in animal DNA: The species and tissue specificity. *Biochimica et Biophysica Acta (BBA) - Nucleic Acids and Protein Synthesis* **299** (3): 397-403.
- Venkat, S., Apte, S. K., Chaubey, R. C., Chauhan, P. S. (2001). Radioadaptive response in human lymphocytes in vitro. *Journal of Environmental Pathology, Toxicology and Oncology* **20** (3): 165-75.

Vesselinovitch, S. D., Simmons, E. L., Mihailovich, N., Rao, K. V., Lombard, L. S. (1971). The effect of age, fractionation, and dose on radiation carcinogenesis in various tissues of mice. *Cancer Research* **31** (12): 2133-42.

Vilenchik, M. M., Knudson, A. G. (2000). Inverse radiation dose-rate effects on somatic and germ-line mutations and DNA damage rates. *Proceedings of the National Academy of Sciences* **97** (10): 5381-5386.

Walsh, P., Erlich, H., Higuchi, R. (1992). Preferential PCR amplification of alleles: mechanisms and solutions. *Genome Research* **1** (4): 241-250.

Wang, G., Cai, L. (2000). Induction of cell-proliferation hormesis and cell-survival adaptive response in mouse hematopoietic cells by whole-body low-dose radiation. *Toxicological Sciences* **53** (2): 369.

Wang, L., Wang, F., Guan, J., Le, J., Wu, L., Zou, J., Zhao, H., Pei, L., Zheng, X., Zhang, T. (2010). Relation between hypomethylation of long interspersed nucleotide elements and risk of neural tube defects. *American Journal of Clinical Nutrition* [ajcn.2009.28858](https://doi.org/10.1093/ajcn/2009.28858).

Ward, J. (1988). *Prog Nucleic Acid Res Mol Biol, Vol. 35*. Cohn, WE (ed.). Academic Press: San Diego, pp 95-125.

Ward, J. F. (1990). The Yield of DNA Double-strand Breaks Produced Intracellularly by Ionizing Radiation: A Review. *International Journal of Radiation Biology* **57** (6): 1141-1150.

Ward, J. F. (1995). Radiation Mutagenesis: The Initial DNA Lesions Responsible. *Radiation Research* **142** (3): 362-368.

Weeks, R., Morison, I. (2006). Detailed methylation analysis of CpG islands on human chromosome region 9p21. *Genes, Chromosomes and Cancer* **45** (4): 357-364.

- Williams, E. S., Klingler, R., Ponnaiya, B., Hardt, T., Schrock, E., Lees-Miller, S. P., Meek, K., Ullrich, R. L., Bailey, S. M. (2009). Telomere Dysfunction and DNA-PKcs Deficiency: Characterization and Consequence. *Cancer Research* **69** (5): 2100-2107.
- Wilson, V. L., Smith, R. A., Ma, S., Cutler, R. G. (1987). Genomic 5-methyldeoxycytidine decreases with age. *Journal of Biological Chemistry* **262** (21): 9948-9951.
- Wojdacz, T., Hansen, L. (2006). Reversal of PCR bias for improved sensitivity of the DNA methylation melting curve assay. *Biotechniques* **41** (3): 274.
- Wojdacz, T. K., Dobrovic, A. (2007). Methylation-sensitive high resolution melting (MS-HRM): a new approach for sensitive and high-throughput assessment of methylation. *Nucleic Acids Research* **35** (6): e41.
- Wojdacz, T. K., Dobrovic, A., Hansen, L. L. (2008a). Methylation-sensitive high-resolution melting. *Nature Protocols* **3** (12): 1903-8.
- Wojdacz, T. K., Hansen, L. L., Dobrovic, A. (2008b). A new approach to primer design for the control of PCR bias in methylation studies. *BMC Research Notes* **1** 54.
- Wolff, E. M., Byun, H.-M., Han, H. F., Sharma, S., Nichols, P. W., Siegmund, K. D., Yang, A. S., Jones, P. A., Liang, G. (2010). Hypomethylation of a LINE-1 promoter activates an alternate transcript of the MET oncogene in bladders with cancer. *PLoS Genetics* **6** (4): e1000917.
- Wolff, G. L., Kodell, R. L., Moore, S. R., Cooney, C. A. (1998). Maternal epigenetics and methyl supplements affect agouti gene expression in Avy/a mice. *The FASEB Journal* **12** (11): 949-957.

- Wong, C.-M., Wong, C. C.-L., Ng, Y.-L., Au, S. L.-K., Ko, F. C.-F., Ng, I. O.-L. (2011). Transcriptional Repressive H3K9 and H3K27 Methylations Contribute to DNMT1-Mediated DNA Methylation Recovery. *PLoS ONE* **6** (2): e16702.
- Wong, K. K., Chang, S., Weiler, S. R., Ganesan, S., Chaudhuri, J., Zhu, C., Artandi, S. E., Rudolph, K. L., Gottlieb, G. J., Chin, L. (2000). Telomere dysfunction impairs DNA repair and enhances sensitivity to ionizing radiation. *Nature Genetics* **26** (1): 85-88.
- Woo, H. D., Kim, J. (2012). Global DNA Hypomethylation in Peripheral Blood Leukocytes as a Biomarker for Cancer Risk: A Meta-Analysis. *PLoS ONE* **7** (4): e34615.
- Woodcock, D. M., Lawler, C. B., Linsenmeyer, M. E., Doherty, J. P., Warren, W. D. (1997). Asymmetric methylation in the hypermethylated CpG promoter region of the human L1 retrotransposon. *Journal of Biological Chemistry* **272** (12): 7810-7816.
- Wright, E. G. (2010). Manifestations and mechanisms of non-targeted effects of ionizing radiation. *Mutation Research/Fundamental and Molecular Mechanisms of Mutagenesis* **687** (1-2): 28-33.
- Wu, H.-C., Wang, Q., Delgado-Cruzata, L., Santella, R. M., Terry, M. B. (2012) Genomic methylation changes over time in peripheral blood mononuclear cell DNA: Differences by Assay Type and Baseline Values. *Cancer Epidemiology Biomarkers & Prevention*: 10.1158/1055-9965.epi-12-0300 June 4, 2012.
- Wu, H. C., Delgado-Cruzata, L., Flom, J. D., Kappil, M., Ferris, J. S., Liao, Y., Santella, R. M., Terry, M. B. (2011). Global methylation profiles in DNA from different blood cell types. *Epigenetics* **6** (1): 76-85.
- Xu, Y., Price, B. D. (2011). Chromatin dynamics and the repair of DNA double strand breaks. *Cell Cycle* **10** (2): 0--1.

Yamamoto, E., Toyota, M., Suzuki, H., Kondo, Y., Sanomura, T., Murayama, Y., Ohe-Toyota, M., Maruyama, R., Nojima, M., Ashida, M., Fujii, K., Sasaki, Y., Hayashi, N., Mori, M., Imai, K., Tokino, T., Shinomura, Y. (2008). LINE-1 hypomethylation is associated with increased CpG island methylation in Helicobacter pylori-related enlarged-fold gastritis. *Cancer Epidemiology Biomarkers & Prevention* **17** (10): 2555-2564.

Yamauchi, K., Kakinuma, S., Sudo, S., Kito, S., Ohta, Y., Nohmi, T., Masumura, K., Nishimura, M., Shimada, Y. (2008). Differential effects of low-and high-dose X-rays on N-ethyl-N-nitrosourea-induced mutagenesis in thymocytes of B6C3F1 gpt-delta mice. *Mutation Research/Fundamental and Molecular Mechanisms of Mutagenesis* **640** (1-2): 27-37.

Yang, A. S., Estecio, M. R., Doshi, K., Kondo, Y., Tajara, E. H., Issa, J. P. (2004). A simple method for estimating global DNA methylation using bisulfite PCR of repetitive DNA elements. *Nucleic Acids Research* **32** (3): e38.

Yauk, C. L., Polyzos, A., Rowan-Carroll, A., Kortubash, I., Williams, A., Kovalchuk, O. (2008). Tandem repeat mutation, global DNA methylation, and regulation of DNA methyltransferases in cultured mouse embryonic fibroblast cells chronically exposed to chemicals with different modes of action. *Environmental and Molecular Mutagenesis* **49** (1): 26-35.

Yu, Y., Okayasu, R., Weil, M. M., Silver, A., McCarthy, M., Zabriskie, R., Long, S., Cox, R., Ullrich, R. L. (2001). Elevated breast cancer risk in irradiated BALB/c mice associates with unique functional polymorphism of the *Prkdc* (DNA-dependent protein kinase catalytic subunit) gene. *Cancer Research* **61** (5): 1820-1824.

Yuhas, J. M., Storer, J. B. (1969). On mouse strain differences in radiation resistance: hematopoietic death and the endogenous colony-forming unit. *Radiation Research* **39** (3): 608-622.

Zaichkina, S., Rozanova, O., Aptikaeva, G., Akhmadieva, A., Klokov, D., Smirnova, H., Balakin, V. (2006). Investigation of the low-dose gamma-irradiation effect on the spontaneous and high-dose radiation-induced level of cytogenetic damage in mouse bone marrow cells in vivo. *International Journal of Low Radiation* **2** (1): 1-12.

Zeng, G., Day, T., Hooker, A., Blyth, B., Bhat, M., Tilley, W., Sykes, P. (2006). Non-linear chromosomal inversion response in prostate after low dose X-radiation exposure. *Mutation Research/Fundamental and Molecular Mechanisms of Mutagenesis* **602** (1-2): 65-73.

Zhang, D., Wang, Y., Bai, Y., Ge, Q., Qiao, Y., Luo, J., Jia, C., Lu, Z. (2008). A novel method to quantify local CpG methylation density by regional methylation elongation assay on microarray. *BMC Genomics* **9** 59.

Zhang, Y., Shu, J., Si, J., Shen, L., Estecio, M. R. H., Issa, J.-P. J. (2012) Repetitive elements and enforced transcriptional repression co-operate to enhance DNA methylation spreading into a promoter CpG-island. *Nucleic Acids Research*: 10.1093/nar/gks429 May 17, 2012.

APPENDIX A: ANALYSIS OF THE EFFECT OF C57BL/6-PKZ1 TRANSGENIC STATUS ON NTS

The effect of the transgenic status of the pKZ1-C57Bl/6 on L1 NTS was analysed (Table 21). There was no difference in the mean L1 NTS between pKZ1-C57Bl/6 transgenic and non-transgenic mice.

Table 21: Independent samples T-test analysis of pKZ1-C57Bl/6 transgenic status.

Transgenic Status	N[#]	Mean	SE	<i>P-value</i>
Transgenic	60	-7.06	0.12	<i>0.726</i>
Non-transgenic	21	-6.97	0.23	

[#]Mice from Section 4.1.4 were used for the analysis.

APPENDIX B: PCR PRIMERS

All primers are shown 5'- 3'.

Bold typeface indicates bisulphite modified bases and biased CpG sites are underlined. *Denotes primers that contain a 5' biotin tag.

Unmod denotes primers specific for bisulphite-unmodified DNA; *mod* denotes primers specific for bisulphite modified DNA; *unbiased* denotes primers unbiased for methylation status; and *unmethylated* denotes primers specific for unmethylated CpGs.

HRM PRIMERS

Kato

F_Kato TAG GAA ATT AGT **TTG** AAT AGG TGA GAG GGT

LINE1

Unbiased

F_unmod_mLINE1 GGG CTG AGG CAG CAC CCT GTG TG

R_unmod_mLINE1 TCC AGA AGC TGT CAG GTT CTC TGG C

F_unbiased_mLINE1* **GGT** TGA GGT AGT **ATT** **TTG** TGT G

R_unbiased_mLINE1 TCC AAA AAC TAT CAA ATT CTC TAA C

Both unbiased primer sets produce a 195 bp amplicon containing 13 CpGs.

Unmethylated

F_umod_unmeth_mLINE1 GCT GAG GCA GCA CCC TGT GTG GGC C

R_umod_unmeth_mLINE1 TCC AGA AGC TGT CAG GTT CTC TGG CGC

F_unmeth_mLINE1*	GTT GAG GTA GTA TTT TGT GTG GGT I
R_unmeth_mLINE1	TCC AAA AAC TAT CAA ATT CTC TAA CAC

Both unmethylated-biased primer sets produce a 193 bp amplicon that contains 11 CpGs.

B1 Mm

F_unmod_unbiased_B1_Mm	AGC CGG GCG TGG TGG
R_unmod_unbiased_B1_Mm	CTT TGT AGA CCA GGC TGG CCT C
F_mod_unbiased_B1_Mm	AGT YGG GYG TGG TGG
R_mod_unbiased_B1_Mm	CTT TAT AAA CCA AAC TAA CCT C

Both B1_Mm primer sets produce a 92 bp amplicon containing 7 CpGs. A Y denotes a degenerate nucleotide – either a C or T.

IAP LTR

F_unmod_unmeth_IAP_LTR	CCA CAT TCG CCG TTA CAA GAT GGC
R_unmod_unmeth_IAP_LTR	CAC CTA AAA ACA TAT CAC T
F_mod_unmeth_IAP_LTR	TTA TAT TTG TTG TTA TAA GAT GG I
R_mod_unmeth_IAP_LTR	CAC CTA AAA CAT ATC ACT

Both IAP_LTR primer sets produce a 141 bp amplicon that contains 6 CpGs.

SEQUENCING PRIMERS

R_pyroprimer	TAT TCAA ACT AAT TTC CTA A
--------------	----------------------------

qRT-PCR PRIMERS**L1-ORF1**

mL1-ORF1aFw	ACTCAAAGCGAGGCAACACTAGA
mL1-ORF1aRv	GTTCCAGATTTCTTTCCTAGGGTTTC
mL1-ORF1bFw	AGGCTACTATACCCAGCCAAACTCT
mL1-ORF1bRv	TACTTTGGTTTCTCCCTCTATGATAATTG

Both the L1-ORF1a and 1b primer sets produce a 54 bp amplicon.

L1-ORF2

mL1-ORF2aFw	CCTCCATTGTTGGTGGGATT
mL1-ORF2aRv	GGAACCGCCAGACTGATTTTC
mL1-ORF2bFw	CTGGCGAGGATGTGGAGAA
mL1-ORF2bRv	CCTGCAATCCCACCAACAAT

The L1-ORF2a primer set produces a 62 bp amplicon, while the L1-ORF2b primer set produces an amplicon of 55 bp.

Coch (Coagulation Factor C homologue)

F_Coch	TGGCACTAATGTTGGGAATTGG
R_Coch	TTCACTGGCTTGAACGAGACC

Polr2c (polymerase (RNA) II (DNA directed) polypeptide C)

F_Polr2c CCAATTCCATTCGGAGGGTCT

R_Polr2c ATGGCTATTATGGGCACCTCT

The *Polr2c* primers were obtained from PrimerBank (ID: 253735706b2) and produce a 49 bp amplicon.

Rn18s (ribonucleotide protein subunit 18)

F_Rn18s CGGACAGGATTGACAGATTG

R_Rn18s CAAATCGCTCCACCAACTAA

The *Rn18s* primers were obtained from RTPrimerDB (ID: 3879) and produce an 83 bp amplicon.

Spi-c (transcription factor spi-c)

F_Spi-c CACCAATCCGTACAGAACATAGC

R_Spi-c TTCCTCCCTTTTGCTGGAAGA

The *Spi-c* primers were obtained from PrimerBank (ID: 165932334b3) and produce a 70 bp amplicon.

APPENDIX C: SOLUTIONS AND BUFFERS

All chemicals used were of analytical grade.

AGAROSE GEL ELECTROPHORESIS

0.5 x Tris-Borate EDTA (TBE) Buffer

45 mM Tris base

45 mM Boric acid

1 mM Sodium EDTA

2% Agarose gel

2% (w/v) of agarose (Scientifix, Australia) in 0.5 x TBE Buffer

6 x Ficoll Loading Buffer

0.25% (w/v) Bromophenol Blue

15% (v/v) Ficoll (Pharmacia type 400)

WESTERN BLOT

Histone Lysis Buffer

0.01 M Tris-HCl pH 6.5

0.05 mM Sodium Bisulphite

1% Triton X-100

0.01 M MgCl₂

8.6% sucrose

Tris-EDTA

0.01 M Tris pH 7.4

0.013 M EDTA

1 x Running Buffer

0.025 M Tris base

0.192 M Glycine

0.06% SDS

4 x Loading Buffer

8% SDS

40% Glycerol

0.4 M DTT

0.08% Bromphenol Blue

0.25 M Tris HCl

1 x Transfer Buffer

0.025 M Tris

0.192 M Glycine

20% Methanol

0.05% SDS

10 x Tris Buffered Solution (TBS)

0.154 M Trizma HCl

1.37 M NaCl

pH 7.6

1 x TBS-Tween (TBS-T)

1 x TBS solution

0.001% Tween-20

IMMUNOHISTOCHEMISTRY

APES solution

2% (v/v) aminopropylethoxysilane (APES) in absolute ethanol.

2% Formaldehyde

Prepared from 4% paraformaldehyde.

Blocking Solution

0.1% Tween-20

5% Goat serum

APPENDIX D: L1 PROMOTER AND ORF SEQUENCES

3331 AACAGGTGAGAGGGTCCGC **CAGAGAA**CCTGACAGCTTCTGGAACAGGCAGAACACAGAGGGG**GCTGAGGCAGCACCCCTKTGTGGGCCGGG**

3421 **GACAGCCRGCCACCKTC**CGGR **CCRGAGGACAGGTGCCYRCCCGCTGGGGAGGCGRCCTAAGCCACAGCAGCAGCG****STCG****CCATCTTGG?**

3511 **CCGRGACCCGCCGA**ACTTAGGAAATTAGTCTGAACAGGTGAGAGGGTGC**CC****MAGAGAA**CCTGACAGCTTCTGGAA**ACAGGCCGGAAGCACAG**

3601 **AGGCGCTGAGGCAGCACCC**TTTGTGGGCCGGGGACAGCCAGCCACCGTCCGG **ACCGGAGGACAGGTGCCCGCCCGGCTGGGGAGGCGGCC**

3691 **TAAGCCACAGCAGCAG****CGGTACCATCTTGGT**CCGAGACCCCGGA**ACTTAGGAAATTAGTCTGAACAGGTGAGAGGGTGC****CC****CAGAGAA**

3781 **CCTGACAGCTTCTGGAACAGGCAGAACACAGAGCGCTGAGGCAGCACCC**TTTGTGGGCCGGGGACAGCCGGCCACCTTCCGG **ACCGGA**

3871 **GGACAGGTGCCACCCGGCTGGGGAGGCGGCCTAAGCCACAGCAGCAG****CGGTCCGCATCTTGGT**CCGAGACTCCAAGGA**ACTTAGGAAT**

3961 **TTAGTCTGCTTAGGTGAGAGTCTGTACCACCTGGGA**ACTGCCAAAGCAACACAGTGTCTGAGAAAGGTCTGTTT**TTGGGCC**ATCTTCTTC

4051 GGCCAGGAGAGGTCCAATACAAGATATCTGCGCACCTTCCCTGTAAGAGAGCTTGCCAGCAGAGAGTGTCTGAGCACTGAAACTCAG

4141 AGGAGAGAATCTGTCTCCAGGTCTGTGATAGACGGTAACAGAATCACCAGAAGAACAATCTCTAAACAGAGTCAACTATAACTACTAA

4231 CTCCAGAGATTACCAGATGGCGAAAGGTAACCGGAGAACTTACTAACAGGAACCAAGACCCTACCATCACCAGAACCCAGCACACC
-M--A--K--G--K--R--R--N--L--T--N--R--N--Q--D--H--S--P--S--P--E--P--S--T--P

4321 CACTTCGCCCACTCCAGGGACCCCAACACACCTGAGAACCTAGACCTAGATTTAAAGCATATCTCATGATGATGGTAGAGGACATCAA
--T--S--P--S--P--G--D--P--N--T--P--E--N--L--D--L--D--L--K--A--Y--L--M--M--M--V--E--D--I--K

4411 GAAGGACTTTAATAAATCACTTAAAGAAATACAGGAGAACTGCTAAAGAGTTACAAGTCTTAAAGAAAAACAGGAAAAACAAATCAA
--K--D--F--N--K--S--L--K--E--I--Q--E--N--T--A--K--E--L--Q--V--L--K--E--K--Q--E--N--T--I--K

4501 ACAGGTAGAAGTCTTACAGAAAAAGAGGAAAAACATACAAACAGGTGATGGAAATGAACAAAACCTACATAGACCTAAAAAGGGAAGT
--Q--V--E--V--L--T--E--K--E--E--K--T--Y--K--Q--V--M--E--M--N--K--T--I--L--D--L--K--R--E--V
mL1-OrflaFw mL1-OrflaRv

4591 AGACACAATAAAGAAA**ACTCAAAGCGAGGCAACACTAGAGATA****GAAACCCCTAGGAAAGAAATCTGGAACC**CATAGATTTGAGCATCAGCAA
--D--T--I--K--K--T--Q--S--E--A--T--L--E--I--E--T--L--G--K--K--S--G--T--I--D--L--S--I--S--N

4681 CAGAATACAAGAGATGGAAGAGAGAATCTCAGGTGCAGAAGATTCATAGAGAACATCGGCACAACAATCAAAGAAAAATGGAAAAATGCAA
--R--I--Q--E--M--E--E--R--I--S--G--A--E--D--S--I--E--N--I--G--T--T--I--K--E--N--G--K--C--K

4771 AAAGATCTTAACCTCAAATATCCAGGAAATCCAGGACACAATAAGAAGACCAAACGTACGGATAATAGGAGTGGATGAGAATGAAGATTT
--K--I--L--T--Q--N--I--Q--E--I--Q--D--T--I--R--R--P--N--V--R--I--I--G--V--D--E--N--E--D--F

4861 TCAACTCAAAGTCCAGCAAACATCTTCAACAAAATTATGAAGAAAACCTCCCAAATCTAAAGAATGAGATGCATATGAACATACAAGA
--Q--L--K--G--P--A--N--I--F--N--K--I--I--E--E--N--F--P--N--L--K--N--E--M--H--M--N--I--Q--E

4951 AGCCTACAGAACTCAAATAGACTGGACCAGAAAAGAAATTCCTCCCGACACATAAATCAGAACATCAAATGCCTAAATAAAGATAG
--A--Y--R--T--P--N--R--L--D--Q--K--R--N--S--S--R--H--I--I--I--R--T--S--N--A--L--N--K--D--R

5041 AATACTAAAAGCAGTAAGGAAAAAGTCAAGTAACATATAAAGGCAAGCCTATCAGAATTACACCAGATTTTCCACCAGAGACTATGAA
--I--L--K--A--V--R--E--K--G--Q--V--T--Y--K--G--K--P--I--R--I--T--P--D--F--S--P--E--T--M--K
mL1-OrflaFw mL1-OrflaRv

5131 AGCCAGAAGAGCCTGGACAGATGTTATACAGACACTAAGAGAACCAAACTGCAGCCC**AGGCTACTATACCAGCCAACTCTCAATTAT**
--A--R--R--A--W--T--D--V--I--Q--T--L--R--E--H--K--L--Q--P--R--L--L--Y--P--A--K--L--S--I--I
mL1-OrflaRv

5221 **CATAGAGGGAGAAACCAAGTA**TTCCACGACAAAACCAATTCAGCATTATCTCTCCACGAATCCAGCCCTTCAAAGATAATAACAGA
--I--E--G--E--T--K--V--F--H--D--K--T--K--F--T--H--Y--L--S--T--N--P--A--L--Q--K--I--I--T--E

5311 AAAAAACCAATACAAGAACGGGAACAACGCCCTAGAAAAACAAGAAGGTAATCCCTCAACAAACCTAAAAGAAGACAGCCACAAGAACA
--K--N--Q--Y--K--N--G--N--N--A--L--E--K--T--R--R--

5401 GAATGCCACCTTTAACAACATAAATAACAGGAAGCAACAATTACTTTTCTTAATATCTCTTAACATCAATGGTCTCAACTCGCCAATAA
-M--P--P--L--T--T--K--I--T--G--S--N--N--Y--F--S--L--I--S--L--N--I--N--G--L--N--S--P--I--

5491 AAAGACATAGACTAACAAACTGGCTACACAACAAGACCAACATTTTGTCTGCTTAAAGGAAACTCATCTCAGAGAAAAAGATAGACACT
K--R--H--R--L--T--N--W--L--H--K--Q--D--P--T--F--C--C--L--K--E--T--H--L--R--E--K--D--R--H--

5581 ACCTCAGAATGAAAGGCTGGAACAATTTTCCAAGCAAAATGGTATGAAGAAACAAGCAGGAGTAGCCATCTAATATCTGATAAGATG
Y--L--R--M--K--G--W--K--T--I--F--Q--A--N--G--M--K--K--Q--A--G--V--A--I--L--I--S--D--K--I--

5671 ACTTCCACCCAAAGTCATCAAGAAAGACAAGAAGGACACTTCACTTCTCATCAAGGTAATAATCCTCCAAGGAACTCTCAATTCTGA
D--F--Q--P--K--V--I--K--K--D--K--K--G--H--F--I--L--I--K--G--K--I--L--Q--E--E--L--S--I--L--

5761 ATATCTATGCTCAAATACAAGAGCAGCCACATTCATAAAGAACTTTAGTAAAGCTCAAAGCACACATTGCGCCTCACACAATAATAG
N--I--Y--A--P--N--T--R--A--A--T--F--T--K--E--T--L--V--K--L--K--A--H--I--A--P--H--T--I--I--

factor binding site, while red text indicates an YY1 transcription factor binding site.

Amino acid sequence is shown below nucleotide sequence within the two ORFs.

ORF1 is highlighted by a green box, while ORF2 is highlighted with a purple box.

ORF1 and 2 forward primer sequences are shown in blue, while reverse primer sequences are shown in pink.

APPENDIX E: TELOMERE LENGTH AND GENOME COPY NUMBER CALCULATIONS

Telomere length and *36B4* genome copy number were determined as outlined in O'Callaghan and Fenech (2011) from standard curves created using the oligonucleotide standards.

Calculation of Telomere Length

To calculate the length of the Telomere oligonucleotide standard the following calculations were performed:

The oligonucleotide has a MW of 26667.2 and is 84 bp. Therefore the weight of 1 x molecule is:

$$\begin{aligned}\text{MW/ Avogadro's number} &= 26667.2/6.02 \times 10^{23} \\ &= 0.44 \times 10^{-19} \text{g}\end{aligned}$$

STD A has 141.6 pg of oligo/ μL (see Table 22)

$$\begin{aligned}&= 141.6 \times 10^{-12} \text{g}/0.44 \times 10^{-19} \\ &= 3.22 \times 10^9 \text{ molecules}\end{aligned}$$

Therefore, the amount of Telomere sequence = $3.22 \times 10^9 \times 84 \text{ bp}$

The length of telomere STD A/ μL = $2.7 \times 10^8 \text{ kb}$.

Telomere oligonucleotide standards**Table 22: Telomere oligonucleotide standard lengths.**

STD	Concentration (pg/ μ L)	Dilution Factor	<i>per μL</i>		<i>per reaction</i>	
			# mol	length (kb)	# mol	length (kb)
A	141.6 [#]	5	3.22E+09	2.70E+08	6.44E+09	5.41E+08
B	28.32	25	6.44E+08	5.41E+07	1.29E+09	1.08E+08
C	5.664	125	1.29E+08	1.08E+07	2.57E+08	2.16E+07
D	1.1328	625	2.57E+07	2.16E+06	5.15E+07	4.33E+06
E	0.22656	3125	5.15E+06	4.33E+05	1.03E+07	8.65E+05
F	0.045312	15625	1.03E+06	8.65E+04	2.06E+06	1.73E+05
G	0.0090624	78125	2.06E+05	1.73E+04	4.12E+05	3.46E+04
H	0.00181248	390625	4.12E+04	3.46E+03	8.24E+04	6.92E+03

[#]Standard A is a dilution of the stock oligonucleotide (708 pg/ μ L).

Calculation of genome copy number

To calculate genome copy number the following calculations were performed (as for the Telomere oligonucleotide standard) for an oligonucleotide standard for the *36B4* gene:

The oligonucleotide has a MW of 23606 and is 77 bp. Therefore the weight of 1 x molecule is:

$$\begin{aligned} \text{MW/ Avogadro's number} &= 23606/6.02 \times 10^{23} \\ &= 3.92 \times 10^{-20} \text{g} \end{aligned}$$

$$\begin{aligned} \text{STD A has } 936.8 \text{ pg of oligo/ } \mu\text{L} &= 936.8 \times 10^{-12} \text{g}/3.92 \times 10^{-20} \\ &= 2.39 \times 10^{10} \text{ copies} \end{aligned}$$

Therefore, there are 1.19×10^{10} diploid genome copies/ μ L of STD A.

[36B4 oligonucleotide standards](#)**Table 23: 36B4 oligonucleotide standard copy numbers.**

STD	Concentration (pg/ μ L)	Dilution Factor	<i>per μL</i>		<i>per reaction</i>	
			# copies	# copies/ diploid genome	# copies	# copies/ diploid genome
C [^]	37.472	125	9.56E+08	4.78E+08	1.91E+09	9.56E+08
D	7.4944	625	1.91E+08	9.56E+07	3.82E+08	1.91E+08
E	1.49888	3125	3.82E+07	1.91E+07	7.65E+07	3.82E+07
F	0.299776	15625	7.65E+06	3.82E+06	1.53E+07	7.65E+06
G	0.0599552	78125	1.53E+06	7.65E+05	3.06E+06	1.53E+06
H	0.01199104	390625	3.06E+05	1.53E+05	6.12E+05	3.06E+05
I	0.002398208	1953125	6.12E+04	3.06E+04	1.22E+05	6.12E+04
J	0.000479642	9765625	1.22E+04	6.12E+03	2.45E+04	1.22E+04

[^]STDs A-B were not included in the 36B4 standard curve.

[Telomere lengths of mice from longitudinal study of methylation in PB in response to low dose radiation](#)

Table 24: Mean length per telomere of PB samples from Chapter 5 (Section 5.1.2.3.1).

	Dose (mGy)	Time post-irradiation (d)	<i>n</i>	Mean Tel length (kb)	SD
Male	0	0	8	34.02	29.41
		420	8	18.02	13.28
	10	0	6	14.78	5.96
		420	6	14.17	10.47
Female	0	0	8	18.83	5.80
		420	8	12.78	7.90
	10	0	9	15.08	8.07
		420	9	19.12	10.56

Table 25: Mean length per telomere of spleen samples from Chapter 5 (Section 5.1.2.4.1).

	Dose (mGy)	Age (months)	<i>n</i>	Mean Tel length (kb)	SD
Male	untreated	2	5	13.18	0.63
	0	18.2 (±0.8)	8	22.90	16.01
	10		6	10.17	5.52
Female	untreated	2	5	14.74	2.20
	0	18.2 (±0.8)	9	43.45	40.92
	10		9	21.26	19.32

APPENDIX F: CELLPROFILER™ PIPELINE

The CellProfiler pipeline used to identify T-cell areas of spleen sections is as follows:

1. DAPI images were used to identify cells using Otsu global 2-class thresholding; where weighted variance was minimised. There was a threshold correction factor of 1, with lower and upper bounds of the threshold of 0 and 1 respectively;
2. FITC images were identified following masking of the DAPI image i.e. regions not stained by DAPI were removed by masking. Primary objects were identified in the masked FITC images with a minimum and maximum diameter set at 30-500 pixel units. A 2-class Otsu global threshold with a correction factor of 1 was used, with lower and upper bounds of the threshold of 0.15 and 1, respectively. Weighted variance was minimised.
3. Image area occupied was measured in the objects of the masked FITC image.

APPENDIX G: PUBLICATIONS ARISING FROM THIS THESIS

Epigenetics 7:1, 92-105; January 2012; © 2012 Landes Bioscience

Sensitive quantitative analysis of murine LINE1 DNA methylation using high resolution melt analysis

Michelle R. Newman,¹ Benjamin J. Blyth,¹ Damian J. Hussey,² Daniel Jardine,³ Pamela J. Sykes^{1*} and Rebecca J. Ormsby¹

¹Hematology and Genetic Pathology; ²Department of Surgery; Flinders University and Medical Centre; ³Flinders Analytical; Flinders University; Bedford Park; Adelaide, SA Australia

Key words: DNA methylation, LINE1, high resolution melt analysis, mouse tissue methylation, heterogeneous methylation

Abbreviations: HRM, high resolution melt; PCR, polymerase chain reaction; 5-aza, 5-aza-2'-deoxycytidine; LI, LINE1, long interspersed elements; NTS, net temperature shift; LC-MS, liquid chromatography-mass spectrometry; PB, peripheral blood

We present here the first high resolution melt (HRM) assay to quantitatively analyze differences in murine DNA methylation levels utilizing CpG methylation of Long Interspersed Elements-1 (LINE1 or L1). By calculating the integral difference in melt temperature between samples and a methylated control, and biasing PCR primers for unmethylated CpGs, the assay demonstrates enhanced sensitivity to detect changes in methylation in a cell line treated with low doses of 5-aza-2'-deoxycytidine (5-aza). The L1 assay was confirmed to be a good marker of changes in DNA methylation of L1 elements at multiple regions across the genome when compared with total 5-methyl-cytosine content, measured by Liquid Chromatography-Mass Spectrometry (LC-MS). The assay design was also used to detect changes in methylation at other murine repeat elements (B1 and Intracisternal-A-particle Long-terminal Repeat elements). Pyrosequencing analysis revealed that L1 methylation changes were non-uniform across the CpGs within the L1-HRM target region, demonstrating that the L1 assay can detect small changes in CpG methylation among a large pool of heterogeneously methylated DNA templates. Application of the assay to various tissues from Balb/c and CBA mice, including previously unreported peripheral blood (PB), revealed a tissue hierarchy (from hypermethylated to hypomethylated) of PB > kidney > liver > prostate > spleen. CBA mice demonstrated overall greater methylation than Balb/c mice and male mice demonstrated higher tissue methylation compared with female mice in both strains. Changes in DNA methylation have been reported to be an early and fundamental event in the pathogenesis of many human diseases, including cancer. Mouse studies designed to identify modulators of DNA methylation, the critical doses, relevant time points and the tissues affected are limited by the low throughput nature and exorbitant cost of many DNA methylation assays. The L1 assay provides a high throughput, inexpensive and sensitive screening tool for identifying and characterizing DNA methylation changes to L1 elements at multiple regions across the genome.

Introduction

Approximately 2–10% of the cytosine residues in the mammalian genome are methylated (5-methyl-deoxycytosine; 5-mdC), predominantly when in sequence with a guanine (termed a CpG dinucleotide) and largely within transcriptionally silent regions of the genome. CpG-rich regions within transcriptionally active gene promoters are generally unmethylated, although it has been reported that only key CpGs within the promoter region need to be (un)methylated to exert control on gene expression.¹ In cancer, DNA methylation changes can occur at individual genes, or across the genome (global methylation), resulting in transcriptionally silent regions becoming demethylated, leading to transcriptional activation, or regions that are normally transcriptionally active rendered silent by aberrant increases in DNA methylation.

The most heavily methylated regions of the genome are DNA sequences belonging to repetitive DNA elements, which comprise approximately 45% of the mammalian genome,² of which 20% consist of Long Interspersed Elements-1 (LINE1 or L1).²⁻⁴ Short Interspersed Elements (SINE) and Long-terminal Repeat elements (LTR) are also distributed throughout the genome and can be methylated. These repeat elements can contain full length coding regions that, upon demethylation, may result in transposition across the genome, which can result in disruption to gene expression and, in some cases, disease.^{5,6} Loss of repeat element methylation can be an early event in carcinogenesis or tumor progression. For example, loss of methylation at intracisternal-A particle (IAP) repeat elements in mice results in active transcription and transposition leading to insertion of the IAP element into the genomic locus of *Notch-1*. This retrotransposition induces

*Correspondence to: Pamela J. Sykes; Email: pam.sykes@flinders.edu.au
Submitted: 09/23/11; Revised: 11/17/11; Accepted: 11/21/11
<http://dx.doi.org/10.4161/epi.71.18815>

expression of an oncogenic transcript of *Notch-1* in thymic tumors.⁷ In several cases, it has been reported that a loss of methylation at repeat elements has resulted in increased chromosomal instability as well as the enhanced development of colorectal cancer, non-small cell lung cancer and bladder tumors.⁸⁻¹⁵

Increasingly, mouse models are being used to study the acute and transgenerational effects of exogenous modulators of global DNA methylation such as diet,¹⁶⁻¹⁸ chemical carcinogens,¹⁹ ionizing radiation,²⁰⁻²⁴ as well as the study of DNA methylation in aging animals.^{25,26} Accordingly, there is an increasing need for sensitive, robust, inexpensive and high throughput methods for the detection of changes to global DNA methylation levels. While High Performance Liquid Chromatography (HPLC) and Liquid Chromatography-Mass Spectrometry (LC-MS) are considered two of the gold standards for assessing total methylated cytosine content due to their high sensitivity, accuracy and reproducibility, they are low-throughput due to the requirements of sample preparation, lengthy analysis procedures and cost per sample. More recently, whole genome sequencing and array technologies such as the *Illumina*, SOLiD (Invitrogen) and 454 platforms (Applied Biosystems) have been used to investigate global CpG methylation. While these platforms are able to determine the methylation status of thousands of genes at the single CpG site-level offering the highest level of resolution, they are not amenable for screening large numbers of experimental samples and the technology is not available to all laboratories. Another common sequencing by synthesis technique used in methylation analysis is pyrosequencing, which offers information about the proportion of methylated cytosines in a target sequence. While this is also a powerful tool, it is limited by the size of the target region and cannot be used to analyze highly polymorphic sequences.

High resolution melt (HRM) PCR is now being used in methylation studies and is capable of detecting single nucleotide differences based on differences in melting temperatures.²⁷ The widespread nature and CpG density of L1 elements has resulted in the utilization of L1 elements to investigate changes in DNA methylation at multiple locations within the genome.²⁸⁻³⁰ We have developed a HRM-PCR to quantitatively detect methylation changes to heterogeneously methylated murine L1 repeat elements as a surrogate marker of widespread alterations to DNA methylation levels. The L1 assay calculates the integral difference in the melt curves of a sample compared with the methylated control sample (termed the Net Temperature Shift-NTS), providing a sensitive, quantitative measurement of differences in methylation. Using the NTS calculation, the assay was shown to detect dose-dependent demethylation of L1 elements induced by a chemical demethylating agent. Application of the assay to various tissues from two common inbred laboratory mouse strains—Balb/c and CBA, demonstrated that the assay could detect differences in methylation between tissue samples that had not been treated with a demethylating agent. We report, for the first time, the relative methylation levels of peripheral blood samples when compared with other murine tissues, which were highly methylated in both mouse strains. The ability to quantitatively measure methylation of mouse PB samples using a high throughput and sensitive screening assay provides a powerful tool

for assessing changes to methylation in response to exogenous and endogenous modulators of methylation in comparison to human studies where repeated sampling of subjects is required.

Results

L1-HRM assay design. We aimed to develop a high-throughput, quantitative assay for the detection of DNA methylation changes by analyzing the CpG methylation status of murine LINE1 (L1) repeat elements using PCR high-resolution melt curve analysis (HRM). The forward primer to a murine L1 element (Accession number: D84931.1) from Kato et al.^{31,32} was used as a query sequence for a BLAT search (genome.ucsc.edu). A target CpG island (containing 13 CpGs) upstream of the Kato primer binding site [located within the open reading frame 2 (ORF2) of the consensus sequence] was identified using MethPrimer³³ and candidate primer sequences that did not contain CpGs were then used to perform an in silico PCR (genome.ucsc.edu). Primer pairs were chosen based on the number of genomic locations predicted to amplify with the candidate primer pair indicating widespread coverage of the L1 elements. The primers were found to amplify L1 elements at numerous locations on each mouse chromosome (data not shown). Successful amplification of murine L1 elements was confirmed by DNA sequence analysis.

HRM analysis is used to distinguish between single nucleotide differences based on the melting temperatures of amplicons.^{27,28,34,35} HRM can be used to differentiate between methylated and unmethylated DNA following treatment of genomic DNA with sodium bisulphite. DNA that is heavily methylated will remain cytosine-rich following bisulphite modification, whereas less methylated DNA will contain a lower GC-content due to the presence of uracil in place of the original unmethylated cytosines. These sequence changes result in melting temperature differences (due to differences in the amount of thermostable GC). Methylated mouse genomic control DNA and an unmethylated control were amplified with the *F_unbiased_mLINE1* and *R_unbiased_mLINE1* primers. A 50% mixture of the two control DNA samples was bisulphite modified and amplified. As expected, the melt curve analysis showed that the methylated control had a higher melt temperature range compared with the unmethylated control DNA. The 50% mixture had a melt temperature range situated between the two control DNA samples (Fig. 1A). The graph of the negative first derivative of the melting curve (-dF/dT) (Fig. 1B) showed that the methylated and unmethylated control samples had only one melt peak each, whereas the 50% mixture of the two control DNA samples had two melt peaks representative of each of the control DNA samples.

Detection of heterogeneous DNA demethylation induced by a chemical demethylating agent. Not all CpG islands will have complete demethylation at every CpG and this will result in a heterogeneous pattern of methylation at any individual CpG dinucleotide.^{28,36-43} In order to investigate if small changes in methylation patterns across numerous L1 elements distributed throughout the genome could be detected with this assay, a mouse hybridoma cell line was treated with two different low doses

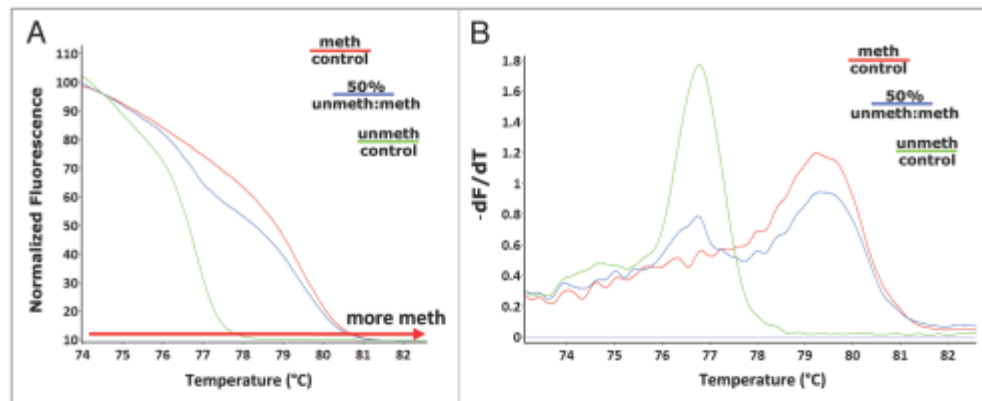


Figure 1. Detection of differences in L1 methylation. Melt curve analysis following amplification with the unbiased L1 primers (*F_unbiased_mLINE1* and *R_unbiased_mLINE1*). (A) The HRM normalized melt curve and (B) the first derivative melt curve ($-dF/dT$) was performed on methylated (red) and unmethylated (green) control DNA as well as a 50% (methylated:unmethylated control) methylated sample (blue).

(0.125 μ M and 0.5 μ M) of the chemical demethylating agent 5-aza-2'-deoxycytidine (5-aza). The melt curves of the samples from each treatment group could be distinguished from the melt profile of the methylated control DNA. A significant difference in melting temperature between the 5-aza treated cells and the vehicle (DMSO) treated control cells was not detected (Fig. 2A). It has been proposed in several reports, that to increase sensitivity to detect small methylation/demethylation events within a large pool of heterogeneously methylated templates, PCR primers may need to enrich for methylated or unmethylated templates.⁴⁴⁻⁴⁶ Using this approach, a new forward and reverse primer pair was designed to match the bisulphite-modified sequence of an unmethylated CpG dinucleotide at the 3' end of each oligonucleotide. Thus, the same region could now be amplified with an unbiased-primer pair (not selective for methylation status) or an unmethylated-biased primer pair (preferentially amplifying L1 sequences with both flanking CpG sites unmethylated). Using the unmethylated-biased primers, a distinct, dose-dependent difference in melt curves was observed for the samples treated with 5-aza compared with the vehicle control and between the two 5-aza doses (Fig. 2B and C). All L1-HRM assays were subsequently performed using the unmethylated-biased primers unless otherwise stated.

Statistical analysis of methylation differences between samples using the net temperature shift. In order to statistically quantify the differences in melt curves observed, a means of deriving the methylation index of a sample based on the melting profile of amplicons was devised. Within the Rotor-Gene Q software, normalized melt curves of all samples were generated. Following this, a control sample was selected (in this instance, the methylated control DNA) and a difference plot of the melt curves compared with the methylated control was generated (Fig. 2C). The difference plot fluorescence value at each temperature point (0.1°C intervals from 74–84°C for a total of 100 readings) within the melt curve was exported to Microsoft Excel. All values within

the melt curve were summed and divided by 100 to give the Net Temperature Shift (NTS) value (Table S1). A greater negative NTS value indicates a greater shift from the methylated control and, thus, a less methylated sample. Using the NTS, a significant dose-dependent demethylation of the L1 elements for samples treated with 5-aza compared with the vehicle control ($p < 10^{-5}$) and between the two 5-aza doses ($p < 10^{-5}$) was observed (Fig. 3A).

To demonstrate that methylation changes were not restricted to L1 elements and that the assay design could be applied to other repeat elements, the NTS calculation was applied to amplicon melt curves from two other DNA repeat elements: mouse B1 (Short Interspersed Elements; SINE family, Mm; located within the first 92 bp of the -130 bp monomeric repeat unit) and Intracisternal-A particle Long-terminal Repeat elements³² (IAP_LTR; located within the 5'LTR of the IAP promoter) (Fig. 3B and C). For both the B1_Mm primers, which were unbiased for methylation, and the unmethylated-biased IAP_LTR element primers, there was a significant difference in the NTS of the 0.125 μ M and 0.5 μ M 5-aza treated samples compared with the vehicle control ($p < 0.05$). Both repeat elements showed strong correlation with the L1 elements ($p < 0.01$); with the IAP_LTR demonstrating greater correlation with the L1 elements than the B1 elements (Table S2).

Validation of the L1-HRM assay. In silico PCR and analysis of L1 repeat element sequences. Sequence analysis of L1-PCR products identified six non-CpG nucleotide positions with more than one defined peak on the sequence chromatogram (data not shown), indicating potential sequence variation. Using the original unbiased L1 primer sequences, the mouse genome was searched by in silico PCR (genome.ucsc.edu) to identify the predicted pool of L1 template sequences. Alignment of 20 randomly selected in silico PCR results revealed ten nucleotide positions with sequence variation and that the frequency of the minority variants occurred in 5–40% of the analyzed templates (Table

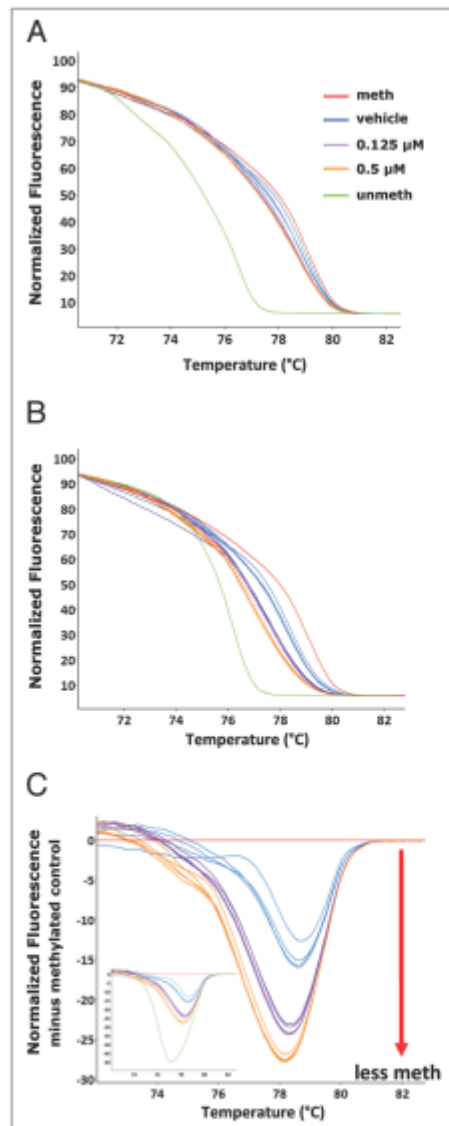


Figure 2. Detection of 5-aza induced partial demethylation. Vehicle control (DMSO) (blue), 0.125 μM (purple) and 0.5 μM (orange) 5-aza treated A11 cell line genomic DNA was amplified following bisulphite modification with the unbiased L1 primers and subjected along with the methylated (red) and unmethylated (green) controls to melt analysis. (A) the normalized HRM melt curve ($n = 3$ samples per treatment group is displayed). The samples were then amplified with unmethylated-biased primers. Melt analysis was performed on the PCR products. (B) The normalized HRM curve and (C) the difference graph (one PCR replicate for each of the $n = 4-5$ samples is displayed; inset is the difference graph with the unmethylated control included).

2). Sequence variants 2, 5 and 7 occurred at the guanine base in CpG dinucleotides (Fig. 4A) and as a result, 10–15% of the L1 elements did not contain a CpG at these sites. All six sequence variants identified from the sequencing of PCR products were observed in the 20 *in silico* predicted L1 template sequences.

Comparison of the L1-HRM assay with pyrosequencing and LC-MS. It was necessary to determine whether the differences in melting temperatures observed were due to differences in cytosine composition following bisulphite modification and not the result of differences in non-CpG sequence variations (Table 2). Analysis of the melt curves for L1 elements amplified from bisulphite unmodified genomic DNA revealed no difference in melt curves between the 5-aza and vehicle control treated samples (data not shown). This indicated that the identified sequence variants were not influencing the differences in melt curves observed, and that the differences were due to cytosine content following bisulphite modification. To confirm this, the L1-HRM PCR products were subjected to pyrosequencing. Pyrosequencing of CpGs 7–12 (Fig. 4A) revealed that each of the six CpG sites in the DNA from the 0.125 μM and 0.5 μM 5-aza treated cells displayed significantly less L1 methylation than the vehicle control (Fig. 4B). The mean percent of L1 methylation across all six CpGs revealed a significant dose-dependent reduction in L1 methylation with increasing concentration of 5-aza (Fig. 4C) and a significant difference between all treatments ($p < 10^{-4}$). CpG 9 demonstrated a greater reduction in methylation compared with the other CpG sites analyzed in the 5-aza treated samples and in comparison with the vehicle control (Fig. 4B).

Liquid Chromatography-Mass Spectrometry (LC-MS) was used to assess total genomic 5-mdC content for comparison with the NTS detection of demethylation. A significant reduction in total genomic 5-mdC content compared with the vehicle control for both 0.125 μM and 0.5 μM treated samples was observed (Fig. 4D). Unlike the HRM assay and pyrosequencing, the LC-MS method was unable to distinguish differences in DNA methylation between the 0.125 μM and 0.5 μM 5-aza treated cells. Bivariate correlations with 5-aza dose for the three assays (Table 3) showed equal and significant negative correlations for NTS vs. 5-aza dose and pyrosequencing mean methylation vs. 5-aza dose, with a weaker but still significant negative correlation between LC-MS 5-mdC content vs. 5-aza dose. The NTS and pyrosequencing mean methylation levels were highly and significantly correlated with each other, while the 5-mdC content by LC-MS, which is not specific for L1 methylation, showed less concordance with the other two methods.

Linearity of the L1-HRM assay. Various ratios of genomic DNA from the 0.5 μM 5-aza treated and vehicle treated samples were made (prior to bisulphite modification) to create heterogeneously methylated samples with predicted mean L1 methylation levels (based on pyrosequencing measurements) between 45.4 and 75.6%. These DNA mixtures were then subjected to the L1-HRM assay to test the sensitivity and linearity of the assay. Linear regression analysis on the standard curve indicated that the NTS was highly linear compared with the predicted L1 methylation levels of the samples ($p < 0.001$; $R^2 = 0.992$) (Fig. 4E). Bonferroni corrected post-hoc analysis revealed that with the

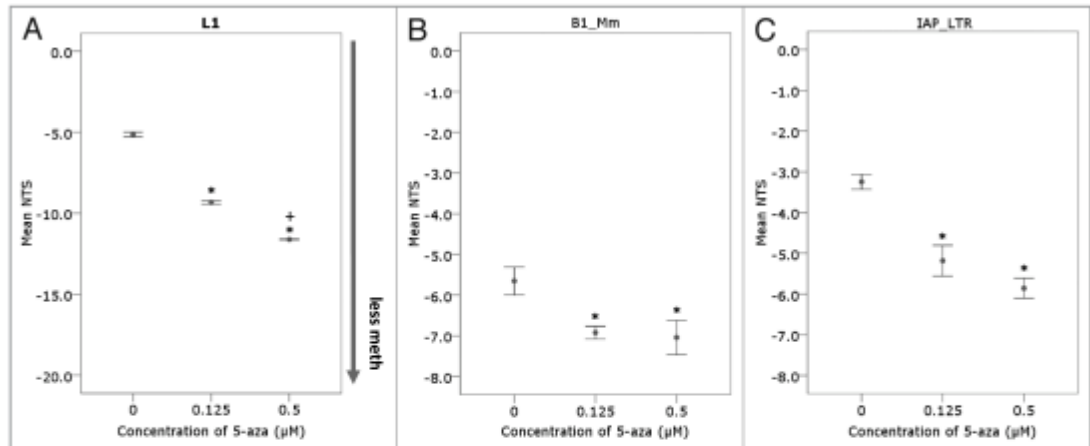


Figure 3. Quantitation of methylation differences using the Net Temperature Shift. The normalized fluorescence at each temperature point on the melt curve were used to calculate the mean NTS of the 5-aza treated samples for (A) L1, (B) murine B1 family Mm (B1_Mm) and (C) Intracisternal-Particle A Long-terminal Repeat (IAP_LTR) repeat elements ($n = 4-5$ samples per treatment group) (* $p < 10^{-5}$ compared with the vehicle control; † $p < 0.05$ compared with the 0.125 μM treated 5-aza samples).

number of replicates used here, an absolute difference of 3% mean L1 methylation or greater could be detected between two mixes of heterogeneously methylated DNA ($p < 0.05$). Comparison of these DNA mixtures by L1-HRM was performed for two separate bisulphite modification reactions and two HRM-PCR runs per modification (shown in Table 4) and revealed that neither bisulphite modification batch nor PCR run made a significant contribution to the overall variance (ANOVA, $p < 0.05$), with the variance largely explained by the predicted methylation levels of the various mixtures ($p < 0.01$).

Detection of tissue and sex specific methylation levels in murine tissues. The L1-HRM assay was then used to detect L1 methylation differences between samples that had not undergone 5-aza induced demethylation, but were expected to be of differing (L1) methylation levels, based on previous reports in references 20, 22 and 47. Mouse strain, gender and the tissues analyzed have been shown to have differences in global DNA methylation levels. Therefore, genomic DNA from male and female Balb/c and CBA mice were analyzed using the unmethylated-biased L1 primers. Analysis of the NTS values revealed that there were both strain and sex based differences in L1 methylation levels; with the peripheral blood samples (PB) displaying the highest L1 methylation and the spleen tissue genomic DNA the lowest. In all mice, the order of L1 methylation from hypermethylated to hypomethylated was as follows: PB>kidney>liver>prostate>spleen (Fig. 5A). For Balb/c mice, higher methylation was observed in the male kidney ($p = 0.03$) and spleen ($p = 0.01$) tissues compared with the females, and for CBA mice, higher methylation was observed in the male kidney ($p = 0.01$), PB ($p = 0.01$) and spleen ($p = 0.028$) tissues relative to female mice. The CBA mice demonstrated higher L1 methylation of the kidney, liver and PB tissues compared with the Balb/c mice ($p < 0.05$). A comparison

of the unbiased primers with the unmethylated-biased primers on the male Balb/c tissues (Fig. 5B) showed hierarchy of tissue L1 methylation that correlated with the NTS for the unmethylated-biased primers ($p < 0.01$, Pearson correlation); however, the unbiased primers did not demonstrate significant differences in L1 methylation between all tissues. For example, the spleen was hypomethylated at L1 elements compared with all other tissues when analyzed with the unmethylated-biased primers (ANOVA, $p < 0.05$); whereas the unbiased primers only demonstrated significant L1 hypomethylation of the spleen when compared with the PB samples (ANOVA, $p = 0.045$).

Discussion

HRM analysis of bisulphite modified DNA templates is used to investigate DNA methylation, with various quantitative calculations of methylation levels employed. These calculations range from comparing Cq values to a standard curve,^{28,46} a calculation based on the temperature at which half of the PCR products have melted,⁴⁸ measuring the height of the differential fluorescence melt peak from a nominated control,⁴⁹ TaqManTM probe technology³⁷ and single dilutions of complex melt curves.³⁶ In these assays, the methylation of a sample is calculated by comparison to a standard curve that is generated using completely methylated and unmethylated control DNA.^{28,36,37,46,48-50} With the exception of Stanzer et al.²⁸ all assays were utilized to investigate gross changes in CpG methylation at single genomic loci in cancer samples. Analysis of the methylation levels of L1 elements using HRM presents a unique challenge due to the number of CpGs within the CpG islands and the abundance and sequence diversity of LINE1 elements throughout the genome. Methylation profiles will be heterogeneous and will produce complex melt

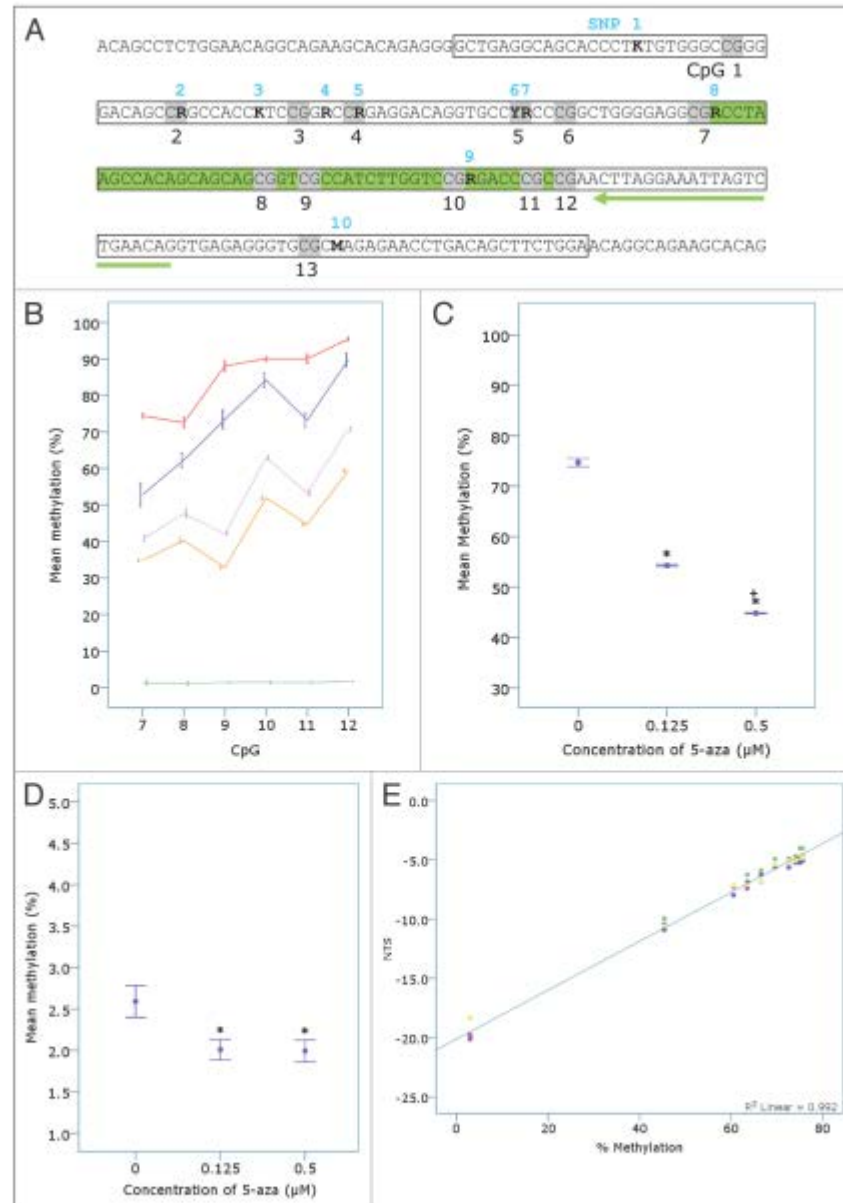


Figure 4. For figure legend, see page 98.

curves that cannot be quantified by comparison to a standard curve of methylated/unmethylated DNA. Our aim was to utilize HRM technology to detect small changes in DNA methylation to L1 elements throughout the genome that can result from

perturbations to the homeostatic environment such as chemical or radiation exposure, dietary changes and aging in mouse studies. As a proof-of-principle, the chemical demethylating agent 5-aza was used to demonstrate the detection of L1 demethylation

Figure 4 (See previous page). Confirmation of the detection of 5-aza induced demethylation by the L1-assay. (A) The L1 sequence as confirmed by DNA sequencing. The location of sequence variants in the target L1 region (boxed region) in unmodified genomic DNA identified from both sequence analysis of L1-PCR products (amplified with *F_unmod_mLINE1* and *R_unmod_mLINE1*) and in *in silico* PCR analysis (see Table 2) are shown in bold, numbered 1–10 in blue and characterized as an R (A/G), K (T/G) or M (A/C). CpGs are shaded and numbered in black 1–13. The L1-HRM PCR products ($n = 4$ –5 samples per treatment group from $n = 1$ bisulphite modification and PCR reaction) were then subjected to pyrosequencing. The pyrosequencing primer is highlighted by the green arrow and the region pyrosequenced is shown in green. (B) The percent methylation of each CpG was plotted and separated by 5-aza concentration (vehicle, blue; 0.125 μM , purple and 0.5 μM , orange) or control DNA status (red, methylated control; green, unmethylated control). (C) The mean methylation of all CpGs pyrosequenced (7–12) was plotted vs. 5-aza concentration ($^*p < 10^{-5}$ compared with the vehicle control; $^*p < 0.05$ compared with the 0.125 μM treated 5-aza samples). (D) Genomic DNA samples ($n = 4$ –5 per treatment group) were subjected to Liquid Chromatography-Mass Spectrometry (LC-MS) and mean percent methylation (5-mdC/dG ratio) for each treatment group plotted ($^*p < 0.05$). (E) Linear regression analysis was performed on the mean NTS for samples of a standard curve ($R^2 = 0.992$; $p < 0.001$). The standard curve was made from mixtures of the vehicle and 0.5 μM 5-aza treated A11 samples (75.6, 75.45, 75.3, 75, 74.09, 72.58, 69.56, 66.54, 63.52, 60.5 and 45.4% methylated) using the mean pyrosequencing values for the two samples. The unmethylated control DNA (~3% methylated) was also included in the L1-HRM PCR reactions. The samples underwent two separate bisulphite modifications and were amplified with the unmethylated-biased primers in two separate PCR reactions per bisulphite modification, prior to melt analysis.

using HRM. Treatment with 5-aza induces significant changes to total genomic 5-mdC levels.^{51,52} In this study, lower doses of 5-aza were used to treat the A11 cells, which underwent only one cell division in order to induce low level demethylation, as would be expected following low level exposure to exogenous or endogenous modulators of DNA methylation. We proposed that treatment would cause partial demethylation resulting in increased heterogeneity across the L1 elements. Initial analysis of the resulting melt curves following amplification with primers unbiased for L1 methylation status demonstrated demethylation of the 5-aza treated cells compared with vehicle treated cells but no difference between the two 5-aza doses. To enhance the detection of small differences in methylation, primers were biased for unmethylated CpGs within the primer binding sites to enrich for the small proportion of samples that had undergone partial demethylation, hypothesizing that CpGs within the target region would also have undergone some partial demethylation. When these primers were applied to the same 5-aza treated samples, we saw differences in the melt curves of the 5-aza treated samples indicating that the biased primers were capable of sensitively detecting small changes in GC content of the L1 elements following bisulphite modification. In order to quantify these small differences, we devised a means of measuring the difference in melt temperature between samples following PCR-termed the Net Temperature Shift (NTS). The NTS quantifies changes in methylation (based on the GC content of the amplicons) compared with a control sample, rather than determining mean percent methylation of a target region, and incorporates all products that melt at each 0.1°C interval within the melt range for an amplified sample. By analyzing the data obtained at all points within the melt curve, all products that are melting are included in the final index of methylation. This approach enables non-uniform melt profiles to be more accurately analyzed in comparison to other reported methods for analyzing HRM data, for example, the T50,⁴⁸ or the differential fluorescence peak,⁴⁹ where only a single point in the melt curve is measured.

It has been reported that 3' end primer biasing can introduce amplification bias-false-positive results.^{44,45,53,54} However, analysis of the L1-HRM PCR products by pyrosequencing confirmed that the L1 elements amplified by the biased primers were heterogeneously methylated and that primer biasing did not enrich for L1 elements that were completely unmethylated at all CpGs. The

mean methylation of all CpGs within the L1 target region analyzed by pyrosequencing confirmed that there was dose dependent demethylation with 5-aza treatment compared with vehicle treated control cells; however, it also demonstrated that the level of demethylation induced by 5-aza was not uniform across all of the CpGs. The sequence heterogeneity of the L1 elements arising from non-CpG sequence variants restricted the pyrosequencing analysis to only 6 out of the 13 CpG dinucleotides. As HRM is used to detect non-CpG polymorphisms, there is the potential for these non-CpG variants to influence the melting profiles of the amplified L1 elements. However, the HRM data showed correlation with total 5-mdC content as determined by LC-MS, which demonstrated a significant, negative correlation with 5-aza dose, indicating that the assay is detecting sequence differences arising from cytosine content following bisulphite modification rather than differences due to sequence diversity. While we observed good correlation between the L1 assay and the LC-MS data, the assay is specific for L1 methylation and may not reflect changes in cytosine content occurring elsewhere. The demonstration of methylation differences between the two 5-aza doses using the L1 assay suggests that either there is a difference in GC content at the L1 elements that is not reflected in the total genomic 5-mdC content, indicating that L1 elements are more sensitive to 5-aza induced demethylation, or that the L1 assay has greater sensitivity to detect very small changes in DNA methylation. L1 elements have been shown in other studies to be relatively resistant to 5-aza induced demethylation compared with other sequences in the genome.⁵⁵ This suggests that the L1 assay is a sensitive assay capable of detecting changes in L1 DNA methylation across the genome.

Irahara et al.⁵⁶ analyzed the precision and reproducibility of pyrosequencing to detect methylation differences, which is reported to be one of the most sensitive methods for methylation analysis. They demonstrated that variability arising from bisulphite modification ranged from 1.2–4.2%, and run to run variation for the pyrosequencing reactions ranged from 1.9–3.8% of the detected mean CpG methylation. The L1 assay presented here was shown to be as sensitive as the gold standard methods, with a 3% difference in NTS between samples detected. The sensitive nature of the L1-HRM assay as a result of biasing the primers was further demonstrated by the strong correlation of the assay with the pyrosequencing results. Assessment of the effect of

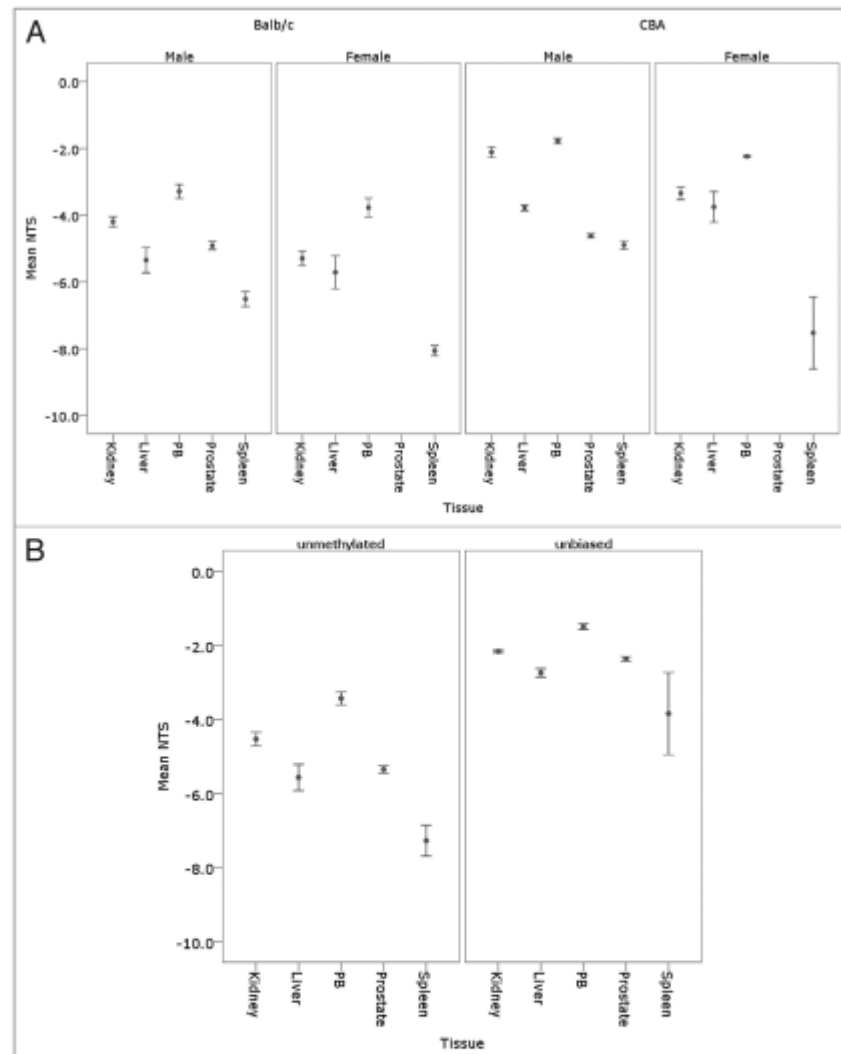


Figure 5. Detection of tissue and sex specific methylation levels in murine tissues. (A) The mean NTS of L1 elements was used to assess DNA methylation levels in the kidney, liver, peripheral blood (PB), prostate and spleen tissues of male ($n = 5$) and female ($n = 5$) Balb/c and CBA mice following bisulphite modification and amplification with the unmethylated-biased primers. (B) The mean NTS of the kidney, liver, PB, prostate and spleen of male Balb/c mice when amplified with the unbiased primers for comparison with the unmethylated-biased primers.

PCR and bisulphite modification reaction variability on detection of methylation differences confirmed that the differences detected between samples was not due to inherent PCR or bisulphite modification variability, but due to differences in cytosine content.

Compared with pyrosequencing, the L1 assay is not limited by the presence of non-CpG sequence variants or the size of the

target region. The target region of a pyrosequencing assay is restricted to ~30 nucleotides, whereas the L1 assay incorporates an entire CpG island consisting of 13 CpGs spanning 192 bp (of the ~6 kb L1 element) and, as we have demonstrated, does not appear to be influenced by the presence of the sequence variants. Economically, the cost to pyrosequence (including specially designed biotin labeled primers, PCR, PCR product

purification, and the pyrosequencing analysis cost) is far greater than performing an in-house PCR reaction with HRM analysis.

Application of the assay to two other murine repetitive DNA elements demonstrated that the assay design can also be applied to other repeat elements. The number of CpGs available for analysis within the smaller B1 elements precluded the design and use of biased primers to enhance sensitivity of detection, while the IAP_LTR element primers could be biased for unmethylated CpGs to enhance sensitivity. While not significant, the IAP_LTR elements displayed a greater NTS difference between the 0.125 μ M and 0.5 μ M treated 5-aza samples relative to the B1 elements. While this may provide further evidence that biasing can increase the sensitivity to detect small changes in cytosine content, it could also indicate that the number of CpGs within a target region influence sensitivity.

We then applied the L1 assay to various tissue samples isolated from two different mouse strains that have been shown to have differences in genomic 5-mdC levels. Our assay revealed tissue and gender specific differences in L1 methylation consistent with the literature^{26,47} where spleen is reported to be hypomethylated when compared with other tissues, in two inbred laboratory mouse strains (Balb/c and CBA) that are commonly used in global DNA methylation studies.^{26,24,25,57-61} The L1 DNA methylation levels of murine peripheral blood have not previously been reported, however it is commonly used to measure methylation changes in humans.^{50,56,62-65} The L1-HRM assay is amenable to the analysis of the small volumes of blood obtained during tail vein bleeds allowing repeated blood sampling and peripheral blood methylation levels to be monitored at various time points from the same mouse.

In summary, the assay provides the ability to quantitatively measure L1 DNA methylation changes where individual CpG methylation data or mean percent (%) methylation is not sought. The assay will provide a useful tool for the ongoing investigation of the transcriptional control of DNA repeat elements and their impact on genomic stability. Furthermore, we propose that the L1-HRM assay is a high throughput and inexpensive screening method for the investigation and identification of small but potentially disease-initiating aberrant methylation changes in *in vivo* mouse models of diseases such as cancer. The assay can also be used to investigate changes that occur with aging, or in response to treatment with or exposure to genotoxins for comparison with human studies, which often utilize serial blood sampling to monitor changes to L1 methylation at multiple concentrations and time points.

Materials and Methods

Cell culture. All murine hybridoma cells were originally derived by fusion of C57Bl/6-pKZ1 transgenic spleen cells with P3653 murine myeloma cells.⁶⁶ All cells were grown in suspension in RPMI 1640 media supplemented with 5% FCS (cat # 10099-141 Invitrogen), 50 IU/mL penicillin and 50 μ g/mL streptomycin (cat # 15070-063, Invitrogen) at 37°C with 5% CO₂. Cells were passaged twice weekly.

5-aza-2'-deoxycytidine treatment. All cells were cultured at a concentration of 2×10^6 during exponential growth phase in 10 mL RPMI 1640 (Flinders University and Medical Centre) in a 25 cm³ tissue culture flask (Nunc). Cells were treated for 24 h with 0.125 μ M or 0.5 μ M 5-aza-2'-deoxycytidine (5-aza; cat #A3656, Sigma-Aldrich) in DMSO (cat # D8418, Sigma-Aldrich) or vehicle control (0.1% DMSO) (n = 5 flasks per treatment group) and then centrifuged for 5 min at 1,200x g, the media removed by aspiration and washed with 10 mL RPMI 1640. Cells were resuspended at a density of 2×10^4 cells per mL in RPMI 1640 and cultured for a further 72 h before pelleting for DNA extraction.

Mice. Three-month old male and female Balb/c and CBA mice (Animal Resource Centre, Perth, Australia) were barrier maintained in micro-isolators at the Flinders University Animal House with a 12 h light/dark cycle. Food and water were given *ad libitum*. All experiments were approved by the Flinders University and Institute of Medical and Veterinary Science Animal Welfare Committees.

Tissue collection. Immediately prior to euthanasia, mice were placed in a holding restraint. The tails were swabbed with ethanol and a small incision was made to the lateral tail vein using a GoldenRod lancet (MEDIpoint Inc.). No more than 100 μ L of peripheral blood (PB) was collected in EDTA-collection tubes (Bectin-Dickinson and Company). Pressure was applied to the wound until bleeding ceased and animals were returned to their cages. Mice were then euthanized by CO₂ asphyxiation and tissues were collected and fresh frozen in OCT cryoprotectant (Tissue-Tek). Tissues were stored at -80°C and PB samples were stored at -20°C until DNA extraction.

DNA samples. Genomic DNA was extracted from cells and tissues using the QIAmp DNA Mini extraction kit (Qiagen). DNA was extracted from three fresh frozen tissue sections (25 μ M) cut using a cryostat (Reichert-Jung Cryocut 1800) or from the frozen blood samples, as per manufacturer's instructions except that DNA was eluted with 2 x 100 μ L aliquots of Buffer AE. For PB samples, DNA was eluted in 1 x 100 μ L aliquot of Buffer AE. DNA was quantified using a Nanodrop 8000 (Thermo Scientific).

Bisulphite modification. Genomic DNA (200 ng for all samples; 40 ng for PB) was bisulphite modified using the Zymo Research EZ DNA Methylation-Gold kit (Zymo Research) as per manufacturer's instructions. Modified DNA was diluted with water (Qiagen, Hilden, Germany) to 10 ng/ μ L (theoretical amount based on genomic DNA concentration input into the bisulphite modification reaction). Unless stated, all DNA underwent two separate bisulphite modification reactions.

Primers. Primers (Geneworks) for LINE1 (Long Interspersed Nucleic Elements-1), B1_Mm (Mm family of SINE, Short Interspersed Nucleic Elements) and IAP_LTR (Intracisternal-A-Particle Long Terminal Repeat element) specific for bisulphite modified DNA were designed using MethPrimer.³³ Pyrosequencing primers and assays were designed using the PSQ Assay Design program (Qiagen). Table 1 outlines the primer sequences and amplicon sizes. Each primer that was designed

Table 1. Primer sequences

Primer biasing	Primer	Sequence	Number of CpGs in target sequence	Amplicon size
	F_kato	TAG GAA ATT AGT TTG AAT AGG TGA GAG GGT		
unbiased	F_unmod_mLINE1	GGG CTG AGG CAG CAC CCT GTG TG	13	195 bp
	R_unmod_mLINE1	TCC AGA AGC TGT CAG GTT CTC TGG C		
	F_unbiased_mLINE1*	GGT TGA GGT AGT ATT TTG TGT G		195 bp
	R_unbiased_mLINE1	TCC AAA AAC TAT CAA ATT CTC TAA C		
unmethylated	F_umod_unmeth_mLINE1	GCT GAG GCA GCA CCC TGT GTG GGC C	11	193 bp
	R_umod_unmeth_mLINE1	TCC AGA AGC TGT CAG GTT CTC TGG CGC		
	F_unmeth_mLINE1*	GTT GAG GTA GTA TTT TGT GTG GGT I		193 bp
	R_unmeth_mLINE1	TCC AAA AAC TAT CAA ATT CTC TAA CAC		
	R_pyroprimer	TAT TCAA ACT AAT TTC CTA A		
	F_unmod_unbiased_B1_Mm	AGC CGG GCG TGG TGG	7	92 bp
	R_umod_unbiased_B1_Mm	CTT TGT AGA CCA GGC TGG CCT C		
	F_mod_unbiased_B1_Mm	AGT YGG GYG TGG TGG		92 bp
	R_mod_unbiased_B1_Mm	CTT TAT AAA CCA AAC TAA CCT C		
	F_unmod_unmeth_IAP_LTR	CCA CAT TCG CCG TTA CAA GAT GGC	6	141 bp
	R_unmod_unmeth_IAP_LTR	CAC CTA AAA ACA TAT CAC T		
	F_mod_unmeth_IAP_LTR	TTA TAT TTG TTG TTA TAA GAT GG I		141 bp
	R_mod_unmeth_IAP_LTR	CAC CTA AAA CAT ATC ACT		

All primers were designed using MethPrimer and UCSC Genome Browser. Bold typeface indicates bisulphite modified bases and biased CpG sites are underlined. Abbreviation: unbiased, unbiased for methylated or unmethylated bisulphite modified genomic DNA; unmeth, unmethylated-biased primers; unmod, unmodified genomic DNA specific primers; B1_Mm, mouse B1 element, family Mm; IAP_LTR, Intracisternal-A-particle Long-terminal Repeat element. *Primers contain a 5' biotin tag.

Table 2. Frequency of detected variants in L1 target sequence

Sequence variant	Type	Frequency in alignment of 20 random in silico PCR results	Detected in L1-PCR product DNA sequencing
1	G > T	10% (T) (2/20)	no
2	G > A	10% (A) (2/20)	yes
3	T > C	5% (C) (1/20)	no
	T > G	5% (G) (1/20)	yes
4	G > A	5% (A) (1/20)	no
5	G > A	15% (A) (3/20)	yes
6	C > T	5% (A) (1/20)	no
7	G > A	10% (A) (2/20)	yes
8	G > A	30% (A) (6/20)	yes
9	G > A	40% (G) (8/20)	yes
10	C > A	5% (A) (1/20)	no

Unmodified genomic DNA specific L1 primers (F_unmod_mLINE1 and R_unmod_mLINE1) were used in an in silico PCR analysis (UCSC Genome). Twenty randomly selected in silico PCR results were aligned and the frequencies of sequence variants detected in the alignment in comparison to the L1-HRM PCR target sequence are shown.

specifically for bisulphite modified DNA failed to amplify unmodified genomic DNA template.

PCR. PCR cycling and HRM were performed on a Rotor-Gene Q (Qiagen). A 20 µL reaction mix consisted of 20 ng

equivalent of bisulphite modified DNA (10 ng of bisulphite modified PB DNA) and a final concentration of: 1x EpiTect HRM PCR Master Mix (cat # 59445, Qiagen), 0.75 µM forward primer and 0.75 µM reverse primer, and water (Qiagen). Cycling conditions for LINE1 were as follows: 95°C for 5 min followed by 35 cycles of 95°C for 20 sec, 60°C for 30 sec and 72°C for 20 sec. Melt curve analysis occurred from 73°C to 84°C rising by 0.1°C/2 sec. Cycling conditions for B1_Mm and IAP_LTR were: 95°C for 5 min followed by 35 cycles of 95°C for 10 sec, 52°C for 15 sec and 72°C for 10 sec for 35 cycles. Melt analysis occurred from 65°C–80°C rising by 0.1°C/2 sec. Each sample was amplified in duplicate per PCR reaction. Unless stated, all samples underwent two separate PCR reactions.

Control DNA. Universal Methylated Mouse DNA (cat # D5012, Zymo Research) was used as a methylated genomic DNA control. Mean methylation of the methylated control was determined to be 86% (±1.3) by pyrosequencing and contain a 5-mC content of 5% (±1.44) by LC-MS. A LINE1 unmethylated control DNA was made as follows. LINE1 sequences from unmodified Universal Methylated DNA were amplified using F_unmod_mLINE1 and R_unmod_mLINE1 (see Table 1). The PCR products were purified using the QIAquick PCR purification kit as per manufacturer's instructions (Qiagen) and 200 ng of the purified PCR products were subjected to bisulphite modification and purification as described above for genomic DNA. Pyrosequencing analysis was performed to confirm that each CpG was unmethylated and was determined to have a mean

Table 3. Correlation of HRM assay with pyrosequencing and LC-MS

	Pearson Correlation Coefficient			
	Treatment	HRM	LCMS	Pyrosequencing (mean methylation)
Treatment	1	-0.952**	-0.391**	-0.952**
Pyrosequencing (mean methylation)	-0.952**	0.913**	0.377**	1
HRM	-0.952**	1	0.387**	0.913**
LCMS	-0.391**	0.387**	1	0.377**

Analysis of the ability of the L1-HRM assay to detect global DNA demethylation in samples treated with 5-aza when compared with pyrosequencing analysis of L1-HRM PCR products and LC-MS analysis of genomic DNA methylation (**p < 0.01).

Table 4. L1-HRM inter- and intra-assay variation

Sample mean meth (%)	Bisulphite modification reaction #1						Bisulphite modification reaction #2						Mean NTS	SD
	PCR 1		PCR 2		Mean NTS	SD	PCR 1		PCR 2		Mean NTS	SD		
	NTS	SD	NTS	SD			NTS	SD	NTS	SD				
45.40	-10.90	0.09	-9.95	0.25	-10.43	0.67	-10.44	0.08	-10.58	0.10	-10.51	0.10	-10.47	0.38
60.50	-7.99	0.07	-7.27	0.11	-7.63	0.51	-7.28	0.08	-7.16	0.01	-7.22	0.08	-7.42	0.36
63.52	-6.87	0.09	-6.26	0.01	-6.57	0.43	-7.40	0.05	-7.08	0.02	-7.24	0.23	-6.90	0.45
66.54	-6.24	0.21	-5.89	0.13	-6.07	0.25	-6.84	0.34	-6.81	0.03	-6.83	0.02	-6.45	0.45
69.56	-5.60	0.08	-4.93	0.00	-5.27	0.47	-5.60	0.06	-5.40	0.09	-5.50	0.14	-5.38	0.30
72.58	-5.64	0.12	-4.89	0.21	-5.27	0.53	-5.11	0.00	-5.11	0.00	-5.11	0.00	-5.19	0.31
74.09	-5.24	0.03	-4.70	0.00	-4.97	0.38	-5.23	0.09	-5.04	0.07	-5.14	0.13	-5.10	0.20
75.00	-5.25	0.03	-4.03	1.01	-4.64	0.86	-4.78	0.05	-4.63	0.03	-4.71	0.11	-4.67	0.60
75.30	-4.71	0.07	-4.68	0.13	-4.70	0.02	-4.74	0.03	-4.64	0.08	-4.69	0.07	-4.69	0.07
75.45	-5.05	0.06	-4.67	0.01	-4.86	0.27	-4.73	0.04	-4.86	0.04	-4.80	0.09	-4.83	0.16
75.60	-5.09	0.03	-4.03	0.72	-4.56	0.75	-4.70	0.06	-4.76	0.16	-4.73	0.04	-4.66	0.50

The 5-aza standard curve made from mixtures of the vehicle and 0.5 μ M 5-aza treated A11 samples (75.6, 75.45, 75.3, 75, 74.09, 72.58, 69.56, 66.54, 63.52, 60.5 and 45.4% methylated) using the mean pyrosequencing values for the two samples, was used to assess intra- and inter-assay variability. Each sample underwent two separate bisulphite modifications and two separate HRM-PCR runs with two PCR reaction duplicates per HRM-PCR.

methylation of 3% representing background noise level. The final product was diluted in water to a concentration at which the C_q (quantification cycle) range was within that of test samples. The unmethylated control DNA was included in each HRM-PCR as a quality control sample.

Sequencing analysis. HRM PCR products were purified using the QIAquick PCR purification kit (Qiagen) and quantified on a Nanodrop 8000 (Thermo Scientific). Sequencing primers are outlined in Table 1. Sequencing reactions were performed by the SouthPath and Flinders Sequencing Facility (Flinders University and Medical Centre, Adelaide, Australia). For pyrosequencing, HRM PCR reaction replicates for each sample (n = 5 per treatment group) were combined and aliquoted into 96-well plates in duplicate in a volume of 10 μ L and sent to EpigenDx (MA) for analysis on a Qiagen-Pyrosequencing PSQ-MD.

Liquid chromatography-mass spectrometry (LC-MS). *DNA hydrolysis.* Genomic DNA was hydrolyzed as outlined in Song et al. Briefly, 250 ng of DNA in a volume of 20 μ L was denatured at 100°C for 3 min and placed on ice. To the DNA, 2 μ L of 0.1 M ammonium acetate (cat # A7330, Sigma-Aldrich), pH 5.3, containing 2 units Nuclease P1 from *Penicillium citrinum* (cat #N8630, Sigma-Aldrich) was added and samples were incubated at 45°C for 2 h. Following this, 2.2 μ L of 1 M ammonium bicarbonate (cat # 09830, Sigma-Aldrich) containing

0.002 units of Phosphodiesterase I from *Crotalus adamanteus* venom (cat # P3243, Sigma-Aldrich) was added and samples were incubated at 37°C for 2 h. Finally, 1 unit of calf intestinal phosphatase (cat # F201-S, Finnzymes) was added and the reaction was incubated at 37°C for 1 h. Hydrolyzed samples were stored at -20°C. Each sample underwent two separate hydrolysis reactions.

LC-MS procedure. LC-MS was performed by Flinders Analytical (Flinders University, Adelaide, Australia). Briefly, Liquid chromatography (LC) separation was performed on a Waters 2695 HPLC (Milford), at a flow rate of 0.25 mL/min with a column temperature of 22°C. The LC column was a Waters Atlantis T3, 2.1 mm x 150 mm, 5 μ m particle (cat # 186003736, Milford). Two buffers were used: mobile phase A-0.1% aqueous formic acid (cat # 06440, Fluka) and mobile phase B-0.1% formic acid in acetonitrile. The LC program was 100% solvent A for 3 min, a linear gradient to 85% solvent A at 15 min then back to 100% solvent A at 15.5 min where it was held for 6.5 min for re-equilibration. A 20 μ L volume of hydrolyzed sample was diluted with 100 μ L of type 1 water (cat # SYNSV00WW, Millipore Synergy System) and transferred to a 250 μ L volume insert inside a 2 mL LC-MS vial and 10 μ L of this solution was injected into the LC. Mass Spectrometry was performed on a Waters Quattro micro, triple quadrupole mass spectrometer (Milford) fitted with

an electrospray source. Positive ion electrospray and multiple reaction monitoring conditions were determined manually using ribonucleoside and deoxyribonucleoside standards at a concentration of 10 µg/mL in water (dC, cat # D3897; C, cat # C122106; U, cat # U3750; 5mC, cat # M4254; T, cat # T9250; dA, cat # D7400; A, cat # A9251; dG, cat # D7145; and G, cat # G6752; Sigma-Aldrich; 5-mdC, cat # N-1044, Jena Bioscience). Quantitation for 5-mdC was monitored with a precursor ion of 242, fragment ion of 126 with a dwell time of 0.1 sec. Cone voltage was 12 V and collision voltage was 8 V. For dG; the precursor ion was 267.8, the fragment ion was 152, dwell time was 0.1 sec, cone voltage was 12 V and collision voltage was 12 V. Each sample was injected in duplicate. Percent methylation was calculated as the ratio of 5-mdC to dG [5-mdC/dG].

Calculation of methylation differences and statistical analyses. Differences in DNA methylation as detected by HRM were calculated using the average difference between the melt curves of a test sample and the methylated control, termed the Net Temperature Shift (NTS), such that a negative NTS results from a shift of a sample's normalized melt curve to the left of the normalized melt curve of the methylated control and indicates that the sample is less methylated. Calculation of the NTS is as follows: within the Rotor-Gene Q program, two normalization regions (at temperatures before and after melt peak temperature) were nominated for HRM analysis. For LINE1, normalization region 1 was between 74–75°C, while normalization region 2 was between 82–84°C. For B1_Mm the regions were: 66–68°C and 79–80°C; for IAP_LTR: 70–72°C, 78–79°C. The subtraction of the methylated control normalized curve from each test normalized curve was performed automatically within the Rotor-Gene Q program and the summed difference of the fluorescence value

at each temperature point (0.1°C intervals) within the entire melt range was divided by 100 to obtain the average distance between the curves, or the NTS. Data were analyzed using the statistical program SPSS Statistics (version 17, SPSS Inc.). The effect of treatment group and the analysis of methylation differences between mouse tissues was first tested by ANOVA, with Bonferroni post-hoc analysis used to compare means between groups. Linear bivariate correlations were analyzed using Pearson correlation. In all cases $p < 0.05$ was considered significant. All means are displayed with error bars representing ± 1 standard error of the mean.

Disclosure of Potential Conflicts of Interest

No potential conflicts of interest were disclosed.

Acknowledgments

We thank Ami-Louise Cochrane, Mark Lawrence, Alex Staudacher and Katrina Bexis for assistance with animal procedures; Dr. Tanya Day for the 5-aza cell culture experiments; and Dr. Tina Bianco-Miotto for critically reading this manuscript. This work was supported by the Low Dose Radiation Research Program, Biological and Environmental Research, US Department of Energy (DE-FG02-05ER64104) and the Flinders Medical Centre Foundation and BHP Billiton Low Dose Radiation Research Scholarship (to M.N.) and the Newell Foundation.

Note

Supplemental material can be found at: www.landesbioscience.com/journals/epi/article/18815

References

- Copley JE, Sater CM, Beckman KB, Martin DL. CpG methylation of a silent controlling element in the murine *Amy* allele is incomplete and unresponsive to methyl donor supplementation. *PLoS ONE* 2010; 5:9055; PMID:20140227; <http://dx.doi.org/10.1371/journal.pone.0090555>.
- Lander ES, Linton LM, Birren B, Nusbaum C, Zody MC, Baldwin J, et al. Initial sequencing and analysis of the human genome. *Nature* 2001; 409:860-921; PMID:11237011; <http://dx.doi.org/10.1038/35057062>.
- Fedorov A. Regulation of mammalian LINE1 retrotransposon transcription. *Cell Tissue Res* 2009; 31:1-13; <http://dx.doi.org/10.1134/S1990519X09010015>.
- Osterag EM. Biology of mammalian L1 retrotransposons. *Annu Rev Genet* 2001; 35:501; PMID:11700292; <http://dx.doi.org/10.1146/annurev.genet.35.102401.091032>.
- Scott AE, Schneckepfer BJ, Abdelraik M, Corney CT, O'Hara B, Rossiter JB, et al. Origin of the human L1 elements: Proposed progenitor genes deduced from a consensus DNA sequence. *Genomics* 1987; 1:113-25; PMID:3692483; [http://dx.doi.org/10.1016/0888-7543\(87\)90003-6](http://dx.doi.org/10.1016/0888-7543(87)90003-6).
- Furano AV, Robb SM, Robb FT. The structure of the regulatory region of the rat L1 (L1Ra, long interspersed repeated) DNA family of transposable elements. *Nucleic Acids Res* 1988; 16:9215; PMID:2845369; <http://dx.doi.org/10.1093/nar/16.19.9215>.
- Howard G, Eigen R, Gaudet E, Jemisch R, Eden A. Activation and transposition of endogenous retroviral elements in hypomethylation induced tumors in mice. *Oncogene* 2008; 27:404-8; PMID:17621273; <http://dx.doi.org/10.1038/sj.onc.1210631>.
- Estéicio MR, Gharibyan V, Shen L, Ibeahim AE, Doshi K, He R, et al. LINE-1 hypomethylation in cancer is highly variable and inversely correlated with microsatellite instability. *PLoS ONE* 2007; 2:399; PMID:17476321; <http://dx.doi.org/10.1371/journal.pone.0000399>.
- Gaudet E, Hodgson JG, Eden A, Jackson-Grusby L, Dausman J, Gay JW, et al. Induction of tumors in mice by genomic hypomethylation. *Science* 2003; 300:489-92; PMID:12702876; <http://dx.doi.org/10.1126/science.1083558>.
- Igarashi S, Suzuki H, Ninuma T, Shimizu H, Nojima M, Iwaki H, et al. A novel correlation between LINE-1 hypomethylation and the malignancy of gastrointestinal stromal tumors. *Clin Cancer Res* 2010; 16:5114-23; PMID:20978145; <http://dx.doi.org/10.1158/1078-0432.CCR-10-0581>.
- Ogino S, Kawasaki T, Nosho K, Ohnishi M, Suemoto Y, Kirkner GJ, et al. LINE-1 hypomethylation is inversely associated with microsatellite instability and CpG island methylase phenotype in colorectal cancer. *Int J Cancer* 2008; 122:2767-73; PMID:18366060; <http://dx.doi.org/10.1002/ijc.23470>.
- Ogino S, Nosho K, Kirkner GJ, Kawasaki T, Chan AT, Scherhammer ES, et al. A cohort study of tumoral LINE-1 hypomethylation and prognosis in colon cancer. *J Natl Cancer Inst* 2008; 100:1734-8; PMID:19033568; <http://dx.doi.org/10.1093/jnci/djn359>.
- Yamamoto E, Toyota M, Suzuki H, Kondo Y, Sanomura T, Murayama Y, et al. LINE-1 hypomethylation is associated with increased CpG island methylation in *Helicobacter pylori*-related enlarged-fold gastritis. *Cancer Epidemiol Biomarkers Prev* 2008; 17:2555-64; PMID:18842996; <http://dx.doi.org/10.1158/1055-9965.EPI-08-0112>.
- Wolff EM, Byun HM, Han HE, Sharma S, Nichols PW, Siegmund KD, et al. Hypomethylation of a LINE-1 promoter activates an aberrant transcript of the MET oncogene in bladders with cancer. *PLoS Genet* 2010; 6:1000917; PMID:20421991; <http://dx.doi.org/10.1371/journal.pgen.1000917>.
- Saino K, Kawakami K, Matsumoto I, Oda M, Watanabe G, Minamoto T. Long interspersed nuclear element 1 hypomethylation is a marker of poor prognosis in stage IA non-small cell lung cancer. *Clin Cancer Res* 2010; 16:2418-26; PMID:20371677; <http://dx.doi.org/10.1158/1078-0432.CCR-09-2819>.
- Sauer J, Jang H, Zimmerly EM, Kim KC, Liu Z, Chanson A, et al. Ageing, chronic alcohol consumption and folate are determinants of genomic DNA methylation, p16 promoter methylation and the expression of p16 in the mouse colon. *Br J Nutr* 2010; 104:24-30; PMID:20236555; <http://dx.doi.org/10.1017/S0007114510000322>.

17. Finnell RH, Spiegelstein O, Włodarczyk B, Triplett A, Pogribny IP, Melnyk S, et al. DNA methylation in FcγR1 knockout mice supplemented with folic acid during gestation. *J Nutr* 2002; 132:2457-61; PMID:12163711.
18. Vanhees K, Coort S, Ruijters EJB, Godschalk RWL, van Schooten FJ, Burjess van Waalwijk van Doorn-Khorrami S. Epigenetics: prenatal exposure to genotoxic leaves a permanent signature on the hematopoietic lineage. *FASEB J* 2011; 25:797-807; PMID:21048042; <http://dx.doi.org/10.1096/fj.10-172155>.
19. Koturbash I, Scherbag A, Sorrentino J, Sexton K, Bodnar W, Swenberg JA, et al. Epigenetic mechanisms of mouse interstrain variability in genotoxicity of the environmental toxicant 1,3-Butadiene. *Toxicol Sci* 2011; 122:448-56; PMID:21602187; <http://dx.doi.org/10.1093/toxsci/kfr133>.
20. Giotopoulos G, McCormick C, Cole C, Zanker A, Jawad M, Brown R, et al. DNA methylation during mouse hematopoietic differentiation and radiation-induced leukemia. *Exp Hematol* 2006; 34:1462-70; PMID:17046565; <http://dx.doi.org/10.1016/j.exphem.2006.06.008>.
21. Pogribny I, Koturbash I, Tryndyak V, Hudson D, Stevenson SM, Sedelnikova O, et al. Fractionated low-dose radiation exposure leads to accumulation of DNA damage and profound alterations in DNA and histone methylation in the murine thymus. *Mol Cancer Res* 2005; 3:553-61; PMID:16254189; <http://dx.doi.org/10.1158/1541-7786.MCR-05-0074>.
22. Pogribny I, Raiche J, Slovack M, Kovalchuk O. Dose-dependence, sex- and tissue-specificity, and persistence of radiation-induced genomic DNA methylation changes. *Biochem Biophys Res Commun* 2004; 320:1253-61; PMID:15249225; <http://dx.doi.org/10.1016/j.bbrc.2004.06.081>.
23. Raiche J, Rodriguez-Juarez R, Pogribny I, Kovalchuk O. Sex- and tissue-specific expression of maintenance and de novo DNA methyltransferases upon low dose X-irradiation in mice. *Biochem Biophys Res Commun* 2004; 325:39-47; PMID:15522198; <http://dx.doi.org/10.1016/j.bbrc.2004.10.002>.
24. Tera R, Kimura Y, Komura J, Miyamura Y, Karishita A, Saeki MS, et al. Effects of X-ray irradiation on genomic DNA methylation levels in mouse tissues. *J Radiat Res (Tokyo)* 1998; 39:271-8; PMID:10196782; <http://dx.doi.org/10.1269/jrr.39.271>.
25. Barboe W, Dupressoir A, Lazar V, Heidmann T. Epigenetic regulation of an IAP retrotransposon in the aging mouse: progressive demethylation and dislodging of the element by its repetitive induction. *Nucleic Acids Res* 2002; 30:2365; PMID:12034823; <http://dx.doi.org/10.1093/nar/30.11.2365>.
26. Singhal RP, Mays-Hoopes LL, Eichhorn GL. DNA methylation in aging of mice. *Mech Ageing Dev* 1987; 41:199-210; PMID:3431172; [http://dx.doi.org/10.1016/0047-6374\(87\)90040-6](http://dx.doi.org/10.1016/0047-6374(87)90040-6).
27. Ririe KM, Rasmussen R, Witwer C. Product differentiation by analysis of DNA melting curves during the polymerase chain reaction. *Anal Biochem* 1997; 245:154-60; PMID:9056205; <http://dx.doi.org/10.1006/abio.1996.9916>.
28. Stamer S, Balic M, Strutz J, Heitner E, Obermair E, Hauser-Kronberger C, et al. Rapid and reliable detection of LINE-1 hypomethylation using high resolution melting analysis. *Clin Biochem* 2010; 43:1445-8; PMID:20883681; <http://dx.doi.org/10.1016/j.clinbiochem.2010.09.013>.
29. Yang AS, Estecio MR, Doshi K, Kondo Y, Tajara EH, Issa JP. A simple method for estimating global DNA methylation using bisulfite PCR of repetitive DNA elements. *Nucleic Acids Res* 2004; 32:38; PMID:14973332; <http://dx.doi.org/10.1093/nar/gnh052>.
30. Bollani V, Schwartz J, Wright R, Lisonjua A, Taramini L, Suh H, et al. Decline in genomic DNA methylation through aging in a cohort of elderly subjects. *Mech Ageing Dev* 2009; 130:234-9; PMID:19150625; <http://dx.doi.org/10.1016/j.mad.2008.12.003>.
31. Kato Y, Kanoda M, Hara K, Kamaki K, Hisano M, Kohara Y, et al. Role of the DNMT3 family in de novo methylation of imprinted and repetitive sequences during male germ cell development in the mouse. *Hum Mol Genet* 2007; 16:2272-80; PMID:17616512; <http://dx.doi.org/10.1093/hmg/ddm179>.
32. Lane N, Dean W, Erhardt S, Hajkova P, Surani A, Walter J, et al. Resistance of IAPs to methylation reprogramming may provide a mechanism for epigenetic inheritance in the mouse. *Genesis* 2003; 35:88-93; PMID:12535790; <http://dx.doi.org/10.1002/gene.10168>.
33. Li L-C, Dahiya R. MethPrimer: designing primers for methylation PCRs. *Bioinformatics* 2002; 18:1427-31; PMID:12424112; <http://dx.doi.org/10.1093/bioinformatics/18.11.1427>.
34. Witwer CT, Reed G, Gundry C, Vandersteen J, Pryor R. High-resolution genotyping by amplicon melting analysis using LCGreen. *Clin Chem* 2003; 49:853; PMID:12765979; <http://dx.doi.org/10.1373/49.6.853>.
35. Gundry CN, Vandersteen J, Reed G, Pryor R, Chen J, Witwer C. Amplicon melting analysis with labeled primers: a closed-tube method for differentiating homozygotes and heterozygotes. *Clin Chem* 2003; 49:396; PMID:12600951; <http://dx.doi.org/10.1373/49.3.396>.
36. Candiani IL, Mikeška T, Hokland P, Dobrovic A. Rapid analysis of heterogeneously methylated DNA using digital methylation-sensitive high resolution melting: application to the CDKN2B (p15) gene. *Epigenetics Chromatin* 2008; 1:7; PMID:19014416; <http://dx.doi.org/10.1186/1756-8935-1-7>.
37. Eads CA, Danenberg KD, Kawakami K, Saltz LB, Blake C, Shibata D, et al. MethyLight: a high-throughput assay to measure DNA methylation. *Nucleic Acids Res* 2000; 28:32; PMID:10734209; <http://dx.doi.org/10.1093/nar/28.8.e32>.
38. Rand KN, Molloy P. Sensitive measurement of unmethylated repeat DNA sequences by end-specific PCR. *Biotechniques* 2010; 49:13-7; PMID:20964632; <http://dx.doi.org/10.2144/000113494>.
39. Fandy TE, Herman JG, Kerns P, Jernitt A, Sugar EA, Choi SH, et al. Early epigenetic changes and DNA damage do not predict clinical response in an overlapping schedule of 5-azacytidine and entinostat in patients with myeloid malignancies. *Blood* 2009; 114:2764-73; PMID:19546476; <http://dx.doi.org/10.1182/blood-2009-02-203547>.
40. Gebhard C, Benner C, Ehrlich M, Schwarzfacher I, Schilling E, Klug M, et al. General transcription factor binding at CpG islands in normal cells correlates with resistance to de novo DNA methylation in cancer cells. *Cancer Res* 2010; 70:1398; PMID:20145141; <http://dx.doi.org/10.1158/0008-5472.CAN-09-3406>.
41. Suzuki S, Oho R, Narita T, Park AJ, Shaw G, Wang C, et al. Retrotransposon silencing by DNA methylation can drive mammalian genomic imprinting. *PLoS Genet* 2007; 3:5; PMID:17432937; <http://dx.doi.org/10.1371/journal.pgen.0030955>.
42. Zhang D, Wang Y, Bai Y, Ge Q, Qian Y, Luo J, et al. A novel method to quantify local CpG methylation density by regional methylation elongation assay on microarray. *BMC Genomics* 2008; 9:59; PMID:18237388; <http://dx.doi.org/10.1186/1471-2164-9-59>.
43. Weeks RJ, Morison I. Detailed methylation analysis of CpG islands on human chromosome region 9p21. *Genes Chromosomes Cancer* 2006; 45:357-64; PMID:16372313; <http://dx.doi.org/10.1002/gcc.20297>.
44. Wojdacz TK, Dobrovic A. Methylation-sensitive high resolution melting (MS-HRM): a new approach for sensitive and high-throughput assessment of methylation. *Nucleic Acids Res* 2007; 35:411; PMID:17289753; <http://dx.doi.org/10.1093/nar/gkm613>.
45. Wojdacz TK, Hansen L. Reversal of PCR bias for improved sensitivity of the DNA methylation melting curve assay. *Biotechniques* 2006; 41:274; PMID:16989087; <http://dx.doi.org/10.2144/000112240>.
46. Kristiansen LS, Mikeška T, Krupp M, Dobrovic A. Sensitive melting analysis after real-time-methylation specific PCR (SMART-MSP): high-throughput and probe-free quantitative DNA methylation detection. *Nucleic Acids Res* 2008; 36:42; PMID:18344521; <http://dx.doi.org/10.1093/nar/gkn113>.
47. Gama-Sosa MA, Migdott RM, Slagel VA, Gibbens S, Kuo KC, Gebelke CW, et al. Tissue-specific differences in DNA methylation in various mammals. *Biochimica et Biophysica Acta* 1983; 740:212-9; [http://dx.doi.org/10.1016/0167-4781\(83\)90079-9](http://dx.doi.org/10.1016/0167-4781(83)90079-9).
48. Smith E, Jones ME, Drew PA. Quantitation of DNA methylation by melt curve analysis. *BMC Cancer* 2009; 9:123; PMID:19393074; <http://dx.doi.org/10.1186/1471-2407-9-123>.
49. Malentacchi F, Furni G, Vinci S, Orlando C. Quantitative evaluation of DNA methylation by optimization of a differential-high resolution melt analysis protocol. *Nucleic Acids Res* 2009; 37:86; PMID:19454604; <http://dx.doi.org/10.1093/nar/gkp383>.
50. Leconte A, Mueller W, Urdangarin E, Lásoco P, Von Dömling A, Castresana J. Detection of methylation in promoter sequences by melting curve analysis-based semiquantitative real time PCR. *BMC Cancer* 2008; 8:61; PMID:18298842; <http://dx.doi.org/10.1186/1471-2407-8-61>.
51. Jüttemann R, Li E, Jaenisch R. Toxicity of 5-aza-2'-deoxycytidine to mammalian cells is mediated primarily by covalent trapping of DNA methyltransferase rather than DNA demethylation. *Proc Natl Acad Sci USA* 1994; 91:11797-801; PMID:7527544; <http://dx.doi.org/10.1073/pnas.91.25.11797>.
52. Mund C, Hackanson B, Szesemann C, Lübbert M, Lyko E. Characterization of DNA demethylation effects induced by 5-aza-2'-deoxycytidine in patients with myelodysplastic syndrome. *Cancer Res* 2005; 65:7086; PMID:16103056; <http://dx.doi.org/10.1158/0008-5472.CAN-05-0695>.
53. Wojdacz TK, Hansen LL, Dobrovic A. A new approach to primer design for the control of PCR bias in methylation studies. *BMC Res Notes* 2008; 1:54; PMID:18710507; <http://dx.doi.org/10.1186/1756-0500-1-54>.
54. Wojdacz TK, Dobrovic A, Hansen LL. Methylation-sensitive high-resolution melting. *Nat Protoc* 2008; 3:1903-8; PMID:19180074; <http://dx.doi.org/10.1038/nprot.2008.191>.
55. Mund C, Hackanson B, Szesemann C, Lübbert M, Lyko E. Characterization of DNA demethylation effects induced by 5-Aza-2'-Deoxycytidine in patients with myelodysplastic syndrome. *Cancer Res* 2005; 65:7086-90; PMID:16103056; <http://dx.doi.org/10.1158/0008-5472.CAN-05-0695>.
56. Irahara N, Noshio K, Baba Y, Shima K, Lindeman N, Harra A, et al. Precision of pyrosequencing assay to measure LINE-1 methylation in colon cancer, normal colonic mucosa and peripheral blood cells. *J Mol Diagn* 2010; 12:177; PMID:20093385; <http://dx.doi.org/10.2353/jmol.2010.090106>.
57. Akagi K, Li J, Stephens RM, Volkovskiy N, Symer DE. Extensive variation between inbred mouse strains due to endogenous L1 retrotransposition. *Genome Res* 2008; 18:869-80; PMID:18381897; <http://dx.doi.org/10.1101/jg.075770.107>.
58. Boulton E, Cole C, Knight A, Cleary H, Snowden R, Plumb M. Low-penetrance genetic susceptibility and resistance loci implicated in the relative risk for radiation-induced acute myeloid leukemia in mice. *Blood* 2003; 101:2349-54; PMID:12411293; <http://dx.doi.org/10.1182/blood-2002-08-2394>.

59. Carole L, Yauk AP, Rowan-Carroll A, Korubash I, Williams A, Korolchuk O. Tandem repeat mutation, global DNA methylation and regulation of DNA methyltransferases in cultured mouse embryonic fibroblast cells chronically exposed to chemicals with different modes of action. *Environ Mut Mutag* 2008; 49:26-35.
60. Plumb M. Genetic instability in radiation-induced leukaemias: mouse models. *Int J Radiat Biol* 1998; 74:711-20; PMID:9881716; <http://dx.doi.org/10.1080/095530098140989>.
61. Yu Y, Okayasu R, Weil MM, Silver A, McCarthy M, Zabridke R, et al. Elevated breast cancer risk in irradiated BALB/c mice associates with unique functional polymorphism of the *Pkb4* (DNA-dependent protein kinase catalytic subunit) gene. *Cancer Res* 2001; 61:1820-4; PMID:11280730.
62. El-Maarri O, Waller M, Behne F, van Ütim J, Singer H, Diaz-Lacava A, et al. Methylation at global LINE-1 repeats in human blood are affected by gender but not by age or natural hormone cycles. *PLoS ONE* 2011; 6:16252; PMID:21311577; <http://dx.doi.org/10.1371/journal.pone.0016252>.
63. Zhu ZZ, Hou L, Bollati V, Taramini L, Marinelli B, Cantonese L, et al. Predictors of global methylation levels in blood DNA of healthy subjects: a combined analysis. *Int J Epidemiol* 2010; PMID:20846947; <http://dx.doi.org/10.1093/ije/dyq154>.
64. Hooker AM, Home R, Morley A, Sykes P. Dose-dependent increase or decrease of somatic intrachromosomal recombination produced by cisposide. *Mutat Res* 2002; 509:117-24; PMID:11890941; [http://dx.doi.org/10.1016/S0027-5107\(02\)00007-6](http://dx.doi.org/10.1016/S0027-5107(02)00007-6).
65. Song L, James S, Kazim L, Karpf A. Specific method for the determination of genomic DNA methylation by liquid chromatography-electrospray ionization tandem mass spectrometry. *Anal Chem* 2005; 77:504-10; PMID:15649046; <http://dx.doi.org/10.1021/ac0489420>.
